

12-2023

## A Study Of The Snd1/Prmt5 Axis In Liver Cancer By Genetic Mouse Models

Tanner Wright

Tanner Wright

Follow this and additional works at: [https://digitalcommons.library.tmc.edu/utgsbs\\_dissertations](https://digitalcommons.library.tmc.edu/utgsbs_dissertations)



Part of the [Genetics Commons](#), and the [Molecular Genetics Commons](#)

---

### Recommended Citation

Wright, Tanner and Wright, Tanner, "A Study Of The Snd1/Prmt5 Axis In Liver Cancer By Genetic Mouse Models" (2023). *Dissertations and Theses (Open Access)*. 1309.

[https://digitalcommons.library.tmc.edu/utgsbs\\_dissertations/1309](https://digitalcommons.library.tmc.edu/utgsbs_dissertations/1309)

This Dissertation (PhD) is brought to you for free and open access by the MD Anderson UTHealth Houston Graduate School at DigitalCommons@TMC. It has been accepted for inclusion in Dissertations and Theses (Open Access) by an authorized administrator of DigitalCommons@TMC. For more information, please contact [digcommons@library.tmc.edu](mailto:digcommons@library.tmc.edu).

A STUDY OF THE SND1/PRMT5 AXIS IN LIVER  
CANCER BY GENETIC MOUSE MODELS

by

*Tanner Janson Wright, B.S.*

APPROVED:

---

Mark T. Bedford, PhD  
Advisory Professor

---

David G. Johnson, PhD

---

Manu M. Sebastian, DVM, PhD

---

Min Gyu Lee, PhD

---

Laura Beretta, PhD

---

Taiping Chen, PhD

APPROVED:

---

Dean, The University of Texas  
MD Anderson Cancer Center UTHealth Houston Graduate School of Biomedical Sciences

A STUDY OF THE SND1/PRMT5 AXIS IN LIVER  
CANCER BY GENETIC MOUSE MODELS

A

Dissertation

Presented to the Faculty of

The University of Texas

MD Anderson Cancer Center UTHealth Houston

Graduate School of Biomedical Sciences

in Partial Fulfillment

of the Requirements

for the Degree of

Doctor of Philosophy

by

Tanner Janson Wright, B.S.

December 2023

## Dedication

*“Wanting the desirable but unattainable is very different from failing to get the desirable and potentially attainable.”*

Sydney Brenner 1996

This work is dedicated to each of the following:

To my mother who gave me the daily charge to “come back better”-

To my father who climbed “the” mountain to be with me-

To Bob who saw something that was worth encouraging to grow-

To my courageous and trusting wife who is the wind in my sails and the sunshine of my day-

And finally, to “Salmon shorts”, the young man who met mocking with courage, abuse with resolution, and persecution with poise- who inspired the change of course that has altered my trajectory forever.

*“Es gibt nichts Gutes, ausser: Man tut es.”*

“There is nothing good unless you do it.”

Erich Kästner

## Acknowledgements

*“Sometimes science is the excuse for exploration. I think it is rarely the reason.”*

George Lee Malory

I express gratitude for my mentor, Dr. Mark Bedford for guiding my development as a scientist line upon line- for being patient as I learned- and for being understanding when duty called. In my experience, he is a mentor any trainee will be happy to learn from.

I also express gratitude for an exceptional and inspiring committee in no special order: Doctors Margarida Albuquerque Almeida Santos, Laura Beretta, Min Gyu Lee, Manu Sebastian, Taiping Chen, and David Johnson. Each member always encouraged growth and taking the next step.

To a second family, the Epigenetics and Molecular Carcinogenesis Department, I owe much and wish to thank all for their gracious help, expertise, and excellence. Everywhere I turned I found a group of welcoming and genuine friends. They weathered both literal and figurative storms as few organizations can. To the entire Smithville/Science Park community, thank you.

This work was greatly aided by Steven Vokes and Ernesto Guccione and the talented scientists in each of their labs.

Finally, I add my thanks to the past and present members of the Bedford Lab as I met them: Jason Friedemann, Cari Sagum, Jianji Chen, Goushen Gao, Fen Yang, Ishita Rehman, Swarnalatha Manickavinayaham, Leilei Shi, Sharad Awasthi, and Isaiah Mixon. Also, a special thanks goes to Yalong Wang and Sabrina Stratton- this work wouldn't exist without you.

*“The important thing about research is that it is new, and is about going where none have gone before, and you have no other recourse but to teach yourself...”*

Sydney Brenner 1996

# A STUDY OF THE SND1/PRMT5 AXIS IN LIVER CANCER BY GENETIC MOUSE MODELS

Tanner Janson Wright, B.S.

Advisory Professor: Mark T. Bedford, Ph.D.

## **Abstract:**

Arginine methylation is an essential post-translational modification (PTM) in cells. Protein arginine methyltransferase 5 (PRMT5) is the primary enzyme that catalyzes symmetric dimethyl arginine (SDMA) and requires methylome protein 50 (MEP50) for stability and enzymatic activity which are necessary for life and development. Effector proteins bind different types of PTM's to facilitate signaling. Staphylococcal nuclease Tudor domain containing 1 (SND1) is an effector that specifically binds SDMA via its single C-terminal Tudor domain. Both SND1 and PRMT5 have been implicated in hepatocellular carcinoma (HCC). SND1 has been confirmed as a driver of HCC using genetically engineered mouse models (GEMMs), though, it remains unknown if loss of SND1 or its methyl reading ability can protect against HCC formation. PRMT5 has been reported as upregulated in many cancers and may predispose hepatocytes to develop HCC. However, it remains to be determined if *Prmt5* overexpression (OE) alone is sufficient to drive HCC. This work utilizes three new GEMMs, namely a *Snd1* KO, *Snd1* Tudor domain mutant (*KI*), and tissue specific *Prmt5* OE mouse, to answer these key questions: 1) Does loss of SND1 or its methyl binding ability impact tumorigenesis? and 2) Does *Prmt5* OE predispose mice to develop HCC? We characterize and validate each of these GEMMs and use a high penetrance HCC assay to determine the role of this effector/writer pair to begin answering these questions. First, the *Snd1* KO and *KI* mice reveal a Tudor domain independent "small" phenotype and reveal distinct transcriptional control by SND1 and its Tudor domain. *Snd1* KO and *KI* mice are further hepatoprotected against carcinogen-induced HCC. Next, *Prmt5* OE mice reveal important insight into PRMT5 biology and suggest that elevated PRMT5 levels do not correlate with elevated SDMA levels. Carcinogenesis studies using two cancer-inducing models further strengthen our understanding of these processes. This work provides important information about the SND1/PRMT5 axis in liver cancer and how this axis may be a viable target for treating HCC.

Table of Contents-

<b>0.1</b>	<b>Approval page</b> .....	<b>i</b>
<b>0.2</b>	<b>Title page</b> .....	<b>ii</b>
<b>0.3</b>	<b>Dedication</b> .....	<b>iii</b>
<b>0.4</b>	<b>Acknowledgements</b> .....	<b>iv</b>
<b>0.5</b>	<b>Abstract</b> .....	<b>v</b>
<b>0.6</b>	<b>List of Illustrations</b> .....	<b>ix</b>
<b>0.7</b>	<b>List of Tables</b> .....	<b>x</b>
<b>0.8</b>	<b>Key abbreviations</b> .....	<b>xi</b>
<b>1</b>	<b>Chapter 1- Introduction</b> .....	<b>1</b>
<b>1.1</b>	<b>Arginine methylation and Tudor domains</b> .....	<b>1</b>
1.1.1	Arginine methylation .....	1
1.1.2	Arginine methyltransferases- “writers” .....	1
1.1.3	Methyl binding effector proteins- “readers” .....	7
<b>1.2</b>	<b>Arginine methylation in cancer</b> .....	<b>11</b>
1.2.1	PRMT5 in cancer .....	12
1.2.2	SND1 in cancer .....	14
<b>1.3</b>	<b>The SND1/PRMT5 axis in hepatocellular carcinoma</b> .....	<b>15</b>
1.3.1	Introduction to HCC .....	15
1.3.2	SND1 OE in clinical samples .....	16
1.3.3	<i>Snd1</i> drives HCC in SB screen .....	16
1.3.4	SND1 drives HCC in OE GEMM .....	17
1.3.5	Evidence for <i>Prmt5</i> in promoting HCC .....	17
<b>1.4</b>	<b>Summary and scope</b> .....	<b>20</b>
<b>2</b>	<b>Chapter 2- Materials and methods</b> .....	<b>22</b>
<b>2.1</b>	<b>Mouse experiments</b> .....	<b>22</b>
<b>2.2</b>	<b>Generation of mouse models</b> .....	<b>22</b>
2.2.1	<i>Snd1</i> KO and KI GEMMs .....	22
2.2.2	PRMT5 OE GEMM .....	23
<b>2.3</b>	<b>MEF isolation and immortalization</b> .....	<b>24</b>
<b>2.4</b>	<b>Genotyping</b> .....	<b>24</b>
2.4.1	DNA extraction .....	24
2.4.2	Genotyping <i>Snd1</i> KO mice .....	25
2.4.3	Genotyping <i>Snd1</i> KI mice .....	25
2.4.4	Genotyping PRMT5 transgenic mice .....	26
<b>2.5</b>	<b>Sequencing</b> .....	<b>26</b>
<b>2.6</b>	<b>Liver harvest for Western blot</b> .....	<b>27</b>
<b>2.7</b>	<b>Western blot analysis</b> .....	<b>28</b>
2.7.2	LI-COR detection by fluorescence- .....	28
2.7.3	Western blot detection by chemiluminescence- .....	29
<b>2.8</b>	<b>Antibodies</b> .....	<b>29</b>
<b>2.9</b>	<b>Peptide pulldown assay</b> .....	<b>30</b>

2.10	RNA-extraction.....	30
2.11	RT-qPCR primers .....	30
2.12	RT-qPCR analysis .....	31
2.13	RNA-sequencing of <i>Prmt5<sup>OE</sup></i> samples.....	31
2.14	DEN injection model .....	32
2.15	Bloodwork .....	32
2.16	BrdU proliferation model .....	33
2.17	<i>In vitro</i> methylation assay .....	33
2.18	Enhancer spray .....	34
2.19	Transient transfection.....	34
2.20	Hydrodynamic Tail Vein Injection .....	34
2.21	Phosphatase inhibitor cocktail .....	35
2.22	Post-DEN treatment necropsy procedure .....	35
2.23	Photoshop courtesy edits .....	36
<b>3</b>	<b>Chapter 3- Characterizing loss or mutation of <i>SND1</i> and the effect on HCC.....</b>	<b>37</b>
3.1	Introduction and scope.....	37
3.2	Generation and validation of <i>Snd1</i> KO and KI mouse lines.....	37
3.2.1	<i>Snd1</i> KO GEMM.....	37
3.2.2	<i>Snd1</i> KI GEMM.....	39
3.2.3	Comparing the phenotype of <i>Snd1</i> mutant mouse models.....	41
3.3	Transcriptional analysis of livers from <i>Snd1</i> mutant mice.....	41
3.4	<b>SND1 Carcinogenesis Models.....</b>	<b>43</b>
3.4.1	DEN carcinogenesis modeling .....	45
3.4.2	BrdU proliferation assay .....	50
3.5	<b>Conclusions and Future Experiments .....</b>	<b>50</b>
3.5.1	<i>Snd1</i> KO and KI mice reveal Tudor independent functions for SND1 .....	50
3.5.2	Transcriptional analysis .....	53
3.5.3	Carcinogenesis modeling .....	54
<b>4</b>	<b>Chapter 4- Characterizing a gain-of-function <i>PRMT5</i> OE mouse and the effect on HCC.....</b>	<b>59</b>
4.1	Generation and validation of a <i>Prmt5</i> OE GEMM .....	59
4.2	Transcriptional analysis of <i>PRMT5</i> OE GEMM.....	70
4.2.1	Alternative splicing in <i>Prmt5</i> OE livers .....	70
4.3	<b><i>PRMT5</i> OE carcinogenesis models.....</b>	<b>72</b>
4.3.1	<i>PRMT5</i> OE in unchallenged normal mice .....	74
4.3.2	Carcinogenesis modeling by DEN-induced HCC .....	74
4.3.3	BrdU injection to measure <i>Prmt5<sup>OE</sup></i> liver proliferation .....	76
4.3.4	Hydrodynamic tail vein injection.....	78
4.4	<b>Discussion.....</b>	<b>80</b>
4.4.1	New insights into the control and activity of <i>PRMT5</i> .....	80
4.4.2	<i>PRMT5</i> OE in carcinogenesis.....	82



<b>5</b>	<b><i>Chapter 5- Summary of conclusions and future directions</i></b> .....	<b>84</b>
5.1	<b><i>Part I- The Reader</i></b> .....	<b>84</b>
5.2	<b><i>Part II- The Writer</i></b> .....	<b>87</b>
<b>6</b>	<b><i>Appendix A- Published review</i></b> .....	<b>90</b>
<b>7</b>	<b><i>Appendix B- Plasmid maps and sequences</i></b> .....	<b>145</b>
<b>8</b>	<b><i>Appendix C- Quantification of myc-Prmt5 OE</i></b> .....	<b>158</b>
<b>9</b>	<b><i>Appendix D- Albumin-Cre documentation</i></b> .....	<b>162</b>
<b>10</b>	<b><i>Appendix E- BioRender license</i></b> .....	<b>163</b>
<b>11</b>	<b><i>Bibliography</i></b> .....	<b>164</b>
<b>12</b>	<b><i>Vita</i></b> .....	<b>195</b>

## List of Illustrations

Figure 1- Arginine methylation pathways in mammals	3
Figure 2- PRMT5 and MEP50 structure and enzymatic processing	4
Figure 3- SND1 graphical structure and protein-protein interaction mapping...	10
Figure 4- <i>Snd1</i> KO GEMM validation	38
Figure 5- <i>Snd1</i> KI GEMM validation	40
Figure 6- Litter and body size of <i>Snd1</i> KO and KI mice	42
Figure 7- RT-qPCR of selected downregulated genes from KO and KI mice	44
Figure 8- Diethylnitrosamine induced HCC grossing and pathology	46
Figure 9- Tumor burden of DEN induced HCC in <i>SND1</i> KO, KI, and WT mice	49
Figure 10- Proliferation assay in <i>Snd1</i> variable mice	51
Figure 11- RT-qPCR of common drug metabolizing cytochromes Cyp3a44 and Cyp2c39	55
Figure 12- <i>Prmt5</i> <sup>OE</sup> GEMM design and sequence validation	61
Figure 13- Western blot and quantification for <i>Prmt5</i> <sup>WT</sup> and <i>Prmt5</i> <sup>OE</sup> from whole cell lysate	63
Figure 14- <i>In vitro</i> methylation of recombinant H4 by <i>Prmt5</i> <sup>WT</sup> and <i>Prmt5</i> <sup>OE</sup> ...	64
Figure 15- Type II methylation of <i>Prmt5</i> <sup>OE</sup> liver tissues	66
Figure 16- Pan-tissue methylarginine comparison	67
Figure 17- Hypermethylation analysis in myc-PRMT5 overexpressing HepG2 cells	68
Figure 18- Hypermethylation analysis in myc-PRMT5 overexpressing HEK293T cells	69
Figure 19- Volcano plot of differentially expressed genes from <i>Prmt5</i> <sup>OE</sup> mice liver	71
Figure 20- <i>Prmt5</i> <sup>OE</sup> alternative splicing events	73
Figure 21- <i>Prmt5</i> <sup>OE</sup> vs <i>Prmt5</i> <sup>WT</sup> pathology and tumor burden for DEN injected mice	75
Figure 22- Proliferation of <i>Prmt5</i> <sup>OE</sup> livers by BrdU incorporation	77
Figure 23- Hydrodynamic tail vein injection of <i>Prmt5</i> <sup>OE</sup> and WT mice	79

## List of Tables

Table 1- Published <i>Prmt5</i> and <i>Mep50</i> conditional knockout mice	5
Table 2- Sampling of Tudor domain proteins and their methyl species binding	8
Table 3- Published roles of PRMT5 in cancer	13
Table 4- Blood analyte comparison of <i>Snd1</i> <i>WT</i> , <i>KO</i> , and <i>KI</i> DEN injected mice	47

## Key abbreviations

ADMA- Asymmetric dimethyl arginine

BrdU- Bromodeoxyuridine

DEN- Diethylnitrosamine

GEMM- Genetically engineered mouse model

HCC- Hepatocellular carcinoma

HTVi- Hydrodynamic tail vein injection

KI- Tudor domain mutant, or knock in

KO- Knockout

MEF- Mouse embryonic fibroblast

MMA- Monomethyl arginine

MEP50- Methylosome protein 50

NAFLD- Non-alcoholic fatty liver disease

NASH- Non-alcoholic steatohepatitis

OE- Overexpression

PRMT5- Protein arginine methyltransferase 5

PTM- Post-translational modification

SDMA- Symmetric dimethyl arginine

SMI- Small molecule inhibitor

SN-domain- Staphylococcal nuclease like domain

SND1- Staphylococcal nuclease and Tudor domain containing 1

# 1 Chapter 1- Introduction

## 1.1 Arginine methylation and Tudor domains

### 1.1.1 Arginine methylation

Arginine is a bulky net positively charged amino acid. This electrophilic nature makes the side chain a reactive substrate for methylation, an abundant post-translational modification (PTM). Like its positively charged sibling lysine, arginine residues are methylated in many proteins which influences protein-protein interaction and signal transduction. This can impact a proteins subcellular localization, modulate addition of other PTMs, or create docking sites for effector proteins to relay cellular signals. While lysine and arginine methylation have some similarities, they are not functionally redundant and serve essential and distinct functions in the cell. A well-recognized biological consequence of protein arginine methylation is the regulation of transcription by either activation or repression by H3R17me2a or H4R3me2s PTMs respectively<sup>1</sup>. Beyond histones, there has been a metaphorical explosion of discovered methylarginine modified proteins and associated pathways with essential biological roles over the last twenty years (79). These targets and pathways of arginine methylation include regulating RNA polymerase II (80), splicing machinery (81), DNA damage repair (82), and potential roles in immunity<sup>2</sup>.

### 1.1.2 Arginine methyltransferases- “writers”<sup>3</sup>”

The family of enzymes that deposit methylarginine marks are the protein arginine

---

<sup>1</sup> There is growing evidence that arginine methylation of histones is important primarily in development given their abundance in gametes compared to somatic cells (Tee, et al.,2010); (Wang, et al.,2014).

<sup>2</sup> These were recently reviewed here (Xu, et al., 2021).

<sup>3</sup> Observations that PTMs on histones were reversible and could be selectively bound by distinct protein domains gave rise to the “Histone Code” hypothesis. This says that PTMs are added or “written” onto proteins which can then be bound or “read” by an effector protein creating an epigenetic code with similarities to the genetic code. Thus, the colloquial terms of “writer” and “reader” can quickly convey the function of many proteins.

methyltransferases (PRMTs) and are sequentially numbered 1-9 in mammals (84, 85). This family is further divided into three types, identified with roman numeral I-III, and are grouped based on the methyl-isomer they catalyze. The guanidyl chemical group at the end of an arginine side chain contains two  $\omega$ -nitrogen ( $\omega$ -N<sup>G</sup>) atoms, distinguished as  $\omega$ -N<sup>G</sup>, and  $\omega$ -N'<sup>G</sup> (said 'omega-prime nitrogen'), and can be methylated in one of three configurations being either monomethylated (MMA), asymmetric dimethylated (ADMA), or symmetric dimethylated arginine (SDMA) (**Figure 1**). Type I PRMTs catalyze MMA and ADMA, Type II PRMTs catalyze MMA and SDMA, and Type III only catalyze MMA (16, 84).

Type I PRMTs are the largest subtype in the family consisting of PRMTs 1,2,3,4 (commonly called CARM1), 6, and 8. PRMT7 is the only Type III PRMT. PRMT5 and PRMT9 are Type II PRMTs, though PRMT5 is widely acknowledged as the major depositor of SDMA because verified PRMT9 substrates remain very limited (86)<sup>4</sup>. As the major Type II PRMT, PRMT5 plays an essential role in development and homeostasis.

Many in-depth reviews have been published about PRMT5 in normal and disease biology. The author has added one such review to this body of literature which is included as appendix A, and ref (16). In brief, PRMT5 is an essential housekeeping gene for development and cellular viability. Structurally, the protein is divided into a TIM domain, characteristic Rosmann fold, and a C-terminal  $\beta$ -barrel (**Figure 2a**) (16). In mice, full body knockout (KO) is early embryonic lethal at the preimplantation stage (77). Almost invariably, conditional KO of PRMT5 is deleterious. Many conditional KOs of PRMT5 have revealed the importance of PRMT5 for life (**Table 1**). This house keeping nature holds true in cell culture as PRMT5 inhibition or knockdown is cytotoxic to cells<sup>5</sup>. PRMT5 is normally found throughout the cell and methylates a variety of proteins. A small sampling of these includes the known SDMA marks on canonical histones, Sm proteins, and

---

<sup>4</sup> See also (Bedford, et al.,2009) and (Blanc, et al.,2017)

<sup>5</sup> Prolonged use of PRMT5 inhibitors at moderate concentrations will lead to drug resistance in cell lines. This is an important consideration as will be discussed later.

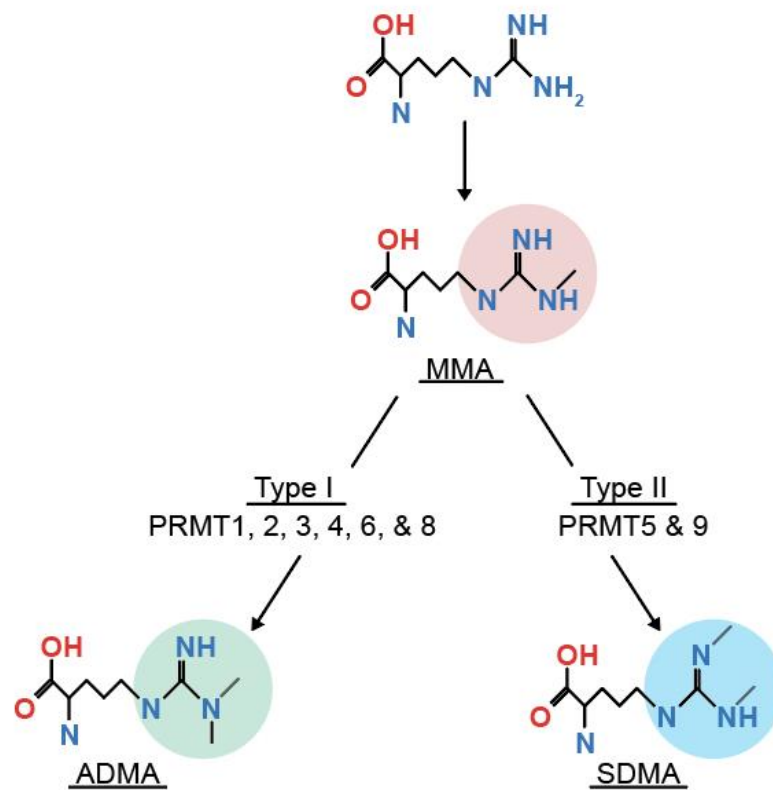


**Figure 1-** Arginine methylation pathway in mammals. Monomethylated arginine (MMA) guanidyl moiety highlighted in “pink”. Asymmetrically dimethylated arginine (ADMA) highlighted in “green” is dimethylation of  $\omega$ -N<sup>G</sup>. Symmetrically dimethylated arginine (SDMA) in “blue” is methylation at  $\omega$ -N<sup>G</sup>,N<sup>G</sup>. All PRMTs facilitate MMA formation.

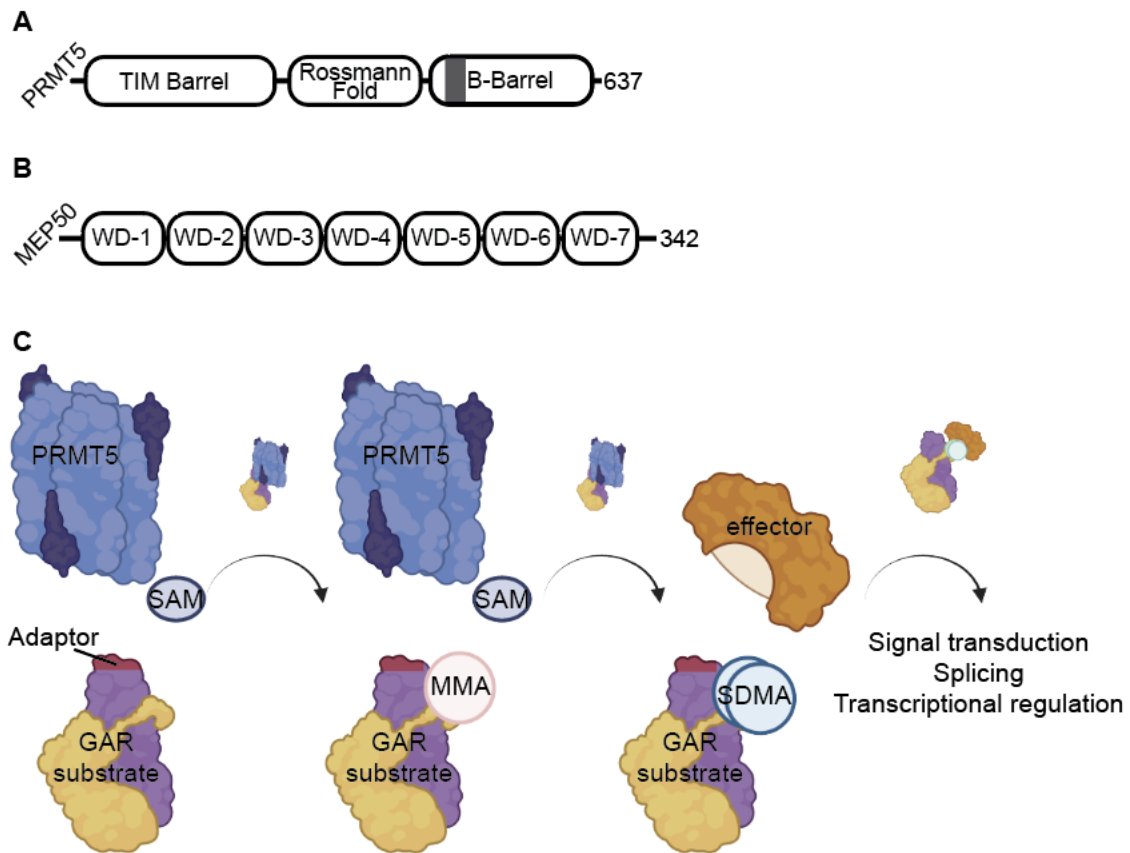


**Figure 2-** PRMT5 and MEP50 structure and enzymatic processing. **a)** PRMT5 graphical structure. The TIM- and  $\beta$ -barrel are needed for oligomerization to MEP50. PRMT5 dimerizes in a head to tail orientation. The canonical Rossman fold is responsible for binding S-adenosyl methionine (SAM), the universal methyl donor. The 60 residue dimerization domain, in “gray”, initiates heterodimerization of the complex (17). Full length protein is needed for enzymatic activity *in vitro*. **b)** MEP50 graphical structure. This protein contains seven tandem WD-domains. These orient into a 7 bladed “propeller” shape. MEP50 binds the TIM containing domain of PRMT5 (17, 19). **c)** Graphical representation of distributive methylation by PRMT5. Which effector binds SDMA modifications will determine what downstream pathways are impacted. Generated with BioRender.



**Table 1-** Published *Prmt5* and *Mep50* conditional knockout mice

Tissue	Conditional allele	Phenotype	Ref
Neuron	Nestin <sup>cre</sup>	- Postnatal lethality (14d) - Neurological disorders; balance, tremors, akinesia (immobility) - Reduced brain size	(5)
Oligodendrocytes <sup>††</sup>	Olig1 <sup>cre</sup>	- Postnatal lethality (14d) - Impaired myelination	(4, 9)
Bone	Prx <sup>cre</sup>	- Long Bone atrophy - Oligodactyly	(11, 12)
Liver	Alb <sup>cre</sup>	- Liver cirrhosis - Nuclear polyploidy	(15)
Blood	Inducible Mx1 <sup>cre</sup>	- Fatal bone marrow aplasia (moribund 16 days post-Cre induction) - Loss of hematopoietic progenitor cells - Splicing defects	(8, 18)
	Vav1 <sup>cre</sup>	- Embryonic lethal (post-day E14.5) - Severe hematopoietic defects and DNA damage accumulation	(19, 20)
T Cell	CD4 <sup>cre</sup>	- Impaired T cell maintenance	(21, 22)
Spermatogenesis	Tnap <sup>cre</sup> , Stra8 <sup>cre</sup>	- Germ cell loss	(27, 28)
Lung	Shh <sup>cre</sup>	- Lethality at birth; respiratory distress cyanosis (suffocation) - Unbranched lung development	(33)
(Primary lung epithelial cells) <sup>*†</sup>	Constitutively active Cre	- Impaired cellular growth and proliferation	(38)
Muscle stem cell <sup>†††</sup>	Pax7 <sup>cre-ER</sup>	- Depletion of muscle stem cells - Lack of muscular regeneration	(39)
Pancreatic beta cells	Pdx1 <sup>cre-ER</sup>	- Impaired glucose tolerance - Reduced insulin expression	(41)
Prostate <sup>*</sup>	PPR2Bi-Cre	- Impaired ductal structure - Altered secretory proteins and androgen receptor expression	(47)

\*MEP50 knockout system- MEP50 conditional knockouts are expected to mimic PRMT5 KO systems.

† *Ex vivo* conditional knockout

†† This experiment provided an *in vivo* phenotype for the observation of myelin basic protein as a robust PRMT5 substrate (55).

††† This report suggests a distinct genetic regulation for developmental vs adult stem cell maintenance as embryonic myogenesis was unaffected in *Prmt5* KO mice.

myelin basic protein<sup>6</sup>. PRMT5 requires a cofactor, the WD repeat protein methylosome protein 50 (MEP50), for protein stability and enzymatic activity (**Figure 2b**) (17, 88, 89). This is perhaps best illustrated by the following observations. First, purification of truncated PRMT5 proved to be inactive. Only co-expression of full length PRMT5 with MEP50 results in an enzymatically active methylosome that can be crystalized (17)<sup>7</sup> (89). Second, knockdown of MEP50 results in decreased PRMT5 protein<sup>8</sup> (88). Together, PRMT5 and MEP50 hetero-octamerize to form a methylosome complex which typically methylates proteins at glycine- and arginine-rich (GAR) motifs or proline-glycine motifs<sup>9</sup> (90). The current model of PRMT5 mediated methylation shows that PRMT5 works in a distributive manner (91) and is recruited to substrates via substrate adapter proteins (92). This is to say that PRMT5 loads S-adenosylmethionine (SAM), the universal methyl donor, into the Rossmann fold followed by modular substrate adapters bringing PRMT5 into proximity of the target GAR motif to catalyze  $\omega$ -N<sup>G</sup>-monomethylation (92). PRMT5 is released from the substrate to reload with SAM and then tries to relocate the substrate to complete the  $\omega$ -N<sup>G</sup>,  $\omega$ -N<sup>G</sup>-SDMA modification (**Figure 2c**). Adapter proteins allow for spatiotemporal control over possible versus actual substrate methylation in addition to control by PTM of PRMT5<sup>10</sup>. Once a substrate is methylated with SDMA, effector binding proteins can bind SDMA and serve as scaffolding for processes like splicing, transcriptional regulation, and signal transduction, each of which is well-recognized as downstream effects of PRMT5 methylation. Thus, methylation is able to impact many cellular processes. Conditional KO of *Prmt5* gives clear

---

<sup>6</sup> In considering known and purported PRMT5 substrates it is important to note that PRMT5 has some affinity for  $\alpha$ -Flag antibodies. Thus, PRMT5 is co-immunoprecipitated in over 90% of Flag-based pull downs. A repository of spurious affinity artifacts is collected in the “CRAPome” (Mellacheruvu, et al.,2013). Herein we note just a few established PRMT5 substrates.

<sup>7</sup> From this report, the authors note that full length PRMT5 expressed in insect cells formed dimers and was biochemically active, but formed aggregates and couldn't be crystalized.

<sup>8</sup> Of note, systemic loss of MEP50 is also embryonic lethal in mice, albeit by day E8.5 rather than before preimplantation like *Prmt5* KO mice.

<sup>9</sup> GAR motifs typically have a 'GRR' or GRG amino acid sequence and are the preferred substrate motif for PRMT5. However, it can also methylate PGM motifs. Most PRMTs prefer either GAR or PGM motifs, like PRMT1 that prefers GAR, while CARM1 prefers PGM.

<sup>10</sup> PRMT5 can be post-translationally modified to regulate its activity. Phosphorylation by mutant Janus kinase decreases activity while other phospho-sites modulate interaction with substrates. Methylation by CARM1 at R505 increases activity. PRMT5 PTMs were recently reviewed here (Hartley, et al.,2020).

evidence of the importance of *Prmt5*, though it is not known if overexpression (OE) of *Prmt5* has a phenotype- or if *Prmt5* OE will drive hypermethylation of substrates.

Loss of *Prmt5* using a conditional KO approach have conclusively shown *Prmt5* is essential for development and for maintaining homeostasis. On the other hand, PRMT5 has been implicated in nearly as many types of cancer which will be described further in section 1.2. PRMT5 and SDMA will be the topic of chapter 4. Chapter 3, however, will deal primarily with a specific effector that binds, or colloquially “reads”, SDMA.

### 1.1.3 Methyl binding effector proteins- “readers”

Methylation is recognized by many protein domains across dozens of effector proteins. Tudor domains, which are characterized by a 4-5  $\beta$ -stranded aromatic cage that docks on methylated substrates, can recognize lysine-methylation and is the only domain to date which recognizes methyl-arginine residues (94, 95). The Tudor protein domain was first identified from a protein with the same name containing 11 Tudor repeats in *Drosophila melanogaster*. Tudor domains often occur in a tandem array but can occur singly. Individual Tudor domains exhibit amino acid specificity<sup>11</sup>, though some proteins with multiple Tudors can read both methyl-lysine and methyl-arginine marks by individual Tudors, as in the case with Spindlin1<sup>12</sup> (**Table 2**) (30, 31, 96, 97). In addition to amino acid specificity, Tudor domains have methyl-species (that is mono-, di-, di-asymmetric, di-symmetric, or tri-methylation) specific recognition. To date, relatively few methyl-arginine readers have been identified<sup>13</sup>.

---

<sup>11</sup> Methyl-lysine vs. methyl-arginine specificity is thought to be facilitated by an additional  $\alpha$ -helix and two additional  $\beta$ -strands called an “extended Tudor” (Liu, et al.,2010).

<sup>12</sup> Spindlin1 is a histone reader with 3 tandem Tudor domains. The first and second Tudors exhibit crosstalk by reading a combination H3K9me3 with H3R8me2a mark. This combination reading is a recent discovery and illustrates the possible combinatorial power of “the histone code”.

<sup>13</sup> There is, currently, a paradox in that Type II PRMTs, which have few writers, have several effectors that bind SDMA, while Type I PRMTs which are more numerous have fewer known effectors for ADMA (Wright, et al.,2021). Whether this discrepancy is biologically driven or is an artifact of technological limitations remains to be determined. As PRMT5 is the major depositor of SDMA in the cell, more SDMA binding effectors points to the importance of the associated methyltransferases.

**Table 2-** A sampling of Tudor domain proteins and their methyl-species binding.

Methyl Lysine			Methyl Arginine		
Protein	Methyl species	Ref	Protein	Methyl species	Ref
53BP1	Kme2; H4K20me2	(1)	SMN	SDMA	(13)
JMJD2a	H3K4me3 H4K20me3	(1)	SND1 <sup>†</sup>	SDMA	(1, 16)
Spindlin1- 3 <sup>rd</sup> Tudor	Unknown		TDRD 1,2,6,8 (Germ cell)	SDMA	(16)
Spindlin1- 2 <sup>nd</sup> Tudor	H3K4me3 H3K9me3	(30, 31)	SPF30	SDMA	(13)
PHF20	H3K4me2	(37)	TDRD3	ADMA	(53)
SGF29	H3K4me3	(59)	TDRD17 (mitochondria)	ADMA	(63)
UHRF1	H3K9me3, H3K4me0/1	(70)	Spindlin1- 1st Tudor	ADMA	(31, 71)
SHH1	H3K9me3	(72)			
PHF1	H3K36me3	(76)			

<sup>†</sup>Also known as TSN, p100, and TDRD11

Staphylococcal nuclease Tudor domain containing 1 (SND1) is a unique protein that has both protein- and nucleic acid-binding properties<sup>14</sup>. SND1 functions primarily as a RNA processing protein. Structurally, it contains four tandem SN-like domains (SN-domains) followed by a fifth SN-domain that is split by a Tudor domain (**Figure 3**). SND1 is expressed in most cell types but is enriched for in exosome and lipid secreting cells like liver, pancreas, and mammary tissues (16, 99). Within the cell, SND1 can shuttle freely between the nucleus and cytoplasm, but will form foci within stress granules in response to cellular stress (66, 67, 100-102) . SN-domains have been identified as important for several biological processes including this stress granule formation, transcriptional coactivation (58, 75, 103), exosome processing (104), and binding RISC factors for RNA degradation (105-107) (**Figure 3**). The C-terminal Tudor domain, on the other hand, binds various splicing factors (68, 71, 73) and PIWI1/Miwi proteins to facilitate noncoding RNA biogenesis (1). Protein-protein interaction mapping reveals that SND1 generally interacts with either the Tudor or SN-domains. SND1 Tudor domain has preferential binding to SDMA<sup>15</sup> (108). Indeed, we and others have identified that SND1 is able to bind SDMA modified E2F peptides (58, 109, 110). Recently mass spectrometry results from an SND1-BioID2 avidin purification returned many novel potential SND1-binding proteins (101). This suggests that there may yet be more unidentified proteins that SND1 can bind through its Tudor domain. Because SND1 preferentially recognizes SDMA, and because PRMT5 deposits nearly all SDMA in the cell, PRMT5 and SND1 form a writer/reader pair.

As mentioned above, SND1 is ubiquitously expressed (111), but is enriched for in exosome secreting cells such as the liver and pancreas (16, 112). Unlike KO of the writer PRMT5, SND1 loss does not exhibit embryonic lethality. This has been known for a time, but the SND1 KO

---

<sup>14</sup> Also known as TSN, p100, and TDRD11.

<sup>15</sup> Friberg et al were the first to identify that the SND1 Tudor domain preferentially binds SDMA over ADMA modified ligands. Additionally, they did not observe methyl-lysine binding for unmodified, mono-, di-, or trimethylated states.

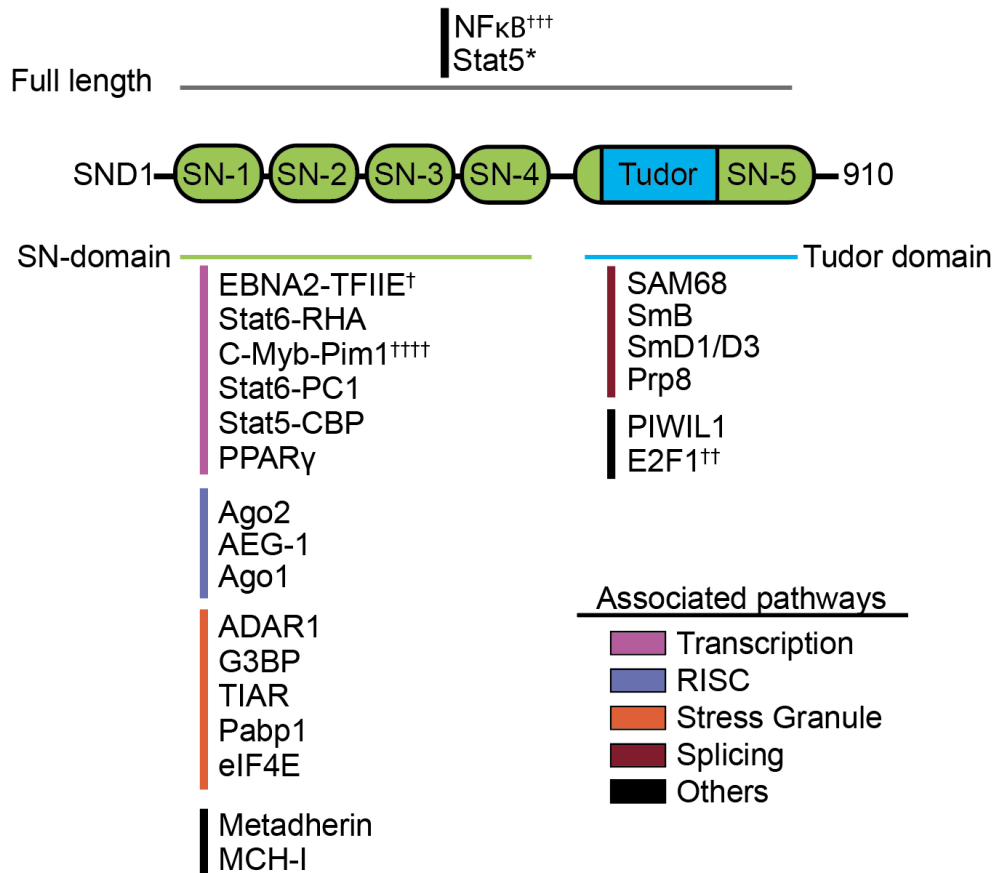


**Figure 3-** SND1 graphical structure and protein-protein interaction mapping to Tudor and SN-domains. Adapted from Gutierrez-Beltran (2016). STAT6-CBP (14); PPAR $\gamma$  (29); STAT6-RHA (36); STAT6-PC1 (52); STAT5 (57); E2F1 (50, 58); EBNA2 (60); Metadherin (61); NF- $\kappa$ B (62); AEG-1 (64); Ago1, Ago2, TIAR, Pabp1, eIF4E (65); G3BP (66); ADAR1 (67); Prp8 (68); SmB, SmD1/D3 (17, 69) (71); SAM68 (73); PIWI (1); MHC-I (74).

<sup>†</sup> SND1 binds EBNA2 via TFIIIE. Primary sequence of the interfacing acidic domain of EBNA2 and TFIIIE $\alpha$  or - $\beta$  reveal no obvious GAR motif to serve as a substrate for PRMT5 methylation and subsequent SND1 Tudor binding. Thus, transcriptional coactivation may be achieved via nuclease domain interaction. This has yet to be determined empirically either way, however.

<sup>††</sup> This interaction has only been shown using peptides.

<sup>†††</sup> It is unknown what domains of SND1 interact with NF $\kappa$ B.

<sup>††††</sup> C-Myb-Pim1 activity is strengthened by full length SND1 and is decreased in  $\Delta$ C terminal mutants (75).

<sup>\*</sup>Both the Tudor domain and the SN-domains can pull down STAT5. It is biologically unknown why this particular target interacts with both types of domains.

phenotype was only recently published<sup>16</sup> (101, 113). However, the pathology and phenotype of an SND1 Tudor domain mutant mouse has not been described. We highlight the phenotype of a *Snd1 KO* genetically engineered mouse model (GEMM) and present a SND1 Tudor domain dead (KI) mutant mouse in chapter 3.

## 1.2 Arginine methylation in cancer

There is a growing appreciation of the role of arginine methylation in cancer at large. H4R3me2a and H3R8me2a, deposited by PRMT1 and PRMT2 respectively, are key marks of proliferation, migration, stemness, and differentiation– all of which are important cancer related processes<sup>17,18</sup>. Also linked to transcriptional control, tumor suppressors and CDK inhibitors can be silenced transcriptionally by H4R3me2s which is deposited by PRMT5. Recently, it was shown that NFIB methylation by CARM1 is needed for small cell lung cancer development which mediates an opening of chromatin states (115) . CARM1 also promotes error-prone non-homologous end joining DNA damage repair by repressing R-loop formation in ovarian cancers (116).

In the last decade, there has been a substantial increase in the number of publications and interest in targeting PRMTs (117). The availability and potency of small molecule inhibitors (SMI) have allowed many groups to study PRMTs in cancer. Many cancers are very sensitive to PRMT inhibitors, which have revealed the roles of PRMTs in splicing, DNA damage response, tumor immunity (118), and cellular signaling in cancer.

Both PRMT5 and SND1 have been implicated in a variety of cancers, especially liver cancer. Here, we briefly explore the role of each the writer and reader in cancer broadly speaking then look more closely at liver cancer in section 1.3.

---

<sup>16</sup> SND1 KO mice have been available for several years (Fu, et al.,2018); (Su, et al.,2015); (Wang, et al.,2021).

<sup>17</sup> H3R8me2a has primarily been shown at the enhancers and promoters of growth and survival related genes (Dong, et al.,2018).

<sup>18</sup> See also (Blanc, et al.,2017).

### 1.2.1 PRMT5 in cancer

The role of PRMT5 in cancer is a substantial study by itself (**Table 3**). Yet, there are some common themes in PRMT5 research which hint at its overall role in neoplasms. As a sampling, PRMT5 has been shown to be overexpressed in glioblastoma, melanoma, breast, liver, prostate, pancreatic, bladder, ovarian, lymphoma, lung, and colorectal cancers (references in **Table 3**). Across the spectrum, PRMT5 improves the viability and proliferation of cell types, though through tissue specific molecular targets. Also interconnecting these findings is that targeting PRMT5 impairs cellular viability and has potential to serve as an anticancer therapy.

Cancer cells are very sensitive to loss of PRMT5<sup>19</sup>. To date, there are no known functional homologs of PRMT5<sup>20</sup>, and the PRMT5-MEP50 complex has several targetable folds<sup>21</sup>. Each of these facts has contributed to this protein being an active area of research in pharmacology. There are at least 14 unique compounds which selectively target PRMT5, many of which have made it to clinical trials and beyond (119). The targetable folds and the many SMI alludes to the several mechanisms of action (MOA) of these compounds including three combinations of SAM and substrate cooperative/competitive molecules, a PROTAC degrader, and covalent binding that blocks binding of SAM and peptide substrates (120) (121) (also see appendix A). The most recent MOA to be published is based on the sensitivity of PRMT5 to a natural feedback inhibitor, 5'-methylthioadenosine (MTA). MTA is a natural metabolite of the methionine cycle and byproduct of methylation that inhibits PRMT5 as a negative feedback modulator. Normally, methylthioadenosine phosphorylase (MTAP) processes MTA through its next step in the cycle, but in MTAP deleted cells, MTA accumulates as it cannot be processed by normal means thereby naturally inhibiting PRMT5. This new compound is a MTA-cooperative inhibitor that exhibits

---

<sup>19</sup> Virtually every reference from **Table 3** includes experiments which utilize siRNA to knockdown PRMT5 or SMI to decrease PRMT5 activity. Invariably,  $\alpha$ -PRMT5 treated cells show decreased proliferation and viability.

<sup>20</sup> There have been no functional homologs of PRMT5 identified to date. This may partially explain why cells are so sensitive to  $\alpha$ -PRMT5 treatments. PRMT5 facilitates virtually all SDMA in the cell and so cells enter crisis upon loss of the primary Type II PRMT.

<sup>21</sup> Truncated PRMT5 is inactive (Antonyamy, et al.,2012). Thus, pharmacologically targeting even a portion of the protein can be an effective means of disrupting normal PRMT5 function.



**Table 3-** Published roles of PRMT5 in cancer

Cancer Type	PRMT5 related effect	Ref
Glioblastoma	Proliferation, migration, differentiation	(2-4)
Melanoma	Proliferation, increase in p27, alternative MDM4 splicing	(6-8)
Breast	Proliferation, inhibit apoptosis, FOXP1 recruitment for transcription	(10) (19)
Hepatocellular carcinoma	Proliferation via ERK signaling, HNF $\alpha$ repression promoting EMT, <i>de novo</i> lipogenesis	(23-26)
Prostate	Transcriptional cofactor for Sp1 and Brg1 promoting cancer androgen receptor expression.	(32)
Pancreatic	Proliferation, silencing of FBW7 to promote the Warburg effect	(34, 35)
Bladder	Increases proliferation and colony forming capacity, apoptosis suppression	(40)
Ovarian	Proliferation and correlation with tumor burden and worse prognosis	(42)
Lymphoma	Proliferation, increase in cyclin D1, c-myc, and survivin protein <sup>†</sup>	(43-46)
Lung	Enhanced cell growth via decrease in GLIPR1, Leprel1 and BTG2 (tumor suppressors), and increase in FGFR and HER (growth factors) proteins.	(48, 49)
Colorectal	Invasion, differentiation	(50, 51)
Leukemia (MLL <sup>††</sup> )	Proliferation, self-renewal and differentiation block	(54)
Multiple myeloma	Interaction promoting NF $\kappa$ B induced cellular growth	(56)

<sup>†</sup> This occurs via H3R8me2s repressive marks at promoters for regulators of WNT/ $\beta$ -catenin signaling.

<sup>††</sup> Mixed lineage leukemia. Interestingly, leukemia's have more sensitivity to PRMT5 inhibition than lymphatic cancers.

synthetic lethality in *Mtap* deleted cells (122). The potential of this drug is to specifically target MTAP delete cells while being ineffective in healthy cells<sup>22</sup>. The effectiveness of all of these compounds in cells and mice has encouraged research into their potential use as anti-cancer therapies.

While knockdown and inhibition of PRMT5 informs our understanding of PRMT5 in normal biology, it is also important to understand how the amount of PRMT5 makes a difference in normal and diseased states. PRMT5 is overexpressed in many cancer types and is thought to cause hypermethylation of methyl substrates, which will lead to transcriptional activation and promote cellular growth. As PRMT5 is involved in splicing, this regulation of oncolytic activity or oncosuppression by treatment with SMI could also occur at the splicing level. However, it has not been determined if PRMT5 OE alone is sufficient to induce tumorigenesis.

### 1.2.2 SND1 in cancer

*Snd1* has been implicated primarily in breast (124, 125), glioma (126), colon (127), lung, and liver cancer (112, 128-130) specifically with upregulation of the protein. To date, SND1 is thought to be oncogenic by increasing stabilizing factors, like Metadherin<sup>23</sup>, and by degrading tumor suppressor RNA directly or indirectly. SND1 pulls down principally with RNA binding proteins, suggesting it may also impact oncogenic RNAs. In recent review, a positive feedback loop was described for TGF $\beta$ -SND1 expression which may also serve in promoting cancer signaling (131). While involved in many tissues, SND1 is abundant in the liver making this role of SND1 in liver cancer of special interest.

---

<sup>22</sup> *Mtap* deletion is present in 15% of solid tumors (Kalev, et al.,2021).

<sup>23</sup> Metadherin is involved with RISC and plays an important role in miRNA processing. It is frequently upregulated in cancer (Blanco, et al., 2011).

### 1.3 The SND1/PRMT5 axis in hepatocellular carcinoma

Liver cancer is a major health concern worldwide. Hepatocellular carcinoma (HCC) is the most common form of liver cancer and has a high mortality (132). *Prmt5* has been implicated in HCC, but the data has been circumstantial. On the other hand, *Snd1* has been robustly reported as overexpressed in clinical HCC samples implicating it as a potentially important axis of study. Additionally, *Snd1* has been shown to drive HCC formation by multiple groups using GEMMs. These include two independent mutagenic Sleeping Beauty (SB) transposon screens and a tissue-specific conditionally active *Snd1 OE* mouse model. This section will first briefly introduce HCC, followed by describing the relevant SND1 information, and concluding with presenting evidence of PRMT5 in HCC.

#### 1.3.1 Introduction to HCC

Liver cancer is the third leading cause of cancer mortality to a third of the world's population, and is fourth overall (132). HCC is the most common form of primary liver cancer, reportedly contributing 75-90% of hepatic cancers (133, 134). Risk factors are well documented including alcohol abuse, chronic inflammation, obesity, aflatoxin or carcinogen exposure, type two diabetes, and the most prominent factor, hepatitis infection. These etiologies and tumor biology confound treatment options as most liver tumors are immunologically cold, chemoresistance is common, and many tumors are deemed inoperable due to patient health and late-stage diagnosis<sup>24</sup> (136, 137). One of the challenges in treating HCC has been a limited understanding of the molecular drivers of the disease. Further study of genetic and epigenetic drivers of HCC to identify novel and potentially actionable pathways remains an important need at large.

---

<sup>24</sup> A general review of these current standard therapies was recently published (Llovet, et al.,2021).

### 1.3.2 SND1 OE in clinical samples

There are at least two studies that show the OE of *Snd1* in a clinical setting. The first uses tissue microarray wherein there is an upregulation of SND1 in 74% of tissues compared to normal tissues (64). Also, a pan-cancer analysis from TCGA data also indicated *Snd1* upregulation in many cancer types (112). Further, *Snd1* expression was correlated with a worse overall survival and disease-free survival in both glioblastomas and HCC. Various mutations of *Snd1* improved patient outcomes of overall survival, disease-specific survival, disease-free survival, and progression-free survival (112). Together, these are hallmarks of oncogenic drivers and implicate SND1 as involved in HCC.

### 1.3.3 *Snd1* drives HCC in SB screen

SB mutagenesis is a powerful tool that has been used to screen for potential oncogenes for nearly two decades (138). The SB transposon has undergone substantial genetic engineering to create increasingly potent and focused tool enzymes (139). Simply, SB mutagenesis uses a two-part insertion program to randomly incorporate a transposon vector into the host genome. The transposon vector contains promoter sequence and inverted stop codons. Splice donor and splice acceptor regions within the transposon allow the vector to insert a viral promoter or stop codon throughout the genome including into genes. A promoter incorporated vector will allow for amplification of oncogenes, while stop codons inserted into tumor suppressors will effectively silence their expression by the bi-directional stop-codon. Next-gen sequencing of tumor tissues then allows for identifying insertion sites and identification of potential driver genes<sup>25</sup>. The improved transposase iteration, SB11, was used for the studies that identified *Snd1* as a potential driver in both SB screens using a chronic hepatitis and *Pten* null mouse respectively<sup>26</sup>. In both

---

<sup>25</sup> These are an in-depth review of this system (Copeland, et al.; (Moriarity, et al., 2015).

<sup>26</sup> B6.129 (Bard-Chapeau, et al.,2014) and B6.C (Kodama, et al.,2018) backgrounds.

models, insertion of the transposon upstream of *Snd1*, thereby amplifying the gene, was a potent driver of HCC (128, 130).

#### 1.3.4 SND1 drives HCC in OE GEMM

Independently, a second group identified *Snd1* as a *bona fide* driver of HCC. An exogenous copy of Myc-tagged human *Snd1* was cloned behind the albumin promoter to create a liver-specific *Snd1* OE mouse<sup>27</sup>. This mouse developed histologically verifiable HCC spontaneously. When these mice were exposed to carcinogen, they had an exacerbated tumorigenic response with more aggressive tumor growth<sup>28</sup> (129).

Within this same study, authors used a general nuclease inhibitor, pdTp<sup>29</sup>, to target SND1 in tumor-initiating cells and HCC xenografts to show proof of concept that SND1 inhibition may impair tumorigenesis. These results support the need to better understand SND1 biology and if targeting SND1 may have therapeutic action against this axis. However, none of these approaches break down the functional domains of SND1 to determine if the Tudor domain is needed for these processes.

#### 1.3.5 Evidence for *Prmt5* in promoting HCC

PRMT5 has become an increasingly prominent topic in the HCC literature in recent years. However, the data remains circumstantial, and it is unknown if PRMT5 itself can drive liver cancer or if these correlations are byproducts of cancer cells evolving to meet biochemical demands. The reported literature thus far implicates PRMT5 in this disease by correlating protein level with disease, impacting an epithelial to mesenchymal transition (EMT), and promoting hepatocyte function. Each of these topics and examples are described in further detail in appendix A.

---

<sup>27</sup> B6CBAF1 genetic background.

<sup>28</sup> Expression of myc-SND1 quantitatively increased SND1 levels by approximately three-fold. Of interest, the mutagenic SB screen identified that insertion of an oncogenic transposon upstream of *Snd1* increased its expression by approximately two-fold (Bard-Chapeau). Thus, each of these reports support that a comparative moderate increase of SND1 is oncogenic.

<sup>29</sup> 3',5'-deoxythymidine bisphosphate.

#### 1.3.5.1 Correlation of PRMT5 levels and disease

PRMT5 has been shown to be overexpressed in HCC and correlates with a worse prognosis (23, 26, 142-144). High levels of PRMT5, shown with mRNA (142) or protein (26, 143), decreased survival and increased recurrence (26, 144). Interestingly, mRNA level does not always match protein level and *Prmt5* mRNA is highly varied in different HCC cell lines and in resected liver tissue (142). One explanation for high protein level is the observation that PRMT5 interacts with the long intergenic non-coding RNA 1q21.2<sup>30</sup>. This interaction allows PRMT5 to escape proteasomal degradation. Accumulation of this non-coding RNA correlated with tumor size, alpha-fetoprotein (AFP)<sup>31</sup>, and hepatitis B surface antigen levels (145). The stabilization of PRMT5 protein could explain the phenomenon of increased protein levels while some mRNA databases don't identify increased *Prmt5* levels in HCC.

#### 1.3.5.2 PRMT5 facilitates EMT related pathways

EMT is part of the classic hallmark of cancer, invasion and metastasis, from the year 2000. This descriptive characteristic can be influenced by many different pathways<sup>32</sup>. E-cadherin depletion is one such pathway that may be impacted by PRMT5. The PRMT5-MEP50 complex binds to AJUBA, a key scaffolding protein for SNAIL. Recruitment of these factors to the *E-cadherin* enhancer can repress its expression, with protein turnover depleting E-cadherin levels (146). Invasiveness, a next step of transition, is also impacted by PRMT5 controlling protein levels of matrix metalloproteinase 2 (23, 25)<sup>33</sup>. Expression of the liver-specific transcription factor hepatocyte nuclear factor 4 $\alpha$  (HNF4 $\alpha$ ) is a cellular defense against dedifferentiation in

---

<sup>30</sup> Also called LINC01138

<sup>31</sup> AFP is a common blood contaminant in patients with HCC.

<sup>32</sup> "Hallmarks" of cancer are primarily descriptive of cellular states rather than mechanistic explanation of cellular function. Thus, a hallmark like "evasion of apoptosis" or "invasion and metastasis" could impact hundreds of possible targets to achieve this behavior. Hence, EMT is less of a defined biochemical/molecular state, and is more a way to describe the overall cellular behavior.

<sup>33</sup> This relationship of PRMT5 to matrix metalloproteinase 2 was shown in a PRMT5 knockdown and PRMT5 competent lines respectively. It was not shown if this was transcriptionally regulated, splicing impacted, or protein stability influenced.

hepatocarcinogenesis. H4R3me2s marks from PRMT5 at the *Hnf4a* promoter repress its transcription, thereby promoting cancer stemness and implicating PRMT5 as oncogenic (25).

#### 1.3.5.3 Increased hepatocyte function by Prmt5 transcriptional control

Steatosis<sup>34</sup> is preliminary to developing HCC. Thus, hepatocytes with overactive *de novo* lipid production is often concurrent with hepatic damage and increased risk of developing liver disease and cancer (147). Sterol regulatory element-binding protein 1 (SREBP1) is a central transcription factor that controls genes involved in synthesizing various lipids. PRMT5 methylates SREBP1 stabilizing the transcription factor and promoting gene expression. Overexpressing *Prmt5* in HepG2 cells increases intercellular triglycerides, which is reversible with its knockdown<sup>35</sup> (24). Taken together, PRMT5 promotes *de novo* lipogenesis, a key pathway that increases risk of developing HCC<sup>36</sup>.

It remains an important question to answer if PRMT5 activity is directly oncogenic in a hepatic setting. The findings to date have looked at PRMT5 in pre-diseased states. Thus, the findings that show PRMT5 promoting tumorigenesis could arise from other factors driving disease and transformation. Additionally, dependencies on PRMT5 could be the byproduct of overall cellular toxicity to inhibiting PRMT5 rather than specifically targeting oncogenic effects themselves. Thus, the direct role of PRMT5 in promoting HCC remains to be determined.

---

<sup>34</sup> Fatty liver disease. The major risk factors of this fatty buildup in the liver is obesity and diabetes. This pathology is precursor to developing nonalcoholic fatty liver disease (NAFLD) and nonalcoholic steatohepatitis (NASH).

<sup>35</sup> Additionally, deletion of SREBP1 GAR motif (GAGRG- amino acids 365-369) impedes triglyceride accumulation in HepG2 cells.

<sup>36</sup> There is evidence that PRMT5 methylates E2F1 to influence cellular fates and cellular signaling (Cho, et al.,2012); (Zheng, et al.,2013); (Roworth, et al.,2019); (Su, et al.,2015); (Barczak, et al.; (Pastore, et al.,2020). This may have substantial roles in HCC, especially given an expanding understanding of E2F1 in HCC (Farra, et al.,2017). Thus, PRMT5 could be important for driving HCC by altering cellular signaling.

## 1.4 Summary and scope

In cells, arginine methylation is an essential PTM for normal development and homeostasis. PRMT5 is the primary enzyme that catalyzes SDMA and requires MEP50 for protein stability and enzymatic activity. Conditional KO of *Prmt5* is deleterious or even lethal in most tissues which has broadened our understanding of the role and function of PRMT5 in development and disease. However, it is not known if there is a phenotype for overexpressing PRMT5 in specific tissues. PRMT5 related proteins and pathways are important in the liver, giving us an interest in studying PRMT5 OE in the liver.

Effectors bind PTM's to facilitate downstream signaling and activity. SND1 is a SDMA specific binder via its single C-terminal Tudor domain. Protein-protein interaction mapping identifies most proteins interact with either the SN- or Tudor domain of the protein. There may be additional targets of the Tudor domain which are yet to be identified. The phenotype for a *Snd1* full body KO mouse was recently published. However, it is unknown what phenotypic changes are dependent on the Tudor domain of SND1.

Both PRMT5 and SND1 have been implicated in cancer at large and in HCC. SND1 is reported as increased in patient samples of HCC and has been confirmed as a driver of HCC using GEMMs. However, it remains unknown if SND1 loss can protect against HCC development. Further, it is unknown if the Tudor domain plays a part in this process. **We hypothesize that the SND1 Tudor domain is critical for the oncogenic functions of SND1.** Upstream of the SND1 Tudor domain, PRMT5, the writer of SDMA, has been reported to have a role in HCC by predisposing hepatocytes to develop HCC by impacting cancer transformation pathways. However, it remains to be determined if *Prmt5 OE* alone is sufficient to drive HCC formation. **We hypothesize that liver-specific *Prmt5 OE* will be oncogenic.**

This work utilizes three GEMMs to test these hypotheses, namely an *Snd1 KO*, *Snd1 KI*, and *Prmt5 OE* mouse, none of which have previously been published. For clarity and convenience in reading, the work is divided into two parts. First are the new findings of the reader



function of SND1. The second part contains the work done on the writer, PRMT5. Follows is a summary of conclusions written in the same order and giving an analysis of the results and the value of this work.

## **2 Chapter 2- Materials and methods**

### **2.1 Mouse experiments**

All mice used for experiments were age and sex matched as indicated. Every mouse experimental protocol was reviewed and approved by the Institutional Animal Care and Use Committee at MD Anderson Cancer Center (ACUF# 00001090-RN03).

### **2.2 Generation of mouse models**

#### **2.2.1 *Snd1* KO and KI GEMMs**

Both *Snd1* KO and KI mice were generated using CRISPR/Cas9 gene-editing technology. sgRNA, donor DNA, and Cas9 protein were from Horizon Discovery. *Snd1* KI mice were generated using sgRNA targeting tyrosine 766 of *Snd1*, donor DNA encoding the tyrosine to leucine substitution (Y-to-L mutation) were designed by Horizon Discovery. An *AvrII* restriction site was also introduced into the donor DNA for easy genotyping. To generate the *Snd1* KO and KI mice, the sgRNA, Cas9 protein, and donor DNA (for *Snd1* KI mice generation) were micro-injected into 1-cell FVB embryos. The injected embryos were transferred into pseudo-pregnant recipient female mice. Genomic DNA from the resultant pups was isolated and used for PCR genotyping. PCR products were purified and sequenced to identify heterozygous mice as founders. The founders were backcrossed with FVB strain background mice for four generations to separate any potential off-target event. The sequences of sgRNAs and donor DNA are as follows:

*Snd1*-KO sgRNA: tccttcgcaagaagctgattGGG; *Snd1*-KI sgRNA: catgtctctacatcgactaCGG

*Snd1-Kl* donor DNA: CATTGCAGGTACCGCGCCCGGGTAGAAAAGGTGGAGTCCCCTGCCA  
AAGTGCATGTCTTCTACATCGACCTAGGCAACGTGAGTGCTGGGACCAGGGTGGAAAACA  
GGCAAGGCAGGGACCATTGGGCACAG

### 2.2.2 PRMT5 OE GEMM

B6/C3H<sup>PRMT5</sup> mice were generated using homologous recombination of donor plasmid into the mouse genome by the Vokes Lab at The University of Texas, Austin. A V5-tagged full length murine *Prmt5* adjacent to an IRES and full length murine MEP50 (with a C-terminal BGH polyadenylation signal) sequence was cloned into the pROSA26PA targeting plasmid. This pROSA26PAS-V5-*Prmt5-Mep50* vector was then transfected into embryonic stem cells and subjected to antibiotic selection. Resistant cells were genotyped to identify those that had undergone homologous recombination. Genotyping primers amplified the entire V5-tag, beginning at the second loxP site and ending within the V5-*Prmt5* transgene. Samples without the transgene have no amplicon from this primer set. These cells were microinjected into a blastocyst and transferred into female mice. The resulting chimeric pups were bred to create heterozygous founders. Genomic DNA from the resultant pups was isolated and used for PCR genotyping founders. Founders were backcrossed with B6/C3H mixed background mice for four generations to separate any potential off-target event. The V5-*Prmt5-Mep50* sequence combined with the Rosa26 targeting sequence is included in appendix B.

Swiss-Webster Albumin-Cre mice were a gift from the David Johnson Lab, which were originally in an FVB background purchased from JAX laboratory (see appendix D). Swiss-Webster Albumin-Cre mice were backcrossed into B6/C3H background for 4 generations to generate a B6/C3H<sup>Alb-Cre</sup> mouse. PRMT5 OE mice were generated by crossing B6/C3H<sup>PRMT5</sup> and B6/C3H<sup>Alb-cre</sup> mice. Genomic DNA from pups was used to identify bi-transgenic, or bi-genic, mice.

## **2.3 MEF isolation and immortalization**

We set up a timed pregnancy, and harvested embryos at 12.5-14.5 days post-crossing. Mothers were sacrificed for 5min using CO<sub>2</sub> and let sit for 3 min in cage to allow additional coagulation. Embryos were removed and placed in 1x PBS. We separated embryo's and gently removed them from their sack. Embryos were decapitated and eviscerated, and the remaining tissue was minced and kept in trypsin (Sigma, cat# T2601) for >30min at 37°C. Trypsin was quenched, and samples homogenized by pipetting in a large volume of FBS containing culture media. The solution was then filtered using a 70um filter (Falcon, cat# 352350). Cells (in the flow through) were plated in 15cm plates and maintained in a designated and separate tissue culture setting. MEFs were genotyped by genomic tissue extraction from yoke sacks using Qiagen DNEasy blood and tissue kit (cat# 69506) according to the manufactures instructions and genotyped as described below.

## **2.4 Genotyping**

### **2.4.1 DNA extraction**

Routine genotyping DNA template was obtained by clipping ~2mm of each mouse tail from 4–7-day old pups and performing a NaOH based DNA extraction. Expanded, tail clips were boiled in 300uL 50mM NaOH for 30 min at 95°C followed by adding 25uL 10mM pH 6.8 TrisHCl and centrifuging at 15,000xg for 10 min. DNA was stored at 4°C following centrifugation. Genomic DNA for sanger sequencing of MEF genotyping was obtained from tissues collected during MEF generation using Qiagen DEasy blood and tissue kit according to the manufacture's recommendation.

#### 2.4.2 Genotyping *Snd1* KO mice

*Snd1* KO mice were genotyped as previously described (151). In brief, genomic DNA extracted from pup tail clips and used as a template for amplification of the target gene region by PCR, to yield a 456bp PCR product. All genotyping PCR reactions utilized GoTaqGreen PCR Master mix (Promega, cat# M7123). The PCR product was split into two aliquots, and a *Snd1* wild-type (*WT*) control PCR product was added to one of the two aliquots. The PCR products were denatured and annealed before digestion with T7E1 endonuclease. The digested materials were then separated by electrophoresis through a 2% agarose gel. In the absence of an added *Snd1* *WT* control PCR product, only the heterozygous PCR samples were efficiently cleaved by T7E1, resulting in smaller cleaved products (228 bp/227 bp); in the presence of the added *Snd1* *WT* control PCR products, the *Snd1* KO samples are separated from the *Snd1* *WT* samples, as the added *Snd1* *WT* control PCR products resulted in the formation of heteroduplexes with the *Snd1* KO samples that are sensitive to cleavage by T7E1.

*Snd1*-KO genotyping forward primer: TTTAGGAGGCCCTGAGTGTG

*Snd1*-KO genotyping reverse primer: CAGGGCTGCTAGAGGTATGC

#### 2.4.3 Genotyping *Snd1* KI mice

*Snd1* KI mice were genotyped using genomic DNA extracted from either tail clips from pups or extracted tissues and subjected to amplification by PCR using the primers described below for 28 cycles. Amplicons were digested overnight with *AvrII* (New England Biolabs) using their recommended protocol and were visualized following electrophoresis through a 2% agarose gel. Digested PCR products from homozygous *KI* mice resulted in two bands (261bp/145bp), whereas products from heterozygous *KI* mice displayed 3 bands (406bp/261bp/145bp), representing *WT* and *KI* alleles.

*Snd1*-KI genotyping forward primer: TATTAATCTGCTGCCCCGTGCT

*Snd1*-KI genotyping reverse primer: GAAGAGTGGCGGTGACCAATA

#### 2.4.4 Genotyping PRMT5 transgenic mice

Genotype of the B6/CH3<sup>PRMT5</sup> mice was determined using PCR amplification of genomic DNA for the V5-tag. Using the primers below, genomic DNA was PCR amplified for 34 cycles and visualized using electrophoresis through a 2% agarose gel with gel red (Millipore, SCT123). A 189bp amplicon indicated the presence of at least one copy of the *V5-Prmt5* transgene.

*V5-Prmt5* genotyping forward primer: CCCAGTGTGTCAGCTATTTC

*V5-Prmt5* genotyping reverse primer: GAAGTTATTTTGTGCGACGCT

We likewise genotyped for Albumin-Cre in the respective mice using a four-primer PCR approach with to amplify the Albumin-Cre transgene and an internal PCR control. B6/CH3<sup>Alb</sup> positive samples resulted in a 500bp Albumin-Cre and 324bp control amplicons while samples lacking Albumin-Cre only showed a 324bp control amplicon.

*Albumin-Cre* forward primers: CCAGGCTAAGTGCCTTCTCTACA

*Albumin-Cre* reverse primers: AATGCTTCTGTCCGTTTGCCGGT

Internal PCR control forward primer: CTAGGCCACAGAATTGAAAGATCT

Internal PCR control reverse primer: GTAGGTGGAAATTCTAGCATCATCC

#### 2.5 Sequencing

Genomic DNA was purified from MEF tissues using a DNeasy kit as described above. Purified DNA was PCR amplified using High-fidelity Taq-polymerase (New England Biolabs, 0491L) and run on a 2% agarose gel to confirm the appropriate size of amplicon and lack of off-target amplification in WT samples. Samples were then purified using a Qiagen QIAquick PCR purification kit (cat# 28104) according to the manufacture's recommendations. Amplicons were then sequenced through the MD Anderson Sanger sequencing services.

*Snd1* KO and *Snd1* KI genomic DNA samples were amplified using the genotyping primers shown above.

*Prmt5*<sup>OE</sup> genomic DNA was amplified using six primer sets with overlapping 3' to 5' ends to amplify the complete *V5-Prmt5* and *Mep50* sequences. Due to the repetitive nature of IRES sequences, this portion of the transgene was excluded from PCR amplification and sequencing.

*V5-Prmt5* set 1.1 forward: GAAGTTATTTTGTGCGACGCT

*V5-Prmt5* set 1.1 reverse: GGAGGTCAGCTCCAATTT

*V5-Prmt5* set 2.1 forward: GTGGCATAACTTTTCGGACTCT

*V5-Prmt5* set 2.1 reverse: CCCAGAAGCTCACTGACAATAA

*V5-Prmt5* set 2.2 forward: AGCTGACCTCCCGTCTAAT

*V5-Prmt5* set 2.2 reverse: TGCTCACGCCATCATCTTT

*V5-Prmt5* set 3.1 forward: CTCCGGAGAAAGCTGACATTAT

*V5-Prmt5* set 3.1 reverse: CCTAGGAATGCTCGTCAAGAAG

*Mep50*<sup>trans</sup> set 4.2 forward: GAGTCAAATGGCTCTCCTCAA

*Mep50*<sup>trans</sup> set 4.2 reverse: CTA CTGTCCTCACTACATGAAAGAA

*Mep50*<sup>trans</sup> set 5.1 forward: AGCTGTCAGTGGTAGCAAAG

*Mep50*<sup>trans</sup> set 5.1 reverse: TAGGAAAGGACAGTGGGAGT

## 2.6 Liver harvest for Western blot

Livers were extracted from 2-month-old male mice and washed in ice cold 1x PBS to remove surface blood. Liver chunks were taken in pie-shaped pieces from outside to center of the largest lobe and flash frozen in liquid nitrogen, storing at -80 for short term storage, and stored in liquid nitrogen for long term storage. During protein extraction, frozen liver chunks were weighed and added to 0.5mL/0.1g tissue lysis buffer. Liver lysis buffer for protein extraction was T-PER tissue protein extraction reagent (Thermo, 78510) with 1x Protease inhibitor cocktail set 1 and 1x phosphatase inhibitor cocktail. Tissue was homogenized in Dounce with tight pestle six times on ice. Slurry was then ultracentrifuged at 74k RPM for 60 min at 4°C. After ultracentrifugation, lipid layer was removed, and solution was flash frozen in liquid nitrogen as aliquots. Relative protein

concentration was obtained using Bio Rad protein assay dye reagent concentrate (Bio Rad, 5000006).

## **2.7 Western blot analysis**

Cultured cells were lysed in 1x RIPA buffer containing 1x protease inhibitor cocktail set 1 (Millipore, cat# 535142), and 1x phosphatase inhibitor cocktail (shown below). Equivalent protein concentrations were boiled in 1xSDS laemmli buffer for 10 min. Boiled samples were loaded and run in 10-15% in-house prepared polyacrylamide gels.

### *2.7.1.1 In-house prepared gradient polyacrylamide gels*

Gels were made with: 30% Acrylamide bis (BioRad, Cat# 1610158), 1:1 diluted SDS solution 20% (BioRad, Cat# 1610418), N,N,N',N' tetramethyl ethylenediamine (Acros Organics, Cat#420580050), and ammonium persulfate (Sigma, Cat# A3678-100G). Polyacrylamide gel was then transferred to a methanol activated 0.45um PVDF membrane (Millipore, Cat# 88518) using semi-wet transfer.

### **2.7.2 LI-COR detection by fluorescence-**

Wash buffer contained 1x PBS with 0.5% Tween20 (BioRad, Cat# 1610781) (PBS-T), and blocking buffer contained 3-5% nonfat powdered milk (LabScientific, Cat# M0841) dissolved in PBS-T (X% milk). After transfer, PVDF membranes were blocked for 1hr in 3% milk followed by incubating with primary antibody overnight. Rabbit and mouse primary antibodies were co-incubated overnight. Membranes were washed in cold water followed by two PBS-T washes for 12 min each. Respective secondary fluorescent antibody was next added in 3% milk for 1.5 hrs while rocking in the dark then washed twice in water for 12 min each.



### 2.7.3 Western blot detection by chemiluminescence-

PVDF membranes were blocked for 1hr in 5% milk followed by incubating overnight with 1° antibody. This was followed by three 10 min washes in PBS-T. 2° antibody was added for 1hr of rocking at RT followed by three PBS-T washes at 10 min each. Membranes were developed using Western Lighting (Perkin Elmer, 203-21341).

## 2.8 Antibodies

The following antibodies were used: name; company, catalog number.

$\beta$ -Actin; Sigma, A1978

BrdU; BD BioScience, 8309543

MEP50; Cell signaling technology, 2018S

Myc-tag; CST, 2276S

ADMA- Developed by NEP and reported in (152)

MMA- Developed by NEP and reported in (152)

SDMA- Developed by NEP and reported in (152)

PRMT5; Cell signaling technology, 799985

SND1; Active Motif, 61473

SND1; Bethyl, Cat# A302-883A

V5-tag; Ab Cam, ab27671

$\alpha$ -Rabbit IgG Alexa fluor secondary; Invitrogen, YA354845

$\alpha$ -Mouse IgG Alexa fluor secondary; Invitrogen, VK307586

Streptavidin-HRP; Pierce, 21126

$\alpha$ -Rabbit IgG HRP secondary, Cell Signaling Technology, 7074

ECL  $\alpha$ -mouse IgG HRP; GE Healthcare, NXA931

## 2.9 Peptide pulldown assay.

Streptavidin beads (Millipore, Cat# 16-126) were pre-washed with cell lysis buffer before incubation with biotinylated GAR-un/Rme2s peptides (10ug) in 500  $\mu$ l cell lysis buffer for 1h at 4°C with rocking for conjugation. Lysis buffer was composed of the following Sigma compounds: 50mM sodium diphosphate (Cat# S0751-100G), 300mM sodium chloride (Cat# S9888-25G), 10mM imidazole (Cat# I5513-25G) all adjusted to pH 8.0. The conjugated peptide-beads complex was then incubated with cell lysates prepared from primary MEFs for 1h at 4°C with rocking. After incubation, the bound proteins were eluted by addition of SDS-Lammeli buffer for western blot analysis. GAR peptide sequences are as follows with SDMA marked by “\*”:

GAR-un peptide: GGRGRGGGFRGRGRGGGG-BIOTIN

GAR-Rme2s peptide: GG[R\*\*]G[R\*\*]GGGF[R\*\*]G[R\*\*]G[R\*\*]GGGG-BIOTIN

## 2.10 RNA-extraction

Total RNA was harvested from 2-month-old mice using the manufacturer recommendations for total RNA harvesting using TRIzol reagent (Ambion, 368708) and Qiagen RNeasy Plus mini kit (cat#74136). Samples were run through a second round of isopropanol cleanup to increase purity of total RNA.

## 2.11 RT-qPCR primers

Primers were designed using the NIH Primer-BLAST software. Using accession numbers and requiring primer pair to be separated by at least one intron in genomic DNA. Primers were chosen based on having similar amplicon size, T<sub>m</sub>, 3' GC clamp, similar GC content, low similarity to off target sites, and covering junction sites.

Saa1 F: CATTGTTCACGAGGCTTTCC; Saa1 R: CTGAGTTTTTCCAGTTAGC

Saa2 F: CATTATTGGGGAGGCTTTCC; Saa2 R: CTCCATCTTTCCAGCCAGC  
Lcn2 F: TGAAGGAACGTTTCACCCGC; Lcn2 R: CCATTGGGTCTCTGCGCATC  
Orm2 F: CGCTGTTGGAAGCTCAGAACC; Orm2 R: TAGGACAGCCGCACCAATGA  
Moxd1 F: ATCACCCGAACATGCCCGAT; Moxd1 R: CCTCCGTGCGGGATTATCGT  
Cyp3a44\_set 1 F: CTGAGCTTTCTCAGTGTCTGTG; R: GATCCCATGAGAAACGGTGAAG  
Cyp3a44\_set 2 F: CTCATTCTGCCCTTCTCAG; R: GGTATGGGGATTGGGACTCT  
Cyp2c39\_set 1: AGGTCTGCATCATTCTCGCT; R: ACCTGGACAGGATTGCAGAAGG  
Cyp2c39\_set 2: ACCTCTTTGCTGCAGGGACA; R: GGGCTGCGGTGTCTACCAAT

## 2.12 RT-qPCR analysis

RNA was harvested from liver tissue as described above. A cDNA library was generated with an iScript cDNA Synthesis Kit (BioRad, Cat# 1708891) using the manufacturer's recommended volumes and thermocycler conditions, before dilution in nuclease free water. From the diluted library, 20 ng cDNA was added to 500 nM primers in recommended volumes of 1x iTaq Universal SYBR Green Supermix (BioRad, Cat# 1725122) in 384 well plates. Thermocycler conditions were: step 1 - 95°C for 5 min; step 2 - 95°C for 15 sec, 60°C for 1 min; repeat step 2 39x; step 3 - 65°C for 5 sec, and 95°C 50 sec. Expression change was calculated using  $\Delta\Delta C_t$  methodology. Expressly,  $C_t$  values of *Gapdh* were obtained for each biological replicate. The  $\Delta C_t$  was next calculated as the difference of each raw  $C_t$  value from the respective biological housekeeping gene average. The average  $\Delta C_t$  was obtained for only the biological WT control for each gene of interest. The  $\Delta\Delta C_t$  was then calculated as the difference between each  $\Delta C_t$ , and the average  $\Delta C_t$  of the biological WT control. We then calculated and reported  $2^{-\Delta\Delta C_t}$ .

## 2.13 RNA-sequencing of *Prmt5*<sup>OE</sup> samples

Total RNA was purified as above and the RNA-seq library was prepared with an Illumina TruSeq stranded mRNA kit (Medgenome) and sequencing was performed using a NovaSeq

(PE150) machine. Paired-end sequencing was performed to a depth of 40 million reads (80M total). The RNA-seq raw reads were mapped to the mouse genome GRCm38(mm10) and the raw read count for genes was analyzed by the bioinformatics tool “featureCounts” (<https://subread.sourceforge.net/featureCounts.html>). The normalized read count was generated from built-in functions in DESeq2. The differential expression analysis was performed with a DESeq2 bioconductor R package using a cutoff of FDR  $q \leq 0.05$ . Differentiated genes were further analyzed by GSEA from Broad Institute (<https://www.gsea-msigdb.org/gsea/index.jsp>).

#### **2.14 DEN injection model**

DEN (Sigma, N0258-1G), also known as N-nitrosodiethylamine, was diluted to 2 mg/mL in sterile 0.9% saline and stored at 4°C. All DEN injections were performed on 14-day old male mice. Pups were interperitoneally injected with 20 mg/kg DEN using a 1mL TB/insulin style syringe and moved into a fresh Innovive cage for 14 days post-injection to allow drug wash out, switching the cage and weaning at 7 days post-injection. After wash-out, mature mice were then moved into normal caging and allowed to grow tumors for 272-274 days. We excluded females from DEN studies as they develop HCC in <30% of DEN injections with varied penetrance (153). This is compared with nearly 100% penetrance in males. Increased HCC incidence in males is also seen in humans. Thus, DEN induced HCC is a non-optimal approach for directly comparing tumorigenesis in females but is excellent for foundational HCC studies in males.

#### **2.15 Bloodwork**

>400uL whole blood was collected from sacrificed mice directly from the heart and immediately placed in a 1.5mL green capped lithium heparin tube (BD Microtainer, 365965). Analytes were then measured using an Intregra 400 plus machine from Roche.

## 2.16 BrdU proliferation model

Pups were injected with DEN as described above. 24hrs post-DEN injection, mice received a 15mg/kg BrdU (Selleckchem, S7918) injection interperitoneally. After 1hr intercalation period, livers were harvested and stored in 10% formalin (Fisher Chemical, SF100-4) prior to paraffin emending and sectioning. Whole liver sections were taken from each mouse and stained with BrdU antibody. Liver section slides were analyzed by counting total cells and BrdU positive cells in an area of 600um x 700um, approximately 1300 hepatocytes. Each slide was counted twice, with each genotype contributing three individual mice. Slides were analyzed using ImageScope v 12.4.3.5008.

## 2.17 *In vitro* methylation assay

Livers were harvested from two-month-old mice from *Prmt5 OE* and *Prmt5 WT* littermates. Livers were washed in ice cold sterile PBS prior to cutting into 20-50mg wedge shaped slices and flash frozen in liquid nitrogen. 20mg frozen liver chunks were pulverized in liquid nitrogen using a mortar and pestle and the powder dissolved into 1mL PBS+0.5%Tween with 1x Protease inhibitor cocktail set 1 and 1x phosphatase inhibitor cocktail. Cellular slurry was then put into a glass Dounce and plunged 7 times with a loose pestle. The lysate was then spun at 15,000xg at 4°C. Following the spin, the following was added for the positive control samples: 16.5uL sterile PBS, 0.67ug PRMT5/MEP50 complex (Reaction Biology, HMT-22-148) enzyme, 1uL adenosyl-L-methionine, S-[methyl-<sup>3</sup>H] (<sup>3</sup>H-SAM) (Perkin Elmer, NET155V001MC) and 1.5ug Recombinant Histone H4 (New England BioLabs, M2504S). The following was added for their respective samples: 17.5mL liver lysate, 1.5ug recombinant Histone H4, 1uL <sup>3</sup>H-SAM and 1uL MS023 (Sigma, cat# SML1555). Reactions were pipetted to mix and incubated at 30°C for 60 min or the respective number of minutes. The reaction was stopped by adding 5x SDS-buffer with bromophenol blue with β-mercaptoethanol and boiling for 10 min. Samples were then run on a 15% poly acrylamide gel at 150V for 70min. Sample was semi-wet transferred onto PVDF

membranes at 75V for 75 min. The membrane was then air dried then sprayed with homemade enhance solution (recipe below) twice, drying between, followed by exposing radiosensitive film for one week at -80 degrees C.

### **2.18 Enhancer spray**

In-house enhance spray was generated from a recipe shared from Pål Falnes at the University of Oslo. We added the following to the respective final concentrations: 2-methylnaphthalene (Sigma Alderich, cat# M5700-500G), 57%; Pentyl acetate (Sigma, 109584-250MI), 40%; and 2,5 Diphenyloxazole (D210404), 2.5%. Once mixed, the solution was stored in the chemical fume hood at room temperature in a spray bottle.

### **2.19 Transient transfection**

Six-well plates were seeded to 30% confluency 24hrs prior to transfection. 18ug polyethylenimine (PEI) was incubated with 6ug myc-PRMT5 plasmid DNA in 100uL optimem (Gibco, 31985062) for 10min at room temperature. This full volume was then added to a single well and media changed after 5 hours. In non-transfected cells, Epz015666 (Sigma, cat# SML1421) was added to 10uM final concentration on the same day in an equal number of cells. 72 hours post-transfection, empty vector-transfected, myc-PRMT5 transfected, and Epz015666 treated non-transfected cells were harvested using a cell scraper and processed for western blot analysis as described above. The myc-PRMT5 plasmid was a gift from the Stephane Richards lab.

### **2.20 Hydrodynamic Tail Vein Injection**

Hydrodynamic tail vein injection followed the protocol set forth previously (154-156). pT3-EF1a-*c-myc* (p-c-myc), px330- $\alpha$ *Tp53* (p- $\alpha$ *Tp53*), and SB13 plasmids were a gift from the Ernesto Guccione Lab from Ichan School of Medicine at Mount Sinai. Five-week-old male mice were placed under a 125-watt heat lamp for 5 min to dilate tail veins. While tails were dilating, DNA for

p-c-myc, p- $\alpha$  *Tp53*, and SB13 was diluted to 10mg/kg for the first two and 2.5mg/kg for the latter into 10% of the mice mass in 0.9% sterile saline. Single mice were restrained using a TV-150 Braintree Scientific Inc with a standard barrel (sku# TV-150 STD) and tail cleaned with 70% ethanol. Using a 27.5-gauge needle in a 3mL sterile syringe, 10% of the mouse mass by volume was injected into the tail vein over the course of ~5 seconds. Mice were immediately removed from the restraint and placed into a fresh cage and observed for wellbeing until they returned to normal activity.

Mice were followed for thirty days with daily observation. On the thirtieth day, surviving mice were sacked and livers excised. Terminal mouse mass and liver mass was obtained for each mouse surviving to day thirty. Necropsies were performed and mice were checked for distal lesions. Following hepatectomy, if tumor lesions were distinguishable, they were excised and arrayed onto white paper and photographed. Livers were saved in 10% formalin for downstream H&E staining.

## **2.21 Phosphatase inhibitor cocktail**

1000X concentration phosphatase inhibitor cocktail was prepared from the following: 1M sodium orthovanadate, 1M sodium molybdate, 4M sodium tartrate, 1M sodium fluoride, 2mM Imidazole, 2mM  $\beta$ -glycerophosphate, and 1mM sodium pyrophosphate. All compounds were solubilized in water.

## **2.22 Post-DEN treatment necropsy procedure**

DEN-induced tumorigenesis mice were allowed to age for an additional 272-274 days post-DEN injection. Upon sacrifice, terminal mouse mass was obtained.  $\geq 400\mu\text{L}$  blood was taken from the heart followed by a full necropsy. Livers were excised and terminal liver mass obtained. Photographs were obtained of each mouse and liver. Mice were examined for additional neoplasms throughout the organism. 3 ~100mg pie shaped section was taken from the large

lobe of each of the mice and flash frozen in liquid nitrogen or OCT. Remaining liver and any other lesion containing tissues were fixed in 10% formalin for downstream H&E staining.

### **2.23 Photoshop courtesy edits**

Photos of tumor grossing have been courtesy edited to remove residual blood and normalize colors to fix differences between cameras. Under the “image” tools and “adjust” ribbon, the “shadow and highlights” dialog box was used to increase the “amount”, “tone”, and “radius” options under the shadows option. Values were adjusted till color saturations were similar between photographs taken with different cameras. Next, peripheral blood was removed using the “stamp” tool to mimic adjacent clean areas of the image.



## Part I- The Reader

### **3 Chapter 3- Characterizing loss or mutation of SND1 and the effect on HCC**

#### **3.1 Introduction and scope**

SND1 is involved in several biological processes. It is not known what the phenotype of an SND1 Tudor domain mutant is or if there are transcriptionally regulated genes under the control of the Tudor domain. Loss of the Tudor domain alone may contribute to the KO phenotype. SND1 has been identified as a driver of liver cancer when overexpressed. However, it is unknown if SND1 loss can protect against tumor development. Further, it is unknown if the Tudor domain is needed for driving tumorigenesis. **We hypothesize that the SND1 Tudor domain is important for developing HCC.** Two GEMMs were recently developed in our lab for SND1 studies, namely a *Snd1* whole body KO mouse (*Snd1 KO*) and a *Snd1* Tudor domain mutant (*Snd1 KI*) mouse. These mice are functionally validated, and their transcriptome analyzed. We then chemically induced liver cancer in these mice to study the impact of *Snd1* loss or mutation on tumor formation.

#### **3.2 Generation and validation of *Snd1 KO* and *KI* mouse lines**

##### **3.2.1 *Snd1 KO* GEMM**

First, a *Snd1 KO* mouse line that expressed no SND1 (*Snd1 KO*) was generated. These were generated in our lab by using a CRISPR/Cas9 guide RNA to target the third exon of SND1, corresponding to the SN-1 domain<sup>37</sup> (**Figure 4a**). The sgRNA and purified Cas9 protein were micro-injected into 1-cell embryos and transferred into pseudo-pregnant female mice to complete gestation. Random mistakes in DNA damage repair will result in a subset of these pups having an out-of-frame genetic deletion in the targeted sequence. This mutation becomes the target of

---

<sup>37</sup> Developed by Y. Wang.

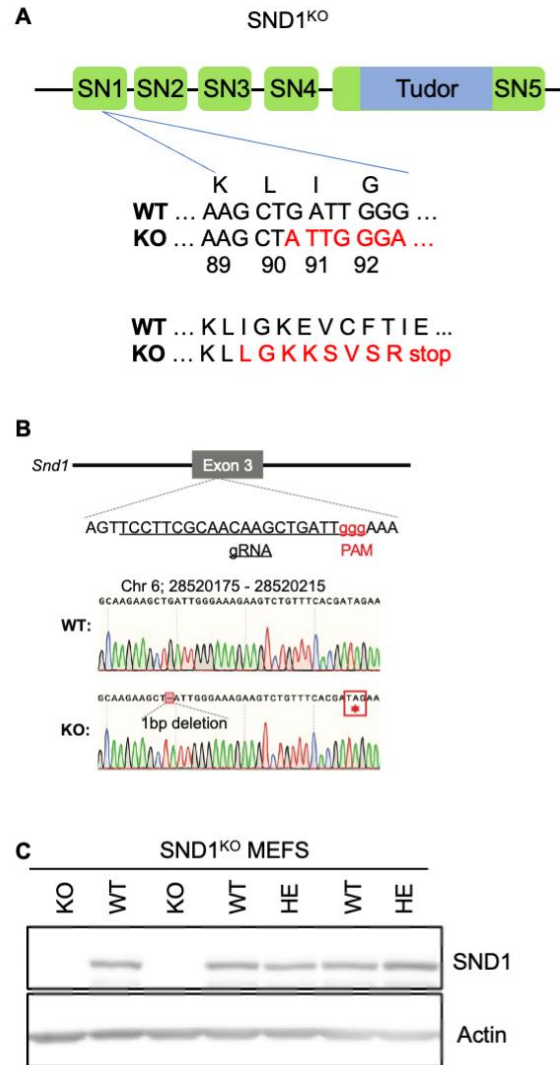


**Figure 4-** *Snd1* KO GEMM validation: **a)** Graphical structure of WT SND1 with *KO* design schematic. Expanded below is WT codons in black with amino acid translation above and amino acid number beneath. Frame shift highlighted in red. Below is WT and KO amino acid sequence, with red indicating frameshift translation. **b)** Screen shot of sanger sequencing for annotated *WT* and *KO* samples with gRNA and PAM sequence highlighted. **c)** Western blot of MEFs from heterozygous *Snd1* *KO* crosses.

genotyping. We obtained genomic DNA from one *Snd1 KO* pup and Sanger sequenced the target region which revealed a single nucleotide deletion that resulted in a frame shift at amino acid 90, and introducing a premature stop codon corresponding to I99 (**Figure 4a,b**). This founder was backcrossed into FVB background mice for four generations to reduce chances of off-target effects of non-specific CRISPR/Cas9 cleavage. Heterozygous *Snd1 KO* mice were intercrossed, and mouse embryonic fibroblasts (MEFs) were generated from 12 days post-coitus (dpc) mouse embryos. Western analysis of these MEFs isolated from a single litter indicated that *Snd1 KO* samples did not express detectable protein (**Figure 4c**, lane 1 and 3). The epitope that is recognized by this antibody (Active Motif) is within the 4<sup>th</sup> SN-domain. To confirm successful knockout, we used a second antibody raised to the N-terminus of SND1 (Bethyl) which binds the 100-150 amino acid in the SN-1 domain. No protein was detected with this antibody indicating successful *Snd1 KO*<sup>38</sup>.

### 3.2.2 *Snd1 KI* GEMM

The structure of the SND1 Tudor domain has been resolved with at least two different SDMA modified peptides. This reveals a four-residue aromatic cage involving F740, Y746, Y763 and Y766 whereupon mutation of any of these residues results in a dramatically reduced binding<sup>39</sup> (1). Having validated the Y766 residue as necessary for SDMA binding, we proceeded with generation of a mouse expressing a full length SND1 protein with a single mutation in the Tudor domain (*Snd1 KI*)<sup>40</sup>. This was done by micro-injecting purified Cas9 protein, sgRNA, and donor DNA to permit homologous recombination at the Y766 site. The mutation was also designed to introduce a novel *AvrII* restriction enzyme site for genotyping (**Figure 5a**). We validated the founder by Sanger sequencing and backcrossed into a FVB background against off-target effects for four generations as before (see section 3.2.1). As designed, *Snd1 KI* mice

---

<sup>38</sup> Data not shown.

<sup>39</sup> This finding was validated by Y. Wang using recombinant GST-Tudor fusion protein with a Y766L mutation in a peptide pull down. Mutant SND1 was unable to pull down SDMA modified GAR peptide.

<sup>40</sup> Developed by Y. Wang.

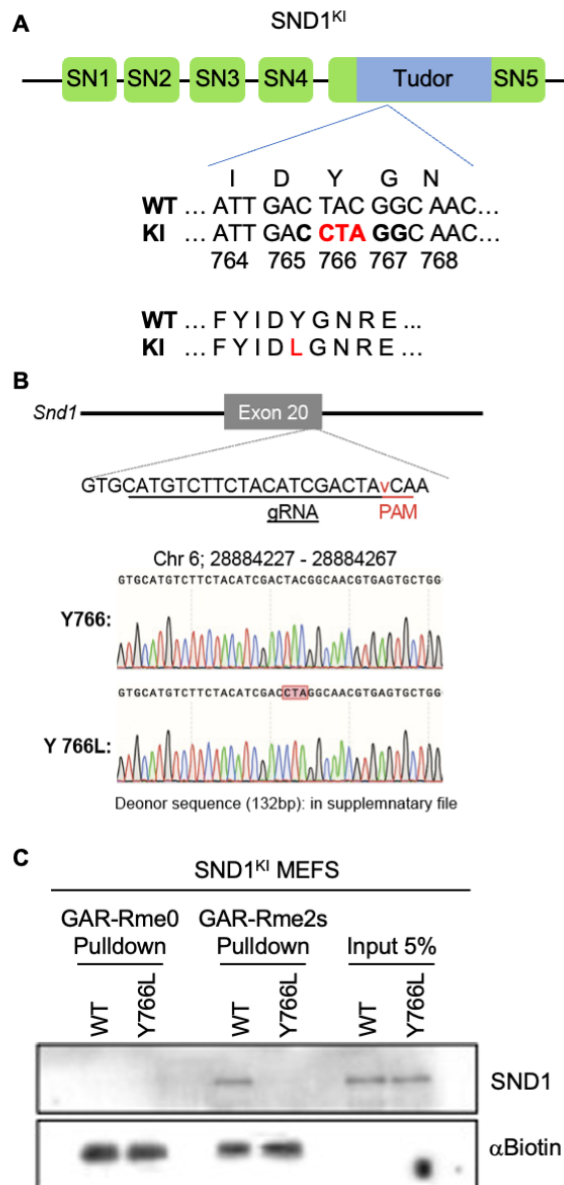


**Figure 5- *Snd1* KI GEMM validation:** **a)** Graphical structure of *Snd1* KI mouse. Expanded portion is *WT* and *KI* design sequence. *Y766L* mutation highlighted in red. *WT* translation above, amino acid residue number below. **b)** Annotated screenshot of *WT* and *KI* mouse sanger sequence with gRNA and PAM sequence. **c)** Peptide pulldown from *WT* and *KI* MEFs. Pull down used a GST-tagged SDMA modified GAR peptide (GAR-Rme2s).

harbored the Y766L mutation and *AvrII* restriction site (**Figure 5b**). As before, heterozygous *Snd1 KI* mice were intercrossed, and MEFs were generated from 12dpc mouse embryos. Protein extracts from *Snd1 WT* and homozygous *Snd1 KI* MEFs were used in pulldown assays with SDMA methylated and unmethylated GAR peptides. The SDMA-GAR peptide pulled down SND1 from *WT*, but not *KI* samples (**Figure 5c**). This validated that *Snd1 KI* mice produce a full length SND1 that cannot read SDMA.

### 3.2.3 Comparing the phenotype of *Snd1* mutant mouse models

While breeding the *Snd1* mouse lines, we noticed a slight decrease in fertility in the *Snd1 KO* mice. *Snd1 KO* mating cages were monitored for infanticide or postnatal mortality. From our observations, birthed pups consistently reached maturity. *Snd1 KO* litters from homozygous crosses had significantly fewer pups, while *Snd1 KI* litters from homozygous crosses did not have a significant change in litter size compared to age matched *WT* mice<sup>41</sup> (**Figure 6a**). This keeps with observations in both *Drosophila* and *Mus*, as *Snd1* has been implicated in spermatogenesis (94, 157). We also noticed that *Snd1 KO* males were not successful breeders after 4 months of age. Following heterozygous crosses, we observed a decreased mass in both 4-week-old male and female *Snd1 KO* mice (**Figure 6b**), consistent with previous reports (101). One copy of *Snd1* was sufficient to rescue the mass difference between *KO* and *WT* mice. This difference in size was not present in the *Snd1 KI* mice indicating *Snd1* has a role in development and growth that is unaffected by our Tudor domain mutation.

### 3.3 Transcriptional analysis of livers from *Snd1* mutant mice

In mice, *Snd1 OE* promotes HCC (128-130). Therefore, we sought to determine how loss of SND1 or mutation of the SND1 Tudor domain might influence gene expression that could ultimately impact oncogenic pathways in the liver. A *Snd1 KO* gene expression profile was

---

<sup>41</sup> Heterozygous *KO* crosses were not tested for fertility.

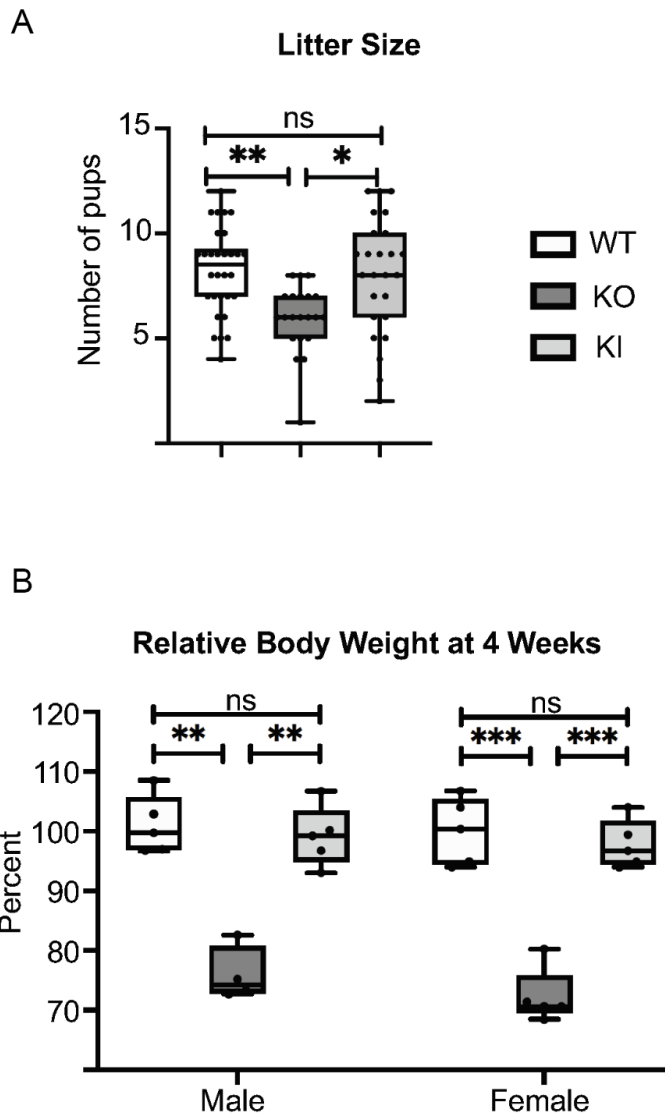


**Figure 6-** Litter and body size of *Snd1* KO and *Snd1* KI mice. **a)** Litter size of *Snd1* KO and *Snd1* KI homozygous crossed mice. Points represent the number of pups per litter. Pups were counted on the day of birth. Litters n = 21, 30 and 25 for WT, KO, and KI, respectively. **b)** The relative body mass of 4-week-old *Snd1* KO and *Snd1* KI mice resulting from heterozygous crosses. n = WT (3m, 5f), KO (3m, 5f) and KI (5m, 5f). Statistical t-test, two-tailed unpaired, P-value \* $<0.05$ ; \*\* $<0.01$ ; \*\*\* $<0.001$ .

recently published by the Silvennoinen group (101). We noted that several of the top downregulated genes included acute inflammatory response genes involved in innate immunity.

As chronic inflammation is a known driver of HCC, we tested the RNA level of the top dysregulated inflammatory response genes by qPCR. *Saa1*, *Saa2*, *Orm2*, and *Lcn2* were all significantly downregulated in *Snd1 KO* and *Kl* liver samples compared to *WT* (**Figure 7a**). These genes, which play a major role in innate immunity, are known to be regulated by IL6/STAT3 signaling in the liver. However, lipopolysaccharide (LPS) activation of IL6 is not negatively impacted in *Snd1 KO* bone marrow derived macrophages (101). Thus, currently it is unclear how SND1 regulates the expression of acute phase proteins.

The top dysregulated gene in the published *Snd1 KO* transcriptional analysis was *Moxd1*, a monooxygenase that localizes to the endoplasmic reticulum (158). Beyond structural similarity to other DBH<sup>42</sup> like proteins (159) and localization, little is known about the normal function of this protein<sup>43</sup>. Interestingly, we saw downregulation of *Moxd1* by qPCR in *Snd1 KO*, but a significant upregulation in *Snd1 Kl* mice (**Figure 7b**). This altered difference between *Snd1 KO* and *Snd1 Kl* livers could be indicative of distinct transcriptional profiles for both genotypes.

Taken together, the downregulation of acute phase response proteins (APPs) indicate loss of SND1 or its methyl reading capacity may impact gene expression related to liver function<sup>44</sup>. Further, the SND1 Tudor domain may have distinct transcriptional control over select targets.

### 3.4 SND1 Carcinogenesis Models

Moderate increase in SND1 is sufficient to promote HCC. With carcinogenic challenge, three-fold SND1 OE resulted in increased tumor burden and a doubling of liver weight (129). Two-fold OE was sufficient to drive tumorigenesis in *Pten*<sup>-/-</sup> mice (128) (see also footnote 28).

---

<sup>42</sup> Dopamine-beta-hydroxylase.

<sup>43</sup> A PubMed search identifies fewer than 30 publications in the last 25 years concerning *Moxd1*, nearly all having been published in the last 5 years. The primary topics described in these are for *Moxd1* in cancer and ER stress induced apoptosis.

<sup>44</sup> See section 3.5.3.2 for description of APPs.

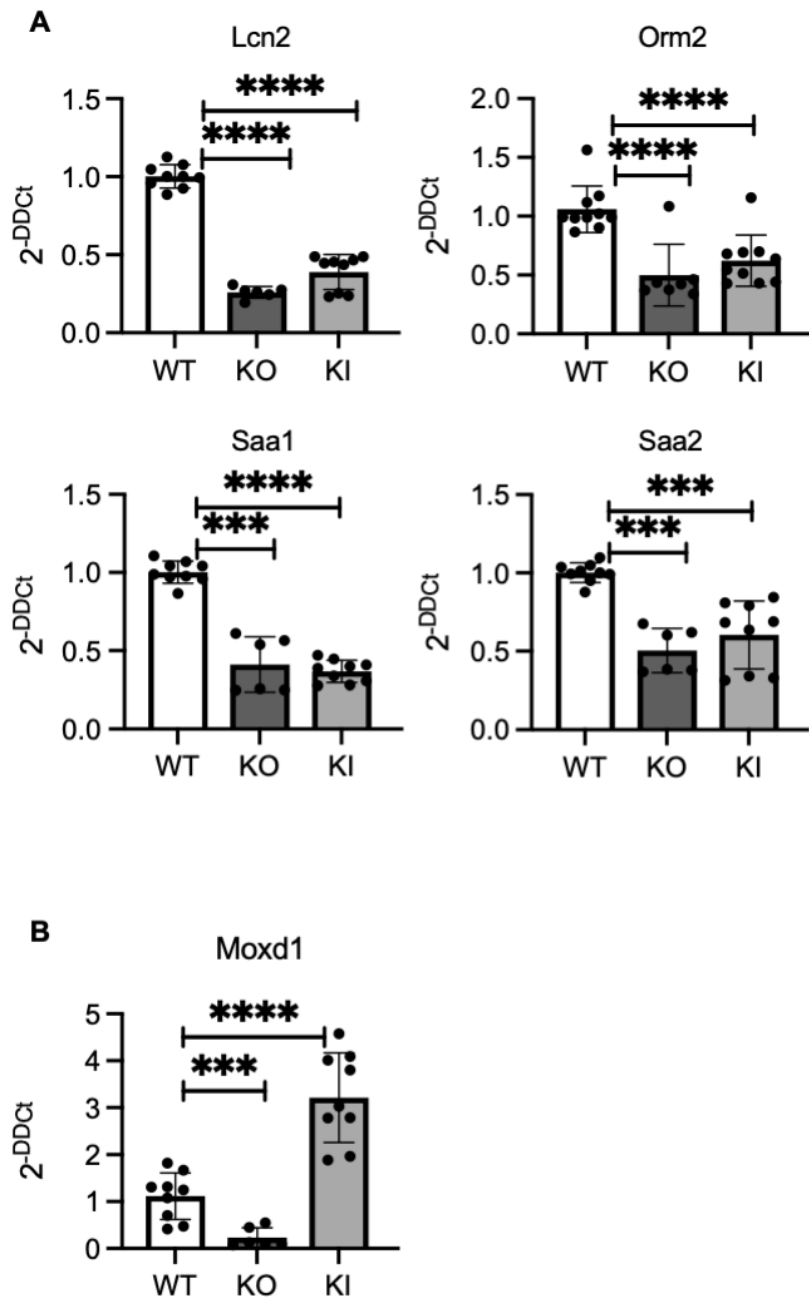


**Figure 7-** RT-qPCR of selected downregulated genes from *KO* and *KI* mice, performed in triplicate for 3 WT, 2 KO, and 3 KI independent biological replicates for each genotype. Statistical t-test, two-tailed unpaired, P-value \*\*\*<0.001; \*\*\*\*<0.0001. **a)** Acute phase response proteins are downregulated in published *Snd1* *KO* transcriptome analysis. **b)** Top dysregulated gene in published *Snd1* *KO* dataset.



From a clinical standpoint, a two-fold increase in SND1 protein levels were observed in 70% of human HCC samples contained on a tissue microarray (112). To determine if loss of SND1 or mutation of the SND1 Tudor domain might have the opposite effect and be protective against HCC development, we treated mice with the carcinogen diethylnitrosamine (DEN).

### 3.4.1 DEN carcinogenesis modeling

DEN has been known to be carcinogenic for over 60 years and is well established as a chemical tool for studying carcinogenic liver injury in mice<sup>45</sup> (153, 160, 161). In cells, DEN is activated by cytochrome P450 enzymes that generate alkylating metabolites which modify DNA bases<sup>46</sup>. Alkylated bases activate the DNA damage response which can result in cell death, proliferative response, and random oncogenic mutations. Tailored feeding and injection protocols can allow study of different classifications of liver cancer<sup>47</sup>. Single injection in two-week-old pups is sufficient to drive liver carcinogenesis in virtually 100% of male mice after nine months which recapitulates a toxic exposure to a carcinogen (153). This tumorigenic penetrance makes this chemical useful for comparing liver tumorigenesis in different genotypes. We injected two-week-old male pups with DEN in *Snd1 KO*, *KI*, and *WT* control mice and assessed tumor development at nine months post-injection (**Figure 8a**). Gross examination of whole liver from 9-month-old mice showed both larger and more abundant surface nodules in *WT* mice than in either *Snd1 KO* or *KI* mice (**Figure 8b**).

A common way of confirming tumorigenesis in DEN and other HCC modeling is to identify an increase in liver contaminants in the blood that can indicate liver damage. To some degree, this can be used to determine how advanced liver disease has become. We collected whole blood from all injected mice and measured the level of 16 analytes. Only total protein and albumin

---

<sup>45</sup>“On the morphology of diethylnitrosamine induce liver changes and tumors in rats” (PMID: 13776439) was published in 1961 (original in German). The “nitrosamine” family of chemicals, however, have been known to be carcinogenic for even longer.

<sup>46</sup> This occurs by hydroxylation by various *Cyp* superfamily genes, which creates a reactive -OH group that can covalently link to nucleic acids (Liu, et al.,2005).

<sup>47</sup> For example, these can include co-injection with CCl<sub>4</sub> for liver fibrosis and hepatitis associated HCC or include high-fat diet to look at non-alcoholic fatty liver disease associated HCC.

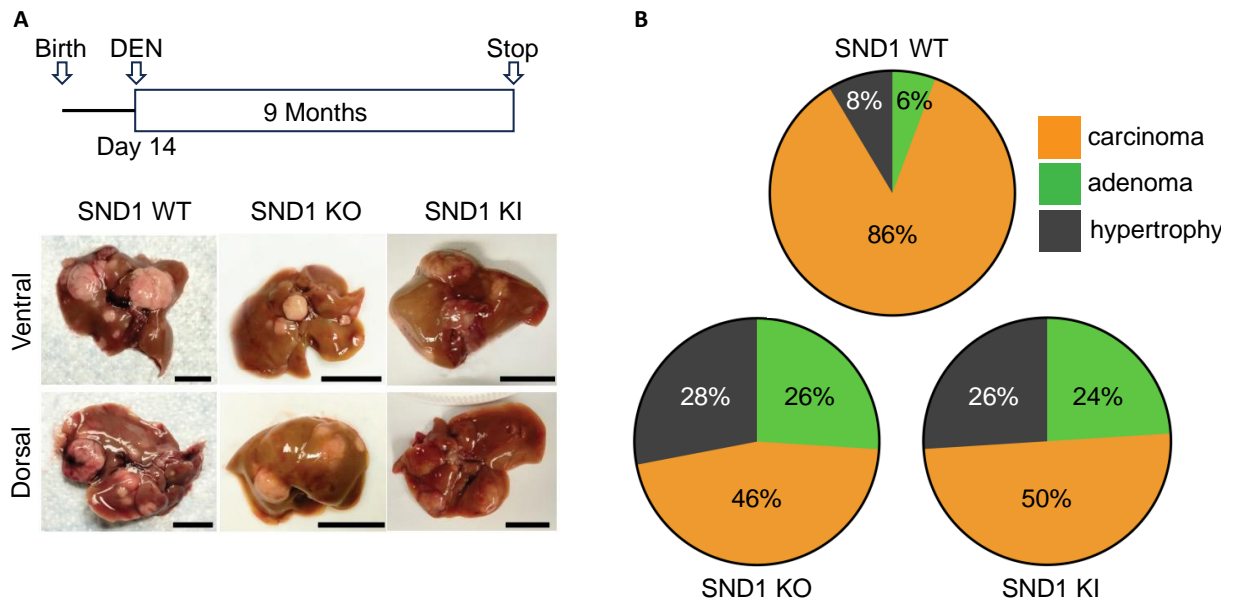


**Figure 8-** Ditethylnitrosamine (DEN) induced HCC grossing and pathology: **a)** Top, schematic of DEN injection schedule. Only male mice were used for DEN injection studies.  $n = WT (28); KO (10)$  and  $KI (10)$ . All mice survived to nine-month termination. (Bottom) Representative images of whole liver with gallbladder (scale bar = 1 cm). Ventral and dorsal respective to mouse orientation. **b)** Ratio of observed pathologies from liver lobe sections representing all 240 lobes from 48 mice ( $n = 50$  lobes from each of  $KO$  and  $KI$  and 140 from  $WT$ ). Hepatocellular carcinoma and adenocarcinoma were binned together as carcinoma.

**Table 4-** Blood analyte comparison of *Snd1* WT, KO, and KI DEN injected mice. Statistical t-test, two-tailed unpaired, P-value, significance <0.05. Significant values in bold.

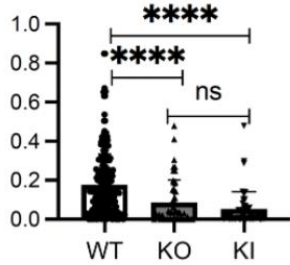
		DEN Injected		
	Analyte	WT avg	KO avg	KI avg
Analyte	Albumin (g/dL)	3.99	<b>3.5</b>	<b>3.59</b>
	ALT (U/L)	251	183.5	95.8
	Calcium mg/dL	10.9	10.9	<b>10.23</b>
	Phosphorus mg/dL	9.29	<b>10.27</b>	8.81
	Glucose mg/dL	242.2	245.9	265.4
	Total Protein g/dL	6.14	<b>5.53</b>	<b>5.39</b>
	ALP (U/L)	102.7	89	84
	AST (U/L)	193.8	169.9	309
	BUN (mg/dL)	24.99	25.39	<b>21.7</b>
	Chloride (mg/dL)	109.3	110.6	109.65
	Globulin (g/dL)	2.148	2.005	<b>1.794</b>
	Potassium (mEq/L)	10.04	10.40	9.974
	LDH (U/L)	1039	660	1095
	Sodium (mEq/L)	151.5	152.2	150.6

levels were significantly lower in both *Snd1 KO* and *KI* mice compared to *WT* (**Table 4**). As the remaining 14 analytes were not uniformly altered, and as we did not measure blood analyte levels of non-injected mice, we determined that we could not use blood analytes as a measure of liver disease.

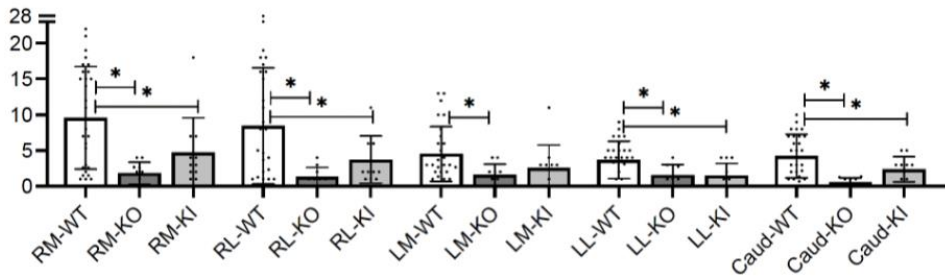
To compare overall tumor burden and to create a quantitative comparison of neoplastic growth rather than gross observation, we established a pipeline to assess tumor type, average tumor-foci, and average tumor area. In brief, we sectioned all five liver lobes from each mouse and performed H&E staining on each section. These sections were digitally scanned with an Aperio AT2 slide scanner and analyzed with ImageScope software to determine the number of tumor foci and the ratio of tumor to tissue area for each section. These images were then read and scored by a pathologist for tumor type; either hepatocellular carcinoma and adenocarcinoma (binned as carcinoma), adenoma, and hepatocellular hypertrophy (indicating an absence of either tumor type) (**Figure 8b**). Compared to *Snd1 WT* mice, *KO* and *KI* mice had a greater proportion of liver sections with hypertrophy (8% vs 28% and 26%, respectively) and adenomas (6% vs. 26% and 24%, respectively). This corresponded to fewer carcinomas (88% vs 46% and 50% respectively). This shift in pathology is relevant as HCC progresses through worsening disease states in humans. Carcinomas are typically more aggressive than adenomas and define later stage HCC. The mean ratio of tumor to section area was significantly decreased in *Snd1 KO* and *KI* mice compared to *WT* controls (**Figure 9a**). A deeper analysis of individual liver lobes revealed the mean number of tumor foci was significantly lower in all five *KO* lobes and in four of five lobes from *KI* sections compared with *WT* (**Figure 9b**).

Liver index is the ratio of liver mass to mouse mass and is a common metric of tumor burden. In principle, the greater the index, the greater the tumor burden. The body mass of one-month-old male and female *Snd1 KO* mice was reduced by approximately 20% (**Figure 6b**). This was independently noted that *Snd1 KO* mice have smaller body size and livers at 2 months (101). In the case of DEN-treated mice, this mass difference was lost at 9-months, while liver mass was

**A** Tumor area of section



**B** Average foci per lobe section



**C** Liver index

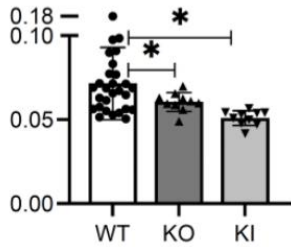


**Figure 9**-Tumor burden of DEN-induced HCC in *Snd1* KO, KI, and WT mice. **a)** Percent tumor area per section area of all tumor types from the livers in **Figure 8b**. Area obtained using ImageScope software and plotted as the ratio of tumor to liver area. Percent tumor area used for statistical test, two-tailed unpaired, P-value \*\*\*\*<0.0001. **b)** Number of tumor foci per lobe section from the livers analyzed in a. Sections with hypertrophy had no foci. Right medial (RM), right lateral (RL), left medial (LM), left lateral (LL), and caudate (Caud). Statistical t-test, two-tailed unpaired. P-value \*<0.05. **c)** Ratio of liver plus gallbladder mass to full mouse from the livers analyzed in a. Mouse liver mass obtained post-sacrifice, prior to further manipulation. Statistical t-test, two-tailed unpaired. P-value \*<0.05.

significantly decreased in both *Snd1* mutant lines compared to *WT*. This resulted in the mean liver index being significantly lower in the mutant compared to *WT* lines (**Figure 9c**).

Several metrics were obtained to determine the extent of tumor burden between chemically induced HCC between *Snd1 WT*, *KO*, and *KI* mice. Comparison of pathologies, the ratio of tumor to tissue, number of foci, and liver index all indicate that either loss of SND1 or incapacitation of the Tudor domain confers hepatoprotection against DEN-induced HCC.

### **3.4.2 BrdU proliferation assay**

To understand the mechanism of how SND1 mutant mice developed less tumors in a DEN induced cancer setting, we tried to determine if proliferation was altered. Liver KO of a master cell cycle regulator, retinoblastoma protein (RB), show increased proliferation in response to DEN treatment (163). Similarly, we injected two-week-old pups with DEN followed by BrdU as previously described. BrdU staining revealed that *Snd1 KO* mice were unable to induce a proliferative response to DEN treatment, while *Snd1 KI* mice did (**Figure 10**).

## **3.5 Conclusions and Future Experiments**

Structure/function studies of SND1 *in vivo* provide valuable insight into the potential importance of its scaffolding, nuclease, and methyl-reader properties. This work provides evidence for distinct roles of the SN- and Tudor domains in development, in transcription, and development of HCC.

### **3.5.1 *Snd1 KO* and *KI* mice reveal Tudor independent functions for SND1**

Homozygous KO of *Snd1* results in a small body size and reduced fertility. This observation is Tudor domain independent as the *Snd1 KI* mice have no discernable change in

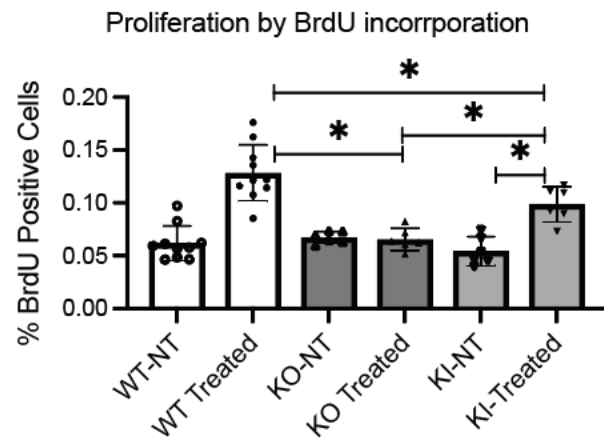


**Figure 10-** Proliferation assay in *Snd1* variable mice: **a)** Mice were treated with either DEN (Treated), on non-treated (NT) as a control. For each experimental condition, mice n=3, each sample was counted twice. Sampling area was 600umx700um, ~1300 cells per count, reporting the percent (%) BrdU positive cells. Statistical t-test, two-tailed unpaired, P value  $* < 0.05$ .

size or fertility. It is not known if the small body size and reduced fertility are linked, however. Here we hypothesize that these phenotypes may be independent from each other.

#### 3.5.1.1 Proposed explanations for a small body size of *Snd1* KO mice

Currently, we do not know mechanistically why *Snd1* KO mice have a small body size. An early hypothesis was that this phenotype might be linked to lipid metabolism as SND1 is known to be involved in lipid synthesis<sup>48</sup>. However, there is no data to support that deletion of lipid-synthesis-associated interacting proteins would result in a small body size. SND1 is involved in many other processes which may impact body size. Published RNA-seq dataset identifies that under normal conditions, full-length SND1 controls transcription of a few genes, which expands in response to a stress stimulus<sup>49</sup> (101). However, there is no indication that these targets influence total body size. SND1 is involved in RISC activity, stress granule formation, splicing, and protein processing at the ER which implicates many potential cellular pathways that could impact body size. Identifying other genetic knockouts in these pathways that phenocopy the *Snd1* KO GEMM will be important in identifying the cause of small body size from loss of SND1.

#### 3.5.1.2 Reduced fertility in *Snd1* KO mice

One copy of *Snd1* is sufficient to rescue a reduced fertility phenotype. This rescue is independent of the Tudor domain. However, it is not clear if this is because of SN-domain scaffolding or SN-domain nuclease activity. As examples of these functions, CA- and UA- rich miRNAs can be directly degraded by SND1 during G1/S phase (167, 168). Also, SND1 is recruited to RISC as a scaffolding protein for the complex and binds many different RNA-binding proteins for transcriptional regulation (**Figure 3**). Accordingly, decreased fertility could be

---

<sup>48</sup> As early as 2000, SND1 was shown to be involved with lipid droplets in mammary tissues in mice and cows (Keenan, et al.,2000). Importantly, SND1 does not appear to be exported in exosomes, but rather functions in lipogenesis itself. Sucrose gradient reveals SND1 pulls down with endoplasmic reticulum and golgi proteins (Garcia-Arcos, et al.,2010). Finally, overexpressing SND1 in rat HCC cells deregulates cholesterol synthesis (Navarro-Imaz, et al.,2016).

<sup>49</sup> SND1 has a dynamic control in response to stimuli. This includes recruitment to stress granules in repose to heat shock (Gao, et al., 2010).



impacted in any number of pathways through these enzymatic or structural roles. Of note, loss of SND1 in *Drosophila* exhibit decreased spermatogenesis and a faster reduction in fertility with age (169). As we noticed males had difficulty mating after 4 months, this could indicate that *Snd1* KO mice have impaired spermatogenesis resulting in reduced fertility. This can be tested by TUNEL<sup>50</sup> staining and tracking the fertility over time of *Snd1* KO male mice (170). Another possible reason for observing decreased fertility is that *Snd1* KO embryos could be developmentally impaired and absorbed by the mother. A series of timed pregnancies and inspecting the number of embryos will determine if *Snd1* loss compromises some embryos.

### 3.5.2 Transcriptional analysis

We were able to validate a group of the top dysregulated genes from a published dataset within a separate mouse. This similarity of differentially expressed genes indicates that our *Snd1* KO mouse is similar to the published datasets even though the knockouts were generated in different mouse backgrounds (FVB and C57BL/6N, respectively).

We identified that several APPs are downregulated in both *Snd1* KO and *Snd1* KI mice, implicating the Tudor domain as involved in their expression. As we see with *Moxd1*, this is the first indication that a Tudor domain mutant SND1 may have a distinct transcriptional profile from a full body *Snd1* KO (**Figure 7**). The next steps in understanding the transcriptional control of the SND1 Tudor domain will be a robust analysis of the transcriptome of both *Snd1* KO and KI samples by ChIP-seq and CUT&RUN. SND1 is known to bind SDMA modified SmB/B' and SmD1/D3 which are core proteins of the spliceosome (71). It remains to be determined if *Snd1* KO can alter global splicing, and further, if Tudor domain mutation will phenocopy a splicing defect of loss of SND1.

---

<sup>50</sup> TUNEL- Terminal deoxynucleotidyl transferase dUTP nick end labeling.

### 3.5.3 Carcinogenesis modeling

We found that the loss of either SND1 or its Tudor domain reader function has a protective role in DEN-induced tumorigenesis (**Figure 8** gross tumor observations and pathologies and **Figure 9** tumor burden). The mechanism for protection remains to be determined. We propose two means of protection by changes in transcriptional regulation from the loss of SND1. Though preliminary results implicate transcriptional regulation, we note that these processes may be transcriptionally independent. Following these considerations will be a description of how to leverage the vulnerability of SND1 loss with our current understanding of SND1 in hepatocarcinogenesis.

#### 3.5.3.1 Transcriptional control of DEN metabolizing enzymes

Cytochromes are involved in drug processing in the liver. In hepatocytes, DEN is hydroxylated by cytochrome P450 proteins, upon which hydroxy-DEN will alkylate DNA and initiate a DNA damage response<sup>51</sup> (162, 171-173). The cytochrome P450 3a (Cyp3a) family is reported to be involved in metabolizing 30-60% of current pharmaceuticals and may be involved in DEN processing<sup>52</sup> (174). Cytochrome expression can be suppressed by repressing cytokine signaling via the JAK/STAT signaling (172). SND1 is a transcriptional co-activator by binding STAT6 and RNA Polymerase II (175). Thus, loss of SND1 could result in loss of STAT-mediated transcription of cytochrome proteins. It has been noted that different cytochrome family members were dysregulated in *Snd1* KO mice (101). As a pilot test, qPCR of a few Cyp2 and Cyp3a family members, known to be involved in drug and DEN processing show decreased mRNA in *Snd1* KO and *KI* mice (**Figure 11**). This decrease in cytochrome P450 proteins could result in decreased metabolism of DEN, lowering the exposure to the carcinogen. A more in-

---

<sup>51</sup> Cyp2a6, Cyp2E1, and Cyp2C11 have been shown to be directly involved in DEN metabolism. There may be additional cytochromes which can hydroxylate DEN.

<sup>52</sup> Mechanistic drug activation by cytochromes is an ongoing field of research.

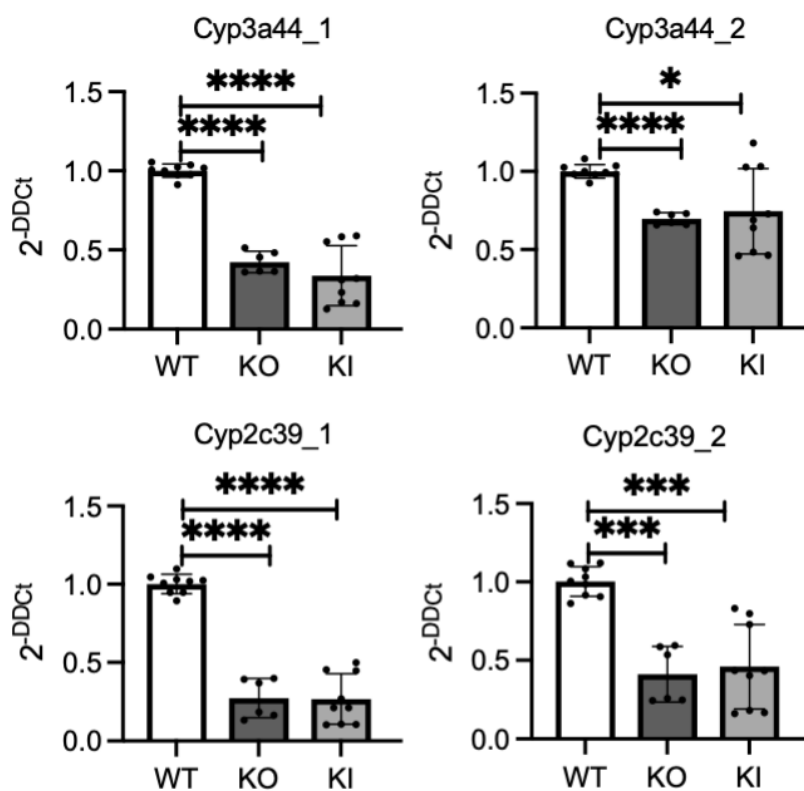


**Figure 11-** RT-qPCR of common drug metabolizing cytochromes Cyp3a44 and Cyp2c39. n= 3 WT, 2 KO, and 3 KI independent biological replicates run in triplicate. Statistical t-test, two-tailed unpaired, P-value \*<0.05; \*\*\*<0.001; \*\*\*\*<0.0001. Two different primer pairs were used for each gene.

depth analysis of DEN activating cytochromes and systemic transcriptional analysis will provide additional insight into this possible mechanism.

### 3.5.3.2 *Transcriptional control of APPs*

Transcriptome analysis of SND1 loss in the liver reveals that some of the top differentially expressed (DE) genes encode APPs, which we validated by RT-qPCR (**Figure 7**) (101). The acute-phase response is part of a general, systemic response to infections and tissue damage. By definition, proteins whose plasma concentrations change by at least 25% in response to pro-inflammatory stimuli are termed APPs (176). APPs are produced primarily in the liver and their production is triggered by inflammatory interleukin-6 (IL-6). It is unclear whether the induced APPs are bystanders or participants in carcinogenesis (177). However, chronic inflammation is a hallmark of HCC formation. If APPs are indeed participants in the development of HCC, then their reduced expression in *Snd1 KO* and *Kl* livers might be responsible for the hepato-protective effect we observe after DEN-treatment.

### 3.5.3.3 *Transcription-independent function of SND1*

SND1 pulls down primarily with RNA-binding proteins. Indeed, most of the known SND1 protein-protein interactions are mediated through SN-domains (see **Figure 3**). RISC, stress granule formation, signal transduction, and splicing are each SND1 related, transcriptional-independent processes which could impact tumorigenesis. Additionally, there may be unknown mechanisms of SND1 recruitment or scaffolding which may be important for cancer.

As an example, subcellular localization of SND1 can impact its scaffolding and RNA processing functions. SND1 is phosphorylated at T103 which allows localization to stress granules. Kinase inhibition decreases SND1<sup>T103</sup> phosphorylation and impairs recruitment to stress granules. Further, phospho-site mutant T103A lost interaction with G3BP, a key protein in stress granule formation (102). It is thought that this recruitment will impact protein-RNA aggregation (65) and processing of specific cytoplasmic RNAs (178). SND1 is recruited to stress

granules via poly-ADP ribose PTMs (179), thus serving as a scaffold to recruit RISC components, like Ago1/2 (180). Thus, known and potentially unknown scaffolding functions of SND1 may impact tumorigenesis independent of transcription.

#### 3.5.3.4 Leveraging the vulnerability in HCC to loss of SND1

There are many mouse models for studying HCC in mice. These include GEMMs, exposure to carcinogenic agents, induction of liver disease<sup>53</sup>, xenograft, and cancer cell injection modeling<sup>54</sup>. A number of GEMMs can induce spontaneous tumor development by manipulating a single gene under an albumin promoter including *Pten*<sup>-/-</sup> (182), *p53*<sup>-/-</sup> (183), *Snd1 OE* (129), and *Tak1*<sup>-/- 55</sup> (184). Deletion of a second gene decreases tumor latency, as is seen with co-deletion of *Akt1/2* (185) or *Pten/Grp94* (186). Also, carcinogen exposure in these experimental models can decrease latency and recapitulate specific liver disease/damage states that are clinically relevant, including heterogenous genomic mutational burden.

The most frequent genetic alterations in HCC are *Tert* promoter amplification, *Tp53* mutation or deletion, and *Ctnnb1* or *Arid2* mutation. Remaining recurrent genetic aberrations make up less than 10% of clinical cases each (187). It is generally thought that ethnicity, etiology, and environmental exposure all contribute to this perplexing heterogeneity in HCC. Adding to this complexity, the liver exhibits inter- and intra-lobular heterogeneity in gene expression profiles further confounding genetic considerations alone (188). Given the heterogeneity of liver cancer (135, 187, 189), we deemed that DEN injections provides valuable proof of principle of the potential vulnerability of HCC by specifically targeting SND1<sup>56</sup>. This work indicates that inhibition of the SND1 Tudor domain may provide a druggable target to treat HCC.

The methylarginine reader function of SND1 can be therapeutically targeted in two ways; either by 1) limiting the available SDMA marks recognized by the SND1 Tudor domain by

---

<sup>53</sup> This can be through high fat diet, alcohol-induced liver disease, or cholestasis.

<sup>54</sup> An extensive review on each of these approaches was recently published (Brown, et al.,2018).

<sup>55</sup> Also known as MAPK3K7.

<sup>56</sup> DEN induces extensive, random DNA damage in cells.

inhibiting the methyltransferase that deposits SDMA (i.e., using PRMT5 inhibitors), or 2) developing small molecule inhibitors that dock into the aromatic cage of the SND1 Tudor domain to block interaction of this domain with SDMA. Many PRMT5 inhibitors have been developed (190), but PRMT5 has many substrates and is often essential for cell viability. Importantly, analysis of copy number alteration has identified a recurrent homozygous deletion of CDKN2A and MTAP in HCC primary tumors (191), which would make this HCC-subset selectively sensitive to MTA-cooperative PRMT5 inhibitors. Of note, many cell types will develop resistance to prolonged treatment with PRMT5 inhibitors, though this may sensitize cells to other therapeutic strategies. PRMT5 inhibitor-resistant *Kras* mutant/*Tp53*-null lung adenocarcinoma cells exhibited an acquired paclitaxel sensitivity that was specific to resistant cells (192). As PRMT5 impacts many different processes, there may be other acquirable vulnerabilities that have not yet been discovered.

Alternatively, inhibitors could be developed that block the ability of the SND1 Tudor domain to read SDMA marks. Because the SND1 Tudor selectively binds SDMA, this would impact fewer cellular targets and could be less toxic to cells. Notably, SMN is another reader of PRMT5-catalyzed SDMA marks and inhibitors that block the SMN Tudor/SDMA interaction have recently been described (193). Also, localization and protein-protein interaction of SPF30, a single Tudor domain-containing protein, could be disrupted with a SMI<sup>57</sup> (194). Discovery of these Tudor domain SMIs set a precedent for successfully adopting this approach.

---

<sup>57</sup> SPF30 is also known as SMNDC1.

## Part II- The Writer

### **4 Chapter 4- Characterizing a gain-of-function PRMT5 OE mouse and the effect on HCC**

PRMT5 is the major type II arginine methyltransferase responsible for virtually all SDMA in the cell. MEP50 is an essential cofactor for the methylosome complex. Much of our understanding of the protein has come from knockout studies and cancer related studies. Both approaches reveal PRMT5 is essential for life and has important roles in disease. While PRMT5 loss is detrimental, *Prmt5 OE* is associated with oncogenic pathways and tendencies<sup>58</sup>. However, the impact of PRMT5 to promote *de novo* disease has yet to be determined. PRMT5 related proteins and pathways are important in the liver, sparking our interest in the potential role of *Prmt5* in hepatocarcinogenesis. *Prmt5 OE* is thought to be disease promoting. **We hypothesize that liver-specific *Prmt5 OE* will result in hypermethylation of substrates that lead to changes in transcription and splicing.** Related to disease, **we hypothesize that liver-specific *Prmt5 OE* will sensitize hepatocytes to develop HCC.** Follows is the generation and functional validation of a liver-specific *Prmt5 OE* GEMM and induced HCC modeling to study the impact of *Prmt5 OE* on tumor formation. The results of these experiments provide valuable insight into PRMT5 biology for normal and diseased states.

#### **4.1 Generation and validation of a *Prmt5 OE* GEMM**

There is a plethora of tissue-specific PRMT5 knockout mouse models (see **Table 1**). However, *Prmt5 OE* studies have, to date, been restricted to tissue culture methods and bacterially derived vectors. There has yet to be published a genetically engineered PRMT5 overexpressing mouse model. One of the challenges of creating an active *Prmt5 OE* system is that PRMT5 requires the cofactor MEP50 for protein stability and enzymatic activity (17, 89) . To meet this need, the Vokes Lab from the University of Texas, Austin, developed a tissue-specific

---

<sup>58</sup> These include increased proliferation and survival, repression of tumor suppressors.

inducible *Prmt5 OE* mouse model. This was done by generating a PRMT5-MEP50 conditionally activatable vector (see appendix B for plasmid map and sequence). The construct contains a Lox-Stop-Lox sequence preceding a V5-tagged murine *Prmt5* (V5-PRMT5), followed by an internal ribosomal entry site (IRES) and murine *Mep50* (MEP50<sup>trans</sup>) sequence (**Figure 12a**). Thus, *Prmt5 OE* can be selectively induced through constitutively active tissue-specific or drug induced-Cre expression. This construct was cloned and ligated into a Rosa26 targeting vector to allow homologous recombination of the transgene into the genome. This KI vector was transfected into embryonic stem cells and subjected to antibiotic selection. Resistant cells were genotyped to identify those that had undergone homologous recombination. These cells were microinjected into a blastocyst and transferred into female mice<sup>59</sup>. The resulting chimeric pups were bred to create heterozygous founders. Transgenic mice were PCR genotyped using primers against the entire V5-tag, beginning at the second *loxP* site and ending within the V5-*Prmt5* transgene. We received mice from the Vokes lab and confirmed genotyping by their standard. To confirm insertion of the entire transgene and to check for mutations, the length of the transgene was divided into five sections and new primers designed with overlapping ends of 50-100bp<sup>60</sup> (**Figure 12b**). PCR amplicons of each section of transgene were Sanger sequenced and revealed complete inclusion of the construct and was free from mutation.

In chapter 3, we describe how loss of SND1 Tudor domain was hepatoprotective against carcinogen-induced HCC. It has been shown that *Snd1 OE* can induce HCC and drive tumor formation (129). As the SND1 Tudor domain is important in the liver and is well established as an SDMA binder, and as PRMT5 is the primary enzyme responsible for adding SDMA in the cell, we sought to determine if *Prmt5 OE* could phenocopy *Snd1 OE* in the liver. We crossed and backcrossed albumin-cre (Alb-cre) mice from a Swiss-Webster background into B6/C3H mice<sup>61</sup>.

---

<sup>59</sup> Of note, these B6/C3H mice were heavily mixed. Extensive inbreeding periodically gave rise to traditional B6 colors, but most mice maintained B6/C3H pattern, especially when crossed with Cre-containing mice.

<sup>60</sup> IRES contain highly repetitive sequences that are difficult to sequence and can be problematic in PCR amplification. Accordingly, this section of the transgene was excluded from PCR amplification and subsequent sequencing.

<sup>61</sup> These Alb-cre mice were a gift from the David Johnson lab.



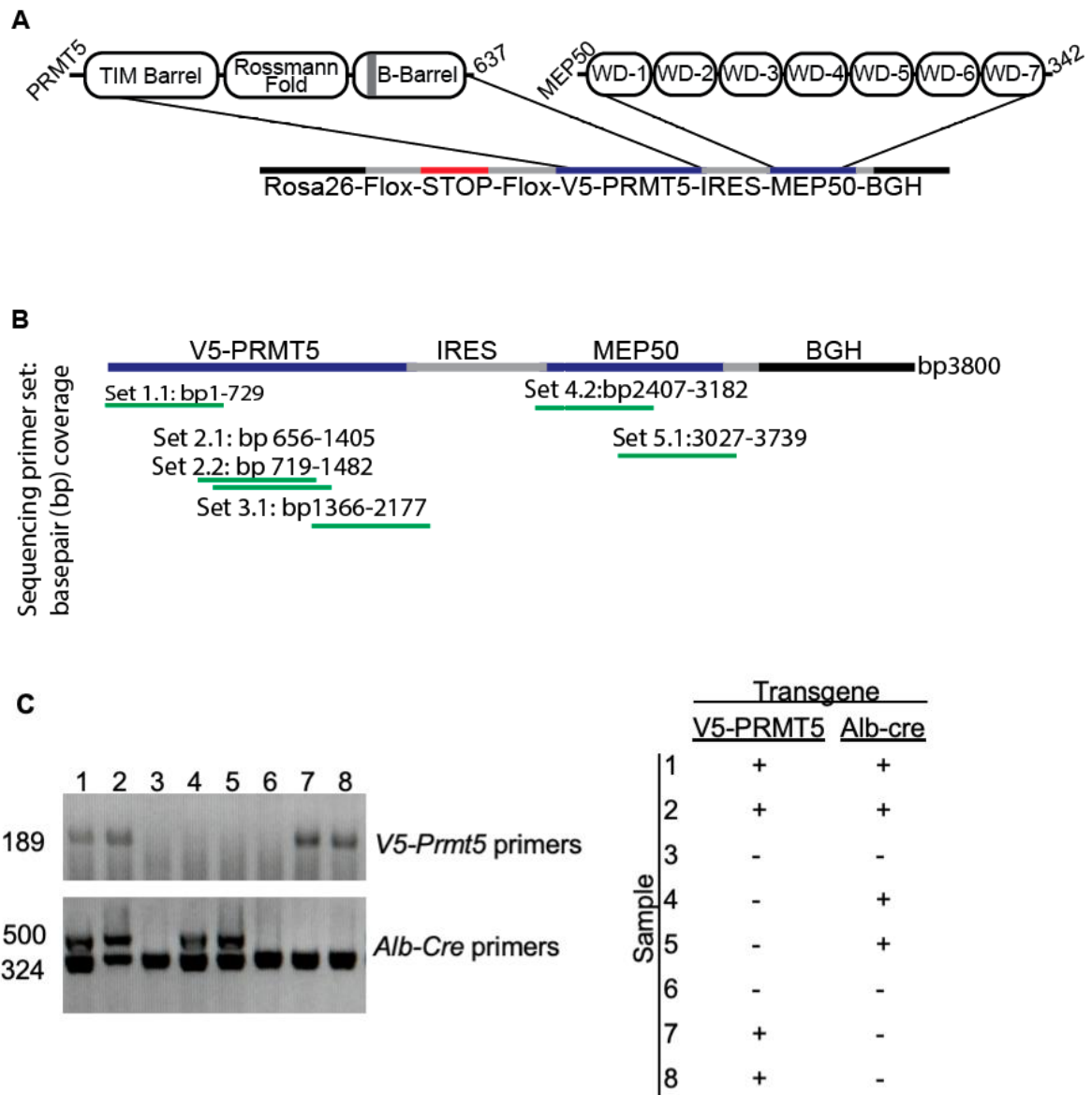


**Figure 12- *Prmt5*<sup>OE</sup> GEMM design and sequence validation. a) *Prmt5*<sup>OE</sup> transgene schematic. b) *Prmt5* transgene amplicon design. Predicted amplicon coverage in green and base pair (bp) coverage. Primer set 2.2 was included to cover a short section of DNA with limited coverage by sets 2.1 and 3.1. c) Genotyping pups from a B6/C3H<sup>PRMT5/WT</sup> heterozygous mice crossed with B6/C3H<sup>Alb-Cre/WT</sup> heterozygous mice showing all four possible genotypes. 500bp band represents Alb-cre transgene. Lower 324bp band is an internal PCR control to confirm presence of DNA. B6/C3H<sup>PRMT5/Alb-cre</sup> (*PRMT5*<sup>OE</sup>) in samples 1 and 2. B6/C3H<sup>PRMT5</sup> in 7 and 8. B6/C3H<sup>Alb-cre</sup> in 4 and 5. B6/C3H<sup>WT</sup> (negative for both transgenes) in 3 and 6.**

Following these backcrosses, the F4 generation of Alb-cre mice were crossed with the PRMT5 transgenic mice to investigate the PRMT5 axis in the liver. Resulting pups had three possible genotypes with normal PRMT5 expression: B6/C3H without either transgene, B6/C3H with only the *V5-Prmt5* transgene (B6/C3H<sup>PRMT5</sup>), and B6/C3H with only Alb-cre transgene (B6/C3H<sup>Alb-cre</sup>) (these three are collectively referred to hereafter as PRMT5<sup>WT</sup>, or WT). Only pups containing both the *V5-Prmt5* and *Alb-Cre* transgene could express the V5-PRMT5 transgene (B6/C3H<sup>PRMT5/AlbCre</sup>, hereafter called PRMT5<sup>OE</sup>, or OE) (**Figure 12c**).

We sought to confirm and quantify tissue specific OE of PRMT5 in the liver. By western blot, *Prmt5*<sup>OE</sup> liver tissues revealed a 75 kDa doublet corresponding to endogenous and V5-tagged PRMT5. Neither the doublet nor V5-tagged protein were observed in *Prmt5*<sup>WT</sup> samples (**Figure 13a** first, second and third row; **b**, quantification). Total MEP50 was increased only in *Prmt5*<sup>OE</sup> samples (**Figure 13a** fifth row; **c**, quantification). Comparing total PRMT5, endogenous protein (lower band, first and third row) was significantly increased in *Prmt5*<sup>OE</sup> over *WT* samples (**Figure 13a,b**). This observation can be explained by the increase of total MEP50 enabling the stabilization of the endogenous protein. Knockdown of PRMT5 or MEP50 will concomitantly decrease expression of the other, so this finding fits with reciprocal observations (88).

We sought to confirm that the V5-PRMT5 protein was enzymatically active. However, as PRMT5 dimerizes with itself, we were unable to separate ectopically expressed PRMT5 from endogenous enzyme. Rather, we used a variation of a traditional *in vitro* methylation assay to assess total PRMT5 activity using whole-cell lysate to look at ectopic plus endogenous PRMT5 activity<sup>62</sup>. We used recombinant histone H4 as substrate combined with adenosyl-L-methionine, S-[methyl-<sup>3</sup>H] (<sup>3</sup>H-SAM) in the presence of *Prmt5*<sup>WT</sup> or *Prmt5*<sup>OE</sup> whole-cell lysate from livers as the PRMT5 enzyme source. We also included a Type-I arginine methyltransferase inhibitor, MS023, to exclude potential methylation signal from enzymes other than PRMT5. Recombinant

---

<sup>62</sup> For reference, a traditional *in vitro* methylation assay includes recombinant substrate, along with adenosyl-L-methionine, S-[methyl-<sup>3</sup>H] as a radioactive label, and purified enzyme from either bacterial or mammalian cells. The resultant methylation from this biochemical assay can be visualized using PAGE and flouorography.

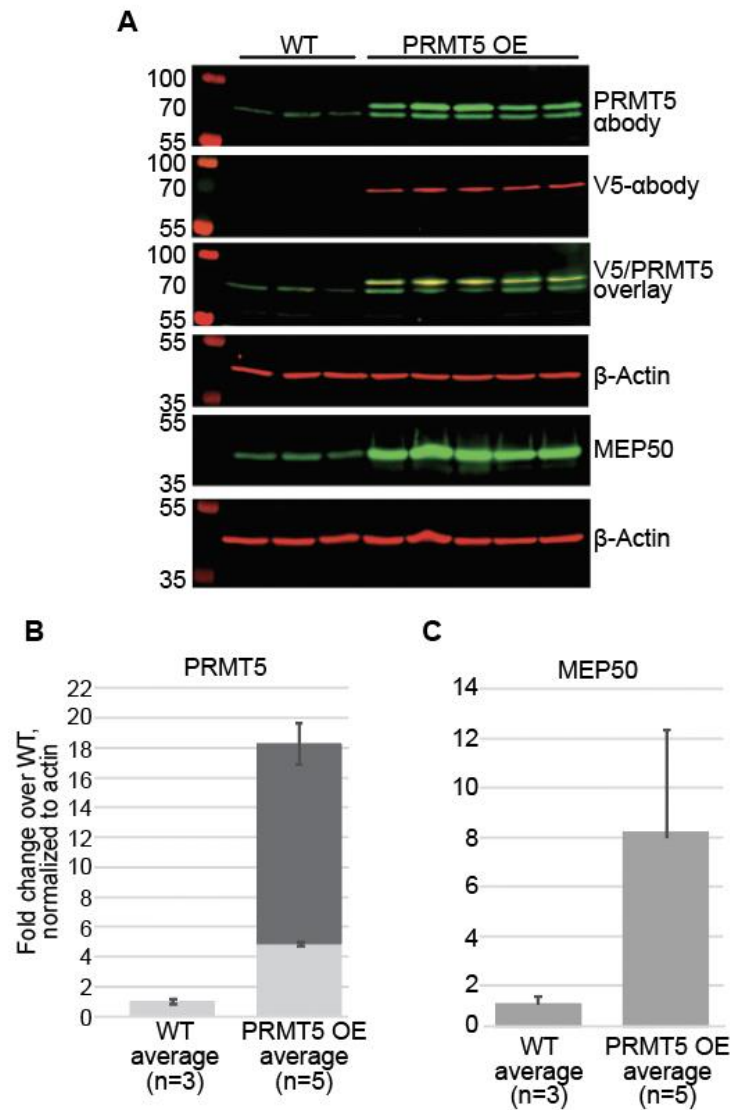


**Figure 13-** Western blot and quantification for *Prmt5<sup>WT</sup>* and *Prmt5<sup>OE</sup>* from whole-cell lysate tissues. **a)** Western blot of whole-cell lysate from livers from respective genotypes. **b)** Fold change of endogenous and V5-PRMT5 normalized to actin. Quantified using LI-COR quantification tool. **c)** Fold change quantification of total MEP50 over *Prmt5<sup>WT</sup>* samples normalized to actin. Quantified using LI-COR quantification.

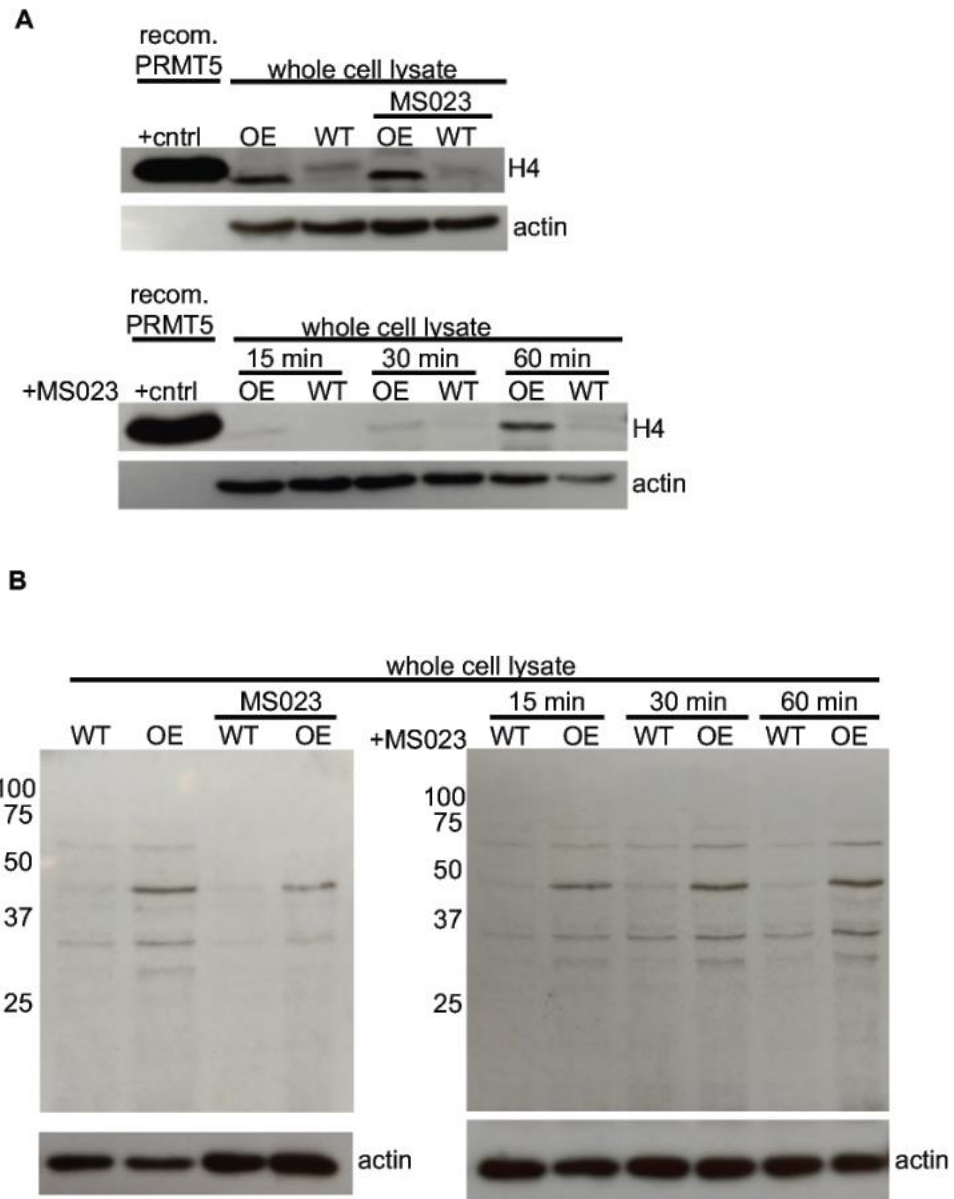


**Figure 14-** *In vitro* methylation of recombinant H4 by *Prmt5<sup>WT</sup>* and *Prmt5<sup>OE</sup>* liver whole-cell lysate. **a)** Positive control (+cntrl) recombinant PRMT5/MEP50 with recombinant H4 (H4) substrate and <sup>3</sup>H-SAM. Top, whole-cell-lysate with added H4 in *Prmt5<sup>OE</sup>* or *Prmt5<sup>WT</sup>* whole-cell lysate with or without Type I PRMT inhibitor (MS023). H4 blot is the fluorograph of the radioactive signal, and actin loading a western blot of the same membrane. Bottom, time course stopping the reaction at 15 min, 30 min, or 60 min respectively all in the presence of MS023. **b)** Complete fluorograph (and loading western below) of whole cell lysate without H4 substrate with and without MS023 (left) and time course with MS023 (right).

H4 methylation was increased in *Prmt5<sup>OE</sup>* sample (**Figure 14a**, top). A time course experiment in the presence of MS023 also showed time-dependent increase of methylation (**Figure 14a**,bottom). Further, we observed an increase in global methylation in *Prmt5<sup>OE</sup>* lysates compared with *Prmt5<sup>WT</sup>* samples (**Figure 14b**). These data, along with our sequencing validation, confirm that the *Prmt5<sup>OE</sup>* mouse is a functional OE GEMM.

In PRMT5 knockdown or inhibition studies, global decrease of SDMA is used to show effective impairment. Conversely, we anticipated that such a dramatic quantitative increase of endogenous and exogenous PRMT5 would result in a marked increase of SDMA. However, MMA and SDMA were only subtly increased in a few targets (**Figure 15a,b** respectively). This raised an important functional question about the role of excess PRMT5 in the cell. While PRMT5 is indispensable for most cell types, it is unknown if increased PRMT5 protein level corresponds to increased SDMA levels.

As a baseline, we tested global methylation of several different cell types of different tissue origins (**Figure 16**). While PRMT5 levels were consistent between cell types, SDMA levels differed substantially. This supports that PRMT5 methylates targets in a tissue specific manner. Transient transfection of myc-tagged PRMT5 (myc-PRMT5) in HEPG2 and HEK293T (293T) cells resulted in abundant accumulation of myc-PRMT5 in these cell types<sup>63</sup> (**Figure 17, Figure 18** respectively). Yet, even with discernibly increased PRMT5 by western blot, a concomitant global hypermethylation was not observed<sup>64</sup>. Changes in MMA and ADMA were not detected.

Taken together, the *Prmt5<sup>OE</sup>* mouse is a functional PRMT5 overexpressing GEMM. These mice exhibit an eighteen-fold increase in total PRMT5. PRMT5 OE in these mice as in HepG2 and 293T cell lines results in minor hyperproliferation of a few targets. These might suggest that SDMA levels are heavily methylated with normal PRMT5 levels and increasing PRMT5 does not increase SDMA levels.

---

<sup>63</sup> This myc-PRMT5 vector is very high expressing and is the standard vector used to purify PRMT5 from mammalian cells for *in vitro* methylation assays.

<sup>64</sup> PRMT5 OE was quantified as >10 and >200 fold increase in HepG2 and HEK293T lines respectively. Quantification included in appendix C.

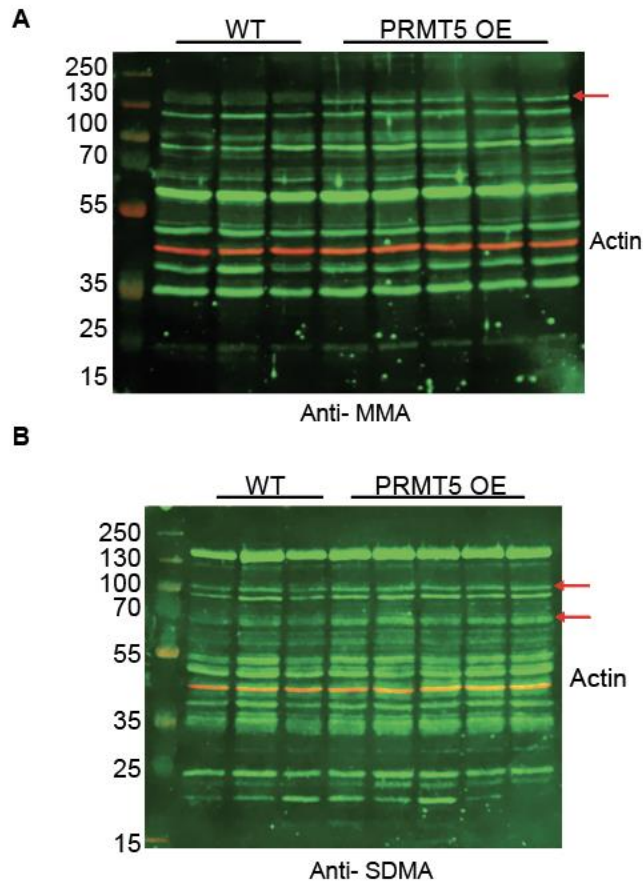


**Figure 15-** Type II methylation of *Prmt5 OE* liver tissues. **a)** Western blot of whole-cell lysate from *Prmt5<sup>WT</sup>* and *OE* mouse livers from **Figure 13a** probing for monomethyl arginine (MMA) using a custom  $\alpha$ -pan-MMA antibody.  $\alpha$ MMA rabbit primary antibody and  $\alpha$ - $\beta$ -actin mouse primary antibody allow co-immunoblotting of target and loading control. **b)** Whole-cell lysate western blot from **Figure 13a** tissues against symmetric dimethylarginine (SDMA) using a custom  $\alpha$ -pan-SDMA antibody.

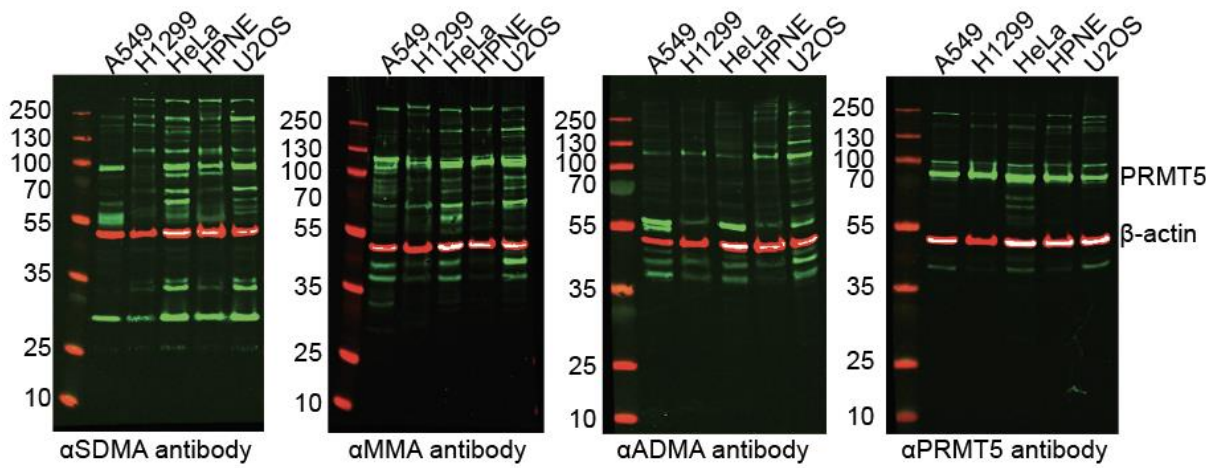


**Figure 16-** Pan-tissue methylarginine comparison. Western blot of equal cell counts of A549, H1292, HeLa, and U2OS cell lines compared for SDMA, MMA, ADMA, or PRMT5 respectively.

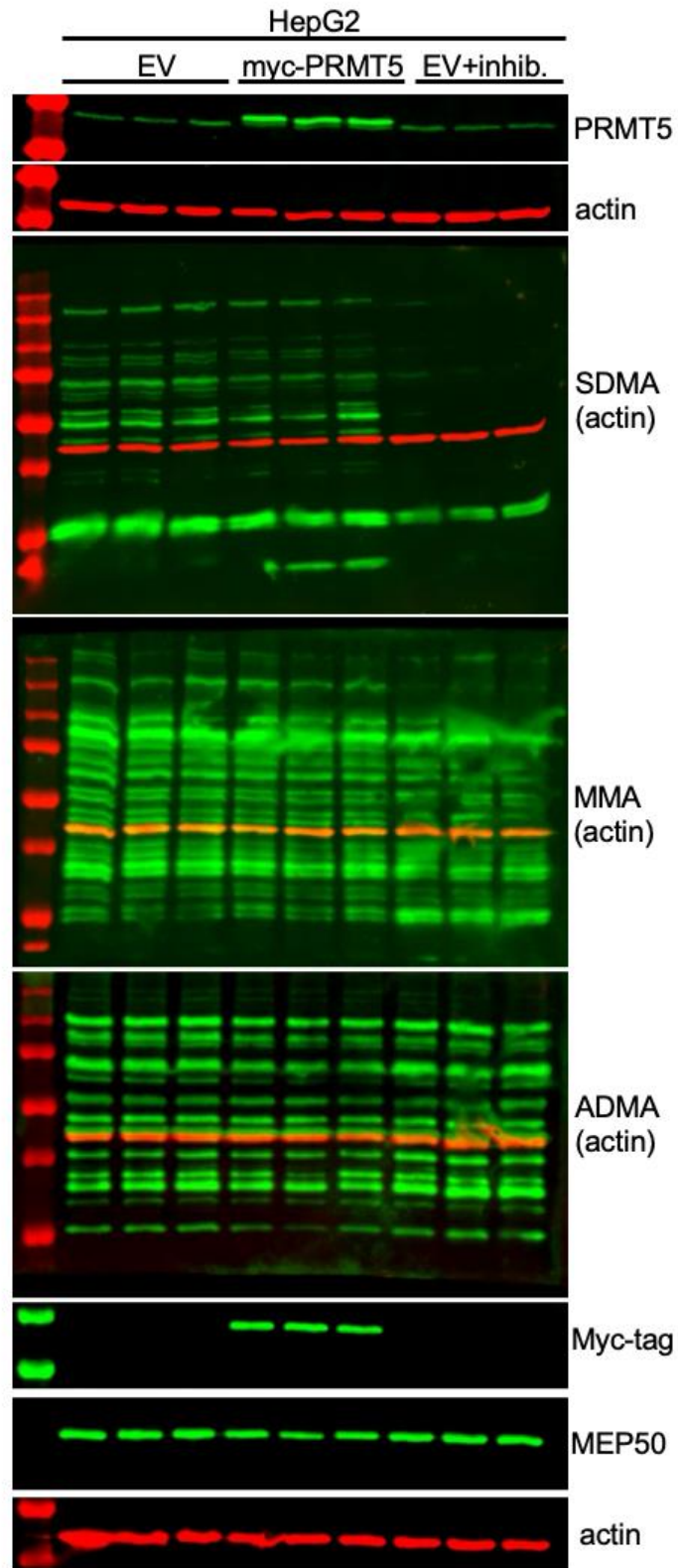


**Figure 17-** Hypermethylation analysis in myc-PRMT5 overexpressing HepG2 cells. Three 35mm wells were transfected with empty vector (EV), myc-tagged PRMT5 (myc-PRMT5), or EV plus 10uM Epz015666 (inhib.) PRMT5 inhibitor in triplicate. Cells were harvested after 72 hours and probed with respective antibodies.



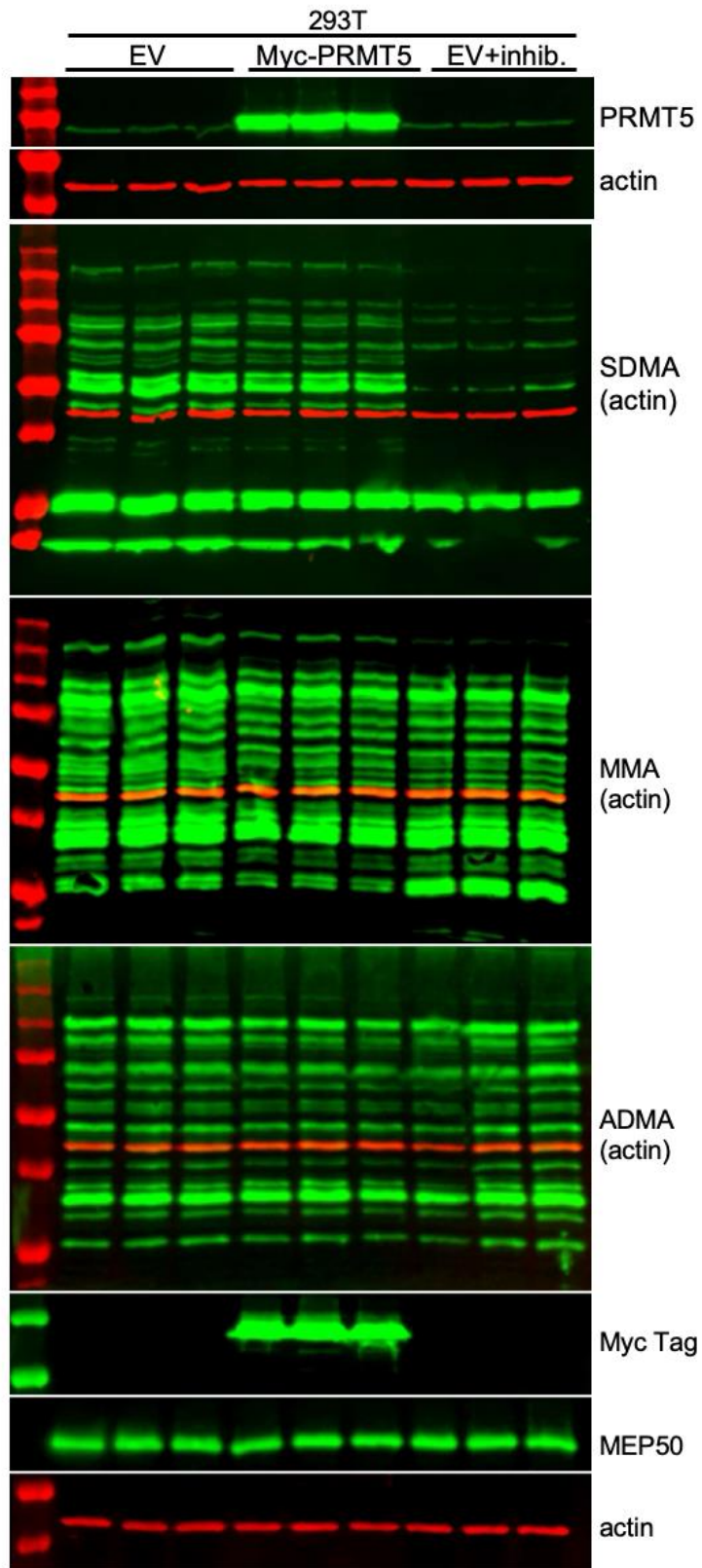


**Figure 18-** Hypermethylation analysis in myc-PRMT5 overexpressing HEK293T (293T) cells. Three 35mm wells were transfected with empty vector (EV), myc-tagged PRMT5 (myc-PRMT5), or EV plus 10uM Epz015666 (inhib.) PRMT5 inhibitor in triplicate. Cells were harvested after 72 hours and probed with respective antibodies.

## 4.2 Transcriptional analysis of PRMT5 OE GEMM

PRMT5 is known to regulate transcription by methylating histones and transcription factors. Further, splicing proteins are known to be symmetrically dimethylated by PRMT5. Loss of PRMT5 results in altered transcriptional profiles and splicing (5). To determine if *Prmt5* OE could inversely alter either of these processes, we performed RNA-sequencing (RNA-seq) of total RNA collected from the livers of three two-month-old *Prmt5*<sup>WT</sup> and *Prmt5*<sup>OE</sup> male mice and compared the expression profiles to each other.

We visualized the DE genes by volcano plot and observed limited changes in transcriptional regulation (**Figure 19**). Principle component analysis of *Prmt5*<sup>OE</sup> to *Prmt5*<sup>WT</sup> samples did not cluster into distinct genotypes (not shown). Thus, transcriptional differences between genotypes were limited.

### 4.2.1 Alternative splicing in *Prmt5* OE livers

To determine if splicing was impacted by *Prmt5* overexpression, alternative splicing events were identified using replicate multivariate analysis of transcript splicing (rMATS) for *Prmt5*<sup>OE</sup> and *Prmt5*<sup>WT</sup> mice. This approach allows for both calling of splicing events and visualization of global changes to splicing.

To explain the visualization, alternative splicing events are determined by aligning sequencing reads and categorizing variations between WT and experimental (in our case OE) RNA samples. These events are divided into five categories being alternative 3'/5' splicing sights (A3SS or A5SS respectively), mutually exclusive exons (MXE), retained introns (RI), or skipped exons (SE). The read counts are then normalized for each gene individually. The difference of the normalized counts is reported as the 'inclusion level'. An 'inclusion level' that is less than zero is enriched in experimental samples while a level of greater than zero is enriched in normal samples. A false discovery rate (FDR) is also calculated for each counted gene to determine

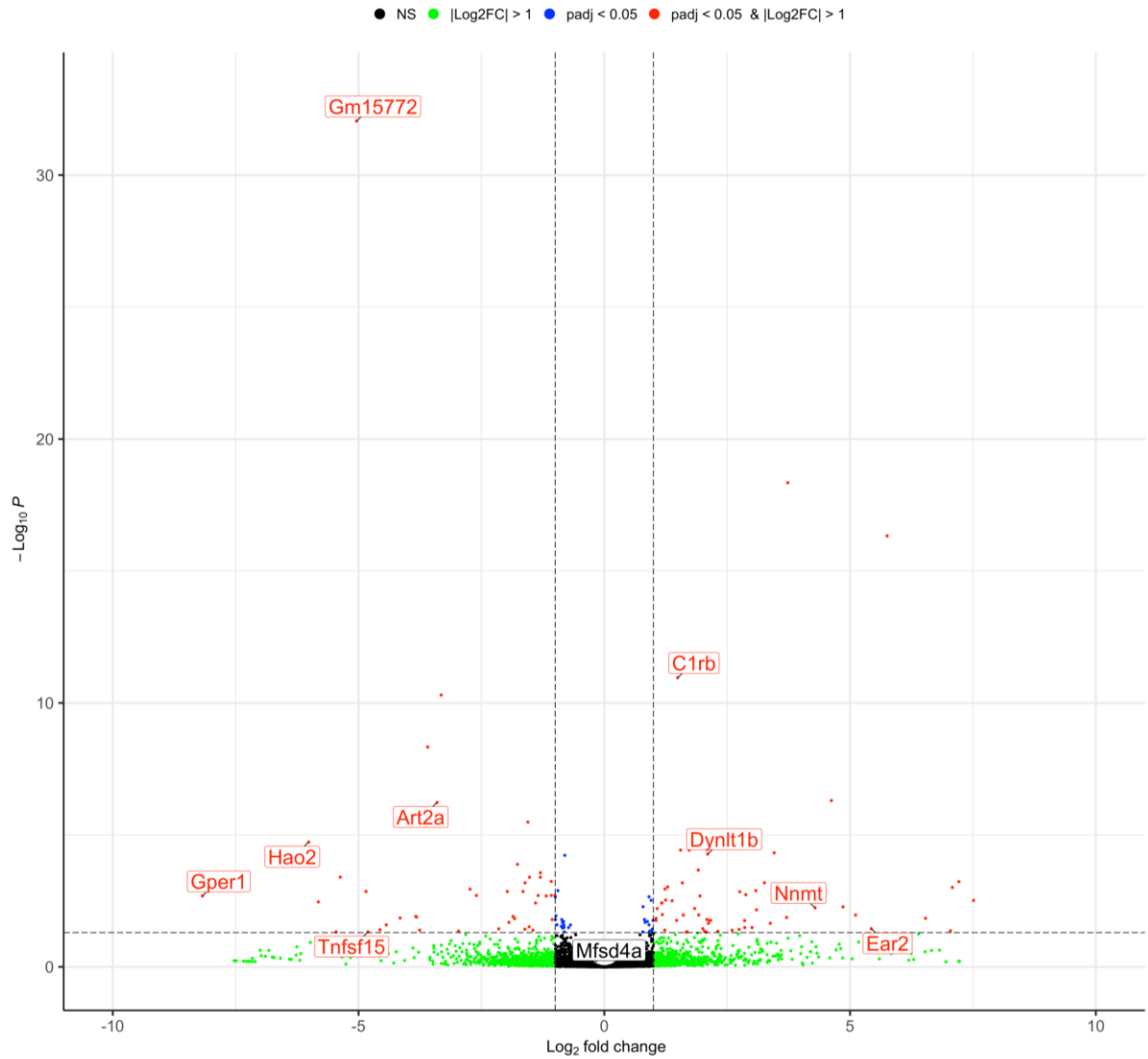


**Figure 19**-Volcano plot of differentially expressed (DE) genes from *Prmt5*<sup>OE</sup> mice liver. Top DE genes identified in red. DE upregulated genes, 42. DE downregulated genes, 52.

statistical significance<sup>65</sup>. Using a FDR of <0.1, the 'inclusion level' of significant splicing events can be visualized for global changes in splicing. A skewing of the average inclusion level, or in the distribution of significant events, will indicate a substantial shift in alternative splicing. As a second measure, graphing the significant FDR can show a change in distribution of significant events as a measure of confidence in called events. A skew towards zero indicates greater confidence in accurate calling of splicing events.

Comparing the splicing events from *WT* to *OE* mice, we graphed the 'inclusion level' of significant events with a false discovery rate (FDR) of <0.1. Distribution of 'inclusion level' were not skewed to either genotype across the five alternative splicing event types (**Figure 20a**). Further, the FDR distribution of all significant splicing events skew towards 0, indicating that false positives are unlikely for identified splicing events (**Figure 20b**). We identified the top DE genes in *OE* mice relative to *WT* and compared these to the genes with significant alternative splicing (FDR <0.1). None of the top dysregulated genes from *OE* mice had alternative splicing with a FDR <0.1. Taken together, *Prmt5 OE* in the liver had limited effect on splicing and transcription which may reflect the fact that we do not observe a major impact on SDMA level, upon PRMT5 OE.

### 4.3 PRMT5 OE carcinogenesis models

PRMT5 is involved in many different cancer types (**Table 3**). In most of these settings, PRMT5 level is correlated with a worse prognosis, and knockdown or inhibition is cytotoxic to cells. There is preliminary evidence that PRMT5 plays a role in HCC by impacting some of the pathways that drive HCC. However, the previous work implicating PRMT5 in cancer has been in established cancer settings. It has yet to be identified if PRMT5 is able to function as a *de novo*

---

<sup>65</sup> Working with large data sets, multiple testing limits the effectiveness of standard statistical p-values, especially with gene sets which have thousands of tests. One method for resolving multiple testing is to use FDR cut offs in place of p-values. Typically, a FDR of <0.1 is used as a significance cut off.

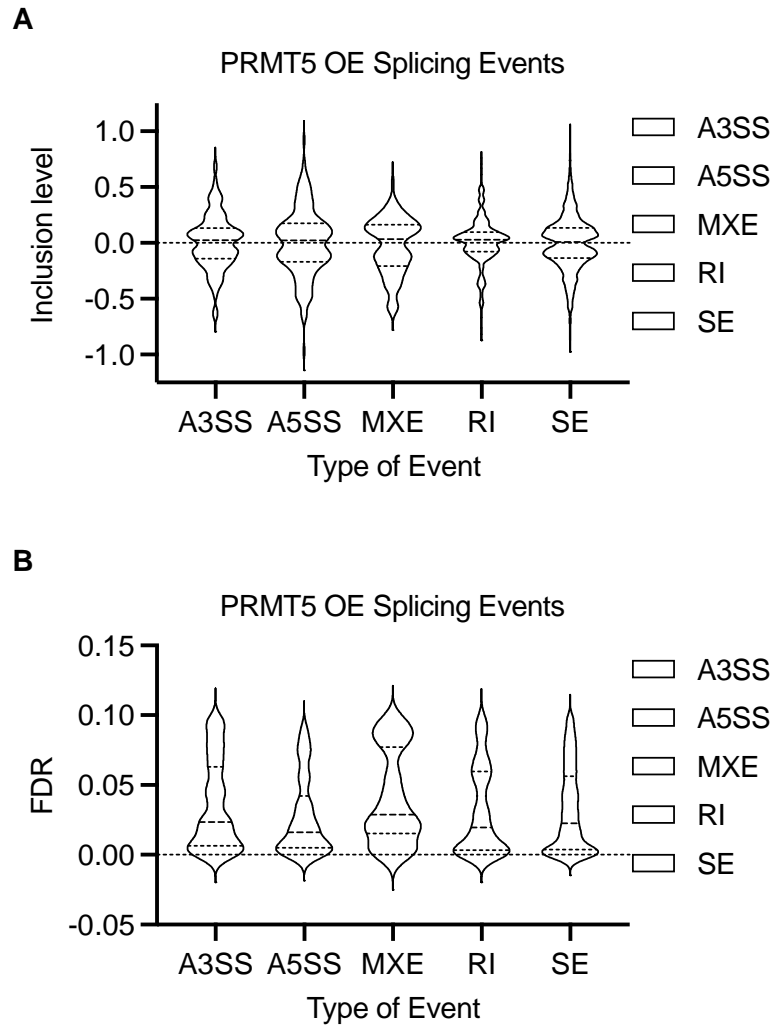


**Figure 20-** *Prmt5*<sup>OE</sup> alternative splicing events. Events are noted as alternative 3' start site (A3SS), alternative 5' start site (A5SS), mutually exclusive exons (MXE), retained introns (RI), and skipped exons (SE). **a)** Inclusion level is the difference between reads from WT to OE samples. An inclusion level that is less than 0 is enriched in OE samples while a level >0 is enriched in WT samples. Splicing events, n= A3SS (230); A5SS (166); MXE (88); RI (219); SE (785). **b)** False discovery rate (FDR) for splicing events in **a**.

oncogenic driver in the liver. We sought to determine if *Prmt5 OE* itself could drive tumorigenesis in non-cancer transformed cells.

#### 4.3.1 PRMT5 OE in unchallenged normal mice

Previous work has correlated PRMT5 level with disease progression in established liver cancer settings. However, whether *Prmt5 OE* can drive tumor formation in non-cancerous tissues has yet to be determined. *Snd1 OE* mice developed spontaneous HCC lesions in 50% of male mice at 12-months-old. Additionally, for other GEMMs with spontaneous HCC formation, macroscopic tumors develop in a range of 4-20 months. *Prmt5<sup>OE</sup>* mice had no gross or histologically evident tumors up to 18 months, and livers appeared healthy like *Prmt5<sup>WT</sup>* littermates (data not shown). This indicated that alone, *Prmt5 OE* in the liver was insufficient to drive neoplastic growth.

Clinical HCC forms in the background of other hepatic diseases like cirrhosis, hepatitis, and fibrosis. Genetic mouse models of HCC can be improved by altering multiple genes. As an example, c-Myc expression in the liver alone is insufficient to drive tumorigenesis, while concomitant knockdown of *Tp53* can drive HCC in a matter of weeks (155). Likewise, addition of carcinogen can stimulate carcinogenesis and reduce tumor latency (181). While *Prmt5<sup>OE</sup>* mice did not develop spontaneous tumors, this did not preclude that *Prmt5 OE* may predispose hepatocytes to develop tumors upon exposure to carcinogen exposure or hepatic insult.

#### 4.3.2 Carcinogenesis modeling by DEN-induced HCC

As described in chapter 3, we performed DEN injections in both *Prmt5<sup>WT</sup>* (including both B6/C3H<sup>PRMT5</sup> and B6/C3H<sup>Alb-cre</sup> genotype) and *Prmt5<sup>OE</sup>* mice<sup>66</sup>. *Prmt5<sup>WT</sup>* and *Prmt5<sup>OE</sup>* livers were grossly indistinguishable, developing many surface nodules in both lines (**Figure 21a**). To compare tumor burden and the extent of neoplastic growth between *Prmt5<sup>WT</sup>* and *Prmt5<sup>OE</sup>* mice

---

<sup>66</sup> For reference, two-week-old pups receive a single intraperitoneal injection of DEN and age for 9 months.

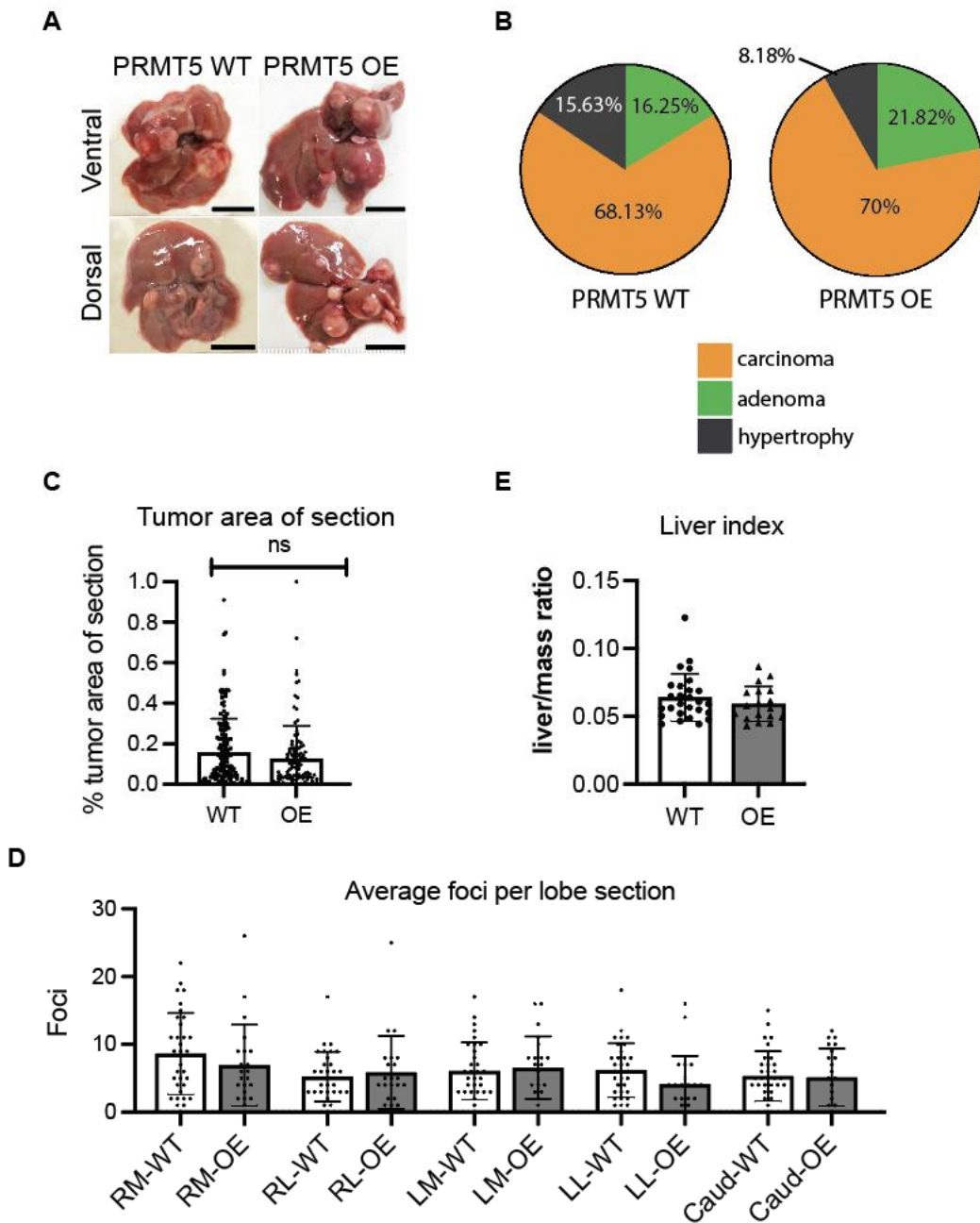


**Figure 21-** *Prmt5*<sup>OE</sup> vs *Prmt5*<sup>WT</sup> pathology and tumor burden for DEN injected mice: **a)** Only males were used for injection studies. n=WT (33); OE (22). Representative images of liver and gallbladder (scalebar 1cm). Images courtesy edited. **b)** Ratio of observed pathologies from liver lobe sections representing all 265 lobes from 53 mice (lobes/mice n= WT (155/31); OE (110/22)). **c)** Percent tumor area per section area of all tumor types from the livers in b obtained using ImageScope and plotted as the ratio of tumor to liver area. Software calculated areas were used for statistical test; Statistical t-test, two-tailed, unpaired. **d)** Number of tumor foci per lobe section from liver sections in b. Sections with hepatocellular hypertrophy had no foci. Statistical t-test, two-tailed, unpaired. **e)** Ratio of liver plus gallbladder mass to total mouse mass representing the livers in b. Mouse liver mass obtained post-sacrifice, prior to further manipulation. Statistical t-test, two-tailed unpaired.

we followed the pipeline established for the *Snd1* mutant mice (described in 3.4.1)<sup>67</sup>. Binned pathologies revealed a small tendency towards disease in *Prmt5*<sup>OE</sup> mice over *WT* samples with carcinomas (70% vs. 68.13%, respectively) and adenomas (21.82% vs. 16.5%, respectively) being slightly elevated. (**Figure 21b**). Hypertrophy was slightly decreased (8% vs. 15.63%, respectively). However, the mean ratio of tumor to section area was not significantly different (**Figure 21c**). Also, we compared the number of foci by individual lobes, and saw no lobe had a significant change in number of tumors between genotypes (**Figure 21d**). As a last comparison of tumor burden, liver index was also unchanged (**Figure 21e**).

Taken together, *Prmt5 OE* was insufficient to drive an exacerbated tumorigenic response in DEN-induced HCC. This implies that PRMT5 may not have a driving role in promoting liver disease.

#### 4.3.3 BrdU injection to measure *Prmt5*<sup>OE</sup> liver proliferation

Unchecked cellular proliferation is a common metric to show improved cancer forming capacity. High PRMT5 levels are generally thought to increase proliferation, while targeting PRMT5 by SMI or siRNA decreases proliferation<sup>68</sup>. We sought to determine if *Prmt5 OE* might impact cellular proliferation in hepatocytes, and further, if hepatocytes might respond with a proliferative response to carcinogen treatment<sup>69</sup>. Two-week-old pups were injected with BrdU, or DEN+BrdU. *Prmt5*<sup>OE</sup> livers did not exhibit increased proliferation with or without DEN treatment as measured by BrdU incorporation (**Figure 22**). It remains to be determined why PRMT5 OE in hepatocytes suppressed proliferation in response to DEN treatment.

---

<sup>67</sup> For reference, the pipeline is described as follows: “we sectioned all five liver lobes from each mouse and performed H&E staining on each section. These sections were digitally scanned with an Aperio AT2 slide scanner and analyzed with ImageScope software to determine the number of tumor foci and the ratio of tumor to tissue area for each section. These images were then read and scored by a pathologist for tumor type.” See pg 43

<sup>68</sup> Proliferation sensitive cancer types include: lung (Liu, et al.,2021), breast (Han, et al., 2020), glioblastoma (Yan, et al.,2014), hepatic and colorectal cancers (Ji, et al., 2017).

<sup>69</sup> Two-week-old pups are still developing their digestive organs and thus have residual cellular growth in the liver. It was unknown if *Prmt5 OE* might increase or decrease this residual growth.



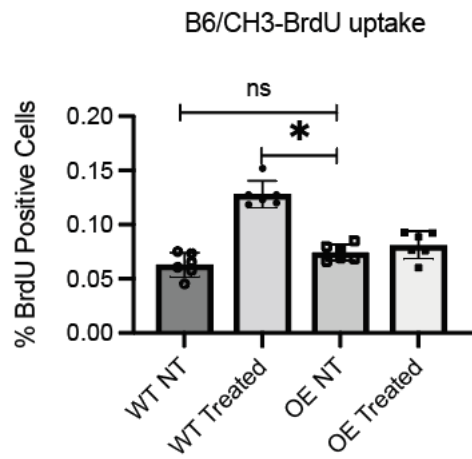


**Figure 22-** Proliferation of *Prmt5<sup>OE</sup>* livers by BrdU incorporation. For each experimental condition, n=3, each sample counted twice. Counting area of 600umx700um, ~1300 cells per count. Statistical t-test, two-tailed unpaired, P value \*<0.05.

#### 4.3.4 Hydrodynamic tail vein injection

*Prmt5* OE was insufficient to drive an exacerbated tumorigenic response in DEN-induced HCC. However, we could not exclude the possibility that a clinically relevant genetic predisposition to cancer may provide a permissible setting for PRMT5 driven HCC. We identified hydrodynamic tail vein injection (HTVi) as a means of inducing HCC with a targeted genetic perturbation. HTVi is a recently developed method for introducing self-incorporating oncogenic plasmids which recapitulate genetic drivers of liver cancer and can be applied to any genetic background to study tumorigenesis<sup>70</sup>. In brief, oncogenic *MYC* (*c-myc*),  $\alpha$ *Tp53* siRNA, and SB encoded vectors are diluted in a large volume of saline and tail vein injected into adult mice in a few seconds<sup>71</sup> (155)<sup>72</sup>. This over-pressurizes the capillaries leading to cardiac congestion, and capillaries dilate for the liver to uptake the excess fluids, including the oncogenic plasmid<sup>73</sup> (156, 198). SB transposes *c-myc* and  $\alpha$ -*Tp53* sequences into the genome of hepatocytes, and results in developing tumors in 21-30 days (155). As *Tp53* alterations and *c-myc* contribute to approximately 40% of HCC combined, HTVi is a suitable alternative for looking at the effect of *Prmt5* OE in a system genetically predisposed to develop HCC.

We injected four-week-old *Prmt5*<sup>WT</sup> and *Prmt5*<sup>OE</sup> with 10ug *c-Myc*, 10ug  $\alpha$ *Tp53*, and 2.5ug SB vectors into a pilot study number of male mice (see appendix B for plasmid maps) (**Figure 23a**). Thirty days post-injection, mice were severely diseased with aggressive hepatic malignancies. However, we were unable to identify substantial differences between tumorigenesis in *Prmt5*<sup>OE</sup> and *Prmt5*<sup>WT</sup> samples (**Figure 23b**).

---

<sup>70</sup> This approach was described in 1999 to deliver luciferase reporter plasmid to the liver (Liu, et al., 1999). This was followed by proposing this as a means of gene therapy but has most recently been suggested as a means of studying carcinogenesis (Molina-Sánchez, et al., 2020).

<sup>71</sup> For reference, mice are injected with 10% of their body mass in volume. Thus, a 20g mouse would receive a 2mL injection of plasmid diluted in 0.9% saline.

<sup>72</sup> This group recently tested combinations of 23 oncogenes and tumor suppressors and found 9 combinations that resulted in liver tumor formation. Among these combinations, *c-myc* and  $\alpha$ -*Tp53* were among the most potent combinations at generating liver tumors.

<sup>73</sup> The large volume is also thought to dilute cytoplasmic nucleases which degrade cytoplasmic DNA. Experiments with smaller injection volumes have lower transfection efficiency, even when increasing the concentration of injected DNA (Lecocq, et al., 2003).

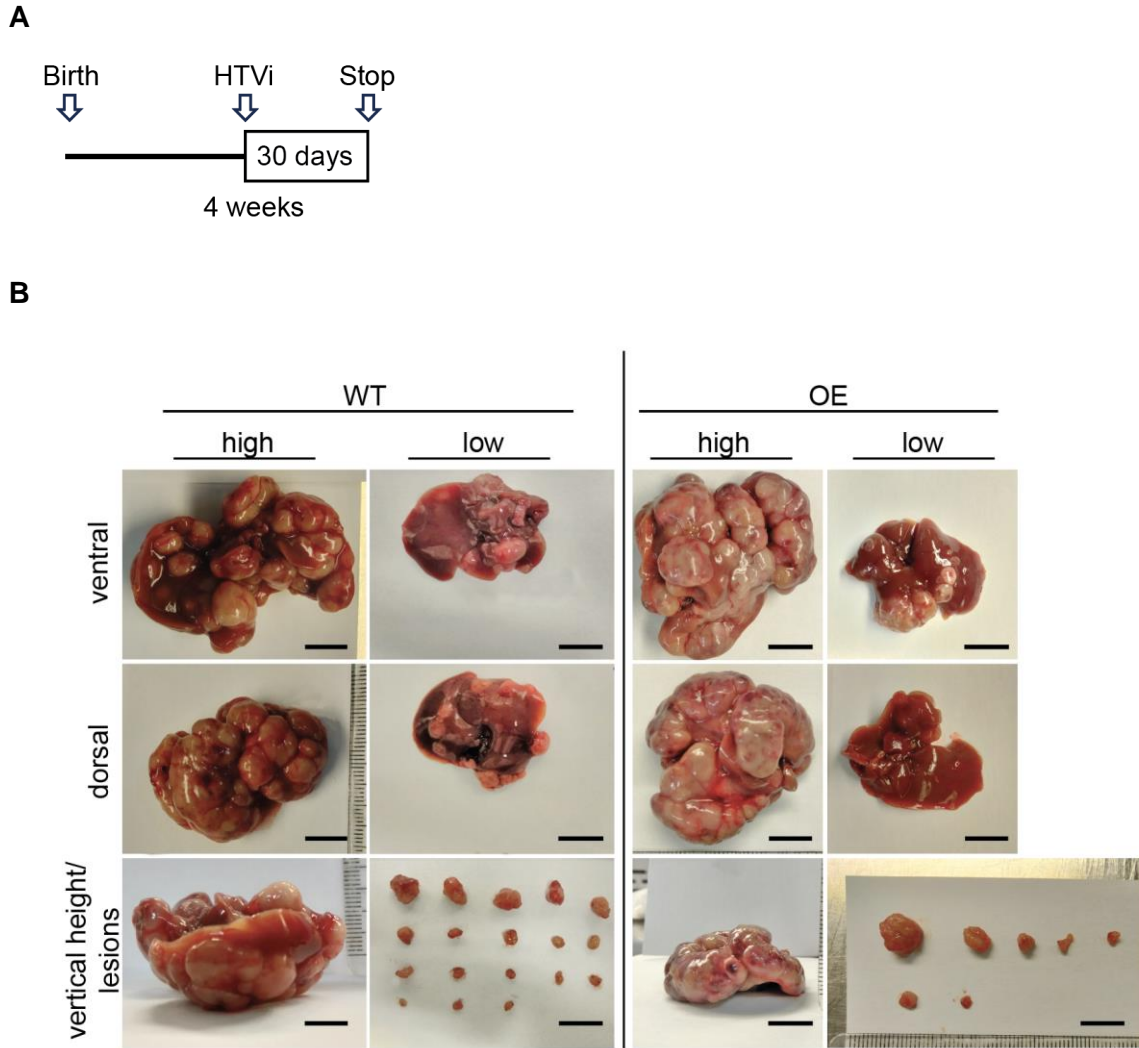


**Figure 23-** Hydrodynamic tail vein injection (HTVi) of *Prmt5<sup>OE</sup>* and *WT* mice: **a)** Visual schematic of injection schedule. **b)** Representative images of *Prmt5<sup>WT</sup>* (n=5) and *Prmt5<sup>OE</sup>* (n=5) mice with most and least aggressive tumorigenesis. Pathology confirmed as HCC. Pathological gross examination describes high tumor burden as “containing multiple expansive vascular masses present in all lobes with extensive fibrotic scarring. Also, displacement of liver tissue with palpable and visible replacement of parenchyma.” Images are courtesy edited. Scale-bar, 1cm.

## 4.4 Discussion

Homeostasis and health are maintained by constantly adjusting the balance of biological macromolecules. PRMT5 is an essential housekeeping gene that provides virtually all the SDMA requirements of the cell. This impacts protein-protein interaction, splicing, transcriptional regulation, and more. Conditional KO is deleterious in every tissue tested (**Table 1**) clearly marking this enzyme as essential for development and life. There remains much to be discovered about how PRMT5 concertos with cellular control for methylation of targets. This work provides new insights into PRMT5 biology.

### 4.4.1 New insights into the control and activity of PRMT5

We generated a liver-specific *Prmt5* OE GEMM. Exogenous V5-tagged PRMT5 and total MEP50 were substantially increased which significantly stabilized endogenous PRMT5. It is generally thought that increase in total PRMT5 may induce hyperproliferation in cells. However, *Prmt5* OE in mouse livers resulted in only a modest increase in SDMA. Using a high protein expressing plasmid encoding myc-PRMT5, we showed that transient PRMT5 OE in HepG2 and Hek293T cells exhibit limited hyperproliferation. This may be due to tight regulation of the enzyme, substrates of PRMT5 being heavily methylated under normal conditions, or adapter protein availability mediating enzymatic activity.

#### 4.4.1.1 Regulation of PRMT5 to mediate methylation

PRMT5 is under considerable control in cells. Phosphorylation and adapter proteins regulate the recruitment of PRMT5 to various substrates (92, 93, 199). **Figure 16** shows extant tissue specific arginine methylation. Further, our whole-cell lysate *in vitro* methylation assay shows an increase in signal after cells were lysed (**Figure 14b**). This is likely from substrates that don't encounter each other within the cell, but which do when the cell is lysed. PRMT5 was found to be localized to the cytoplasm in prostate cancer, and forced re-localization to the nucleus

inhibited growth (200). Indeed, subcellular localization of PRMT5 has a role in disease and development<sup>74</sup>. Determining more about substrate recruitment and PRMT5 localization in specific tissues may ultimately help in developing even more selective PRMT5 inhibitors to target a specific group of substrates or protein-protein interactions. The spatiotemporal control of substrate methylation is an area of ongoing research and is aided by knowing that protein abundance may have less impact on disease than substrate recruitment and activation of the enzyme.

#### 4.4.1.2 *Substrates are heavily methylated with normal levels of PRMT5*

Another potential reason for seeing a minimal increase in global SDMA could be that substrates of PRMT5 are heavily methylated with normal levels of PRMT5. Whole-cell lysate from *Prmt5*<sup>OE</sup> livers (**Figure 15**) or myc-PRMT5 transfected cells (**Figure 17** and **Figure 18**) show hypermethylation of a select few targets. Remaining SDMA-modified substrates show no difference in SDMA<sup>75</sup>. Thus, increasing PRMT5 may have little effect on driving hypermethylation because low levels of PRMT5 are sufficient for heavily methylating most PRMT5 substrates. Indeed, this is supported as *Prmt5*<sup>+/-</sup> (heterozygous) mice are viable and normal, indicating that even half the normal level of PRMT5 is sufficient for cellular SDMA needs (8, 77).

#### 4.4.1.3 *Adaptor proteins availability mediating PRMT5 enzymatic activity*

Adaptor proteins are important for bringing the PRMT5/MEP50 complex and target substrates into proximity for methylation. This allows for spatiotemporal and modular control over symmetric methylation. Several adaptors have been identified including RIOK1 (202), COPR5

---

<sup>74</sup> PRMT5 localization plays an important role in development and specific cell types and is discussed at length here (Stopa, et al.,2015).

<sup>75</sup> Authors note: As with all experiments, these experiments are only as good as the reagents. Pan-methyl antibodies are inherently biased towards the epitope used to generate them. The antibodies used for these experiments may only recognize heavily methylated substrates, or the methylated substrates which are most abundant. However, even if these antibodies are unable to recognize methyl-substrates that are being hypermethylated in PRMT5<sup>OE</sup> mice, there are yet no discernable liver related diseases with hepatic-specific *Prmt5* OE, bringing into question if hypermethylation is important.

(203), pICln (204), Blimp1 (205), Sharpin (206), and OXR1A (207). Mulvaney et al. recently identified a conserved amino acid motif that they term a “PRMT5 binding motif” between RIOK1, COPR5, and pICln that docks into groove in PRMT5 to facilitate methylation (92). Different adaptors facilitate increased methylation of various targets. For instance, COPR5 recruits the PRMT5/MEP50 complex to nucleosomes which is necessary for myogenic differentiation (208) while pICln promotes PRMT5/MEP50 and Sm binding to facilitate splicing (209). However, it is not known if an increase in adaptor proteins can promote an increase in methylation by the PRMT5/MEP50 complex.

#### 4.4.2 PRMT5 OE in carcinogenesis

Liver specific *Prmt5* OE mice did not develop spontaneous liver tumors, nor did they have an exacerbated tumorigenic response to DEN-induced HCC (**Figure 21**) or HTVi (**Figure 23**). However, PRMT5 inhibition has clearly been shown as a potential anticancer therapy. The new class of MTAP-dependent PRMT5-MTA cooperative inhibitors are even more selective by having increased toxicity against *Mtap*<sup>-/-</sup> cells, which is very often co-deleted with *Cdkn2a* in cancer<sup>76</sup> (122, 123, 211) (see also section 1.2.1). Further, eight phase I/II PRMT5 inhibitor clinical trials were underway as of mid-year, 2022 (119). Indeed, PRMT5 inhibition has potent anti-proliferative effects in many cancer types (see **Table 3**).

Our data suggests that PRMT5 may not function as a driver in neoplasms but is essential for cellular viability. We propose that cancer correlated amplification of *Prmt5* may be an adaptation of cancer cells to meet the extensive protein synthesis requirements of rapidly dividing cells. Normal mitotic cells must completely duplicate their genome and generate enough protein for both daughter cells to be self-sufficient. Normally, cell-cycle signaling can allow adequate time and material for faithful genomic reproduction and ample protein production. However, in cancer cells, which escape cell cycle regulation, the cell must rapidly produce protein without the

---

<sup>76</sup> *Mtap* is deleted in over 90% of *Cdkn2a*<sup>-/-</sup> cancers (Zhang, et al., 1996).

protection of cell-cycle signaling to mediate division upon suitable conditions. Importantly, both full body and conditional *Prmt5* KO GEMMs reveal that PRMT5 is essential for many processes. Thus, cancer cells may adapt by increasing PRMT5 protein levels to accommodate the splicing, signal transduction, PTM, and transcriptional regulation demands of uncontrolled cell growth. Thus, inhibition of PRMT5 may decrease cell viability by starving cells of essential arginine methylation in cancer cells.

## 5 Chapter 5- Summary of conclusions and future directions

This work provides important insight into the basic functions of both SND1 and PRMT5 and their role in disease. This is accomplished by generating three novel mouse models, namely a *Snd1 KO*, a *Snd1 KI*, and *Prmt5 OE* GEMM. We functionally characterize each of these mice and identify important characteristics of how each mouse responds to induced carcinogenesis. This work reveals the SND1/PRMT5 axis may be a targetable axis to treat HCC using available or novel small molecule inhibitors. There is much that can yet be learned from these GEMMs about this axis in normal and disease settings.

### 5.1 Part I- The Reader

We identify that *Snd1 KO* mice have a small phenotype and reduced fertility that is independent of the Tudor domain (**Figure 6**). From our observations in mice and known observations from *Drosophila* (169), reduced fertility may arise from an impaired spermatogenesis. However, it remains to be determined if there are maternally linked meiotic differences in *Snd1 KO* mice that impact reproduction. Fertility tracking of both male and female mice will help elucidate if loss of SND1 also impairs oogenesis. Regardless of male/female reproductive differences with loss of SND1, since a reduction in litter (mouse) and brood (fly) sizes increases in severity with time, this suggests that SND1 may have an important role in cellular maintenance of undifferentiated cells. To this point, oncogenes often impact cellular stemness, and *Snd1 OE* primary liver cells were able to expand cancer stem cells<sup>77</sup> (129). Thus, SND1 may have important roles in cell stemness that can impact fertility.

Recent mass spectrometry analysis of the SND1 complex from 293T cells identified many novel SND1 binding proteins (101). However, it remains to be determined what protein-protein interactions are specifically facilitated by the Tudor-domain. A BioID2-HA tagged SND1 and

---

<sup>77</sup> In this experiment, WT primary hepatocytes formed abortive spheres. However, *Snd1 OE* hepatocytes could form spheres that could gradually grow and expand.



Tudor domain mutated SND1 mass spectrometry pulldown may provide important insight into key protein-protein interactions that are important in a variety of tissues. This may also help distinguish potential interactions that are important for the small phenotype. Further, this could be done in hepatocytes to determine potential interactions that may be involved in normal liver function and tumorigenesis.

*Snd1 KO* and *Snd1 KI* mice have a reduced expression of key APPs (**Figure 7**). This reduction could have an impact on the overall ability of mice to respond to hepatic stress and inflammation. However, it is not clear how SND1 regulates APPs<sup>78</sup>. Further work is needed to identify if the hepatic-inflammatory response differs with *Snd1* loss or mutation. An important next step will be to identify how APP expression changes in response to DEN treatment or to other hepatic strains like alcohol consumption. Further, it is not known how chronic inflammation is impacted by reduced APP expression. Crossing the *Snd1 KO* and *Snd1 KI* mice to a hepatitis prone mouse model may determine if there are changes in chronic hepatic inflammatory responses, and thereby if inhibiting SND1 activity may have an anti-inflammatory effect. To this point, NF- $\kappa$ B activation is upregulated in *Snd1 OE* cells (62), which transcriptionally upregulates inflammatory response genes<sup>79</sup>. Use of a general nuclease inhibitor, pdTp, decreased nuclear phospho-p65, indicating SND1 inhibition may decrease inflammatory response transcription (129).

It remains to be determined if there is crosstalk between the SN- and Tudor domains. **Figure 7b** and unpublished data suggests there may be additional transcriptional SN/Tudor domain crosstalk that impacts transcription in Tudor-mutant SND1 mice. These results should be followed up to determine the extent of Tudor domain mediated transcription. CUT&RUN or similar ChIP-seq approaches may identify specific targets of SND1 Tudor dependent transcription.

---

<sup>78</sup> LPS triggered induction of IL-6 similar to *Snd1 WT* and *KO* macrophages.

<sup>79</sup> This occurs by phosphorylation of p65, thereby re-localizing this protein to the nucleus and transcriptional upregulation of inflammatory genes.

The *Snd1* KO and KI mice are hepatoprotected and develop less tumors than WT mice in DEN-induced carcinogenesis (**Figure 8** and **Figure 9**). However, there remain several questions about how loss of SND1 or its methyl-reading ability decreases tumor burden in these mice. Moving forward, work is needed to determine 1) if the SN-domains of SND1 are involved in promoting tumors, and 2) if loss of SND1 can protect against other types of induced HCC.

#### 5.1.1.1 *Are SN-domains involved in promoting tumors?*

First, it remains to be determined if hepatoprotection is a SN-domain independent process. The SND1 Tudor domain may be necessary for its recruitment for SN-domains to impact RNA processing. A mis-localization of RNA processing proteins may dysregulate RNA processing and could thereby impact tumor formation. Thus, an important next step will be to determine if mutation of the SN-domains can impact tumorigenesis. Progressively shorter nuclease domain truncations reveal that all four-SN domains are needed for nuclease activity. This was explained by molecular modeling that showed adjacent SN-domains sandwich double stranded nucleic acids in a single orientation for digestion (212). Thus, a truncated SND1 will be unable to create a concave tertiary fold to bind nucleic acids. From this, either point mutation of enzymatic residues or n-terminally truncating SND1 may be enough to disrupt SND1 for these experiments.

#### 5.1.1.2 *Are Snd1 KO and KI mice hepatoprotected with other types of inducible-HCC?*

Second, there are many types of inducible HCC, each of which allow researchers to study a particular subtype of HCC. For instance, high fat diet in transgenic MUP-uPA mice can be used for studying steatosis and NASH associated HCC to study inflammation associated HCC<sup>80</sup> (213). Alternatively, expression of hepatitis B surface antigen allows for study of Hepatitis induced

---

<sup>80</sup> Major urinary protein-urokinase-type plasminogen activator (MUP-uPA) transgenic mice express high amounts of this fusion protein in the liver. These mice undergo transient ER stress, and ultimately develop NASH and HCC.

tumorigenesis<sup>81</sup> (214). Crossing both a *Snd1 KO* and *Snd1 KI* mice into a model that is genetically predisposed to develop HCC will help determine if targeting SND1 may reduce carcinogenesis from other etiologies.

It should be noted that not all liver diseases ultimately progress to become HCC. We observed that *Snd1 KO* and *KI* mice can still develop HCC, but with more mice harboring early stages of the disease (**Figure 8**). Thus, loss of SND1 may impact early processes of tumorigenesis, and thus may impact risk factors that ultimately lead to HCC. Thus, these SND1 altered mice may also provide insight into novel treatment for basic liver disease such as diabetes and fibrosis. However, it first needs to be determined if loss of SND1 impacts specific process associated with these diseases.

## 5.2 Part II- The Writer

We developed the first liver specific *Prmt5 OE* mouse. This mouse is viable and expresses a V5-tagged PRMT5 and MEP50 that can increase total PRMT5 activity (**Figure 13** and **Figure 14**). Herein we determine an important piece of PRMT5 biology, namely that PRMT5 OE alone does not induce hypermethylation. We propose that PRMT5 methylation is highly controlled, with most targets being heavily methylated with normal levels of PRMT5. *Prmt5<sup>OE</sup>* mice have very mild SDMA hypermethylation (**Figure 15**). Comparing MMA, ADMA, and SDMA in multiple cell types, arginine methylation exhibits tissue specificity (**Figure 16**). Finally, transiently expressed myc-PRMT5 did not show a dramatic increase in SDMA (**Figure 17** and **Figure 18**). This is important for understanding how PRMT5 activity is controlled in the cell and may help develop substrate targetable PRMT5 inhibitors.

PRMT5 conditional knockouts have greatly expanded our understanding of PRMT5. In this same way, the *Prmt5<sup>OE</sup>* mice will be valuable for determining the effects of *Prmt5 OE* in other tissue types. PRMT5 methylation of histones is important in development and is correlated with

---

<sup>81</sup> These models can be paired with aflatoxin or DEN exposure to exacerbate tumorigenic response and look at specific subtypes of liver disease.

proliferation. However, it is not known if *Prmt5 OE* can alter the proliferation or development of germ cells or other continuously dividing cells. Hepatocytes can regenerate, but this is usually in the context of cellular damage. Thus, it will be important to determine if *Prmt5 OE* impacts cells which are continually dividing and have more pluripotency.

We propose targeting the SND1/PRMT5 axis in HCC by use of PRMT5 inhibitor to impair SND1 methyl reading function. This is not the first work to propose the use of PRMT5 inhibition to treat liver cancer. However, there are disparate conclusions about the pharmacological efficacy of using PRMT5 inhibitors in the liver that both support and refute their use.

L. Huang et al (2018) showed high fat diet was able to induce PRMT5 expression, decrease AKT signaling, and transcriptionally decrease mitochondrial biogenesis pathways<sup>82</sup>. Mitochondrial dysfunction plays a role in liver disease, including diabetes and NAFLD. In liver cells, PRMT5 knockdown or inhibition decreased peroxisome proliferator-activated receptor  $\gamma$ -coactivator 1 $\alpha$  (PGC-1 $\alpha$ ), a master transcription factor for genes involved in energy metabolism. Thus, use of PRMT5 inhibitors may prevent liver disease by increasing mitochondrial biogenesis (215).

However, J. Wang et al generated a PRMT5 liver specific conditional knockout mouse that shows a liver cancer promoting phenotype resulting from hepatic loss of PRMT5. These mice develop liver fibrosis and cirrhosis at 6 and 12 months respectively, with 50% mortality at 16 months. These results suggest prolonged use of PRMT5 inhibitors may have the opposite desired effect in livers by inducing fibrosis and polyploidization of nuclei (42).

Taken together, it remains to be determined how PRMT5 inhibition impacts liver tumor formation<sup>83</sup>. The recently developed MTAP-dependent inhibitors may have greater therapeutic

---

<sup>82</sup> Induction of PRMT5 expression by diet is independent of obesity. Mice with dominant mutations in the agouti locus will develop several metabolic diseases including obesity with age. PRMT5 levels were unchanged in obese-normal chow agouti mice, but upregulated in high fat chow fed non-mutant mice.

<sup>83</sup> Adipogenesis and atherosclerosis risk were recently assessed in mice with PRMT5 inhibitor treatment (Zhang, et al.,2023). Though their results were linked to fatty liver disease, they were not further linked to HCC development.

potential by specifically targeting *Mtap*<sup>-/-</sup> cells, thereby circumventing the potential long-term liabilities of inhibiting PRMT5 in the liver. However, these disparate results also support the development of a SND1-Tudor domain small molecule inhibitor. This would target only a subset of PRMT5 methyl-substrates and be more targeted than PRMT5 inhibitors.

## 6 Appendix A- Published review

This section is a reprinting of: Wright T, Wang Y, Bedford MT. The Role of the PRMT5-SND1 Axis in Hepatocellular Carcinoma. *Epigenomes*. 5(1). doi: 10.3390/epigenomes5010002.

Authors Note: This is a review published in 2021 with Multidisciplinary Digital Publishing Institute (MDPI) on the role of the PRMT5/SND1 axis in HCC, and is referenced as a source within as (16). For all articles published in MDPI journals, copyright is retained by the authors. See <https://www.mdpi.com/authors/rights> for details.

# The Role of the PRMT5–SND1 Axis in Hepatocellular Carcinoma

Tanner Wright <sup>1,2</sup>, Yalong Wang <sup>1</sup> and Mark T. Bedford <sup>1,\*</sup>

Received: 13 December 2020

Accepted: 3 January 2021

Published: 5 January 2021

<https://doi.org/10.3390/epigenomes501000>

Publisher’s Note: MDPI stays neutral with regard to jurisdictional claims in published maps and institutional affiliations.

Copyright: © 2021 by the authors. Licensee MDPI, Basel, Switzerland. This article is an open access article distributed under the terms and conditions of the Creative Commons Attribution (CC BY) license (<http://creativecommons.org/licenses/by/4.0/>).

<sup>1</sup>Department of Epigenetics and Molecular Carcinogenesis, The University of Texas MD Anderson Cancer Center, Smithville, TX 78957, USA; TWright3@mdanderson.org (T.W.); YWang68@mdanderson.org (Y.W.)

<sup>2</sup>Graduate Program in Genetics & Epigenetics, UTHealth Graduate School of Biomedical Sciences, The University of Texas MD Anderson Cancer Center Houston, TX 77030, USA

\*Correspondence: [mtbedford@mdanderson.org](mailto:mtbedford@mdanderson.org)

Abstract: Arginine methylation is an essential post-translational modification (PTM) deposited by protein arginine methyltransferases (PRMTs) and recognized by Tudor domain-containing proteins. Of the nine mammalian PRMTs, PRMT5 is the primary enzyme responsible for the deposition of symmetric arginine methylation marks in cells. The staphylococcal nuclease and Tudor domain-containing 1 (SND1) effector protein is a key reader of the marks deposited by PRMT5. Both PRMT5 and SND1 are broadly expressed and their deregulation is reported to be associated with a range of disease phenotypes, including cancer. Hepatocellular carcinoma (HCC) is an example of a cancer type that often displays elevated PRMT5 and SND1 levels, and there is evidence that hyperactivation of this axis is oncogenic. Importantly, this pathway can be tempered with small-molecule inhibitors that target PRMT5, offering a therapeutic node for cancer, such as HCC, that display high PRMT5–SND1 axis activity. Here we summarize the known activities of this writer–reader pair, with a focus on their biological roles in HCC. This will help establish a foundation for treating HCC with PRMT5 inhibitors and also identify potential biomarkers that could predict sensitivity to this type of therapy.

Keywords: arginine methylation; PRMT5; SND1; Tudor-SN; p100; HCC



## 1. Introduction

Signal transduction is the process by which information is relayed through a cell. Extracellular signals, such as growth factors or contact points with other cells, stimulate receptors on the cell surface to initiate this process by converting one stimulus (ligand binding) into another (phosphorylation). This signal initiation event is then propelled through the cytoplasm and into the nucleus using a series of sequential PTM events that rely on “reader” proteins, or effector molecules, to dock onto a specific PTM and then promote the deposition of a new PTM downstream, which in turn is read and relayed by another effector. There is a vast array of different PTMs including, but not limited to, phosphorylation, acetylation, ubiquitination and methylation, which can all be read by specialized protein domains in effector molecules [1]. These globular domain types include SH2s (phosphor-tyrosine readers), FHAs/14-3-3s/BRCTs (phosphor-serine/threonine readers), Bromo/YEATS domains (acetyl-lysine readers), UBA/UIM/GAT/CUE domains (ubiquitinated-lysine readers), Chromo/PHD/Tudor/BAH domains (methylated-lysine readers), and Tudors (methylated-arginine readers). In this review, we will focus on just one single thread in this hairball of signaling networks: the PRMT5–SND1 axis.

Arginine residues are frequently methylated post-translationally, and these modifications come in one of three flavors: monomethylarginine (MMA), asymmetric dimethylarginine (ADMA), or symmetric dimethylarginine (SDMA) (Figure 1). These methyl-mark additions occur at the peripheral omega nitrogen of arginine guanidine moieties commonly seen at glycine- and arginine-rich (GAR) motifs. Protein arginine methyltransferases (PRMTs) are the family of nine closely-related enzymes which deposit all three of these marks [2]. There is a tenth arginine methyltransferase called NDUFAF7, which is not a member of PRMT family, and seems to be a dedicated mitochondrial enzyme [3]. PRMT1 is the primary Type I PRMT, which deposits the majority of ADMA marks. Other Type I PRMTs include PRMT2, PRMT3, PRMT4/CARM1, PRMT6 and PRMT8. PRMT7 is capable of depositing only MMA marks, and it is referred to as a Type III enzyme. That leaves the Type II enzymes, which deposit SDMA marks. PRMT9 has

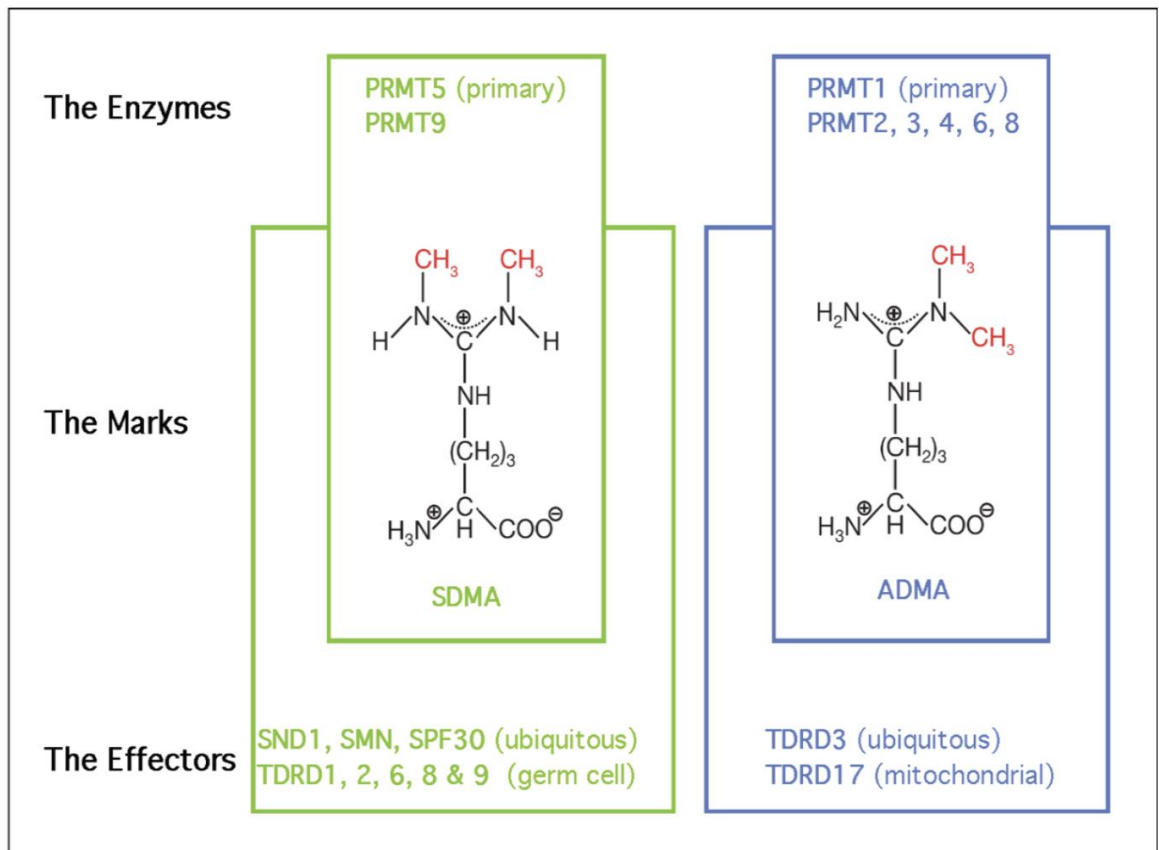


Figure 1. The PRMTs, the marks they deposit, and the effectors of those marks. PRMT5 and PRMT9 deposit the SDMA mark, in “green”. PRMT1-4, 6 and 8 all deposit the ADMA, in “blue”. Methyl groups are highlighted in “red”. The effectors, or readers, of the methyl marks are Tudor domain-containing proteins.

just one known substrate (SAP145) [4], and NDUFAF7 is also dedicated to just one mitochondrial substrate (NDUFS2) [3]. All the remaining proteins marked with SDMA are thought to be PRMT5 substrates. Arginine methylation is a relatively abundant PTM and over the years, a number of studies have reported similar ratios of the different types of arginine methylation in both tissue and cell lines [5–7], which generally breaks down to 1000:5:0.5:0.1 for Arginine:ADMA:SDMA:MMA. So, approximately 0.6% of all arginine residues found in proteins are arginine methylated.

Tudor domains are the only globular folds known to bind methylated arginine motifs [8]. This domain type was first identified in the *Drosophila melanogaster* Tudor protein which contains repeating domains that are present in a number of other proteins in many different species [9]. A detailed understanding of how Tudor domains interact with SDMA motifs was first gleaned from biochemistry and structure studies involving the human survival motor neuron (SMN) protein [10,11], which is mutated in spinal muscular atrophy syndrome. All in all, eight Tudor domain-containing proteins have been reported to be methyl-arginine readers. The vast majority of methyl-arginine readers recognize SDMA motifs, including SMN, SPF30, and SND1, which are ubiquitously expressed, and TDRD1, TDRD2, TDRD6, and TDRD9, which are all germ cell-specific proteins. TDRD3 is currently the only known ADMA motif effector protein that is also ubiquitously expressed (Figure 1).

PRMT5 has emerged as an important player in HCC [12], the fourth leading cause of cancer mortality in the world [13]. This link to HCC is strengthened by the fact that a downstream reader of the PRMT5-deposited SDMA marks—SND1—has been identified as a driver of HCC formation [14], though the precise molecular mechanism of action remains poorly understood. This review focuses on summarizing key biological functions of the PRMT5–SND1 reader–writer pair (Figure 2), then surveys what is known about these proteins as they relate to HCC, and concludes with speculation on unexplored avenues of therapeutic modulation of methylarginine levels in HCC as a potential form of treatment.

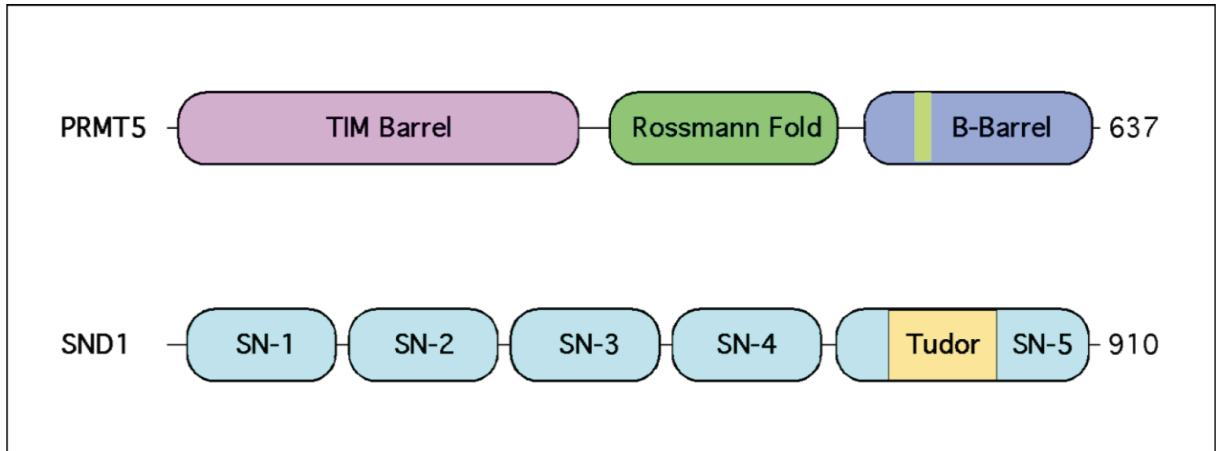


Figure 2. PRMT5 and SND1 structural domains. PRMT5 contains three distinct regions. A triosephosphate isomerase (TIM) barrel, which contains eight consecutive alpha helices, followed by a Rossmann fold, which contains the amino acid residues that bind S-adenosylmethionine. The C-terminus of PRMT5 contains a beta barrel in which the dimerization domain has been mapped. In hetero-octamerization complexing with MEP50, PRMT5 dimerizes head to toe with other PRMT5 proteins. SND1 contains four intact SN-like domains capable of binding nucleic acids and have nuclease activity. A fifth truncated SN-like domain is split by the Tudor.

## 2. Biological Roles of PRMT5—The Primary Depositor of SDMA Marks

PRMT5 is the predominant Type II arginine methyltransferase, indicating that it confers both MMA and SDMA marks on target substrates in a distributive manner [15] (Figure 1). The primary targets of PRMT5 methylation are RNA-binding proteins, epi-genetic modulators and core histones, which has implicated this enzyme in transcriptional regulation and the control of faithful alternative splicing [16]. PRMT5 is not enzymatically active on its own, and is found in a protein complex called the methylosome.

### 2.1. PRMT5 Forms a Stable Complex with MEP50

Regardless of the methylation target, PRMT5 requires the co-factor methylosome protein 50 (MEP50) for stability and enzymatic activity [17]. MEP50 is also referred to as WDR77. Loss of MEP50 results in the destabilization of the PRMT5 protein and vice versa [18]. Enzymatic activity is further dependent on hetero-octamerization of these two proteins to form a complex of four PRMT5 molecules and four MEP50 molecules [19–21]. MEP50 has also been identified as a potential coactivator of the androgen receptor [22], but it is unclear whether PRMT5 is recruited with MEP50 in this context, or whether it functions independently. Importantly, HeLa cell fractionation studies from a sucrose gradient indicate that PRMT5 and MEP50 only occur together and are not found in a complex without the other, nor do they exist in the free un-complexed form [17]. Similar fractionation experiments using *Xenopus* egg extracts and gel filtration also re-veal the existence of a single PRMT5–MEP50 complex and no free monomeric form of either protein [23]. Thus, these two proteins are tightly complexed and likely do not function independently.

### 2.2. The Methylosome is Targeted to Distinct Substrates by Adaptor Proteins

The PRMT5–MEP50 protein complex requires additional adaptor proteins to aid in identifying substrates that will be targeted for symmetric methylation. There are five known adaptors that link the methylosome to its substrates, and these are pICln, RI-OK1, COPR5, Sharpin and OXR1A. pICln is a spliceosome assembly chaperone, which recruits PRMT5 to facilitate the efficient methylation of SmB/B' and SmD1/2 [24,25], as well as a number of

ribosomal proteins [26]. A second adaptor is RIOK1, which is critical for the methylation of nucleolin by PRMT5–MEP50 [27], and is important for pre-rRNA transcription and processing. RIOK1 and pICln compete for binding, suggesting that there may be a common pocket for adaptor protein binding, either on PRMT5 or MEP50 [27]. COPR5 is the third adaptor to be identified, and it recruits PRMT5 activity to nucleosomes to support the deposition of H3R8me2s and H4R3me2s marks, in its role as an epigenetic regulator [28]. The fourth adaptor is Sharpin, and this interaction targets PRMT5 to methylate the transcription factor SKI [29]. Finally, OXR1A also regulates PRMT5's ability to methylate histones, and it is the H3R2me2s methylation that is stimulated by this adaptor [30]. OXR1A and PRMT5 interact in the pituitary gland and regulate growth hormone expression, which in turn impacts liver metabolism. Both RIOK1 and pICln were identified in independent shRNA screens that also identified PRMT5 as a vulnerability in MTAP-null tumors [31–33], further supporting the key role that these adaptors play in helping the PRMT5–MEP50 methylosome find its targets for methylation.

### 2.3. The Identification of PRMT5 Substrates Implicate It in the Regulation of Transcription, Splicing, Signal Transduction and the Repair of DNA Damage

The initial characterization of PRMT5 as an arginine methyltransferase revealed that it methylates H2A and H4, using an in vitro methylation assay [34]. Importantly, the first five residues of H2A and H4 are identical (SGRGK...), and it is the arginine in position 3 that is methylated by PRMT5. Knockout studies showed that the H2AR3me2s modification is particularly sensitive to PRMT5 loss in vivo [35]. Sm proteins were also shown to be methylated by PRMT5 early on in the study of this PRMT [24]. Since then, over the last twenty years, a large number of PRMT5 substrates have been identified [16]. These studies have been spurred on by the development of efficient pan-substrate antibodies that recognize Rme2s marks on different substrates, and can be used to enrich for methylated peptides from tissue and cell extracts, which can then be identified by mass spectrometry. The first such substrate screens were performed by the Richard lab [36], and subsequent screening studies have dramatically expanded on the number of known symmetrically methylated proteins into the 100s [37]. Gene ontology (GO)

analysis of the identified PRMT5 substrates reveals strong enrichment of RNA splicing and processing, as well as PTM regulated gene expression pathways and, to a lesser extent, translation.

#### 2.4. PRMT5 Functional Misdirection Due to Cross-Reactivity with the FLAG Antibody

The PRMT5 field has been confounded by the occurrence of a major artifact of tandem affinity protein (TAP) complex purifications that use the FLAG-tag. Over the years, it is well established that when purifying a FLAG tagged protein using FLAG-M2 beads, a major contaminant is the PRMT5–MEP50 protein complex, because the M2 antibody binds directly to PRMT5 and purifies both it and its associated proteins. This was first reported by Danny Reinberg's lab over 18 years ago [38]. Subsequent studies by the Siekhattar lab reported the same thing [39]. PRMT5 is also listed as a common contaminant of FLAG immunoprecipitation experiments [40]. Most recently, the CRAPome was published, which highlights the major problems with affinity purification-mass spectrometry data sets [41]. Indeed, they showed that 94% of all FLAG purifications data sets detect PRMT5 peptides. Thus, the misassignment of PRMT5 in many FLAG-tagged protein complex purifications has led many researchers astray, and these artifacts have found their way deep into the published literature.

#### 2.5. Mouse Models Reveal a Number of Biological Roles for the Methylosome

It is very likely that loss of PRMT5 and MEP50 in mice will phenocopy each other, as they are codependent on each other for protein stability. Indeed, the interdependence and essentiality of MEP50 and PRMT5 complexing is supported by the fact that the mouse knockouts of both PRMT5 and MEP50 result in early lethal developmental defects. MEP50 knockout mice display an early embryonic lethal phenotype with no null embryos detected at E8.5 [42]. The PRMT5 knockout mice also display a very early embryonic lethal phenotype [35].

The early lethality of these total knockouts has made it necessary to generate conditional alleles for both PRMT5 and MEP50, to help elucidate the biological roles of this protein complex in vivo. Importantly, conditional knockouts of PRMT5 have provided additional insights into its roles in T and B cell development, limb development and neural development [43–47]. A

conditional allele for the study of MEP50 loss in adult mice is also available, but has only been used in two studies related to prostate development [48] and lung development [49], although the conditional knockout was performed *ex vivo* in the latter study.

The first conditional PRMT5 knockout mice were generated by crossing PRMT5<sup>fl/fl</sup> and Nestin<sup>cre</sup> mice, which resulted in postnatal lethality in all homozygous null mice, and implicated PRMT5 in neuronal development [43]. Further exploration determined that this mortality was linked to splicing variations of Mdm4, which induces a p53 response, leading to severe cranial abnormalities. Subsequently, PRMT5 was conditionally knocked out in oligodendrocytes, using Olig1<sup>cre</sup>, and identified as a key factor for myelination [50]. Myelin basic protein has long been known to be a robust substrate for PRMT5 in *in vitro* studies, and the myelination defect in the conditional knockout mice provides *in vivo* evidence for the functional importance of this PTM [51].

A number of additional conditional knockouts of PRMT5 have been performed in adult mice. PRMT5 is also essential for the initiation and maintenance of hematopoiesis [44,52]. Methyl-transferase localization appears to impact the modification of splicing machinery, whereas loss of PRMT5 results in alternative splicing defects via intron retention and exon skipping, which is critical for hematopoietic stem cell quiescence and viability [44,53]. Both conditional knockout and small-molecule inhibitor studies reveal that loss of PRMT5 has anti-tumor activity against MLL-rearranged acute myeloid leukemia (AML) likely due to hypomethylation of essential splicing factor like SRSF1 [54,55], and further vulnerability of cancer to PRMT5 loss is bestowed on the tumors that harbor driver mutation in splicing factors [56]. Using a CD4<sup>cre</sup>, it was recently shown that PRMT5 is dispensable for late T cell development, and is required for peripheral T cell expansion and survival [46]. The removal of PRMT5 activity from pancreatic beta cells, using the Pax<sup>cre</sup>, reveals its role on regulation of insulin expression *in vivo* [57]. PRMT5 has also been shown to play a role in muscle stem cell expansion in adult mice (using Pax7<sup>cre</sup>), but does not seem important for the proliferation and differentiation of myogenic progenitor cells during embryonic development [58].



In a mouse embryo developmental biology setting, PRMT5 has been identified as a key for certain differentiated chondrocytes, and in this case *Prxcre* was used to remove PRMT5 from developing limb buds [59]. Conditional deletion of PRMT5 in hind limbs of mice led to severe phenotypes of atrophied long bone and knee. While essential for some chondrocyte lineages, PRMT5 is dispensable for general chondrocyte maintenance in adult mice. Inactivation of PRMT5 in germ cells (using *Tnapcre*) results in defects in spermatogenesis [60], and loss of PRMT5 in the developing lung epithelial cells (using *Shhcre*) causes defects in branching morphogenesis [61].

Although PRMT5 biology has been studied extensively through conditional knockouts in both adult mice and embryos, far fewer mouse genetic studies have been performed with the other key component of the methylosome—namely MEP50. Importantly, a conditional allele for mouse MEP50 has been generated [48]. However, it has only been used in one study, and that was to investigate the role of MEP50 in the prostate (which we mentioned earlier). Using the *Probasincre* mouse, MEP50 was conditionally removed from all lobes of the developing mouse prostate. This inactivation of PRMT5 had a severe inhibitory effect on prostate development during embryogenesis, which is likely mediated by the deregulation of androgen receptor (AR) target genes due to the ability of MEP50 (and likely PRMT5) to function as an AR cofactor.

While PRMT5 and MEP50 knockouts have been shown to be essential for many key developmental pathways, PRMT5 also harbors many oncogenic characteristics through its ability to repress the expression of the tumor suppressors ST7 and NM23 [62]. Likewise, loss of E-cadherin, a characteristic of epithelial to mesenchymal transition (EMT) which is key for metastasis, is actively repressed through the binding of PRMT5 and AJUBA to SNAIL [63]. Overexpression of PRMT5 further induces hyperproliferation of cell lines in culture [64,65]. In addition, PRMT5 has been shown to be overexpressed in many different cancers including gastric [66], colorectal [67], lung [68,69], lymphoma [64], ovarian [70], melanoma [71], and glioblastoma [72,73]. The focus of this review is on the overexpression of PRMT5 in HCC and there are numerous reports of elevated PRMT5 levels in liver cancer [12,74–78]. Most of these

published studies demonstrate that PRMT5 is overexpressed in many different cancer types, and PRMT5 overexpression correlates with aggressive tumors and poor prognosis. However, it is not clear whether PRMT5 is an oncogenic driver, or whether the elevated PRMT5 levels are an aftereffect of a transformed state. In other words, it is still unknown whether high PRMT5 expression is a cause or a consequence of cellular transformation.

### 3. Biological Roles of SND1—A Major Reader of SDMA Marks

SND1 (also known as TSN, p100, or TDRD11) is a ubiquitously expressed Tudor domain-containing protein [79]. Unique characteristics of SND1 include four tandem SN domains which convey nucleic acid binding and nuclease activity [79,80] (Figure 2). The SN domains are followed by a single Tudor domain that exclusively recognizes SDMA marks, which is fused to a fifth split SN domain [79,81]. This dual ability to simultaneously interface with nucleic and amino acids allows SND1 to impinge on a wide range of different signaling pathways. Some have claimed that this multifacility endows SND1 with the ability to “positively impact all hallmarks of cancer” [82]. Despite its preferential SDMA reading specificity, SND1 has been called a promiscuous binder given its affinity for RNA and DNA, and it regulates multiple pathways that control various aspects of gene expression [83,84].

#### 3.1. The Tudor Domain of SND1 Interacts Selectively with SDMA Marks

Methylated lysine motifs are bound by at least eight different domain types—Chromo, PHD, MBT, Tudor, PWWP, Ank, BAH and WD40 domains. In the case of methylated arginine motifs, only members of the Tudor family are known effectors, with a handful of Tudor domain-containing proteins either binding SDMA or ADMA marks [8]. Importantly, there are a few individual PHD and WD40 domains whose binding affinity is also impacted by arginine methylation. Tudor domains were identified simultaneously by two research groups, which both realized that the *Drosophila melanogaster* Tudor protein contains previously unrecognized repeating domains, which were found in a number of other proteins in many different species [9,85]. Interestingly, SND1 was one of the first proteins to be identified as a Tudor domain-containing protein [85]. Initial structural studies involving the Tudor domain of SND1 identified an

aromatic cage that suggested it might recognize methylated peptide ligands [86]. Subsequent crystal and NMR structural studies found that the extended Tudor domain of fly SND1 bound a short GAR motif from SmB, only when this motif was symmetrically dimethylated [87]. Finally, work involving the human SND1 protein revealed that it bound PIWIL1 in an arginine methylation-dependent manner, with a strong preference for SDMA motifs over ADMA motifs [88]. Thus, SND1 reads marks that PRMT5 deposits.

### 3.2. SND1 as a Transcriptional Coactivator

SND1 was originally identified as a transcriptional coactivator of EBNA2 (Epstein–Barr nuclear antigen-2) [89], which interacts with many general transcription factors and coactivators, and positions SND1 as a central player in transcriptional regulation. Indeed, SND1 has been found to directly engage with a number of transcription factors. Signal transducer and activator of transcription 6 (STAT6) is a key player in transcriptional activation upon IL-4 stimulation. SND1 acts as a transcriptional coactivator by binding the C-terminus of STAT6 along with RNA Polymerase II. In this way, SND1 acts as a bridge between STAT6 nuclear localization and transcriptional activation [90]. A second STAT protein, STAT5, induces transcriptional activation in response to lactogenic hormones, which is facilitated in a similar fashion by SND1 binding the C-terminal transcriptional activation domain [91]. SND1 also functions as a coactivator for the c-Myb transcription factor [92], and in this context it is regulated by phosphorylation. Using a protein domain microarray approach, we identified the Tudor domain of SND1 as a reader of a PRMT5 deposited SDMA motif within the E2F1 transcription factor [81]. E2F proteins are widely known for their central role in transcriptional activity and their close association to proliferation and cancer. Follow-up mechanistic studies by the La Thangue group revealed that the recruitment of SND1 to arginine methylated E2F1, results in cross-talk between transcriptional regulation and altered splicing regulation of a subset of E2F1 transcriptional target genes [93]. Independent luciferase-based assays have validated the ability of SND1 to coactivate E2F1 transcriptional activity [94]. SND1 is also an interactor and coactivator of the transcription factor peroxisome proliferator-activated receptor  $\gamma$  (PPAR $\gamma$ ), and regulates adipogenesis [95]. Thus, SND1 interacts

directly with a number of transcription factors (STAT5/6, c-Myb, E2F1 and PPAR $\gamma$ ) and promotes their transcriptional activity.

### 3.3. SND1 Is a Splicing Factor

The splicing of precursor mRNA is a highly ordered process that is orchestrated by the spliceosome. The spliceosome is composed of five small nuclear ribonucleoprotein particles, which by definition harbor a mix of small nuclear RNAs (snRNAs U1, 2, 4/6 and 5) and proteins (Sm proteins plus additional splicing factors). SND1 interacts with both the RNA and protein components of the spliceosome. Indeed, due to its unique structure, with a Tudor domain for protein binding and SN domains for RNA binding, it plays a role in spliceosome complex formation. The Tudor domain of SND1 interacts directly with the arginine methylated forms of SmB/B' and SmD1/D3 [96], and also the splicing factor Sam68 [97]. The interaction of SND1 with the U RNAs is likely mediated through the Sm core proteins, which bind directly to U1, U2, U4, U5, and U6 snRNAs, as the Tudor domain of SND1 can pulldown U RNAs, but the SN domains cannot [98].

As mentioned above, SND1 directly associates with a number of transcription factors. It has been proposed that the recruitment of SND1 by transcription factors to enhancer/promoter elements can directly impact the alternative splicing of the transcripts that are being activated by that particular transcription factor, at least in the case of E2F1 [93]. In summary, PRMT5 is a key regulator of RNA splicing [55], and as an effector molecule for SDMA marks deposited by PRMT5, it is not surprising that SND1 is also integral to the maintenance of normal splicing programs that can go awry in a cancer setting.

### 3.4. SND1 Regulates RNA Stability

Apart from splicing, SND1 is involved in many other aspects of RNA biogenesis. SND1 is not only a component of the spliceosome, but also the RNA-induced silencing complex (RISC), which are both ribonucleoprotein particles. The RISC is a "carrier" of miRNA and siRNA, which when loaded with Argonaute can target mRNA for cleavage to regulate gene expression. A biochemical purification of RISC in *Drosophila* identified SND1 along with Argonaute 2 and VIG-

1 [99], and SND1 is enriched in size fractionated extracts that also contain the 250 kDa miRNA complex. SND1 was also confirmed to be a component of the mammalian RISC enzyme. SND1 was shown to have ribonuclease activity that is specific for inosine-containing dsRNAs [100], and it was subsequently found that SND1 selectively degrades a highly edited pri-miR-142 that is not processed by Drosha [101]. SND1 has four intact SN domains (the 5th SSN domain is split by the Tudor domain), and structural studies have revealed that a minimum of two tandem SN domains are necessary and sufficient for RNA binding [102]. Recent studies have found that SND1 is involved in regulating the turnover of a sub-set of mature miRNAs with a common CA/UA dinucleotide sequence signature [103]. This process is known as Tudor-staphylococcal/micrococcal-like nuclease (TSN)-mediated miRNA decay (TumiD), and it is promoted by the UPF1 helicase [104]. Thus, as a component of RISC, SND1 is actively involved in processing miRNAs.

### 3.5. SND1 as a Component of Exosome Cargo

Extracellular vesicles (EVs), including exosomes and microvesicles, carry high levels of SND1 as part of their secreted cargo. Exosomes are critical carriers of molecular and signaling information in the extracellular environment of organ systems, where they transfer molecules from one cell to another via membrane vesicle trafficking. Exosomes are approximately 100 nm in size, and are produced in the endosomal compartment (the Golgi network) of most eukaryotic cells. With the development of cancer, exosomes become important messenger packages that “speak to” the tumor microenvironment. The first hint that SND1 was sorted into vesicles came from a study showing the presence of SND1 protein in lipid droplets that are generated by milk secreting cells [105]. Subsequent work has revealed that EVs are enriched for miRNAs, mRNAs and Ago2, which a key protein component of RISC [106–108]. SND1 is also an integral component of RISC [99], and it is thus not surprising that it is also part of these miR-NA/Ago-enriched EVs. An analysis of the changes in the protein composition of exosomes, after ionizing radiation, reveals an increase in SND1 [109]. In addition, patient urinary EVs, which are secreted by bladder cancer cells also contain high levels of SND1 [110]. Exosome-mediated intracellular

communication within the tumor microenvironment seems to play an important role in the development and progression of HCC [111].

### 3.6. SND1 Expression Patterns at the RNA and Protein Levels

Detailed profiling of SND1 expression has found it to be ubiquitously expressed, with the highest expression in proliferating cells and active secretory organs such as exocrine pancreas, lactating mammary glands and the liver [112]. Western analysis of SND1 reveals that it is most highly expressed in the pancreas and the liver [88] (see Figure S1 in Liu et. al., 2010). We have reproduced this data and also see a very similar expression pattern (Figure 3). RNA-seq analysis, curated by the NCBI, was performed on 27 different human tissues from 95 individuals, and also reveals fairly ubiquitous RNA expression of SND1, with approximately a two-fold variable between tissues (Figure 3A). We performed Western analysis on protein extracted from a panel of cell lines, and we observed ubiquitous expression of SND1, albeit at varying levels (Figure 3B). When comparing the protein and RNA expression of SND1, there seems to be a disconnect between the high protein levels of SND1 in pancreas and the liver, and the equal and ubiquitous RNA expression of SND1 in different human tissues. This observation could be explained by the post-transcriptional regulation of SND1 possibly by the proteasome. Indeed, mass spectrometric analysis of SND1 reveals at least 10 different lysine residues that can be ubiquitinated (see the CTS—PhosphoSite database). However, no studies have yet been performed to evaluate the protein stability of SND1 in different tissue settings. Alternatively, certain organs such as the liver and pancreas harbor levels of exosome activity, and SND1 may be sorted and secreted in the tissues from these organs, resulting in extracellular accumulation and retention.

### 3.7. Mouse Models of SND1 Overexpression Support Its Potential Oncogenic Functions

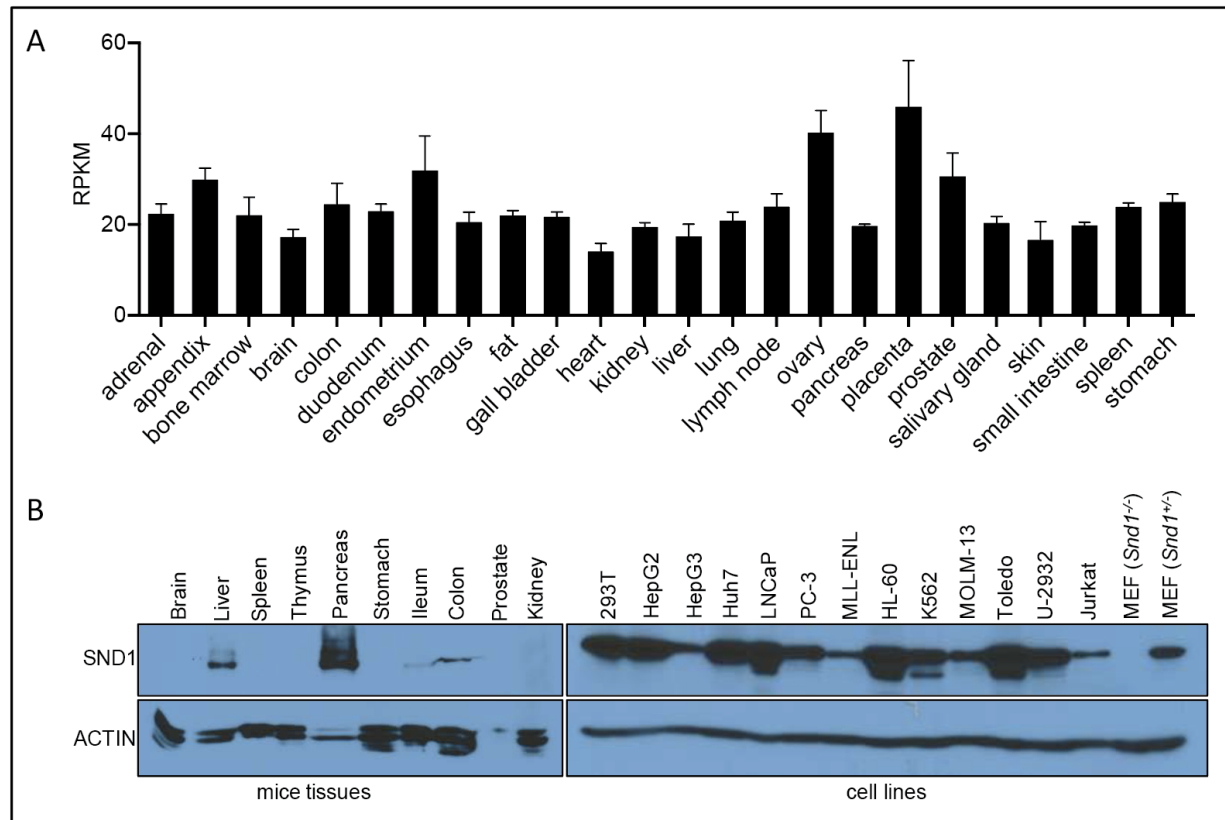


Figure 3. SND1 RNA and protein expression. **(A)** SND1 RNA expression in different human tissues. Data was obtained from PRJEB4337 (<https://www.ncbi.nlm.nih.gov/bioproject/PRJEB4337/>). The expression values of SND1 in 24 human tissues were obtained from RNA-seq RPKM (Reads Per Kilobase per Million mapped reads) values and analyzed by Graphpad. **(B)** SND1 protein expression in different cell lines and mice tissues. MEF were generated from E13.5 mouse embryo following a standard 3T3-MEF generation protocol. MEF cells and other cell lines were lysed. Total cell lysates were analyzed by Western blotting. Different tissues from 8-week-old FVB mice were homogenized and lysed, total tissue lysates were analyzed by Western blotting. The antibodies used were anti-SND1 (Bethyl, #A302-883A) and anti-ACTIN (Sigma, #A1978).

been generated [95], but the knockout phenotype was never presented, and these mice were only ever used to generate SND1 knockout mouse embryonic fibroblasts (MEFs) for further analysis [94,113]. Phenotyping performed by the mouse genome informatics (MIP) project at the Jackson Labs and the international mouse phenotyping consortium (IMPC), which both perform high-throughput phenotyping of spontaneous and trapping mutant mice, suggests that the SND1 knockout is partially viable, with knockout mice appearing at lower than expected Mendelian ratios (approximately 50% of the expected ratio). This data suggests that adult SND1 knockout mice will be available for detailed analysis (albeit at low numbers). However, very little information has yet been gleaned from the systemic knockout of SND1. It would be very informative to compare an SND1 knockout phenotype to a SND1 Tudor-dead knockin phenotype, as this would reveal the importance of the methylarginine reader abilities of SND1, and reveal what signaling pathways are dependent of SND1's ability to read PRMT5 deposited marks, and what SND1 functions are independent of PRMT5 activity.

An overexpression model has revealed that SND1 is a driver for HCC when the induction of expression is focused on the liver, using an Albumin promoter (see section 4.2) [14]. Similar overexpression models for PRMT5 would be extremely valuable to investigate whether this mouse would phenocopy the SND1 as a driver of HCC. Although we have generated other PRMT overexpression transgenic mouse models (including PRMT1, CARM1 and PRMT6) [114], the PRMT5 overexpression transgenic mouse has not yet been developed.

### 3.8. Mouse Syngeneic Tumor Models Reveal a Role for SND1 (and PRMT5) in Antitumor Immunity

The melanoma B16F10 cell line has been used to investigate the role of SND1 in facilitating immune evasion of tumor cells [115]. B16F10-SND1-KO cells were transferred into the flank of syngeneic mice and monitored over a number of days. The resulting tumor size and weight were smaller for growths seeded with SND1-KO cells than in the control parental cell. Furthermore, it was found that SND1-null tumors elicited a robust immune response, when compared to the parental cells. This suggests that the loss of SND1 may sensitize tumors to



immune checkpoint inhibitors. Importantly, very similar experiments involving siRNA-mediated PRMT5 knockdown or PRMT5 inhibition by small-molecule treatment in B16F10 cells also showed that the presence of PRMT5 activity attenuates immune checkpoint therapy [116]. Thus, the loss of either PRMT5 or SND1 will convert an immunologically “cold” microenvironment into a “hot” one, further supporting a mechanistic link between this writer–reader pair. HCC may be sensitized to respond to immune checkpoint inhibitors (which block PD1, PD-L1 and CTLA-4 activity) by prior treatment with PRMT5 inhibitors.

### 3.9. SND1 Is Likely an Oncogene

Like PRMT5 [16], SND1 is upregulated in many different cancer types [117,118]. There is a particular interest in HCC, stemming from the observation made ten years ago, that SND1 protein levels are elevated in HCC and that its expression increases with the stage of the disease [119]. Interestingly, the analysis of RNA expression data-bases (TCGA and GEO) does not support a role for SND1 expression in the clinical progression of liver cancer [117], but the analysis of protein expression by immunohistochemistry does [119]. This suggests that SND1 may be post-transcriptionally regulated in certain tissues, as we have eluded to above (Figure 3). We will next summarize the reported roles of PRMT5 and SND1 in HCC, which can serve as a pre-clinical (mouse) and clinical (human) model system for understanding the link between this enzyme and its effector.

## 4. Hallmarks of HCC

Liver cancer comes in a variety of types and frequencies, from the common HCC and cholangiocarcinoma to the rare liver angiosarcoma and pediatric hepatoblastoma. HCC is cited as constituting approximately 75% of all liver cancers according to the Cancer Treatment Centers of America. Among all cancers, HCC is the fourth leading cause of cancer mortality worldwide [13]. Traditionally, HCC has affected more males than females, though recent studies have begun to suggest occurrence may have less gender disparities than previously thought [120,121]. Induction of HCC is often preceded by other hepatic ailments which ultimately develop into HCC. Non-alcoholic fatty liver disease (NAFLD) is one such malady that ultimately leads to

HCC and is associated with obesity and metabolic syndrome [122,123]. Progression towards HCC from NAFLD often occurs in successive stages from NAFLD which develops into non-alcoholic steatohepatitis (NASH), increasing to fibrosis and cirrhosis, concluding with HCC and metastasis [124].

Atypical lipid accumulation is characteristic of hepatic damage and malignancies and HCC is no exception [125,126]. Hallmark metabolic dysregulation in hepatic tissues include increased de novo synthesis of lipids over extracellular lipid uptake to fulfill the lipid requirements needed for excessive cell division in the transformed state [126–128]. Upswing in lipogenesis arises in part from the liver being the center of lipid synthesis allowing a microenvironment permissible for de novo lipid synthesis. Sterol regulatory element-binding protein (SREBP) is a transcription factor directly upregulated in hepatocytes with active de novo lipogenesis. Accordingly, in HCC and premalignant hepatocytes, lipid accumulation is a tell-tale indicator of increased HCC risk. Lipid accumulation can be grossly visualized as lipid droplets within cells. Additional markers of HCC used in the clinic include measurement of alpha-fetoprotein (AFP), Alanine transaminase (ALT), and Aspartate transaminase (AST). Each of these enzymes, when elevated in the blood stream, can suggest malignancy and dysregulation of hepatocytes as they are typically seen in low abundance extra-hepatically. HCC is highly vascularized allowing excessive signaling and growth factor secretion for rapid expansion of cancer cells and is subsequently supported by sustained nutrient availability [129]. Hepatitis B/C (HBV and HCV, respectively) is the most common risk factor for developing HCC. Many reviews have explored HBV and HCV as they relate to HCC. Interestingly, PRMT5 can methylate the HBV core protein [130], and regulates its nuclear accumulation. Thus, there may be cross-talk between PRMT5–SND1 axis and hepatitis, but this issue will not be further addressed here.

#### 4.1. PRMT5 and HCC

PRMT5 has, in recent years, become an increasingly prominent character in HCC research. Multiple studies have reported a worse prognosis of HCC patients with increased

PRMT5 expression [12,74–76,131]. PRMT5 combined with the lysine methyl-transferase SET8 have been identified as predictors of overall survival and recurrence in HCC patients [131].

EMT and invasion are key hallmarks of metastasis and PRMT5 has been identified as important in both. In vitro knockdown of PRMT5 in HCC and colon cancer cells decreases matrix metalloproteinase-2 expression [75]. This impaired expression decreases invasiveness of these lines along with decreasing proliferation which is supported by another study confirming increased HCC proliferation in PRMT5 competent lines [78]. A current model of E-cadherin depletion, characteristic of EMT, proposes the zinc finger domains of SNAIL directly bind the E-cadherin enhancer. AJUBA links PRMT5–MEP50 complex to SNAIL thereby permitting PRMT5 to mediate the SNAIL-dependent gene repression of E-cadherin [63].

A cellular defense against EMT in hepatocytes is the transcription of hepatocyte nuclear factor 4 $\alpha$  (HNF4 $\alpha$ ). HNF4 $\alpha$  has been shown to re-differentiate HCC cells towards hepatocytes and repress EMT, thereby blocking hepatocarcinogenesis [121,132,133]. While HNF4 $\alpha$  works to drive differentiation towards hepatic cellularity, PRMT5 antagonizes HNF4 $\alpha$  expression assisting in liver cancer stem cell maintenance. In HCC cells, PRMT5 binds H4R3 generating H4R3me2s at the HNF4 $\alpha$  promoter. This methylation of H4R3 represses HNF4 $\alpha$  transcription, while inhibition of PRMT5 activity restores HNF4 $\alpha$  transcription and differentiation activity [78].

Another tumor suppressor, BTG2, is known to suppress proliferation, and is typically inhibited in cancers. While tumor suppressors are commonly inactivated by genetic mutations, deleterious mutations in BTG2 have not to date been identified, suggesting its downregulation may be a result of epigenetic reprogramming. PRMT5 has recently been linked to repressing BTG2 expression (again, in the context of HCC) through ERK signaling, though the mechanism of repression remains unknown [74].

As previously mentioned, lipid accumulation is concurrent with hepatic damage [125]. Lipid accumulation is driven by de novo lipogenesis over extracellular uptake, implying that drivers of lipid synthesis harbor oncogenic potential in hepatocytes. Sterol regulatory element-

binding protein 1 (SREBP1) is a transcription factor that regulates the expression of genes involved in the synthesis of fatty acids, triglycerides and phospholipids, and has recently been shown to directly interact with PRMT5 [134]. Furthermore, PRMT5 methylates SREBP1, which stabilizes this transcription factor and helps promote the expression of its target genes and consequently also de novo lipogenesis. The overexpression of PRMT5 in HepG2 cells increases the levels of intracellular triglyceride levels, and conversely, the knockdown of PRMT5 results in a decrease in Oil red-O staining (a marker for intracellular lipid droplet accumulation). Furthermore, the overexpression of SREBP1 causes an increase in Oil red-O staining, which is not observed when the mutant form of SREBP1 (that cannot be methylated by PRMT5) is overexpressed. Thus, PRMT5 promotes de novo lipogenesis by methylating a single site on SREBP1 [134].

Long non-coding RNAs (lncRNAs) have emerged as key regulators of normal physiology as well as pathogenesis. Long intergenic non-coding RNA 1q21.2 (LINC01138) has been shown to correlate with PRMT5 expression as well as HCC tumor size, AFP levels, and hepatitis B surface antigen levels. PRMT5 and LINC01138 were shown to interact in HCC, which allowed PRMT5 to evade proteasomal degradation [77]. Increased PRMT5 stability may explain why we see increased protein expression of PRMT5, but not an increase in PRMT5 mRNA levels in some patient samples.

Recent findings reveal that PRMT5, in combination with SND1, promotes the dynamic regulation of E2F1 target genes. PRMT5 has been shown to promote cell growth, which contrasts to PRMT1 asymmetric dimethylation of E2F1 which promotes apoptosis [67,81]. PRMT5 methylation of E2F1, and the subsequent recognition of this methylated site by SND1, expands traditional E2F1 transcriptional control of genes to an extended set of targets that are traditionally poorly regulated by E2F. Extended targeting is accomplished by E2F1-dependent alternative splicing of targets. This alternative splicing activity is dependent on both PRMT5 activity as well as SND1 recognition of SDMA marks on E2F1 [93]. While PRMT5 driven proliferation via E2F1 methylation has been identified, it remains unclear whether this signaling pathway is active or

important for the development of HCC. However, given the emerging role of E2F1 in HCC [135], the activation of this regulatory node could be a critical consequence of elevated PRMT5 and/or SND1 protein levels.

#### 4.2. SND1 and HCC

While the role that PRMT5 plays in the development of HCC is largely circumstantial—elevated PRMT5 levels clearly correlate with the promotion of HCC and poor prognosis of these cancer patients—its effector molecule, SND1, is more solidly implicated as a driver of HCC. Indeed, a landmark study of SND1 in HCC emerged from a mouse model with SND1 overexpression [14]. Transgenic mice carrying SND1 under the control of an albumin promoter/enhancer element, selectively overexpress SND1 in the liver, and this is sufficient to drive spontaneous HCC formation with partial penetrance. While half of the overexpressing mice develop HCC spontaneously, all overexpressing mice showed more aggressive tumors in HCC that is chemically induced by diethylnitrosamine (DEN). Hepatocytes from SND1 overexpressing mice have higher levels of spheroid-generating tumor-initiating cells. Furthermore, SND1 overexpression resulted in a steady proinflammatory state [14], similar to what is seen in chronic inflammation, a central hallmark of HCC progression.

SND1 contributes to alterations in the signaling cascades within HCC that control both transcriptional and post-transcriptional regulation. Angiotensin 2 receptor 1 (AT1R) mRNA stability is augmented through overexpression of SND1 [136]. Importantly, upregulation of AT1R is associated with both the progression of HCC, as well as unfavorable outcomes with respect to overall survival of cancer patients [137]. This increased stability of AT1R mRNA, and subsequent elevation of its protein levels, activates the ERK and SMAD signaling pathways, leading to a downstream increase in TGF $\beta$  signaling in HCC cells [138]. TGF $\beta$  signaling is known to drive proliferation and EMT progression [139]. Furthermore, TGF $\beta$  signaling also induces SND1 transcriptional activation in a feed forward loop [140]. This feed forward activity can be seen in other SND1-regulated pathways including NF- $\kappa$ B and SREBPs [141]. SND1 further promotes proliferative signals by degradation of miRNA via its nuclease domains. Elbarbary et. al. used

transcriptome profiling to identify miRNAs that increase after knockdown or knockout of SND1, and show that these upregulated miRNAs in turn downregulate a cohort of mRNAs that are needed for G1/S transition [103]. We can speculate that the opposite is also true, when SND1 is upregulated, the G1/S transition may be shortened, and this would help explain one of the characteristics of liver cancer, which is a deregulated cell cycle [142].

NF- $\kappa$ B is a transcription factor that regulates innate immunity, and activation of this pathway promotes an inflammatory response and cellular growth. Chronic inflammation has been linked to many cancers, including HCC [143–145]. Indeed, chronic inflammation and hepatic injury serve as malignant drivers and precede 90% of HCC occurrences [146]. SND1 interacts with AEG-1 (also called metadherin) [119], which regulates multiple signaling pathways including NF- $\kappa$ B, PI3K/Akt and Wnt [147]. The activation of the NF- $\kappa$ B pathway by SND1 overexpression is reported to increase onco-genic miRNAs (oncomiRs) such as miR-221, that target and degrade tumor suppressor RNAs [80,148]. SND1 overexpression functions to increase inflammatory driving cytokines to promote HCC formation, as well as factors such as CXCL16 and angiogenin which promote angiogenesis. The inhibition of NF- $\kappa$ B blocks SND1-induced angiogenesis [80]. The benefits, to liver cancer cells, of having elevated SND1 can thus be explained, in part, by its pro-inflammatory and pro-angiogenic roles.

In order for cancer cells to persist and multiply, they evolve aggressive survival responses to stress signals to evade cell death pathways, which represents one of the major hallmarks of cancer. Stress granules are membraneless organelles that collect in the cytoplasm of cells, and serve as a means of stalling cellular machinery while the cell responds to the strain [149]. This suspended state can buy time sufficient for cells to respond with survival signaling, thereby evading apoptosis. SND1 has been shown to be enriched in stress granules induced from oxidative stress [150–152]. Whether SND1's role is primarily as a nuclease or as a recruiting/scaffolding protein remains unclear. It has been noted, however, that phosphorylation of SND1 promotes its binding to G3BP [152], which in turn stimulates stress granule formation, suggesting that SND1 works in a recruiting role in stress granule formation. The ability of SND1

to help liver cancer cells evade cell death is not limited to its role in stress granule formation and function. SND1 can also promote the expression of UCA1 expression in HepG2 and SMMC-7721 cells [153]. UCA1 is an oncogenic lncRNA that has anti-apoptotic activity, and is itself a predictor of poor overall survival for patients with HCC [154]. Thus, high levels of SND1 helps tumor cells evade cell death.

A third survival pathway for cancer cells is DNA damage response. Using a laser microirradiation approach, SND1 is clearly localized to the laser-induced DNA damaged stripes [113]. Mechanistically, SND1 is recruited by PARP1 to damaged DNA, where it serves as a scaffold for chromatin remodeling proteins that then help facilitate DNA repair, such as SMARCA5 and GCN5 [113]. These two proteins are an ATP-dependent remodeler and a histone acetyltransferase, respectively, and they both act at sites of DNA damage to help open up chromatin so that the repair machinery can access the damaged DNA. SND1 overexpression thereby potentially provides a survival advantage in DNA damaged cells [82]. The combination of the liver as the body's de-toxification center, along with the ability of elevated SND1 levels to promote survival advantages under DNA damaging conditions, may partially explain why HCC is often chemoresistant and radioresistant. Targeting SND1 may reverse this resistance.

Like PRMT5, SND1 has been noted to have a variety of functions in lipogenesis. SND1 facilitates lipid droplet formation in mammary cells and hepatocytes. This association is lost in milk globules suggesting that SND1 association is specific to formation, but not maintenance of fat droplets [105,155]. SND1 overexpressing cells show a significantly altered lipoprotein secretion content and are saturated with phospholipids over other metabolically common lipids [156]. SREBPs appear to be regulated by SND1, although the difference in activity between normal and diseased states remains unknown [156]. More recently, it was found that hepatoma cells overexpressing SND1 display low triglyceride synthesis and accelerated cholesterol ester synthesis, likely because fat-ty acids are preferentially used for cholesterol esterification [157]. While profiling the target genes of SND1s transcriptional coactivator activity, using human hepatoma HepG2 cells, it was found that cohort of glycerolipid genes (such as CHPT1, LPGAT1,

PTDSS1 and LPIN1) are regulated by SND1, in response to proinflammatory TNF $\beta$  signaling [83]. SND1 is thus key for sustaining glycerophospholipid homeostasis in human HCC cells. The roles of SND1 in lipid metabolism has recently been reviewed in detail [158].

#### 5. Targeting Elevated SND1 Levels with PRMT5 Inhibitors

As highlighted above, PRMT5 is overexpressed in a large number of different tumor types, and the inhibition of PRMT5 has been linked to tumor regression in mouse models [2,16,54]. These findings indicate that PRMT5 might be a promising therapeutic target for both solid and liquid tumors. Indeed, PRMT5 is currently a very popular target for the development of small-molecule inhibitors by both pharma and biomedical startup companies. A search of the published and patent literature reveals the development of at least 13 distinct PRMT5 inhibitors (Table 1). These inhibitors have six different mechanisms of action (MOA) [159,160], namely (1) inhibitors that compete with SAM (but not the peptide substrate); (2) inhibitors that compete with peptide substrate (but not SAM-competitive); (3) inhibitors that block both SAM and the substrate peptide from binding; (4) covalent inhibitors that form a stable bond with Cys449 in the active site and prevent SAM binding; (5) the development of a PROTAC probe that is based on the GSK3326595 compound, and targets PRMT5 for proteasomal degradation; (6) an allosteric inhibitor which causes the formation of an 11 amino acid acidic loop that blocks both SAM binding and peptide substrate binding.

In addition to the panel of 13 different PRMT5 inhibitors that have been developed, it may be possible to target elevated PRMT5 levels using inhibitors for PRMT1 and perhaps even CARM1 (PRMT4). This is because there is clear evidence of redundancy between different PRMT family members. Indeed, we have shown that PRMT1 and PRMT5 share many substrates [7]. Furthermore, GSK and the Guccione lab have shown that PRMT5 and PRMT1 inhibitors function synergistically to target MTAP-null cancer cells [161] and tumors that are driven by splicing mutations [56]. Finally, using a CRISPR-screening approach, we have found that in the presence



Table 1. PRMT5 inhibitor and their different mechanisms of action.

Company	Compound	Trials	MOA	Ref. or Patent
GSK/ Epizyme	GSK3326595	Ph 1 NCT02783300 Ph 2 NCT03614728	b	[164]
Pfizer	PF-06939999	Ph 1 NCT03854227	a	[165]
Janssen	JNJ64619178	Ph 1 NCT03573310	c	AACR
Prelude	PRT543	Ph 1 NCT03886831	a	[166]
Prelude	PRT811	Ph 1 NCT04089449	a	[166]
Prelude	C449	Pre-clinical	f	[167]
Eli Lilly	LLY-283	Pre-clinical	a	[168]
Argonaut	T1-44	Pre-clinical	b	[169]
Jian Jin	MS4322	Pre-clinical	d	[159]
Merck	Comp 1A	Pre-clinical	e	[160]
Aurigene	AU-14755	Pre-clinical	b	WO2019-180628
Angex	Not named	Pre-clinical	a	WO2019-112719
Jubilant	JPRMT5i	Pre-clinical	b	WO2019-102494

Mechanism of action (MOA): (a) SAM competitive; (b) SAM cooperative and peptide substrate competitive; (c) SAM and peptide substrate competitive; (d) PROTAC degrader; (e) allosteric modulator; and (f) covalent inhibitor. The “WO2019” numbers refer to patent submissions.

of PRMT5 inhibitors cells are sensitized to PRMT1 and CARM1 loss [162]. Thus, it may be important to evaluate the effects of a CARM1 inhibitor (GSK3359088) [163] and a Type I PRMT inhibitor (GSK3368715) [161] for their ability to retard the growth of tumors with elevated PRMT5–SND1 signaling.

## 6. Conclusion and Future Direction

HCC is a major health concern worldwide. It has a 20% five-year survival rate and 1% of the global population are expected to develop HCC in their life time. This disease poses a significant health burden which urges additional study. The majority of therapeutic options are hepatic resection and transplant, though transplant needs far out-weigh available organs [13]. Accordingly, a more comprehensive molecular understanding of HCC development is needed to approach the HCC epidemic. The PRMT5–SND1 axis has emerged recently as a key point of inquiry, though we are far from understanding its intricacies in HCC. A lot of the interest in PRMT5 is driven by the fact that there are now very good inhibitors available that target this enzyme, raising therapeutic hope for diseases that are driven by PRMT5 overexpression, or by increased effector molecule activity (such as SND1 overexpression). SND1 has been shown to be a potent hepatic-oncogene, though many important questions still need to be addressed. Clearly, there remains a lot of low-hanging fruit to be picked; for example: (1) In the context of HHC, is SND1 the primary effector molecule for SDMA marks that are deposited by PRMT5? (2) Does SND1 compete with other Tudor domain-containing proteins such as SMN for binding to PRMT5 deposited marks? (3) Will PRMT5 inhibitors block the oncogenic effects of SND1 overexpression in the liver? (4) How important is the Tudor domain of SND1 for its oncogenic function? Many of these questions will require the development of new genetically engineered mouse models that will facilitate pre-clinical studies. A detailed mechanistic elucidation of the PRMT5–SND1 axis in HCC promises to illuminate novel and rational approaches towards treating this terrible disease.

Author Contributions: T.W. wrote the first draft of this review. M.T.B. then revised the review. Y.W. edited the review and contributed to Figure 2. All authors have read and agreed to the published version of the manuscript.

Funding: M.T.B. is supported by an NIH grant—GM126421.

Conflicts of Interest: M.T.B. is a co-founder of EpiCypher.

## References

1. Chen, J.; Sagum, C.; Bedford, M.T. Protein domain microarrays as a platform to decipher signaling pathways and the his-tone code. *Methods* 2019, 184, 1–12, doi:10.1016/j.ymeth.2019.08.007.
2. Yang, Y.; Bedford, M.T. Protein arginine methyltransferases and cancer. *Nat. Rev. Cancer* 2013, 13, 37–50, doi:10.1038/nrc3409.
3. Rhein, V.F.; Carroll, J.; Ding, S.; Fearnley, I.M.; Walker, J.E. NDUFAF7 methylates arginine 85 in the NDUF52 subunit of human complex I. *J. Biol. Chem.* 2013, 288, 33016–33026, doi:10.1074/jbc.M113.518803.
4. Yang, Y.; Hadjikyriacou, A.; Xia, Z.; Gayatri, S.; Kim, D.; Zurita-Lopez, C.; Kelly, R.; Guo, A.; Li, W.; Clarke, S.G.; Bedford, M.T. PRMT9 is a type II methyltransferase that methylates the splicing factor SAP145. *Nat. Commun.* 2015, 6, 6428, doi:10.1038/ncomms7428.
5. Matsuoka, M. Epsilon-N-methylated lysine and guanidine-N-methylated arginine of proteins. 3. Presence and distribu-tion in nature and mammals. *Seikagaku* 1972, 44, 364–370.
6. Paik, W.K.; Kim, S. *Natural Occurrence of Various Methylated Amino Acid Derivatives*; John Wiley & Sons: New York, NY, USA, 1980; pp. 8–25.
7. Dhar, S.; Vemulapalli, V.; Patananan, A.N.; Huang, G.L.; Di Lorenzo, A.; Richard, S.; Comb, M.J.; Guo, A.; Clarke, S.G.; Bedford, M.T. Loss of the major Type I arginine methyltransferase PRMT1 causes substrate scavenging by other PRMTs. *Sci. Rep.* 2013, 3, 1311, doi:10.1038/srep01311.
8. Gayatri, S.; Bedford, M.T. Readers of histone methylarginine marks. *Biochim. Biophys. Acta* 2014, 1839, 702–710, doi:10.1016/j.bbagr.2014.02.015.
9. Ponting, C.P. Tudor domains in proteins that interact with RNA. *Trends Biochem. Sci.* 1997, 22, 51–52, doi:S0968-0004(96)30049-2.

10. Friesen, W.J.; Massenet, S.; Paushkin, S.; Wyce, A.; Dreyfuss, G. SMN, the product of the spinal muscular atrophy gene, binds preferentially to dimethylarginine-containing protein targets. *Mol. Cell* 2001, 7, 1111–1117.
11. Selenko, P.; Sprangers, R.; Stier, G.; Buhler, D.; Fischer, U.; Sattler, M. SMN tudor domain structure and its interaction with the Sm proteins. *Nat. Struct. Biol.* 2001, 8, 27–31.
12. Shimizu, D.; Kanda, M.; Sugimoto, H.; Shibata, M.; Tanaka, H.; Takami, H.; Iwata, N.; Hayashi, M.; Tanaka, C.; Koba-yashi, D.; Yamada, S.; Nakayama, G.; Koike, M.; Fujiwara, M.; Fujii, T.; Kodera, Y. The protein arginine methyltransferase 5 promotes malignant phenotype of hepatocellular carcinoma cells and is associated with adverse patient outcomes after curative hepatectomy. *Int. J. Oncol.* 2017, 50, 381–386, doi:10.3892/ijo.2017.3833.
13. Asrani, S.K.; Devarbhavi, H.; Eaton, J.; Kamath, P.S. Burden of liver diseases in the world. *J. Hepatol.* 2019, 70, 151–171, doi:10.1016/j.jhep.2018.09.014.
14. Jariwala, N.; Rajasekaran, D.; Mendoza, R.G.; Shen, X.N.; Siddiq, A.; Akiel, M.A.; Robertson, C.L.; Subler, M.A.; Windle, J.J.; Fisher, P.B.; Sanyal, A.J.; Sarkar, D. Oncogenic Role of SND1 in Development and Progression of Hepatocellular Carcinoma. *Cancer Res.* 2017, 77, 3306–3316, doi:10.1158/0008-5472.CAN-17-0298.
15. Wang, M.; Xu, R.M.; Thompson, P.R. Substrate specificity, processivity, and kinetic mechanism of protein arginine methyl-transferase 5. *Biochemistry* 2013, 52, 5430–5440, doi:10.1021/bi4005123.
16. Kim, H.; Ronai, Z.A. PRMT5 function and targeting in cancer. *Cell Stress* 2020, 4, 199–215, doi:10.15698/cst2020.08.228.
17. Friesen, W.J.; Wyce, A.; Paushkin, S.; Abel, L.; Rappsilber, J.; Mann, M.; Dreyfuss, G. A novel WD repeat protein component of the methylosome binds Sm proteins. *J. Biol. Chem.* 2002, 277, 8243–8247.

18. Gao, G.; Dhar, S.; Bedford, M.T. PRMT5 regulates IRES-dependent translation via methylation of hnRNP A1. *Nucleic Acids Res.* 2017, 45, 4359–4369, doi:10.1093/nar/gkw1367.
19. Timm, D.E.; Bowman, V.; Madsen, R.; Rauch, C. Cryo-electron microscopy structure of a human PRMT5:MEP50 complex. *PLoS One* 2018, 13, e0193205, doi:10.1371/journal.pone.0193205.
20. Ho, M.C.; Wilczek, C.; Bonanno, J.B.; Xing, L.; Seznec, J.; Matsui, T.; Carter, L.G.; Onikubo, T.; Kumar, P.R.; Chan, M.K.; Brenowitz, M.; Cheng, R.H.; Reimer, U.; Almo, S.C.; Shechter, D. Structure of the arginine methyltransferase PRMT5-MEP50 reveals a mechanism for substrate specificity. *PLoS One* 2013, 8, e57008, doi:10.1371/journal.pone.0057008.
21. Antonysamy, S.; Bonday, Z.; Campbell, R.M.; Doyle, B.; Druzina, Z.; Gheyi, T.; Han, B.; Jungheim, L.N.; Qian, Y.; Rauch, C.; Russell, M.; Sauder, J.M.; Wasserman, S.R.; Weichert, K.; Willard, F.S.; Zhang, A.; Emtage, S. Crystal structure of the human PRMT5:MEP50 complex. *Proc. Natl. Acad. Sci. USA* 2012, 109, 17960–17965, doi:10.1073/pnas.1209814109.
22. Hosohata, K.; Li, P.; Hosohata, Y.; Qin, J.; Roeder, R.G.; Wang, Z. Purification and identification of a novel complex which is involved in androgen receptor-dependent transcription. *Mol. Cell. Biol.* 2003, 23, 7019–7029.
23. Wilczek, C.; Chitta, R.; Woo, E.; Shabanowitz, J.; Chait, B.T.; Hunt, D.F.; Shechter, D. Protein arginine methyltransferase Prmt5-Mep50 methylates histones H2A and H4 and the histone chaperone nucleoplasmin in *Xenopus laevis* eggs. *J. Biol. Chem.* 2011, 286, 42221–42231, doi:10.1074/jbc.M111.303677.
24. Meister, G.; Eggert, C.; Buhler, D.; Brahms, H.; Kambach, C.; Fischer, U. Methylation of Sm proteins by a complex containing PRMT5 and the putative U snRNP assembly factor pICln. *Curr. Biol.* 2001, 11, 1990–1994.

25. Pesiridis, G.S.; Diamond, E.; Van Duyne, G.D. Role of pICln in methylation of Sm proteins by PRMT5. *J. Biol. Chem.* 2009, 284, 21347–21359, doi:10.1074/jbc.M109.015578.
26. Paknia, E.; Chari, A.; Stark, H.; Fischer, U. The Ribosome Cooperates with the Assembly Chaperone pICln to Initiate Formation of snRNPs. *Cell Rep.* 2016, 16, 3103–3112, doi:10.1016/j.celrep.2016.08.047.
27. Guderian, G.; Peter, C.; Wiesner, J.; Sickmann, A.; Schulze-Osthoff, K.; Fischer, U.; Grimmmler, M. RioK1, a new interactor of protein arginine methyltransferase 5 (PRMT5), competes with pICln for binding and modulates PRMT5 complex composition and substrate specificity. *J. Biol. Chem.* 2011, 286, 1976–1986, doi:10.1074/jbc.M110.148486.
28. Lacroix, M.; Messaoudi, S.E.; Rodier, G.; Le Cam, A.; Sardet, C.; Fabrizio, E. The histone-binding protein COPR5 is re-quired for nuclear functions of the protein arginine methyltransferase PRMT5. *EMBO Rep.* 2008, 9, 452–458.
29. Tamiya, H.; Kim, H.; Klymenko, O.; Kim, H.; Feng, Y.; Zhang, T.; Han, J.Y.; Murao, A.; Snipas, S.J.; Jilaveanu, L.; Brown, L.; Kluger, H.; Zhang, H.; Iwai, K.; Ronai, Z.A. SHARPIN-mediated regulation of protein arginine methyltransferase 5 controls melanoma growth. *J. Clin. Invest.* 2018, 128, 517–530, doi:10.1172/JCI95410.
30. Yang, M.; Lin, X.; Segers, F.; Suganthan, R.; Hildrestrand, G.A.; Rinholm, J.E.; Aas, P.A.; Sousa, M.M.L.; Holm, S.; Bolstad, N.; Warren, D.; Berge, R.K.; Johanse, R.F.; Yndestad, A.; Krisiansen, E.; Klungland, A.; Luna, L.; Eide, L.; Halvorsen, B.; Aukrust, P.; Bjørås, M. OXR1A, a Coactivator of PRMT5 Regulating Histone Arginine Methylation. *Cell Rep.* 2020, 30, 4165–4178, doi:10.1016/j.celrep.2020.02.063.
31. Kryukov, G.V.; Wilson, F.H.; Ruth, J.R.; Paulk, J.; Tsherniak, A.; Marlow, S.E.; Vazquez, F.; Weir, B.A.; Fitzgerald, M.E.; Tanaka, M.; Bielski, C.M.; Scott, J.M.; Dennis, C.; Soley, G.S.; Boehm, J.S.; Root, D.E.; Golub, T.R.; Clish, C.B.; Bradner, J.E.; Hahn, W.C.; Garraway, L.A. MTAP deletion confers enhanced dependency on the PRMT5 arginine

- methyltransferase in cancer cells. *Science* 2016, 351, 1214–1218, doi:10.1126/science.aad5214.
32. Marjon, K.; Cameron, M.J.; Quang, P.; Clasquin, M.F.; Mandley, E.; Kunii, K.; McVay, M.; Choe, S.; Kernytsky, A.; Gross, S.; Konteatis, Z.; Murtie, J.; Blake, M.L.; Travins, J.; Dorsch, M.; Biller, S.A.; Marks, K.M. MTAP Deletions in Cancer Create Vulnerability to Targeting of the MAT2A/PRMT5/RIOK1 Axis. *Cell Rep.* 2016, 15, 574–587, doi:10.1016/j.celrep.2016.03.043.
33. Mavrakis, K.J.; McDonald, E.R., 3rd; Schlabach, M.R.; Billy, E.; Hoffman, G.R.; deWeck, A.; Ruddy, D.A.; Venkatesan, K.; Yu, J.; McAllister, G.; Stump, M.; deBeaumont, R.; Ho, S.; Yue, y.; Liu, y.; Yan-Neale, Y.; Yang, G.; Lin, F.; Yin, H.; Gao, H.; Kipp, D.R.; Zhao, S.; McNamara, J.T.; Sprague, E.R.; Zheg, B.; Lin, Y.; Cho, Y.S.; Gu, J.; Crawford, k.; Ciccone, D.; Vitari, A.C.; Lai, A.; Capka, V.; Hurov, K.; Porter, J.A.; Tallarico, J.; Mickanin C.; Lees, E.; Pagliarini R.; Keen, N.; Schmelzle, T.; Hofmann, Fl.; Stegmeier F.; Sellers. W.R. Disordered methionine metabolism in MTAP/CDKN2A-deleted cancers leads to dependence on PRMT5. *Science* 2016, 351, 1208–1213, doi:10.1126/science.aad5944.
34. Pollack, B.P.; Kotenko, S.V.; He, W.; Izotova, L.S.; Barnoski, B.L.; Pestka, S. The human homologue of the yeast proteins Skb1 and Hsl7p interacts with Jak kinases and contains protein methyltransferase activity. *J. Biol. Chem.* 1999, 274, 31531–31542.
35. Tee, W.W.; Pardo, M.; Theunissen, T.W.; Yu, L.; Choudhary, J.S.; Hajkova, P.; Surani, M.A. Prmt5 is essential for early mouse development and acts in the cytoplasm to maintain ES cell pluripotency. *Genes Dev.* 2010, 24, 2772–2777, doi:10.1101/gad.606110.
36. Boisvert, F.M.; Cote, J.; Boulanger, M.C.; Richard, S. A Proteomic Analysis of Arginine-methylated Protein Complexes. *Mol. Cell. Proteom.* 2003, 2, 1319–1330.
37. Musiani, D.; Bok, J.; Massignani, E.; Wu, L.; Tabaglio, T.; Ippolito, M.R.; Cuomo, A.; Ozbek, U.; Zorgati, H.; Ghoshdastider, U.; Robinson, R.C.; Guccione, E.; Bonaldi, T.



- Proteomics profiling of arginine methylation defines PRMT5 substrate specificity. *Sci. Signal.* 2019, 12, doi:10.1126/scisignal.aat8388.
38. Nishioka, K.; Reinberg, D. Methods and tips for the purification of human histone methyltransferases. *Methods* 2003, 31, 49–58.
39. Chendrimada, T.P.; Gregory, R.I.; Kumaraswamy, E.; Norman, J.; Cooch, N.; Nishikura, K.; Shiekhattar, R. TRBP recruits the Dicer complex to Ago2 for microRNA processing and gene silencing. *Nature* 2005, 436, 740–744, doi:10.1038/nature03868.
40. Chen, G.I.; Gingras, A.C. Affinity-purification mass spectrometry (AP-MS) of serine/threonine phosphatases. *Methods* 2007, 42, 298–305, doi:10.1016/j.ymeth.2007.02.018.
41. Mellacheruvu, D.; Wright, Z.; Couzens, A.L.; Lambert, J.P.; St-Denis, N.A.; Li, T.; Miteva, Y.V.; Hauri, S.; Sardiu, M.E.; Low, T.Y.; Halim, V.A.; Bagshaw, R.D.; Hubner, N.C.; Al-Hakim, A.; Bouchard, A.; Faubert, D.; Fermin, D.; Dunham, W.H.; Goudreault, M.; Lin, Z.; Badillo, B.G.; Pawson, T.; Durocher, D.; Coulombe, B.; Aebersold, R.; Superti-Ferga, G.; Colinge, J.; Heck, A.J.R.; Choi, H.; Gstaiger, M.; Mohammed, S.; Cristea, I.M.; Bennett, K.L.; Washburn, M.P.; Raught, B.; Ewing, R.M.; Gingras, A.; Nesvizhskii, A.I. The CRAPome: A contaminant repository for affinity purification-mass spectrometry data. *Nat. Methods* 2013, 10, 730–736, doi:10.1038/nmeth.2557.
42. Zhou, L.; Wu, H.; Lee, P.; Wang, Z. Roles of the androgen receptor cofactor p44 in the growth of prostate epithelial cells. *J. Mol. Endocrinol.* 2006, 37, 283–300, doi:10.1677/jme.1.02062.
43. Bezzi, M.; Teo, S.X.; Muller, J.; Mok, W.C.; Sahu, S.K.; Vardy, L.A.; Bonday, Z.Q.; Guccione, E. Regulation of constitutive and alternative splicing by PRMT5 reveals a role for Mdm4 pre-mRNA in sensing defects in the spliceosomal machinery. *Genes Dev.* 2013, 27, 1903–1916, doi:10.1101/gad.219899.113.
44. Liu, F.; Cheng, G.; Hamard, P.J.; Greenblatt, S.; Wang, L.; Man, N.; Perna, F.; Xu, H.; Tadi, M.; Luciani, L.; Nimer, S.D. Arginine methyltransferase PRMT5 is essential for

- sustaining normal adult hematopoiesis. *J. Clin. Invest.* 2015, 125, 3532–3544, doi:10.1172/JCI81749.
45. Litzler, L.C.; Zahn, A.; Meli, A.P.; Hebert, S.; Patenaude, A.M.; Methot, S.P.; Sprumont, A.; Bois, T.; Kitamura, D.; Costanti-no, S.; King, I.L.; Kleinman, C.L.; Richrd, S.; Di Noia, J.M. PRMT5 is essential for B cell development and germinal center dynamics. *Nat. Commun.* 2019, 10, 22, doi:10.1038/s41467-018-07884-6.
  46. Tanaka, Y.; Nagai, Y.; Okumura, M.; Greene, M.I.; Kambayashi, T. PRMT5 Is Required for T Cell Survival and Proliferation by Maintaining Cytokine Signaling. *Front. Immunol.* 2020, 11, 621, doi:10.3389/fimmu.2020.00621.
  47. Norrie, J.L.; Li, Q.; Co, S.; Huang, B.L.; Ding, D.; Uy, J.C.; Ji, Z.; Mackem, S.; Bedford, M.T.; Galli, A.; Ji, J.; Vokes, S.A. PRMT5 is essential for the maintenance of chondrogenic progenitor cells in the limb bud. *Development* 2016, 143, 4608–4619, doi:10.1242/dev.140715.
  48. Gao, S.; Wu, H.; Wang, F.; Wang, Z. Altered differentiation and proliferation of prostate epithelium in mice lacking the androgen receptor cofactor p44/WDR77. *Endocrinology* 2010, 151, 3941–3953, doi:10.1210/en.2009-1080.
  49. Gu, Z.; Zhang, F.; Wang, Z.Q.; Ma, W.; Davis, R.E.; Wang, Z. The p44/wdr77-dependent cellular proliferation process during lung development is reactivated in lung cancer. *Oncogene* 2013, 32, 1888–1900, doi:10.1038/onc.2012.207.
  50. Scaglione, A.; Patzig, J.; Liang, J.; Frawley, R.; Bok, J.; Mela, A.; Yattah, C.; Zhang, J.; Teo, S.X.; Zhou, T.; Chen, S.; Bernstein, E.; Canoll, P.; Guccione, E.; Casaccia, P. PRMT5-mediated regulation of developmental myelination. *Nat. Commun.* 2018, 9, 2840, doi:10.1038/s41467-018-04863-9.
  51. Rho, J.; Choi, S.; Seong, Y.R.; Cho, W.K.; Kim, S.H.; Im, D.S. Prmt5, which forms distinct homo-oligomers, is a member of the protein-arginine methyltransferase family. *J. Biol. Chem.* 2001, 276, 11393–11401.

52. Hamard, P.J.; Santiago, G.E.; Liu, F.; Karl, D.L.; Martinez, C.; Man, N.; Mookhtiar, A.K.; Duffort, S.; Greenblatt, S.; Verdun, R.E.; Nimer, S.D. PRMT5 Regulates DNA Repair by Controlling the Alternative Splicing of Histone-Modifying Enzymes. *Cell Rep.* 2018, 24, 2643–2657, doi:10.1016/j.celrep.2018.08.002.
53. Tan, D.Q.; Li, Y.; Yang, C.; Li, J.; Tan, S.H.; Chin, D.W.L.; Nakamura-Ishizu, A.; Yang, H.; Suda, T. PRMT5 Modulates Splicing for Genome Integrity and Preserves Proteostasis of Hematopoietic Stem Cells. *Cell Rep.* 2019, 26, 2316–2328, doi:10.1016/j.celrep.2019.02.001.
54. Kaushik, S.; Liu, F.; Veazey, K.J.; Gao, G.; Das, P.; Neves, L.F.; Lin, K.; Zhong, Y.; Lu, Y.; Giuliani, V.; Bedford, M.T.; Nimer, S.D.; Santos, M.A. Genetic deletion or small-molecule inhibition of the arginine methyltransferase PRMT5 exhibit anti-tumoral activity in mouse models of MLL-rearranged AML. *Leukemia* 2018, 32, 499–509, doi:10.1038/leu.2017.206.
55. Radzisheuskaya, A.; Shliaha, P.V.; Grinev, V.; Lorenzini, E.; Kovalchuk, S.; Shlyueva, D.; Gorshkov, V.; Hendrickson, R.C.; Jensen, O.N.; Helin, K. PRMT5 methylome profiling uncovers a direct link to splicing regulation in acute myeloid leukemia. *Nat. Struct. Mol. Biol.* 2019, 26, 999–1012, doi:10.1038/s41594-019-0313-z.
56. Fong, J.Y.; Pignata, L.; Goy, P.A.; Kawabata, K.C.; Lee, S.C.; Koh, C.M.; Musiani, D.; Massignani, E.; Kotini, A.G.; Penson, A.; Wun, C.M.; Shen, Y.; Schwarz, M.; Low, D.H.; Rialdi, A.; Ki, M.; Wollmann, H.; Mzoughi, S.; Gay, F.; Thompson, C.; Hart, T.; Barbash, O.; Luciani, G..M.; Szewczyk, M.M.; Wouters, B.J.; Delwel, R.; Papapetrou, E.P.; Barsyte-Lovejoy, D.; Arrowsmith, C.H.; Minden, M.D.; Jin, J.; Melnick, A.; Bonaldi, T.; Abdel-Wahab, O.; Guccione, E. Therapeutic Targeting of RNA Splicing Catalysis through Inhibition of Protein Arginine Methylation. *Cancer Cell* 2019, 36, 194–209, doi:10.1016/j.ccell.2019.07.003.

57. Ma, J.; He, X.; Cao, Y.; O'Dwyer, K.; Szigety, K.M.; Wu, Y.; Gurung, B.; Feng, Z.; Katona, B.W.; Hua, X. Islet-specific Prmt5 excision leads to reduced insulin expression and glucose intolerance in mice. *J. Endocrinol.* 2020, 244, 41–52, doi:10.1530/JOE-19-0268.
58. Zhang, T.; Gunther, S.; Looso, M.; Kunne, C.; Kruger, M.; Kim, J.; Zhou, Y.; Braun, T. Prmt5 is a regulator of muscle stem cell expansion in adult mice. *Nat. Commun.* 2015, 6, 7140, doi:10.1038/ncomms8140.
59. Ramachandran, J.; Liu, Z.; Gray, R.S.; Vokes, S.A. PRMT5 is necessary to form distinct cartilage identities in the knee and long bone. *Dev. Biol.* 2019, 456, 154–163, doi:10.1016/j.ydbio.2019.08.012.
60. Wang, Y.; Zhu, T.; Li, Q.; Liu, C.; Han, F.; Chen, M.; Zhang, L.; Cui, X.; Qin, Y.; Bao, S.; Gao, F. Prmt5 is required for germ cell survival during spermatogenesis in mice. *Sci. Rep.* 2015, 5, 11031, doi:10.1038/srep11031.
61. Li, Q.; Jiao, J.; Li, H.; Wan, H.; Zheng, C.; Cai, J.; Bao, S. Histone arginine methylation by Prmt5 is required for lung branching morphogenesis through repression of BMP signaling. *J. Cell Sci.* 2018, 131, doi:10.1242/jcs.217406.
62. Pal, S.; Vishwanath, S.N.; Erdjument-Bromage, H.; Tempst, P.; Sif, S. Human SWI/SNF-associated PRMT5 methylates histone H3 arginine 8 and negatively regulates expression of ST7 and NM23 tumor suppressor genes. *Mol. Cell. Biol.* 2004, 24, 9630–9645, doi:10.1128/MCB.24.21.9630-9645.2004.
63. Hou, Z.; Peng, H.; Ayyanathan, K.; Yan, K.P.; Langer, E.M.; Longmore, G.D.; Rauscher, F.J., 3rd. The LIM protein AJUBA recruits protein arginine methyltransferase 5 to mediate SNAIL-dependent transcriptional repression. *Mol. Cell. Biol.* 2008, 28, 3198–3207, doi:10.1128/MCB.01435-07.
64. Pal, S.; Baiocchi, R.A.; Byrd, J.C.; Grever, M.R.; Jacob, S.T.; Sif, S. Low levels of miR-92b/96 induce PRMT5 translation and H3R8/H4R3 methylation in mantle cell lymphoma. *EMBO J.* 2007, 26, 3558–3569.

65. Wang, L.; Pal, S.; Sif, S. Protein arginine methyltransferase 5 suppresses the transcription of the RB family of tumor sup-pressors in leukemia and lymphoma cells. *Mol. Cell. Biol.* 2008, 28, 6262–6277, doi:10.1128/MCB.00923-08.
66. Kim, J.M.; Sohn, H.Y.; Yoon, S.Y.; Oh, J.H.; Yang, J.O.; Kim, J.H.; Song, K.S.; Rho, S.M.; Yoo, H.S.; Kim, Y.S.; Kim, J.; Kim, N. Identification of gastric cancer-related genes using a cDNA microarray containing novel expressed sequence tags expressed in gastric cancer cells. *Clin. Cancer Res.* 2005, 11, 473–482.
67. Cho, E.C.; Zheng, S.; Munro, S.; Liu, G.; Carr, S.M.; Moehlenbrink, J.; Lu, Y.C.; Stimson, L.; Khan, O.; Konietzny, R.; McGouran, J.; Coutts, A.S.; Kessler, B.; Kerr, D.J.; La Thangue N.B. Arginine methylation controls growth regulation by E2F-1. *EMBO J.* 2012, 31, 1785–1797, doi:10.1038/emboj.2012.17.
68. Jing, P.; Xie, N.; Zhu, X.; Dang, H.; Gu, Z. The methylation induced by protein arginine methyltransferase 5 promotes tumorigenesis and progression of lung cancer. *J. Thorac. Dis.* 2018, 10, 7014–7019, doi:10.21037/jtd.2018.10.100.
69. Wei, T.Y.; Juan, C.C.; Hsu, J.Y.; Su, L.J.; Lee, Y.C.; Chou, H.Y.; Chen, J.M.; Wu, Y.C.; Chiu, S.C.; Hsu, C.P.; Liu, K.; Yu, C.R. Protein argi-nine methyltransferase 5 is a potential oncoprotein that upregulates G1 cyclins/cyclin-dependent kinases and the phosphoinositide 3-kinase/AKT signaling cascade. *Cancer Sci.* 2012, 103, 1640–1650, doi:10.1111/j.1349-7006.2012.02367.x.
70. Bao, X.; Zhao, S.; Liu, T.; Liu, Y.; Liu, Y.; Yang, X. Overexpression of PRMT5 promotes tumor cell growth and is associated with poor disease prognosis in epithelial ovarian cancer. *J. Histochem. Cytochem.* 2013, 61, 206–217, doi:10.1369/0022155413475452.
71. Nicholas, C.; Yang, J.; Peters, S.B.; Bill, M.A.; Baiocchi, R.A.; Yan, F.; Sif, S.; Tae, S.; Gaudio, E.; Wu, X.; Grever, M.R.; Young, G.S.; Lesinski, G.B. PRMT5 is up-regulated in malignant and metastatic melanoma and regulates expression of MITF and p27(Kip1.). *PLoS One* 2013, 8, e74710, doi:10.1371/journal.pone.0074710.

72. Han, X.; Li, R.; Zhang, W.; Yang, X.; Wheeler, C.G.; Friedman, G.K.; Province, P.; Ding, Q.; You, Z.; Fathallah-Shaykh, H.M.; Gillespie, G.Y.; Zhao, X.; King, P.H.; Nabors, L.B. Expression of PRMT5 correlates with malignant grade in gliomas and plays a pivotal role in tumor growth in vitro. *J. Neurooncol.* 2014, 118, 61–72, doi:10.1007/s11060-014-1419-0.
73. Yan, F.; Alinari, L.; Lustberg, M.E.; Martin, L.K.; Cordero-Nieves, H.M.; Banasavadi-Siddegowda, Y.; Virk, S.; Barnholtz-Sloan, J.; Bell, E.H.; Wojton, J.; Jacob, N.K.; Chakravarti, A.; Nowicki, M.O.; Wu, X.; Lapalombella, R.; Datta, J.; Yu, B.; Gordon, K.; Haseley, A.; Patton, J.T.; Smith, P.L.; Ryu, J.; Zhang, X.; Mo, X.; Marcucci, G.; Nuovo, G.; Kwon, C.; Byrd, J.C.; Chiocca, E.A.; Li, C.; Sif, S.; Jacob, S.; Lawler, S.; Kaur, B.; Baiocchi, R.A. Genetic validation of the protein arginine methyltransferase PRMT5 as a candidate therapeutic target in glioblastoma. *Cancer Res.* 2014, 74, 1752–1765, doi:10.1158/0008-5472.CAN-13-0884.
74. Jiang, H.; Zhu, Y.; Zhou, Z.; Xu, J.; Jin, S.; Xu, K.; Zhang, H.; Sun, Q.; Wang, J.; Xu, J. PRMT5 promotes cell proliferation by inhibiting BTG2 expression via the ERK signaling pathway in hepatocellular carcinoma. *Cancer Med.* 2018, 7, 869–882, doi:10.1002/cam4.1360.
75. Jeon, J.Y.; Lee, J.S.; Park, E.R.; Shen, Y.N.; Kim, M.Y.; Shin, H.J.; Joo, H.Y.; Cho, E.H.; Moon, S.M.; Shin, U.S.; Park, S.H.; Ha, C.J.; Choi, D.W.; Gu, M.B.; Kim, S.; Lee, K. Protein arginine methyltransferase 5 is implicated in the aggressiveness of human hepatocellular carcinoma and controls the invasive activity of cancer cells. *Oncol. Rep.* 2018, 40, 536–544, doi:10.3892/or.2018.6402.
76. Zhang, B.; Dong, S.; Li, Z.; Lu, L.; Zhang, S.; Chen, X.; Cen, X.; Wu, Y. Targeting protein arginine methyltransferase 5 inhibits human hepatocellular carcinoma growth via the downregulation of beta-catenin. *J. Transl. Med.* 2015, 13, 349, doi:10.1186/s12967-015-0721-8.

77. Li, Z.; Zhang, J.; Liu, X.; Li, S.; Wang, Q.; Di, C.; Hu, Z.; Yu, T.; Ding, J.; Li, J.; Yao, M.; Fan, J.; Huang, S.; Gao, Q.; Zhao, Y.; He, X. The LINC01138 drives malignancies via activating arginine methyltransferase 5 in hepatocellular carcinoma. *Nat. Commun.* 2018, 9, 1572, doi:10.1038/s41467-018-04006-0.
78. Zheng, B.N.; Ding, C.H.; Chen, S.J.; Zhu, K.; Shao, J.; Feng, J.; Xu, W.P.; Cai, L.Y.; Zhu, C.P.; Duan, W.; Ding, J.; Zhang, X.; Luo, C.; Xie, W. Targeting PRMT5 Activity Inhibits the Malignancy of Hepatocellular Carcinoma by Promoting the Transcription of HNF4alpha. *Theranostics* 2019, 9, 2606–2617, doi:10.7150/thno.32344.
79. Kim, M.; Ki, B.S.; Hong, K.; Park, S.P.; Ko, J.J.; Choi, Y. Tudor Domain Containing Protein TDRD12 Expresses at the Acro-some of Spermatids in Mouse Testis. *Asian-Australas J. Anim. Sci.* 2016, 29, 944–951, doi:10.5713/ajas.15.0436.
80. Santhekadur, P.K.; Das, S.K.; Gredler, R.; Chen, D.; Srivastava, J.; Robertson, C.; Baldwin, A.S., Jr.; Fisher, P.B.; Sarkar, D. Multifunction protein staphylococcal nuclease domain containing 1 (SND1) promotes tumor angiogenesis in human hepatocellular carcinoma through novel pathway that involves nuclear factor kappaB and miR-221. *J. Biol. Chem.* 2012, 287, 13952–13958, doi:10.1074/jbc.M111.321646.
81. Zheng, S.; Moehlenbrink, J.; Lu, Y.C.; Zalmas, L.P.; Sagum, C.A.; Carr, S.; McGouran, J.F.; Alexander, L.; Fedorov, O.; Munro, S.; Kessler, B.; Bedford, M.T.; Yu, Q.; La Thangue, N.B. Arginine methylation-dependent reader-writer interplay governs growth control by E2F-1. *Mol. Cell* 2013, 52, 37–51, doi:10.1016/j.molcel.2013.08.039.
82. Chidambaranathan-Reghupaty, S.; Mendoza, R.; Fisher, P.B.; Sarkar, D. The multifaceted oncogene SND1 in cancer: Focus on hepatocellular carcinoma. *Hepatoma Res.* 2018, 4, doi:10.20517/2394-5079.2018.34.
83. Arretxe, E.; Armengol, S.; Mula, S.; Chico, Y.; Ochoa, B.; Martinez, M.J. Profiling of promoter occupancy by the SND1 transcriptional coactivator identifies downstream glycerolipid metabolic genes involved in TNFalpha response in human hepatoma cells. *Nucleic Acids Res.* 2015, 43, 10673–10688, doi:10.1093/nar/gkv858.

84. Gutierrez-Beltran, E.; Denisenko, T.V.; Zhivotovsky, B.; Bozhkov, P.V. Tudor staphylococcal nuclease: Biochemistry and functions. *Cell Death Differ.* 2016, 23, 1739–1748, doi:10.1038/cdd.2016.93.
85. Callebaut, I.; Mornon, J.P. The human EBNA-2 coactivator p100: Multidomain organization and relationship to the staphylococcal nuclease fold and to the tudor protein involved in *Drosophila melanogaster* development. *Biochem. J.* 1997, 321 Pt 1, 125–132.
86. Shaw, N.; Zhao, M.; Cheng, C.; Xu, H.; Saarikettu, J.; Li, Y.; Da, Y.; Yao, Z.; Silvennoinen, O.; Yang, J.; Liu, Z.; Wang, B.; Rao, Z. The multifunctional human p100 protein ‘hooks’ methylated ligands. *Nat. Struct. Mol. Biol.* 2007, 14, 779–784, doi:10.1038/nsmb1269.
87. Friberg, A.; Corsini, L.; Mourao, A.; Sattler, M. Structure and ligand binding of the extended Tudor domain of *D. melanogaster* Tudor-SN. *J. Mol. Biol.* 2009, 387, 921–934, doi:10.1016/j.jmb.2009.02.018.
88. Liu, K.; Chen, C.; Guo, Y.; Lam, R.; Bian, C.; Xu, C.; Zhao, D.Y.; Jin, J.; MacKenzie, F.; Pawson, T.; Min, J. Structural basis for recognition of arginine methylated Piwi proteins by the extended Tudor domain. *Proc. Natl. Acad. Sci. USA* 2010, 107, 18398–18403, doi:10.1073/pnas.1013106107.
89. Tong, X.; Drapkin, R.; Yalamanchili, R.; Mosialos, G.; Kieff, E. The Epstein-Barr virus nuclear protein 2 acidic domain forms a complex with a novel cellular coactivator that can interact with TFIIE. *Mol. Cell. Biol.* 1995, 15, 4735–4744, doi:10.1128/mcb.15.9.4735.
90. Yang, J.; Aittomaki, S.; Pesu, M.; Carter, K.; Saarinen, J.; Kalkkinen, N.; Kieff, E.; Silvennoinen, O. Identification of p100 as a coactivator for STAT6 that bridges STAT6 with RNA polymerase II. *EMBO J.* 2002, 21, 4950–4958, doi:10.1093/emboj/cdf463.
91. Paukku, K.; Yang, J.; Silvennoinen, O. Tudor and nuclease-like domains containing protein p100 function as coactivators for signal transducer and activator of transcription 5. *Mol. Endocrinol.* 2003, 17, 1805–1814, doi:10.1210/me.2002-0256.



92. Levenson, J.D.; Koskinen, P.J.; Orrico, F.C.; Rainio, E.M.; Jalkanen, K.J.; Dash, A.B.; Eisenman, R.N.; Ness, S.A. Pim-1 kinase and p100 cooperate to enhance c-Myb activity. *Mol. Cell* 1998, 2, 417–425, doi:10.1016/s1097-2765(00)80141-0.
93. Roworth, A.P.; Carr, S.M.; Liu, G.; Barczak, W.; Miller, R.L.; Munro, S.; Kanapin, A.; Samsonova, A.; La Thangue, N.B. Arginine methylation expands the regulatory mechanisms and extends the genomic landscape under E2F control. *Sci. Adv.* 2019, 5, eaaw4640, doi:10.1126/sciadv.aaw4640.
94. Su, C.; Zhang, C.; Teclé, A.; Fu, X.; He, J.; Song, J.; Zhang, W.; Sun, X.; Ren, Y.; Silvennoinen, O.; Yao, Z.; Yang, X.; Wei, M.; Yang, J. Tudor staphylococcal nuclease (Tudor-SN), a novel regulator facilitating G1/S phase transition, acting as a co-activator of E2F-1 in cell cycle regulation. *J. Biol. Chem.* 2015, 290, 7208–7220, doi:10.1074/jbc.M114.625046.
95. Duan, Z.; Zhao, X.; Fu, X.; Su, C.; Xin, L.; Saarikettu, J.; Yang, X.; Yao, Z.; Silvennoinen, O.; Wei, M.; Yang, J. Tudor-SN, a novel coactivator of peroxisome proliferator-activated receptor gamma protein, is essential for adipogenesis. *J. Biol. Chem.* 2014, 289, 8364–8374, doi:10.1074/jbc.M113.523456.
96. Gao, X.; Zhao, X.; Zhu, Y.; He, J.; Shao, J.; Su, C.; Zhang, Y.; Zhang, W.; Saarikettu, J.; Silvennoinen, O.; Yao, Z.; Yang, J. Tudor staphylococcal nuclease (Tudor-SN) participates in small ribonucleoprotein (snRNP) assembly via interacting with symmetrically dimethylated Sm proteins. *J. Biol. Chem.* 2012, 287, 18130–18141, doi:10.1074/jbc.M111.311852.
97. Cappellari, M.; Bielli, P.; Paronetto, M.P.; Ciccocanti, F.; Fimia, G.M.; Saarikettu, J.; Silvennoinen, O.; Sette, C. The transcriptional co-activator SND1 is a novel regulator of alternative splicing in prostate cancer cells. *Oncogene* 2014, 33, 3794–3802, doi:10.1038/onc.2013.360.
98. Yang, J.; Valineva, T.; Hong, J.; Bu, T.; Yao, Z.; Jensen, O.N.; Frilander, M.J.; Silvennoinen, O. Transcriptional co-activator protein p100 interacts with snRNP proteins

- and facilitates the assembly of the spliceosome. *Nucleic Acids Res.* 2007, 35, 4485–4494, doi:10.1093/nar/gkm470.
99. Caudy, A.A.; Ketting, R.F.; Hammond, S.M.; Denli, A.M.; Bathoorn, A.M.; Tops, B.B.; Silva, J.M.; Myers, M.M.; Hannon, G.J.; Plasterk, R.H. A micrococcal nuclease homologue in RNAi effector complexes. *Nature* 2003, 425, 411–414, doi:10.1038/nature01956.
  100. Scadden, A.D. The RISC subunit Tudor-SN binds to hyper-edited double-stranded RNA and promotes its cleavage. *Nat. Struct. Mol. Biol.* 2005, 12, 489–496, doi:10.1038/nsmb936.
  101. Yang, W.; Chendrimada, T.P.; Wang, Q.; Higuchi, M.; Seeburg, P.H.; Shiekhattar, R.; Nishikura, K. Modulation of microRNA processing and expression through RNA editing by ADAR deaminases. *Nat. Struct. Mol. Biol.* 2006, 13, 13–21, doi:10.1038/nsmb1041.
  102. Li, C.L.; Yang, W.Z.; Chen, Y.P.; Yuan, H.S. Structural and functional insights into human Tudor-SN, a key component linking RNA interference and editing. *Nucleic Acids Res.* 2008, 36, 3579–3589, doi:10.1093/nar/gkn236.
  103. Elbarbary, R.A.; Miyoshi, K.; Myers, J.R.; Du, P.; Ashton, J.M.; Tian, B.; Maquat, L.E. Tudor-SN-mediated endonucleolytic decay of human cell microRNAs promotes G1/S phase transition. *Science* 2017, 356, 859–862, doi:10.1126/science.aai9372.
  104. Elbarbary, R.A.; Miyoshi, K.; Hedaya, O.; Myers, J.R.; Maquat, L.E. UPF1 helicase promotes TSN-mediated miRNA de-cay. *Genes Dev.* 2017, 31, 1483–1493, doi:10.1101/gad.303537.117.
  105. Keenan, T.W.; Winter, S.; Rackwitz, H.R.; Heid, H.W. Nuclear coactivator protein p100 is present in endoplasmic reticulum and lipid droplets of milk secreting cells. *Biochim. Biophys. Acta* 2000, 1523, 84–90, doi:10.1016/s0304-4165(00)00106-9.

106. Valadi, H.; Ekstrom, K.; Bossios, A.; Sjostrand, M.; Lee, J.J.; Lotvall, J.O. Exosome-mediated transfer of mRNAs and microRNAs is a novel mechanism of genetic exchange between cells. *Nat. Cell Biol.* 2007, 9, 654–659, doi:10.1038/ncb1596.
107. Makarova, J.A.; Shkurnikov, M.U.; Wicklein, D.; Lange, T.; Samatov, T.R.; Turchinovich, A.A.; Tonevitsky, A.G. Intracellular and extracellular microRNA: An update on localization and biological role. *Prog Histochem. Cytochem.* 2016, 51, 33–49, doi:10.1016/j.proghi.2016.06.001.
108. Nakamura, K.; Sawada, K.; Yoshimura, A.; Kinose, Y.; Nakatsuka, E.; Kimura, T. Clinical relevance of circulating cell-free microRNAs in ovarian cancer. *Mol. Cancer* 2016, 15, 48, doi:10.1186/s12943-016-0536-0.
109. Jelonek, K.; Wojakowska, A.; Marczak, L.; Muer, A.; Tinhofer-Keilholz, I.; Lysek-Gladysinska, M.; Widlak, P.; Pietrowska, M. Ionizing radiation affects protein composition of exosomes secreted in vitro from head and neck squamous cell carcinoma. *Acta Biochim. Pol.* 2015, 62, 265–272, doi:10.18388/abp.2015\_970.
110. Silvers, C.R.; Miyamoto, H.; Messing, E.M.; Netto, G.J.; Lee, Y.F. Characterization of urinary extracellular vesicle proteins in muscle-invasive bladder cancer. *Oncotarget* 2017, 8, 91199–91208, doi:10.18632/oncotarget.20043.
111. Wu, Q.; Zhou, L.; Lv, D.; Zhu, X.; Tang, H. Exosome-mediated communication in the tumor microenvironment contributes to hepatocellular carcinoma development and progression. *J. Hematol. Oncol.* 2019, 12, 53, doi:10.1186/s13045-019-0739-0.
112. Fashe, T.; Saarikettu, J.; Isomaki, P.; Yang, J.; Silvennoinen, O. Expression analysis of Tudor-SN protein in mouse tissues. *Tissue Cell* 2013, 45, 21–31, doi:10.1016/j.tice.2012.09.001.
113. Fu, X.; Zhang, C.; Meng, H.; Zhang, K.; Shi, L.; Cao, C.; Wang, Y.; Su, C.; Xin, L.; Ren, Y.; Zhang, W.; Sun, X.; Ge, L.; Silvennoinen, O.; Yao, Z.; Uang, X.; Yang, J. Oncoprotein Tudor-SN is a key determinant providing survival advantage under DNA damaging stress. *Cell Death Differ.* 2018, 25, 1625–1637, doi:10.1038/s41418-018-0068-9.

114. Bao, J.; Di Lorenzo, A.; Lin, K.; Lu, Y.; Zhong, Y.; Sebastian, M.M.; Muller, W.J.; Yang, Y.; Bedford, M.T. Mouse Models of Overexpression Reveal Distinct Oncogenic Roles for Different Type I Protein Arginine Methyltransferases. *Cancer Res.* 2019, 79, 21–32, doi:10.1158/0008-5472.CAN-18-1995.
115. Wang, Y.; Wang, X.; Cui, X.; Zhuo, Y.; Li, H.; Ha, C.; Xin, L.; Ren, Y.; Zhang, W.; Sun, X.; Ge, L.; Liu, X.; He, J.; Zhang, T.; Zhang, K.; Yao, Z.; Yang, X.; Yang, J. Oncoprotein SND1 hijacks nascent MHC-I heavy chain to ER-associated degradation, leading to impaired CD8(+) T cell response in tumor. *Sci. Adv.* 2020, 6, doi:10.1126/sciadv.aba5412.
116. Kim, H.; Kim, H.; Feng, Y.; Li, Y.; Tamiya, H.; Tocci, S.; Ronai, Z.A. PRMT5 control of cGAS/STING and NLRC5 path-ways defines melanoma response to antitumor immunity. *Sci. Transl. Med.* 2020, 12, doi:10.1126/scitranslmed.aaz5683.
117. Cui, X.; Zhang, X.; Liu, M.; Zhao, C.; Zhang, N.; Ren, Y.; Su, C.; Zhang, W.; Sun, X.; He, J.; Gao, X.; Yang, J. A pan-cancer analysis of the oncogenic role of staphylococcal nuclease domain-containing protein 1 (SND1) in human tumors. *Genomics* 2020, 10.1016/j.ygeno.2020.06.044, doi:10.1016/j.ygeno.2020.06.044.
118. Tsuchiya, N.; Ochiai, M.; Nakashima, K.; Ubagai, T.; Sugimura, T.; Nakagama, H. SND1, a component of RNA-induced silencing complex, is up-regulated in human colon cancers and implicated in early stage colon carcinogenesis. *Cancer Res.* 2007, 67, 9568–9576, doi:10.1158/0008-5472.CAN-06-2707.
119. Yoo, B.K.; Santhekadur, P.K.; Gredler, R.; Chen, D.; Emdad, L.; Bhutia, S.; Pannell, L.; Fisher, P.B.; Sarkar, D. Increased RNA-induced silencing complex (RISC) activity contributes to hepatocellular carcinoma. *Hepatology* 2011, 53, 1538–1548, doi:10.1002/hep.24216.
120. Petrick, J.L.; Kelly, S.P.; Altekruse, S.F.; McGlynn, K.A.; Rosenberg, P.S. Future of Hepatocellular Carcinoma Incidence in the United States Forecast Through 2030. *J. Clin. Oncol.* 2016, 34, 1787–1794, doi:10.1200/JCO.2015.64.7412.

121. Fekry, B.; Ribas-Latre, A.; Baumgartner, C.; Mohamed, A.M.T.; Kolonin, M.G.; Sladek, F.M.; Younes, M.; Eckel-Mahan, K.L. HNF4alpha-Deficient Fatty Liver Provides a Permissive Environment for Sex-Independent Hepatocellular Carcinoma. *Cancer Res.* 2019, 79, 5860–5873, doi:10.1158/0008-5472.CAN-19-1277.
122. Seyda Seydel, G.; Kucukoglu, O.; Altinbasv, A.; Demir, O.O.; Yilmaz, S.; Akkiz, H.; Otan, E.; Sowa, J.P.; Canbay, A. Economic growth leads to increase of obesity and associated hepatocellular carcinoma in developing countries. *Ann. Hepatol.* 2016, 15, 662–672, doi:10.5604/16652681.1212316.
123. Singal, A.K.; Hasanin, M.; Kaif, M.; Wiesner, R.; Kuo, Y.F. Nonalcoholic Steatohepatitis is the Most Rapidly Growing Indication for Simultaneous Liver Kidney Transplantation in the United States. *Transplantation* 2016, 100, 607–612, doi:10.1097/TP.0000000000000945.
124. Tarao, K.; Tanaka, K.; Nozaki, A.; Sato, A.; Ishii, T.; Komatsu, H.; Ikeda, T.; Komatsu, T.; Matsushima, S.; Oshige, K. Efficacy and safety of dual therapy with daclatasvir and asunaprevir in elderly patients. *World J. Hepatol.* 2017, 9, 544–550, doi:10.4254/wjh.v9.i11.544.
125. Gu, J.; Yao, M.; Yao, D.; Wang, L.; Yang, X.; Yao, D. Nonalcoholic Lipid Accumulation and Hepatocyte Malignant Transformation. *J. Clin. Transl. Hepatol.* 2016, 4, 123–130, doi:10.14218/JCTH.2016.00010.
126. Rysman, E.; Brusselmans, K.; Scheys, K.; Timmermans, L.; Derua, R.; Munck, S.; Van Veldhoven, P.P.; Waltregny, D.; Daniels, V.W.; Machiels, J.; Vanderhoydonc, F.; Smans, K.; Waelkens, E.; Guido, V.; Swinnen, J.V. De novo lipogenesis protects cancer cells from free radicals and chemotherapeutics by promoting membrane lipid saturation. *Cancer Res.* 2010, 70, 8117–8126, doi:10.1158/0008-5472.CAN-09-3871.
127. Bhalla, K.; Hwang, B.J.; Dewi, R.E.; Twaddel, W.; Goloubeva, O.G.; Wong, K.K.; Saxena, N.K.; Biswal, S.; Girnun, G.D. Metformin prevents liver tumorigenesis by inhibiting

- pathways driving hepatic lipogenesis. *Cancer Prev. Res.* 2012, 5, 544–552, doi:10.1158/1940-6207.CAPR-11-0228.
128. Jacobs, R.J.; Voorneveld, P.W.; Kodach, L.L.; Hardwick, J.C. Cholesterol metabolism and colorectal cancers. *Curr. Opin. Pharmacol.* 2012, 12, 690–695, doi:10.1016/j.coph.2012.07.010.
129. Zhu, A.X.; Duda, D.G.; Sahani, D.V.; Jain, R.K. HCC and angiogenesis: Possible targets and future directions. *Nat. Rev. Clin. Oncol.* 2011, 8, 292–301, doi:10.1038/nrclinonc.2011.30.
130. Lubyova, B.; Hodek, J.; Zabransky, A.; Prouzova, H.; Hubalek, M.; Hirsch, I.; Weber, J. PRMT5: A novel regulator of Hepa-titis B virus replication and an arginine methylase of HBV core. *PLoS One* 2017, 12, e0186982, doi:10.1371/journal.pone.0186982.
131. Lin, Z.; Jia, H.; Hong, L.; Zheng, Y.; Shao, W.; Ren, X.; Zhu, W.; Lu, L.; Lu, M.; Zhang, J.; Chen, J.. Prognostic impact of SET do-main-containing protein 8 and protein arginine methyltransferase 5 in patients with hepatocellular carcinoma following curative resection. *Oncol. Lett.* 2018, 16, 3665–3673, doi:10.3892/ol.2018.9083.
132. Yin, C.; Lin, Y.; Zhang, X.; Chen, Y.X.; Zeng, X.; Yue, H.Y.; Hou, J.L.; Deng, X.; Zhang, J.P.; Han, Z.G.; Xie, W. Differentiation therapy of hepatocellular carcinoma in mice with recombinant adenovirus carrying hepatocyte nuclear factor-4alpha gene. *Hepatology* 2008, 48, 1528–1539, doi:10.1002/hep.22510.
133. Ning, B.F.; Ding, J.; Yin, C.; Zhong, W.; Wu, K.; Zeng, X.; Yang, W.; Chen, Y.X.; Zhang, J.P.; Zhang, X.; Wang, H.; Xie, W. Hepatocyte nuclear factor 4 alpha suppresses the development of hepatocellular carcinoma. *Cancer Res.* 2010, 70, 7640–7651, doi:10.1158/0008-5472.CAN-10-0824.
134. Liu, L.; Zhao, X.; Zhao, L.; Li, J.; Yang, H.; Zhu, Z.; Liu, J.; Huang, G. Arginine Methylation of SREBP1a via PRMT5 Pro-motes De Novo Lipogenesis and Tumor Growth. *Cancer Res.* 2016, 76, 1260–1272, doi:10.1158/0008-5472.CAN-15-1766.

135. Farra, R.; Grassi, G.; Tonon, F.; Abrami, M.; Grassi, M.; Pozzato, G.; Fiotti, N.; Forte, G.; Dapas, B. The Role of the Transcription Factor E2F1 in Hepatocellular Carcinoma. *Curr. Drug Deliv.* 2017, 14, 272–281, doi:10.2174/1567201813666160527141742.
136. Pauku, K.; Kalkkinen, N.; Silvennoinen, O.; Kontula, K.K.; Lehtonen, J.Y. p100 increases AT1R expression through inter-action with AT1R 3'-UTR. *Nucleic Acids Res.* 2008, 36, 4474–4487, doi:10.1093/nar/gkn411.
137. Ji, Y.; Chen, H.; Gow, W.; Ma, L.; Jin, Y.; Hui, B.; Yang, Z.; Wang, Z. Potential biomarkers Ang II/AT1R and S1P/S1PR1 predict the prognosis of hepatocellular carcinoma. *Oncol. Lett.* 2020, 20, 208, doi:10.3892/ol.2020.12071.
138. Santhekadur, P.K.; Akiel, M.; Emdad, L.; Gredler, R.; Srivastava, J.; Rajasekaran, D.; Robertson, C.L.; Mukhopadhyay, N.D.; Fisher, P.B.; Sarkar, D. Staphylococcal nuclease domain containing-1 (SND1) promotes migration and invasion via angiotensin II type 1 receptor (AT1R) and TGFbeta signaling. *FEBS Open Bio* 2014, 4, 353–361, doi:10.1016/j.fob.2014.03.012.
139. Katsuno, Y.; Lamouille, S.; Derynck, R. TGF-beta signaling and epithelial-mesenchymal transition in cancer progression. *Curr. Opin. Oncol.* 2013, 25, 76–84, doi:10.1097/CCO.0b013e32835b6371.
140. Yu, L.; Liu, X.; Cui, K.; Di, Y.; Xin, L.; Sun, X.; Zhang, W.; Yang, X.; Wei, M.; Yao, Z.; Yang, J. SND1 Acts Downstream of TGF-beta1 and Upstream of Smurf1 to Promote Breast Cancer Metastasis. *Cancer Res.* 2015, 75, 1275–1286, doi:10.1158/0008-5472.CAN-14-2387.
141. Ochoa, B.; Chico, Y.; Martinez, M.J. Insights Into SND1 Oncogene Promoter Regulation. *Front. Oncol.* 2018, 8, 606, doi:10.3389/fonc.2018.00606.
142. Bisteau, X.; Caldez, M.J.; Kaldis, P. The Complex Relationship between Liver Cancer and the Cell Cycle: A Story of Multiple Regulations. *Cancers* 2014, 6, 79–111, doi:10.3390/cancers6010079.

143. Caselmann, W.H. Pathogenesis of hepatocellular carcinoma. *Digestion* 1998, 59 (Suppl. 2), 60–63, doi:10.1159/000051425.
144. Mauad, T.H.; van Nieuwkerk, C.M.; Dingemans, K.P.; Smit, J.J.; Schinkel, A.H.; Notenboom, R.G.; van den Bergh Weerman, M.A.; Verkruisen, R.P.; Groen, A.K.; Oude Elferink, R.P.; van der Valk, M.A.; Borst, P.; Offerhaus, G.J.A. Mice with homozygous disruption of the *mdr2* P-glycoprotein gene. A novel animal model for studies of nonsuppurative inflammatory cholangitis and hepatocarcinogenesis. *Am. J. Pathol.* 1994, 145, 1237–1245.
145. Pikarsky, E.; Porat, R.M.; Stein, I.; Abramovitch, R.; Amit, S.; Kasem, S.; Gutkovich-Pyest, E.; Urieli-Shoval, S.; Galun, E.; Ben-Neriah, Y. NF-kappaB functions as a tumour promoter in inflammation-associated cancer. *Nature* 2004, 431, 461–466, doi:10.1038/nature02924.
146. Bishayee, A. The role of inflammation and liver cancer. *Adv. Exp. Med. Biol.* 2014, 816, 401–435, doi:10.1007/978-3-0348-0837-8\_16.
147. Dhiman, G.; Srivastava, N.; Goyal, M.; Rakha, E.; Lothion-Roy, J.; Mongan, N.P.; Miftakhova, R.R.; Khaiboullina, S.F.; Rizvanov, A.A.; Baranwal, M. Metadherin: A Therapeutic Target in Multiple Cancers. *Front. Oncol.* 2019, 9, 349, doi:10.3389/fonc.2019.00349.
148. Pineau, P.; Volinia, S.; McJunkin, K.; Marchio, A.; Battiston, C.; Terris, B.; Mazzaferro, V.; Lowe, S.W.; Croce, C.M.; Dejean, A. miR-221 overexpression contributes to liver tumorigenesis. *Proc. Natl. Acad. Sci. USA* 2010, 107, 264–269, doi:10.1073/pnas.0907904107.
149. Song, M.S.; Grabocka, E. Stress Granules in Cancer. *Rev. Physiol. Biochem. Pharmacol.* 2020, 10.1007/112\_2020\_37, doi:10.1007/112\_2020\_37.
150. Gao, X.; Ge, L.; Shao, J.; Su, C.; Zhao, H.; Saarikettu, J.; Yao, X.; Yao, Z.; Silvennoinen, O.; Yang, J. Tudor-SN interacts with and co-localizes with G3BP in stress granules under stress conditions. *FEBS Lett.* 2010, 584, 3525–3532, doi:10.1016/j.febslet.2010.07.022.



151. Weissbach, R.; Scadden, A.D. Tudor-SN and ADAR1 are components of cytoplasmic stress granules. *RNA* 2012, 18, 462–471, doi:10.1261/rna.027656.111.
152. Su, C.; Gao, X.; Yang, W.; Zhao, Y.; Fu, X.; Cui, X.; Zhang, C.; Xin, L.; Ren, Y.; Li, L.; Shui W.; Yang, X.; Wei, M.; Yang, J. Phosphorylation of Tudor-SN, a novel substrate of JNK, is involved in the efficient recruitment of Tudor-SN into stress granules. *Biochim. Biophys. Acta Mol. Cell Res.* 2017, 1864, 562–571, doi:10.1016/j.bbamcr.2016.12.018.
153. Cui, X.; Zhao, C.; Yao, X.; Qian, B.; Su, C.; Ren, Y.; Yao, Z.; Gao, X.; Yang, J. SND1 acts as an anti-apoptotic factor via regulating the expression of lncRNA UCA1 in hepatocellular carcinoma. *RNA Biol.* 2018, 15, 1364–1375, doi:10.1080/15476286.2018.1534525.
154. Yao, F.; Wang, Q.; Wu, Q. The prognostic value and mechanisms of lncRNA UCA1 in human cancer. *Cancer Manag. Res.* 2019, 11, 7685–7696, doi:10.2147/CMAR.S200436.
155. Garcia-Arcos, I.; Rueda, Y.; Gonzalez-Kother, P.; Palacios, L.; Ochoa, B.; Fresnedo, O. Association of SND1 protein to low density lipid droplets in liver steatosis. *J. Physiol. Biochem.* 2010, 66, 73–83, doi:10.1007/s13105-010-0011-0.
156. Palacios, L.; Ochoa, B.; Gomez-Lechon, M.J.; Castell, J.V.; Fresnedo, O. Overexpression of SND p102, a rat homologue of p100 coactivator, promotes the secretion of lipoprotein phospholipids in primary hepatocytes. *Biochim. Biophys. Acta* 2006, 1761, 698–708, doi:10.1016/j.bbalip.2006.05.005.
157. Navarro-Imaz, H.; Chico, Y.; Rueda, Y.; Fresnedo, O. Channeling of newly synthesized fatty acids to cholesterol esterification limits triglyceride synthesis in SND1-overexpressing hepatoma cells. *Biochim. Biophys. Acta Mol. Cell Biol. Lipids* 2019, 1864, 137–146, doi:10.1016/j.bbalip.2018.11.004.
158. Navarro-Imaz, H.; Ochoa, B.; Garcia-Arcos, I.; Martinez, M.J.; Chico, Y.; Fresnedo, O.; Rueda, Y. Molecular and cellular insights into the role of SND1 in lipid metabolism. *Biochim. Biophys. Acta Mol. Cell Biol. Lipids* 2020, 1865, 158589, doi:10.1016/j.bbalip.2019.158589.

159. Shen, Y.; Gao, G.; Yu, X.; Kim, H.; Wang, L.; Xie, L.; Schwarz, M.; Chen, X.; Guccione, E.; Liu, J.; Bedford, M.T.; Jin, J. Discovery of First-in-Class Protein Arginine Methyltransferase 5 (PRMT5) Degradors. *J. Med. Chem.* 2020, 63, 9977–9989, doi:10.1021/acs.jmedchem.0c01111.
160. Palte, R.L.; Schneider, S.E.; Altman, M.D.; Hayes, R.P.; Kawamura, S.; Lacey, B.M.; Mansueto, M.S.; Reutershan, M.; Siliphaivanh, P.; Sondey, C.; Xu, H.; Xu, Z.; Ye, Y.; Machacek, M.R. Allosteric Modulation of Protein Arginine Methyltransferase 5 (PRMT5). *ACS Med. Chem. Lett.* 2020, 11, 1688–1693, doi:10.1021/acsmchemlett.9b00525.
161. Gerhart, S.V.; Kellner, W.A.; Thompson, C.; Pappalardi, M.B.; Zhang, X.P.; Montes de Oca, R.; Penebre, E.; Duncan, K.; Boriack-Sjodin, A.; Le, B.; Majer, C.; McCabe, M.T.; Carpenter, C.; Johnson, N.; Kruger, R.G.; Barbash, O. Activation of the p53-MDM4 regulatory axis defines the anti-tumour response to PRMT5 inhibition through its role in regulating cellular splicing. *Sci. Rep.* 2018, 8, 9711, doi:10.1038/s41598-018-28002-y.
162. Metz, P.J.; Ching, K.A.; Xie, T.; Delgado Cuenca, P.; Niessen, S.; Tatlock, J.H.; Jensen-Pergakes, K.; Murray, B.W. Symmetric Arginine Dimethylation Is Selectively Required for mRNA Splicing and the Initiation of Type I and Type III Interferon Signaling. *Cell Rep.* 2020, 30, 1935–1950, doi:10.1016/j.celrep.2020.01.054.
163. Snyder, K.J.; Zitzer, N.C.; Gao, Y.; Choe, H.K.; Sell, N.E.; Neidemire-Colley, L.; Ignaci, A.; Kale, C.; Devine, R.D.; Abad, M.G.; Pietrzak, M.; Wang, M.; Lin, H.; Zhang, Y.W.; Behbehani, G.K.; Jackman, J.E.; Garzon, R.; Vaddi, K.; Baiocchi, R.A.; Ranganathan, P. PRMT5 regulates T cell interferon response and is a target for acute graft-versus-host disease. *JCI Insight* 2020, 5, doi:10.1172/jci.insight.131099.
164. Lin, H.; Wang, M.; Zhang, Y.W.; Tong, S.; Leal, R.A.; Shetty, R.; Vaddi, K.; Luengo, J.I. Discovery of Potent and Selective Covalent Protein Arginine Methyltransferase 5 (PRMT5) Inhibitors. *ACS Med. Chem. Lett.* 2019, 10, 1033–1038, doi:10.1021/acsmchemlett.9b00074.

165. Bonday, Z.Q.; Cortez, G.S.; Grogan, M.J.; Antonysamy, S.; Weichert, K.; Bocchinfuso, W.P.; Li, F.; Kennedy, S.; Li, B.; Mader, M.M.; Arrowsmith, C.H.; Brown, R.J.; Eram, M.S.; Szewczyk, M.M.; Barsyte-Lovejoy, D.; Vedadi, M.; Guccione, E.; Campbell, R.M. LLY-283, a Potent and Selective Inhibitor of Arginine Methyltransferase 5, PRMT5, with Antitumor Activity. *ACS Med. Chem. Lett.* 2018, 9, 612–617, doi:10.1021/acsmchemlett.8b00014.
166. Barczak, W.; Jin, L.; Carr, S.M.; Munro, S.; Ward, S.; Kanapin, A.; Samsonova, A.; La Thangue, N.B. PRMT5 promotes cancer cell migration and invasion through the E2F pathway. *Cell Death Dis* 2020, 11, 572, doi:10.1038/s41419-020-02771-9.
167. Fedoriw, A.; Rajapurkar, S.R.; O'Brien, S.; Gerhart, S.V.; Mitchell, L.H.; Adams, N.D.; Rioux, N.; Lingaraj, T.; Ribich, S.A.; Pappalardi, M.B.; Shah, N.; Laraio, J.; Liu, Y.; Butticello, M.; Carpenter, C.L.; Cresasy, C.; Korenchuk, S.; McCabe, M.T.; McHugh, C.F.; Nagarajan, R.; Wagner, C.; Zappacosta, F.; Annan, R.; Concha, N.O.; Thomas, R.A.; Hart, T.K.; Smith, J.J.; Copeland, R.A.; Moyer, M.P.; Campbell, J.; Stickland, K.; Mills, J.; Jacques-O'Hagan, S.; Allain, C.; Johnston, D.; Raimondi, A.; Scott, M.P.; Waters, N.; Swinger, K.; Boriack-Sjodin, A.; Riera, T.; Shapiro, G.; Chesworth, R.; Prinjha, R.K.; Kruger, R.G.; Barbash, O.; Mohamad, H.P. Anti-tumor Activity of the Type I PRMT Inhibitor, GSK3368715, Synergizes with PRMT5 Inhibition through MTAP Loss. *Cancer Cell* 2019, 36, 100–114, doi:10.1016/j.ccell.2019.05.014.
168. Gao, G.; Zhang, L.; Villarreal, O.D.; He, W.; Su, D.; Bedford, E.; Moh, P.; Shen, J.; Shi, X.; Bedford, M.T.; Xu, H. PRMT1 loss sensitizes cells to PRMT5 inhibition. *Nucleic Acids Res.* 2019, 47, 5038–5048, doi:10.1093/nar/gkz200.
169. Drew, A.E.; Moradei, O.; Jacques, S.L.; Rioux, N.; Boriack-Sjodin, A.P.; Allain, C.; Scott, M.P.; Jin, L.; Raimondi, A.; Handler, J.L.; Ott, H.M.; Kruger, R.G.; McCabe, M.T.; Sneeringer, C.; Riera, T.; Shapiro, G.; Waters, N.J.; Mitchell, L.H.; Duncan, K. W.; Moyer, M.P.; Copeland, R.A.; Smith, J.; Chesworth, Ribich, S.A. Identification of a CARM1

Inhibitor with Potent In Vitro and In Vivo Activity in Preclinical Models of Multiple Myeloma.

Sci. Rep. 2017, 7, 17993, doi:10.1038/s41598-017-18446-z.

End of Appendix A

## 7 Appendix B- Plasmid maps and sequences

SB Plasmid Sequence:

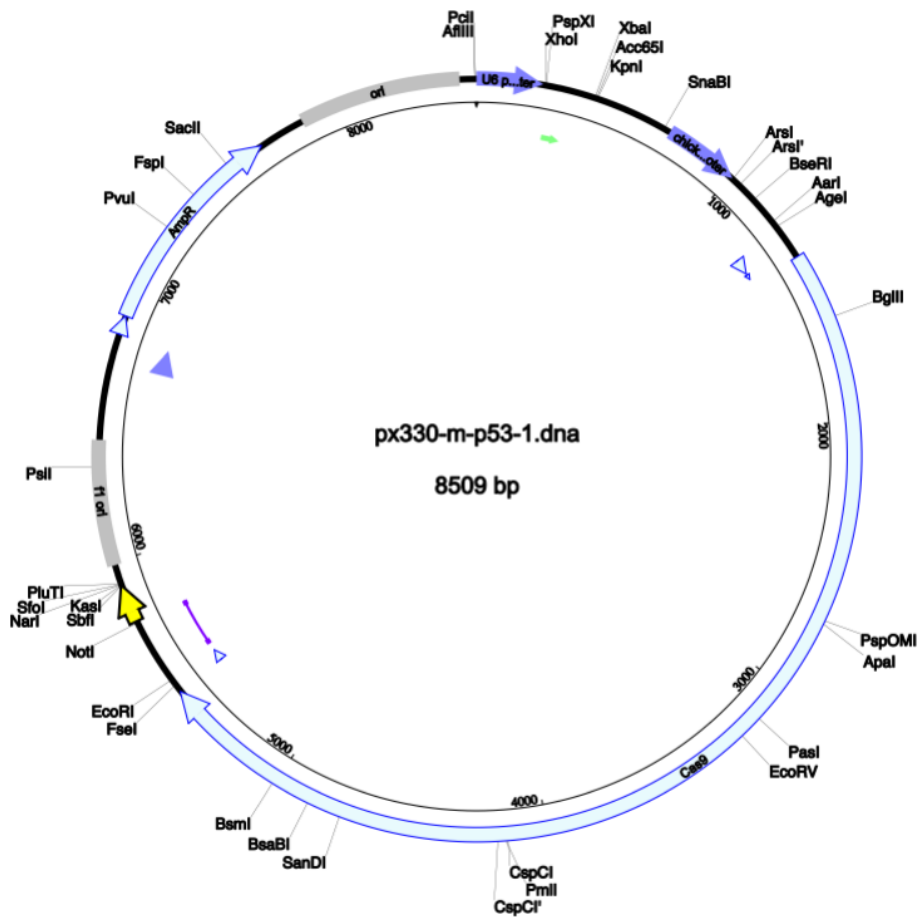
tgccgcatagttaagccagtatctgctccctgctgtgtgtggaggtcgctgagtagtgccgagcaaaaatlaagctacaacaaggc  
aaggcttgaccgacaattgcatgaagaatctgcttagggtaggcgtttgcgctgcttcgcatgtacgggcccagatatacgcgttga  
cattgattattgactagttataatagtaatacaattaccggggcattagttcatagcccataatggagttccgcttacataactacggta  
aatggcccgcctggctgaccgcccacgacccccgccattgacgtcaataatgacgtatgttccatagtaacgccaatagggac  
ttccattgacgtcaatgggtggagatttacggtaaaactgccactggcagtagcatcaagtgtatcatatgccaagtagcggccctatt  
gacgtcaatgacggtaaatggcccgcctggcattatgccagtagcatgaccttagggacttctacttggcagtagcatctacgtatta  
gtcatcgctattaccatgggtgatgcccgtttggcagtagcatcaatgggctggatagcgggttgactcacggggattccaagtccacc  
ccattgacgtcaatgggagtttggcaccaaaatcaacgggacttccaaaatgtcgtacaactccgccccattgacgcaaatg  
ggcgttaggcgtgtacgggtggaggtctatataagcagagctctctggtaactagagaaccactgctactggcttatcgaaatta  
atacgtactactatagggagacccaagctggtagcagctcggatccgacatcatgggaaaatcaaaagaaatcagccaagac  
ctcagagcgaaaattgtagacctccacaagtctgggtcatcctgggagcaatttccaaacgcctggcgttaccacgttcatctgtaca  
aacaatagtagcgaagtataaacacccatgggaccacgcagccgtcataccgctcaggaaggagacgcgttctgtctctagagat  
gaacgtacttgggtgcgaaaatgcaaatcaatcccagaacagcggcaaaaggaccttgaagatgctggagaaaacagggcaca  
aaagtagtctatataccacagtaaaacaggtctctatcgacataacctgaaaggccgctcagcaaggaagaagccactgctccaaa  
accgacataagaaaagccagactacgggttgaactgcacatggggacaaagatcgacttttggagaaatgtcctctggtctgatga  
aacaataatagaactgttggcataatgaccatcgttatgttggaggaagaagggggaggctgcaagccgaagaacacccatcc  
caaccgtgaagcaggggggtggcagcatcatgttgggggtgcttggcagggaggactgggtcacttcacaaaatagatggc  
atcatgaggaaggaaaattatggtatattgaagcaacatcgaagacatcagtcaggaagtaaaagcttggcgaatgggtct  
tccaaatggacaatgacccaagcatacttccaaagtgtggcaaaaatggcctaaggacaacaaagtaaggtattggagtgcca  
tcacaaagccctgacctcaatcctatagaaaatttggggcagaactgaaaaagcgtgtgcgagcaaggaggcctacaaacctga  
ctcagttacaccagctctgtcaggaggaatggggcaaaaatcaccacactattgtgggaagcttgggaaggctacccgaaacggtt  
gacccaagtaaacaaatlaaaggcaatgctaccaaatacagaattctgcagatattccatcacactggcggccgctcagcatgca  
tctagagggccctattctatagtgacacctaataatgctagagctcgtgatcagcctcgactgtgccttctagtggcagccatctgttgg  
cccctccccgtgcttctgacctggaagggtgcccactcccactgctcttccataaaaatgaggaaatgcatcgattgtctgagt  
aggtgtcattctattctgggggtgggggtggggcaggacagcaagggggaggattgggaagacaatagcaggcatgctggggat  
gcggtgggtctatggctctgaggcggaaagaaccagctgcattaatgaatcggccaacgcgcggggagaggcgggttgcgtatt  
gggcgctctccgctcctcgtcactgactcgtcgcctcggctcgtcggctcggcgcgagcggatcagctactcaaggcggtaat  
acggttatccacagaatcaggggataacgcaggaaagaacatgtgagcaaaaaggccagcaaaaaggccaggaaccgtaaaaa  
ggccgctgtgctggcgttttccataggctccgccccctgacgagcatcacaataatcgacgctcaagtcagaggtggcgaacc  
cgacaggactataaagataaccaggcgttccccctggaagctccctcgtcgcctcctgttccgacctgcccgttaccggatacctg  
tccgcttctccctcgggaagcgtggcgttctcatagctcacgctgtaggtatctcagttcgggtgtaggtcgttccgctccaagctggg  
ctgtgtgacgaacccccgttcagcccagcgtgccccttaccggtaactatcgtctgagtccaacccggtaagacacgacttat  
cgccactggcagcagccactggaacaggattagcagagcaggtatgtagggctgtacagagttctgaagtgggtggcctaac  
tacggctacactagaagaacagatattggtatctgcctcgtcgaagccagttacctcggaaaaaaggattggtagctctgatccgg  
caacaaaaccaccgctgtagcgggtggtttttgttgaagcagcagattacgcgcagaaaaaaggatcctaagaagatcctttg  
atctttctacggggtcagcgtcagtggaacgaaaactcaggttaagggttttggatgagattatcaaaaaggatctcacctag  
atccttttaataaaaatgaagtttaaatcaatctaaagatatatgagtaaaacttggctgacagttaccaatgcttaacagtgaggc  
acctatctcagcagatctgtctatttctcatccatagttgctgactccccctcgtgtagataactacgatacgggagggttaccatctg  
gccccagtgctgcaatgataccgcgagaccacgctcaccggctccagattatcagcaataaacagccagccggaaggggccg  
agcgcagaagtgctcctgcaactttatccgcctccatccagctattaattgttggcgggaagctagagtaagtagttcggcagtaata  
gtttgcgcaacggttggcattgctacaggcatcgtggtgtcacgctcgtcgttggatggctcattcagctccgggtcccaacgatca  
agggcagttacatgatccccatggttgcaaaaagcggtagctcctcggctcctccgatcgtgtcagaagtaagttggccgagcgt  
gttatcactcatggtatggcagcactgcataattcttactgtcatgccatccgtaagatgctttctgtgactggtgagtagtcaaccaa  
gtcattctgagaatagtgatgcccgcagcaggttgccttcccggcgtcaatacgggataataccgcgccacatagcagaacttta  
aaagtgtcatcattgaaaacgttctcggggcgaaaaactcgaaggtatcaccgctgttggatccagttcagatgaaccactcgt  
gcaccaactgatctcagcatctttacttccaccagcgttctgggtgagcaaaaacaggaaggcaaaaatccgcaaaaaaggga  
ataagggcgacacggaatgtgaatactcactcttcttttcaatattatgaagcatttatcaggggtattgtctcatgagcggatac  
atattgaaatgatttagaaaaataacaaataggggtccgcgcacatttccccgaaaagtgccacctgacgtcgacggatcggga  
gatctcccgatcccctatggtgactctcagtagcaatctgctctga





caggaaatcggcaaggctaccgccaagtaacttctctacagcaacatcatgaacttttcaagaccgagattaccctggccaacggc  
gagatccggaagcggcctctgatcgagacaaacggcgaaccggggagatcgtgtgggataagggccgggattttgccaccgtg  
cggaaagtgtgagcatgccccagtgaaatcgtgaaaaagaccgaggtgcagacagggcggctcagcaaagagctatcctg  
cccaagaggaacagcgataagctgatgccagaaagaaggactgggaccctaagaagtagggcggctcagacagccccaccg  
tggcctattctgtgctggtggtggccaaagtggaaaagggcaagtccaagaaactgaagagtgtgaaagagctgtggggatcac  
catcatggaagaagcagctcagagaagaatcccatcgactttctggaagccaagggctacaaagaagtgaaaaggacctgat  
catcaagctgcctaagtaactccctgtcagctggaaaacggcgggaagagaatgctggcctctgccggcgaactgcagaagggga  
aacgaactggcctgccctccaaatagtgaacttctgtacctggccagccactatgagaagctgaagggctccccgaggataat  
gagcagaacacagctgttgtggaacagcacaagcactacctggacgagatcatcgagcagatcagcgagttccaagagagtg  
atcctggccgacgtaatctggacaaagtgtgtccgctacaacaagcaccgggataagcccatcagagagcaggccgagaat  
atcatccacctgtttaccctgaccaatctgggagcccctgccgctcaagtaactttgacaccaccatcgaccggaagaggtacacca  
gcaccaagaggtgctggacgccaccctgatccaccagagcatcaccggcctgtacgagacacggatcgacctgtcagctgg  
gaggcgacaaaagggcggcggccacgaaaaagggcggcaggcaaaaaagaaaagtaagaattcctagagctcgtgatc  
agcctcgactgtccttctagtgtccagccatctgttggccctccccgtgacctcctgacctggaaggtgccaactcccactgtcct  
ttcctaataaaaatgaggaaattgcatcgcattgtctgagtaggtgtcattctattctgggggtgggggaggacagcaagggg  
gaggattgggaagagaatagcaggcatgctggggagcggccgaggaaccctagtatggagttggccactccctctctgcgcg  
ctcgtcgtcactgaggccggcgaccaaaggtcgcccgacggcgggctttgccggggcggcctcagtgagcagcagcagcgc  
gcagctgctgcaggggcgctgatgcggtattttctctacgcatctgtgcggtatttcacaccgcatacgtcaaagcaaccatagta  
cgcgccctgtagcggcgattaagcgcggcgggtgtggtggttacgcgcagcgtgaccgctacacttgccagcgccttagcgc  
gctccttgccttctccctctctctcgcacgcttccggcttccccgtaagctctaaatcgggggctcccttaggggtccgatttagt  
gctttacggcacctcgacccccaaaaaactgattgggtgatggttcacgtagtgggccatgcctgatagacgggttttcgccc  
cgttgagtgccacgttcttaatagtgactctgttccaaactggaacaactcaaccctatctgggctattctttgattataagggat  
tttggcatttggcctattggttaaaaaatgagctgatttaaaaaatftaacgcgaatttaacaaaatftaacgtttacaattttatgg  
tgactctcagtaaatctgctctgatgccgatagttaagccagccccgacaccgccaacaccgctgacgcgcccctgacgggc  
ttgtctgctccggcatccgcttacagacaagctgtgaccttccgggagctgatgtgcagaggtttaccgctcatcaccgaaac  
gcgcgagacgaaagggcctcgtgatacgcctattttataggttaatgtcatgataataatggtttcttagacgtcaggtggcactttcgg  
ggaaatgtgcggaaccctattgtttattttctaaatacattcaaatatgtatccgctcatgacataaacctgataaatgcttca  
ataatattgaaaaaggaagagatgagtagtattcaacattccggtgcgcccttattccctttttgcggcattttgccttctgttttgc  
cacc  
agaaacgctggtgaaagtaaaagatgctgaagatcagttgggtgcacgagtggttacatcgaactggatcacaacagcggtaag  
atccttgagagttttgccccgaagaacggtttccaatgatgagcacttttaagttctgctatgtggcgcggtattatcccgtattgacgc  
gggcaagagcaactcggctgcgcgatacactattctcagaatgacttgggtgactcaccagtcacagaaaagcatcttacggat  
ggcatgacagtaagagaattatgcagtgctgcataaccatgagtgataaactgcggccaacttactctgacaacgatcggagg  
accgaaggagctaacccgtttttgcacaacatgggggatcatgtaactgccttgatcgttgggaaccggagctgaatgaagccat  
accaaacgacgagcgtgacaccacgatgcctgtagcaatggcaacaacgttgcgcaaaactattaactggcgaactactactctag  
ctcccggcaacaattaatagactggatggaggcggataaagttgcaggaccacttctgcgctcggccctccgggtggctggttatt  
gctgataaatctggagccgggtgagcgtggaagccgcggtatcattgcagcactggggccagatggttaagccctccgatatcgtagt  
atctacacgacggggagtcaggcaactatggatgaacgaaatagacagatcgctgagataggtgctcactgattaagcattggta  
actgtcagaccaagttactcatatatactttagattgatttaaaacttatttttaatttaaaaggatctaggtgaagatccttttgataatct  
catgacaaaatccctaacgtgagtttctgctcactgagcgtcagacccccgtagaaaagatcaaaggatcctctgagatccttttttc  
tgcgctaatctgctgctgcaaaacaaaaaaccaccgctaccagcgggtgtttgttgcggatcaagagctaccaactcttttccg  
aaggtaactggcttcagcagagcgcagataccaaatactgtccttctagttagccgtagttaggccaccactcaagaactctgtag  
caccgctacatacctcgtctgtaaatctgttaccagtggctgctgccagtggcgataagtcgtgttaccgggttgactcaagac  
gatagttaccggataagggcagcggctcgggctgaacggggggtcgtgcacacagcccagctggagcgaacgacctacaccg  
aactgagatacctacagcgtgagctatgagaaagcggcagcgttccgaaggagaaaggcggacaggtatccggtgaagcggc  
agggctcggaaacaggagagcgcagggagctccaggggaaacgctggtatctttatagctcgtcgggttccgacctctga  
ctgagcgtcagttttgtgatgctcgtcagggggcggagcctatggaaaacgcccagcaacgcggccttttacggttctgcctttt  
gctggcctttgctcacatgt



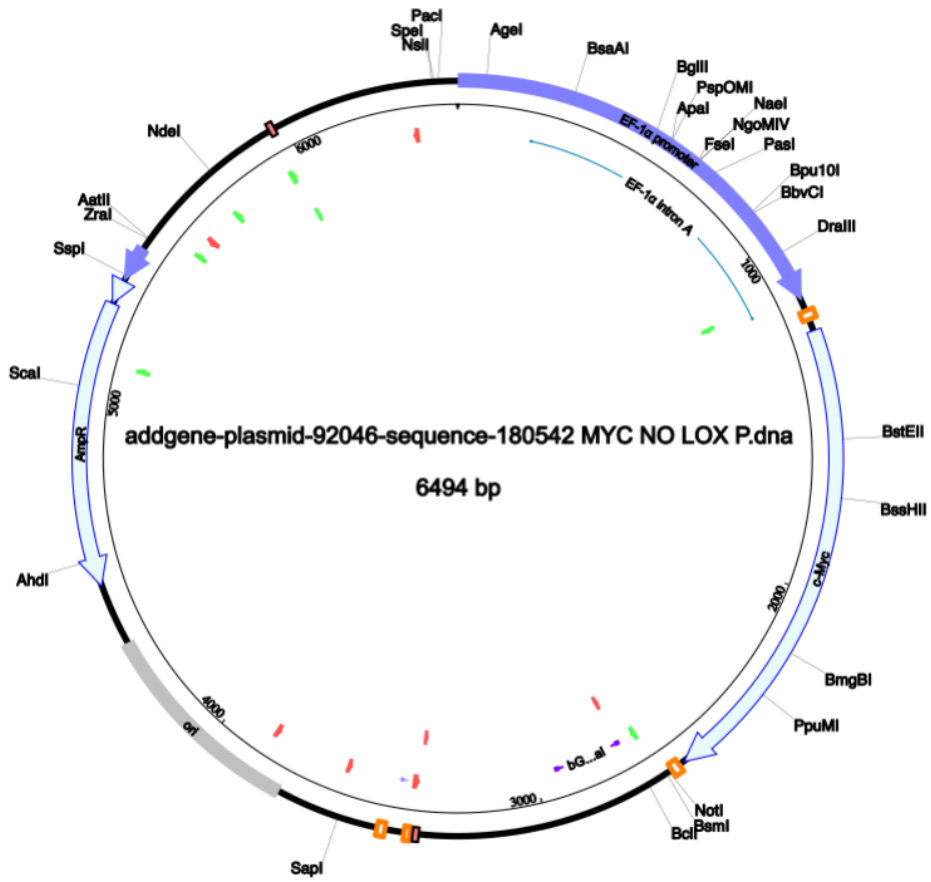


Appendix C Figure 2- p53 plasmid

## Myc Plasmid

ggctccggtgcccgtcagtgggcagagcgcacatcgcccacagtccccgagaagttggggggaggggtcggcaattgaaccggt  
gcctagagaaggtggcgcggggtaaactgggaaagtgatgctgtactggctccgcttttcccgagggtgggggagaaccgat  
ataagtgcagtagtcgcccgtgaacgttcttttcgcaacgggttgcgcccagaacacaggttaagtccggtgtgtggtcccgcggg  
tggcctctttacgggttatggccctgctgctgaattactccacctggctgcagtagctgattctgtatcccagacttcgggttgaag  
tgggtgggagagttcgaggcctgctgctaaggagccccttcgctcgtgcttgattgaggcctggcctggcgctggggccgccc  
cgtgcgaatctggtggcaccttcgcgctgtctcgctgctttcgataagtctctagccatttaaaatgtgatgacctgctgcgacgctttt  
tctggcaagatagctttaaagtcggggccaagatctgcacactggatattcggttttggggccgcccggcgacggggcccgtgc  
gtcccagcgcacatgttcggcgaggcggggcctgagagcgcggccaccgagaatcggacgggggtagtctcaagctggccggc  
ctgctctggtgctgctgcccgcggctgtatgccccgcctggcggaaggctggcccggctggcaccagttgctgagcg  
gaaagatggccgcttccggccctgctgcagggagctcaaaatggaggacgcggcgctgggagagcggcggggtgagtcacc  
cacaaaaggaaaagggccttccgctcagccgctgctcatgtgactccacggagtaccggcgccgctccaggcacctcgatt  
agttctcgagctttggagtagctgctttagttggggggaggggtttatgcatgagttcccacactgagtggtggagactga  
agttaggccagctggcactgtatgaattctccttgaattgcccctttttagttggatcttggtcattctcaagcctcagacagtggtc  
aaagtttttctccattcaggtgctgtaggaattagctgtaccaatacggatatcaacaagttgtacaaaaagcaggctttaa  
ggaaccaattcagtcgactggatccaccatgcccctcaacgttagcttccaacaggaactatgacctgactacgactcggtgca  
gccgtatttctactgagcagaggaggagaacttctaccagcagcagcagagcagagctgacgccccggcgcccagcagg  
atatctggaagaaatcagctgctgcccaccccgcctgtcccctagccgctcgggctctgctgcccctctacgttgcggtc  
acacccttctccctcggggagacaacgacggcggtggcgggagcttctccacggccgaccagctggagatggtgaccgagctgc  
tgggaggagacatggtgaaccagagttcatctgcgacccggagcagagaccttcaaaaaacatcatccaggactgtatg  
ggagcggcttctcggccgccaagctgctcagagaagctggcctcctaccaggctgcgcaagacagcggcagcccga  
accccgcccgcggccacagcgtgctccacctccagctgtacctgagcggcctcagagtgatcgacccc  
tcggtggtcttcccctacccttcaacgacagcagctgcccgaagctgcccctcgaagactccagcgccttctcctcctcggga  
ttctctgctcctcagcggagctcctcccgcagggcagccccgagcccctggtgctccatgaggagacaccgcccaccaccagca  
gagactctgaggaggaacaagaagatgaggaagaaatcgatgttttctgtgaaaaagaggcaggctcctggcaaaaaggtag  
agtctggatcacttctgctggaggccacagcaaacctcctcacagcccactggctcctcaagaggtgccacgttccacacatcagc  
acaactacgcagcgcctccctcactcgggaaggactatcctgctgccaagagggtcaagttggacagtgctcagagctctgagacag  
atcagcaacaaccgaaaatgaccagcccaggctcctcgacaccgaggagaatgcaagaggcgaacacacaacgtcttg  
agcgcagaggaggaacgagctaaaacggagctttttgcccctgctgaccagatcccggagttgaaaacaatgaaaaggccc  
ccaaggtatgtatcttaaaaaagccacagcacaatcctgtccgtccaagcagaggagcaaaagctatttctgaagaggactgtt  
gcgaaacgacgagaacagttgaaacacaaactgaacagctacggaactctgtgaggactcgagatctagaccagcttctt  
gtacaaagtgggtgatatcgcgccgctgactttagttgtggtttgccaactcaatgtatcttcatgctggtatccgctgatcag  
cctcagctgtgcttctagttgccagccatctgttttcccctccccgtgcttccctgaccctggaagggtgccactcccactgtccttc  
ctaataaatgaggaaattgcatcgactgctgagtaggtgcttctattctgggggtgggggtggggcaggacagcaaggggga  
ggattgggaagacaatagcaggcatgctggggatgcggtgggctctatggctctgaggcggatccccttgaatacatccacag  
gtacacctcaattgactcaaatgatgtcaattagctatcagaagcttcaagccatgacatcatttctggaatttccaagctgttaa  
aggcacagtaactagtgtatgtaacttctgaccactggaattgtgatacagtgaaataatctgctgtaacaatt  
gttgaaaaatgactgtgcatgcacaaagtagatgtcctaactgacttgccaaaactattgtttgtaacaagaaattgtgagtagtt  
gaaaaacgagtttaatgactccaactaagtgtatgaaactcggacttcaactgtataggctagagctgacctgcaggcatgcaa  
gcttggcgtaatcatggtcatagctgttctgtgaaattgtatccgctcacaattccacacaacatacagcgggaagcataaagt  
gtaaagcctgggggtcctaagtagtgagtaactcacattaattgctgtgctcactgcccgttccagctcgggaaacctgctgctgc  
cagctgcattaatgaatcgcccaacgcgcccgggagagggcggttgcgtattggcgcttccgcttctcctcctcactgactcgtcgcg  
ctcggctcgtcggctcggcgagcggatcagctactcaaggcggtaatacggttatccacagaatcaggggataacgcaggaa  
agaacatgtgagcaaaaggccagcaaaaggccaggaaccgtaaaaaggccgctgtgctggcgttttccataggctccgcccc  
ctgacgagcatcaaaaaatcgacgctcaagtcagaggtggcgaacccgacaggactataaagataaccaggcgttccccctg  
gaagctcctcgtgctcctcctgttccgaccctgcccctaccggatacctgtccgcttctccctcgggaagcgtggcgcttctcat  
agctcacgctgtaggtatctcagttcgggtgtaggtcgtcctcaagctgggctgtgtgacgaacccccgttcagcccagccgctg  
cgcttaccggtaactatcgtctgagccaacccggtaagacacgacttaccgactggcagcagccactggtaacaggattagc  
agagcggaggtatgtaggggctacagagttctgaagtggtggcctaactacggctacactagaagaacagttttgtatctgcg  
ctctgctgaagccagttacctcggaaaaagagttgtagcttctgatccggcaacaaaccaccgctggtagcgggtgtttttgttg  
caagcagcagattacgcgcagaaaaaaggatctcaagaagatcctttgatctttctacgggtctgacgctcagtggaacgaaa  
actcacgttaagggtttgtcatgagattcaaaaaaggatctcacctagatccttttaataaaaaatgaagtttaaatcaatctaa  
agtataatgagtaaaactggctgacagttaccaatgcttaatcagtgaggcacctatctcagcgtctgtctattcgttcatccatagtt

gcctgactccccgctgtagataactacgatacgggagggcttaccatctgccccagtgctgcaatgataccgagagaccacg  
ctcaccggctccagattatcagcaataaaccagccagccggaagggccgagcgcagaagtggtcctgcaactttatccgcctcca  
tccagcttattaattgttccgggaagctagagtaagtagttcgccagtaaatggttgcgcaacggtgtgcatgctacagggcatcgtg  
gtgtcacgctcgtcgttggatggcttcattcagctccggtcccaacgatcaaggcgagttacatgatccccatggtgtgcaaaaa  
gcggttagctcctcggctcctccgatcgttgcagaagtaagttggccgcagtggtatcactcatggttatggcagcactgcataattctct  
actgtcatgccatccgtaagatgctttctgtgactggtagtactcaaccaagtcattctgagaatagtgatgcggcgaccgagttgct  
ctgccccggctcaatacgggataataccgcgccacatagcagaactttaaagtgctcatcattggaaaacggtcttcggggcgaa  
aactctcaaggatcttaccgctgttgatccagttcgatgtaaccactcgtgcacccaactgatcttcagcatctttacttccaccagc  
gtttctgggtgagcaaaaacaggaaggcaaatgccgcaaaaaaggaataagggcgacacggaaatgtgaatactcactactc  
ttccttttcaatattatgaagcattatcagggttattgtctcatgagcggatacatattgaatgtattagaaaaataaacaatagggg  
ttccgcgcacatttccccgaaaagtgccacctgacgtctaagaaccattattatcatgacattaacctataaaaaataggcgtatcacg  
aggcccttctcgtcgcgcgttccggtgatgacggtgaaaacctctgacacatgcagctcccggagacggtcacagctgtctgtaagc  
ggatgccgggagcagacaagcccgtcagggcgctcagcgggtgtggcgggtgtcggggctggcttaactatgcggcatcaga  
gcagattgtactgagagtgaccatagcgggtgaaataccgcacagatgcgtaaggagaaaataccgcatcagggcgccattcg  
ccattcaggctgcgcaactgtgggaagggcgatcgggtcgggctcttcgctattacgccagctggcgaaagggggatgtgctgca  
aggcgattaagttgggtaacgccagggttccagtcacgacgttgtaaaacgacggccagtgaaatcgagctcgggtaccctacagt  
tgaagtcggaagttacatacactaagttggagtcattaaaactcgttttcaactactccacaaattctgttaacaaacaatagtttgg  
caagtcagttaggacatctacttgtgatgacacaagtcattttccaacaattgtttacagacagattttcacttataattcactgtatc  
acaattccagtggtcagaagtttacatacactaagttgactgtcctttaaacagcttgaaaattccagaaaatgatgtcatggctta  
gaagcttctgatagactaattgacatcatttgagcaattggaggtgtacctgtggatgtattcaaggaattctgtggaatgtgtcagtt  
aggggtgtgaaagtcgccaggtcccagcaggcagaagtatgcaaagcatgcataatcgatactagtttaattaagatcctcttgc  
gctaattggaccttctaggtctgaaaggagtgggaatt



Appendix C Figure 3- c-Myc plasmid

V5-PRMT5 IRES MEP50 sequence: PRMT5 is highlighted in “RED” and MEP50 is highlighted in “ORANGE”

ccccgcggcaggccctccgagcgtggtggagccgttctgtgagacagccgggtacgagtcgtgacgctggaaggggcaagcgg  
gtggtgggcaggaatgcggtccgcccctgcagcaaccggagggggagggagaagggagcggaaaagtctccaccggacgagg  
ccatggctcggggggggggggcagcggaggascgctccggccgacgtctcgtcgtgattggcttcttctcccgccgtgtg  
aaaacacaaatgacgtgtttggtggcgtaaggcgctgtcagttaacggcagccggagtgccagccggcagcctcgtct  
gcccactgggtggggcgggaggtaggtgggtgaggcgagctgnacgtgcccggcggcggcctgaggggggcgggggag  
gggagggaggggtcagcgaagtagctcgcgcgcgagcggcccccaccctccccttcttgggggagtcgtttaccgcccgc  
ggccgggctcgtcgtcgtattggtctcggggccagaaaactggccttgccattggtcgtgttcgtgcaagttgagtcacccgc  
cggccagcggggcggcggaggagcgtcccagggtccggccctcccctggccccgcggcagagtcggccgcgcgcccc  
tgcgcaacgtggcaggaagcgcgcgctggggcggggacgggcagtagggctgagcggctgcccggggcgggtgcaagcacgtt  
tccgactgagttgctcaagagggcgctgctgagccagacctccatcgcgactccggggagtgaggggaaggagcaggggct  
cagttgggctgtttggaggcaggaagcactgtctccaaagtgcctcgtgagttatcagtaagggagctgagtgaggtagggc  
gggagaaggccgacccttcccggaggggggaggggaggtgtgcaataccttctgggagttctcgtcctcctggcttctgagg  
accgccctgggctgggagaatcccctgcccccttcccctcgtgatctgcaactccagcttcttagattaataagggatctgagg  
cgcagtagtccagggttcttgatgatgtcacttctcctgtccctttttccacagctcgcggtgaggacaaactctcgcggtcttc  
cagtgggatcgacggtatcgtagagtcgaggccgctctagagtttaaacgccaccatgaccgagtagaagcccacggtgcgct  
cgccaccgcgcagcagcgtcccaggccgtacgcaccctcgcgcccgttcgcccactaccgcccacgcgccacaccgctc  
atccggaccgccacatcgagcgggtcaccgagctgcaagaactcttctcagcgcgctcgggctgacatcggcaaggtgtggg  
cgcggacgagcggcggcgggtggcggctggaccacgcccggagagcgtcgaagcggggcgggtgtcggcagatcggccc  
cgatggccgagttgagcgggtcccggctggccgcgagcaacagatggaaggcctcctggcggcaccggcccaaggagcc  
cgctgtgttctggccaccgctcgcggcgtcgcggaccaccagggcaagggctgtggcagcggcgtcgtccccggagtgagg  
gcccggagcgcgcccgggtgcccgccttctggagacctccgcgccccgcaacctcccctctacgagcggctcggcttaccgt  
caccgcccagctcagaggtgccgaaggaccgcgacctggtgatgaccgcaagcccgggtgcctgacgcccggcccccacgacc  
cgcagcggccgaccgaaaggagcgcagaccatgcatgatctagagctcgtgatcagcctcagctgtgccttctagtgtg  
ccagccatctgttgtttgcccctccccctgcttcttaccctggaaggtgccactcccactgtccttcttaataaaatgaggaaattg  
catcgcattgtcgtagtaggtgtcattctattctgggggtgggtggggcaggacagcaagggggaggattgggaagacaatagc  
aggcatgtggggaactagtattataatagtaataattacggggctcattagttcatagccatataatggagtccggttacataactac  
ggtaaatggcccgcctggtgaccgcccacgacccccgccattgacgtcaataatgacgtatgtcccatagtaacgccaatag  
ggacttccattgacgtcaatgggtggagtattacggtaaaactgccactggcagtagatcaatgtagatgccaagtagcggcc  
ctattgacgtcaatgacggtaaatggcccgcctggcattatgccagtagatgaccttattgggacttctacttggcagtagatctcgt  
attagtcacgtctattaccatggtcgaggtgagccccacgttctgcttacttcccctctccccccccctcccaccccccaattttgtattt  
atttttttaattttttgtgcagcgtatggggcggggggggggggggggggggggcgcgcccaggcggggcggggcggggcagggg  
cggggcggggcagggcggagaggtgcggcggcagccaatcagagcggcgcgctccgaaagtttctttatggcgaggcggcg  
gcccggcggccctataaaaagcgaagcgcgcccggggcgggagtcgctcgcgctgcctcgcggcggcggcggcggcggcggc  
cgctcgcgcccggcccccggctcgtactgaccggttactcccacaggtgagcgggcccggcggcggcggcggcggcggcggcggc  
attagcgttggttatgacggcgtgtttcttctgtggtcgtgaaagcctgaggggctccgggagggcccttctgtcgggggag  
cggctcgggggtgctgctgtgtgtgctggtgggagcggcggctccgcgctcccggcggctgtgagcgtcggg  
cgcggcggggcgttgtgctcgcgagtgctgcgaggggagcgcggcggggggcgggtccccgcgggtcggggggggctg  
cgaggggaacaaaggctcgtcgggggtgtgctggtgggggggtgagcagggggtgtggcgctcgggtcggggtgcaacccc  
ccctgacccccctcccaggttctgagcacgcccggctcgggtcggggctccgtacggggcgtggcgggggctcggcgt  
gcccggcggggggtggcggcaggtgggggtgccggcggggcggggcggcggcggcggcggcggcggcggcggcggcggcggc  
gcccggcggcccccggagcggc  
agggacttcttctccaaaatctgtgaggagccgaaatctgggagggcggcggcggcggcggcggcggcggcggcggcggcggc  
gtcggcggcggcggcaggaaggaaatgggcccgggagggcctcgtcgtcggcggcggcggcggcggcggcggcggcggcggc  
ggctgtccgcccggggacggctcctcgggggggacggggcagggcgggggtcggcttctggcgtgtgaccggcggctctagag  
cctctgtaaccatgttcatgcttcttcttctacagctcctggcaacgtgctggtattgtgtctcatattttggcaagaattct  
cgacggggaattcggggcccgggggggctagaattcataactcgtatagcacaattacgaagttatgtaggatctgcgactcta  
gaggatctgcgactctagaggatcataatcagccataccacattgtagagtttactgtcttfaaaaaaacctcccacacctcccctg  
aacctgaaacataaaatgaatgcaattgtgtgttaactgtttattgacgttataatggttacaataaagcaatagcatcaaaatt  
cacaataaagcatttttactgactcattctagtgtgtgttgcctcaactcatcaatgtatcttatcatgtctgactctagaggat  
cataatcagccataccacattgtagaggtttactgtcttfaaaaaaacctcccacacctcccctgaaactgaaacataaaatgaatgc

aattgttggtaactgtttattgagcttataatggttacaataaagcaatagcatcacaatttcacaataaagcatttttactgc  
attctagtgtggttgcctaaactcatcaatgtatcttatcatgtctggtatctgcgactctagaggatcataatcagccataccacattgta  
gaggtttactgtcttaaaaaacctcccacacctccccctgaacctgaacataaaatgaatgcaattgtgtgtaactgtttattgca  
gcttataatggttacaataaagcaatagcatcacaatttcacaataaagcatttttactgcattctagtgtgttgcctaaactc  
atcaatgtatcttatcatgtctggtatccccatcaagctgatccggaacccttaataaactcgatagcatacattatac|gaagttatttg  
tcgacgctagcgccacatggggaagccatacctaaccctctttgggtctggatagtacgcgaccctcccgtcggaccgcg  
cgatggcagtcggagggtgctggtggcagccgcgtgtccagcgggagggacctgaattgcgtccccgaatagctgac  
acactgggtgctgtggccaagcaggggttgattcctctgcatgcctgtctccaccgcggttcaagagggagttcattca  
ggaacctgctaagaatcggcctggccccagacacgatcagacctactgctgtcaggaagggactggaatacgttaatt  
gtgggaaagctttctccatggattcatccagactcaaaagtggagaagatccgaaggactctgaagcggctatgttaca  
ggagctgaatttggagcatatctgggtctccagcttctattgccccttaacaggaagataacacgaatctggccagag  
ttctgaccaaccacatccacactggccaccacttctccatgttctggtatgaggggtacccttgggtggcaccagagacctga  
gagatgatgaattgcgaatgccccgactacacacagagggatcagtgaggaagagaagacatggatgtgtggtggc  
ataacttcggactctgtgactatagcaagagaattgcagtagcttctgaattggagctgacctcccgtctaatacagctc  
attgaccgctggcttggagagcccataaagcagccattctcccaccagcatttcttaaccaacaagaaaggatttct  
gttcttctaaagtgcaqcaagggctgatctccggctcctcaagttggaagtgcagttatcatcacqggaaccaaccacc  
actcagagaagggagtctgttctaccctcagacttggaaacttaagccaaaatcgcctccaccatgcctatgagct  
cttggcaaaaggctatgaagactatctgcagctcccactccaqctctgatggacaatctggaatctcagacatagaagtg  
ttgaaaaggacccatcaataactctcaatatcagcaggctattataaatgtttgctagaccgagctaccagaagaagaaa  
aggagaccaatgtccaggtacttatgggtgctgggtgcagggcgggtccttctgtaagcgtctctcgggcagccaaa  
cagggcagcggcgatcaggctgtatgctgtggagaagaaccccaatgctgtgtgagcctagagaactggcagtttg  
aagaatgggggagccaggtgacagttgtctcatcagacatgcgggaatgggtggctccggagaaagctgacattattgt  
cagtgagcttctgggttcttggcacaacgagctgtcacctgagtgctggatggagcacagcacttctgaaagatgat  
ggcgtgagcatccctggagaatacacctcctcctggctccatttctccttaagctgtacaacgaggtccgtgcctgtc  
gggaaaaagaccgcgatcctgagqcacagttgagatgcctatgtggttcggttcacaactccaccagctctctgtc  
ctaagccctgcttaccctcagccatcccaaccgagatcctatgattgacaacaaccgctactgtaccctggagtttctgtg  
gaggtgaacacgggtgcttcatggcttcgaggctactttgagactgtgcttaccgggacatcactctgagtatccgccag  
agactcactctcctggaatgttctcatggttcccatcttctcccattaagcagccatcacgggtgcacgaaggccagaa  
catctgtgtcgttctggcgatgcagcaattccaagaaagtgtgttacgagtgggcggtgacggccccgtctgttcttct  
attcacaaccctaccggccgctcctataaccattggcctctagcccggggatccgcccctctccctccccccccctaacgta  
ctggccgaagccgcttgaataaggccgggtgctgcttatgttatttccaccatattgccgtctttggcaatgtgagggccgg  
aaacctggccctgtctctgacgagcattcctaggggtcttcccctctgcctaaaggaatgcaaggtctgtgaaatgctgaa  
gcagttcctctggaagcttctgaagacaacaacgctgtgagcgacccttgcagcgacggaaacccccacctggcgacaggtg  
cctctgcggccaaaagccagctgtataagatacacctgcaaaggcggcacaacccagtgccacgttgtgagttgtagttg  
aaagagtcaaatggctcctcaagcgtattcaacaaggggtgaaggatgccagaaggtacccattgtatgggatctgatctg  
ggcctcggtacacatgcttacctatgttttagctgaggttaaaaaaacgcttaggcccccgaaaccaggggacgtggttctctgaa  
aaacacgatgataatggtccacatctagaatcgccaagggacaccctcctccgctcgtgccccggcgggcccgagtg  
gaacctgcccccaatgcgcccgatgcatggaacgtcaattggaggctgcacgggtaccggctgatggttccctctgc  
tcgggggtctccagcctgagtggtcgtgctgggtaggttctctgtggttttcaaggatcctagtgcggcccccaacgaag  
gttctgctcgtggtccagaccgaggtgagtagctgacctactgggtgggggacaaggtatcctagtggctt  
ctgattcaggtgctgttgaattgtgggagctagatgagaacgagacacttatagtcagcaagttctgcaagatgagcatga  
tgacattgtgtctactgtcactgtcctgagctctggcacacaagctgtcagtggttagcaagactgctgcatcaaaattggg  
acctggctcagcaggtatcactgaattcataccagctcacgctggacaggttacctgtttgctgcctctccccacaaa  
actctgtgttcttcatgtagtaggacagtagaatttgcctctgggatacccgctgtcccaagccggcatcacagatggc  
tgcaatgcctctggctaccctccctaccgcttggcttggcatcctcagcagaagtgaagtctttgttttgggtgacgagaatgga  
ctgtctcccttggacaccaagaatgcaagctgtaccctcagctcagctgtgcactcccagggtgtcactagactggtat  
tctcccacacagtgctccccctcctgacttctcagtgaaagactgttacttctgtgtgattcaagccttctgaggtgtt  
tagaagtcgagcccacagagacttctgagagatgctacgtggtcctcactcaatcactcccttctaccacagttggctgg  
gaccatcaggtcatccaccatgttgtgcccttagagcctcctccaaacctggacctgacagtttggagtagcccggg  
cgactgtccttctagtggcagccatctgttggctccccctgccttctgacctggaaggtgccactcccactgtccttctta  
ataaaatgaggaaattgcatgcattgtctgagtaggtgtcattctattctgggggggtgggtggggcaggac|agcaagggggagg  
attgggaagacaatagcaggcatgctggggatgctgggtggtctatggggggccgaattcactcctcaggtgagggctgctatca  
gaaggtgtggtggtgtggccaatgccctgctcacaataaccactgagatcttttccctctgccaanaaattatggggacatcatga



ctctcccctagtcaggaagttccccccgccccgagctcgcgctcgtsaggacgtgacaaatggaagtagcacgtctcactagtct  
cgtcagatggacagcaccgctgagcaatggaagcgggtaggccttggggcagcggccaatagcagcttctccttctgcttctg  
gctcagaggtggaaggggtgggtccgggggccccgagcgggctcaggggccccgccccgccccgaaggtcctccg  
gagggccggcattctgcacgctcaaaagcgcacgctgcccgcgtgttctcctctcctcatctccgggcttctgacctgacgtcctc  
gccatggatcctgatgatgttattcttctaatctttgtatggaaaactttctcgtaccacgggactaaacctggtatgtagattccatt  
caaaaaggtatacaaaagccaaaatctggtacacaaggaaatgatgacgatgattggaaagggtttatagtagcacaataaata  
cgacgctcgggatactctgtagataatgaaaaccgctctctggaaaagctggaggcggtgcaaaagtgacgtatccaggactga  
cgaaggttctcgactaaaagtgataatgccgaaactattaagaaagagttaggtttaagctcactgaacctgatggagcaagt  
cggaacggaagagttatcaaaaggtcgggtgatggctcgcgtgtagtctcagcctccctcctgctgaggggagttctagcgttga  
atatattaactgggaacagggcgaagcgttaagcgtagaacttgagattaatgtgaaaccctggaaaacgtggccaagatgc  
gatgatgagatattggctcaagcctgtgcaggaaatcgtgacggcagatctcttctggaaggaacctactctgtggtgtgacataatt  
ggacaaactacctacagagatttaaagctctaaggtaataataaaatctttaaagtgataatgtgttaaactactgattctaattgttgtg  
atcttagattccaacctatggaactgatgaatgggagcagtggtggaatgcagatcctagagctcgtgatcagcctcactgctgctt  
ctagttgccagccatctgtgttgcctccccctgcttccctgacctggaaaggtgccactcccactgctcttctcaataaaatgag  
gaaattgcatcgattgtctgagtaggtgctattctatctgggggtgggggtggggcaggacagcaagggggaggattgggaagac  
aatagcaggcatgctggggatgagggtggctctatggctctgagggcgaagaaccagctggggctcgacctcgagggggggc  
ccggtacattaaatcctgcaggagtagccagctttgtcccttagtgagggttaattgcgcgctggcgtaacatcatggtcatagctgttct  
ctgtgtgaaattgtatccgctcacaattccacacaacatacagcgggaagcataaagttaaagcctggggtgcctaagtagtga  
gtaactcacattaatgctgtcgcctcactgcccgttccagtcgggaacctgctgctgccaagctgcattaatgaatcggccaacgc  
gccccggagagggcgttctgctattgggctctcctcctcctcactgactcgtcgcgctcggctgctcggctgccccgagcggg  
atcagctcactcaaggcggtaatacgggtatccacagaatcaggggataacgcaggaaagaacatgtgagcaaaaggccagc  
aaaaggccaggaaccgtaaaaaggccgcttctgctggcttttccataggtcctccccctgacgagcatcaaaaaatcgacg  
ctcaagtcagaggtggcgaaccgacaggactataaagataccaggcgttccccctggaagctccctcgtcgcctctcctgttcc  
gacctgcccgttaccggatacctgctccgcttctccctcgggaagcgtggcgcttctcatagctcacgctgtaggtatctcagttcgg  
ttaggtcgtcctcaagctgggctgtgtgcacgaacccccgttcagcccagcctgctcgccttatccgtaactatcgtcttgagt  
ccaaccggtaagacacgacttatcgccactggcagcagccactggtaacaggattagcagagcgaggtatgtaggcgggtgtac  
agagttctgaagtggcctactacggctacactagaaggacagatattggtatctcgcctcgtcgaagccagttaccttcggaa  
aaagagttgtagctctgatccggcaacaaccaccgctgtagcgggtggtttttgttgaagcagcagattacgcgcagaaa  
aaaaggatctcaagaagatccttctgatctttctacggggtcgtcagcctcagtggaacgaaaactcacgtaagggattttgtgctag  
attatcaaaaaggatctcactagatccttttaataaaatgaagtttaatacaatctaaagtataatgagtaaactggctgaca  
gttaccaatgcttaacagtgaggcacctatctcagcagatctgtctattctcgttccatagttgctgactccccgctgctgataacta  
cgatacgggagggcttaccatctgccccagtgctgcaatgataccgcgagaccacgctcaccggctccagattatcagcaata  
aaccagccagccggaagggccgagcgcagaagtggtcctgcaactttatccgctccatccagcttataattgttccgggaagct  
agagtaagtagttcggcagtaatagtttgcgcaacgttgttgcattgctacagcagcagctcgtgctgctgttggatggctt  
attcagctccggttccaacgatcaaggcaggttacatgatccccatgttgtgcaaaaaagcgggttagctcctcgtcctccgatcgt  
gtcagaagtaagttggccgaggttatcactcatggttatggcagcactgcataattcttactgcatgccatccgtaagatgctttct  
gtgactggtgagtagtcaaccaagtcattctgagaatagtgatgcggcagcaggtgctcttggccggcgtcaatacgggataata  
ccgcccacatagcagaactttaaagtgctcatcattggaacagttctcggggcgaaaactcaaggatctaccgctgttgag  
atccagttcagatgaaccactcgtgcaccaactgatctcagcatctttactttaccagcgttctgggtgagcaaaaacaggaag  
gcaaaatgccgcaaaaagggaataagggcgacacggaaatgtgaactcactcttcttcttcaatattattgaagcattatca  
gggttattgtctcatgagcggatacatttgaatgtatttagaaaaataaacaataggggttccgcgacatttccccgaaaagtcc  
acctaaattgaagcgttaataattttgttaaattcgcgttaaattttgttaaatacagctcatttttaaccaataggccgaaatcggcaaaa  
tccctataaatcaaaaagaatagaccgagatagggttgaggttgcagtttgaacaagagttccactataaagaacgtggactcc  
aacgtcaaaagggcgaaaaaccgtctatcagggcagtgcccactacgtgaacctaccctaatacagtttttggggtcaggtgc  
cgtaaagcactaaatcggaacctaaagggagccccgatttagagcttgacggggaaagccggcgaacgtggcgagaaagg  
aaggaagaaagcgaagggagcggcgctaggcgctggcaagtgtagcgtcacgctgcgctgaaccaccacccccgg  
cgctaatgcggcgtacagggcgcgtcccattcgccattcaggtcgcgcaactgttgggaagggcgatcgggtcgggctctcgt  
attacgccagctggcgaaagggggatgtgctgcaaggcattaagttgggtaacgccaggggttccagtcacgacgttgaaaa  
gacggccagtgagcgcgtaatacagactcactatagggcgaattggagct



# Vokes Lab Biological Samples Database

Plasmid ID **1712**

Generated By **Jann Uy**

Date Entered **7/28/2017 10:49:48 AM**

Plasmid Name **Rosa26PAS-V5-prmt5-MEP50**

Species

**Mouse**

**Description**

V5-tagged full length mouse prmt5 adjacent to an IRES and full length mouse MEP50. BGH polyadenylation signal attached to MEP50. Cloned into ROSA targeting vector between homology arms.

Note: Construct is unstable and has a propensity to reduce down from 18kb to 5kb.

Amp-25 must be used for all liquid cultures. If using alpha-comp cells, incubate liquid cultures for at least 15 hours. If using a stable cell line, grow at 30°C. Plates must incubate for 24 hours; liquid cultures at least 30 hours.

Original Vector

**p1335**

Size of Vector (bp)

**9897**

Size of Insert (bp)

**8127**

Concentration (ng/ul)

Glycerol Stock #

**G296**

In Situ Probe Enzyme

Notebook Reference

**#74, p101-105**

.GB Sequence File

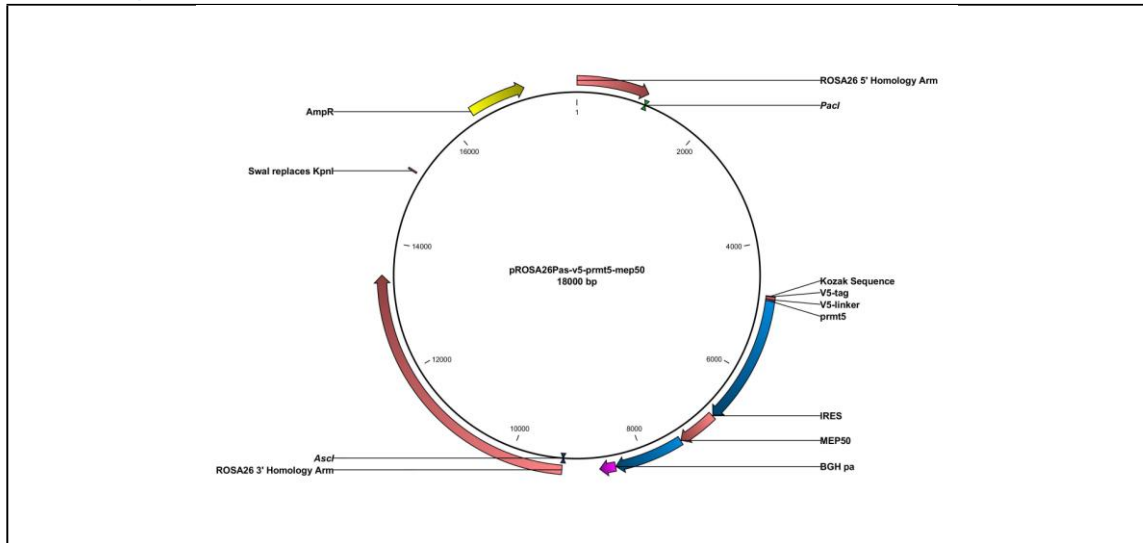


**p1712.gbk**

**Construction Method**

Gel extracted V5-prmt5-MEP50 from p1711 and cloned into gel extracted ROSA targeting vector (p1335, Rosa26Pas) from p1711 using *AscI* and *PacI*.

**Construct Map**



\* REQUIRED FIELD

Save Record

Print Current Record

New Record

## 8 Appendix C- Quantification of myc-Prmt5 OE.

**LI-COR**

Image ID: 0001068\_01  
Acquire Time: Aug 11, 2023 1:44:41 PM

Page 1

### Acquisition Information

#	Image ID	Acquire Time	Channels	Resolution	Intensities	Image Name	Comment	Image Modifications
1	0001068_01	Aug 11, 2023 1:44:41 PM	700 800	125um		0001068_01		

### Image Display Values

Channel	Color	Minimum	Maximum	K
800	Green	0.0000458	0.00286	1



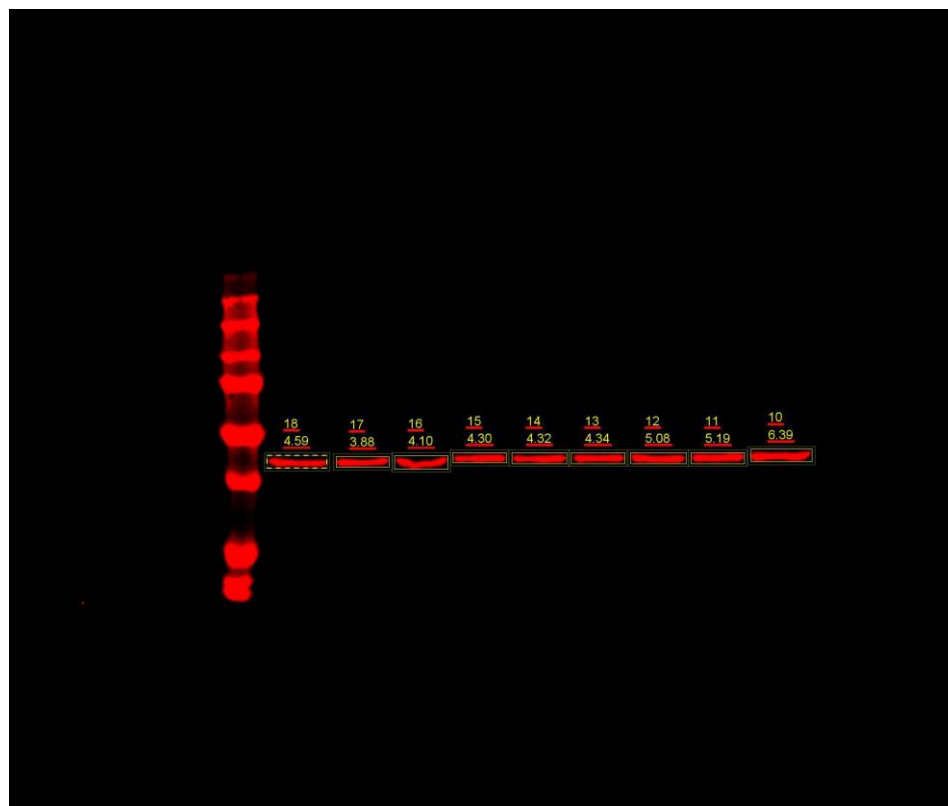
Fig1-  $\alpha$ PRMT5 antibody in Hek293T cells

## Acquisition Information

#	Image ID	Acquire Time	Channels	Resolution	Intensities	Image Name	Comment	Image Modifications
1	0001068_01	Aug 11, 2023 1:44:41 PM	700 800	125um		0001068_01		

## Image Display Values

Channel	Color	Minimum	Maximum	K
700	Red	0.00475	0.0130	1

Fig 2-  $\alpha$ -  $\beta$ -actin antibody in Hek293T cells

Acquisition Information

#	Image ID	Acquire Time	Channels	Resolution	Intensities	Image Name	Comment	Image Modifications
1	0001064_01	Aug 11, 2023 12:54:33 PM	700 800	125um		0001064_01		

Image Display Values

Channel	Color	Minimum	Maximum	K
800	Green	0.0000619	0.000591	1

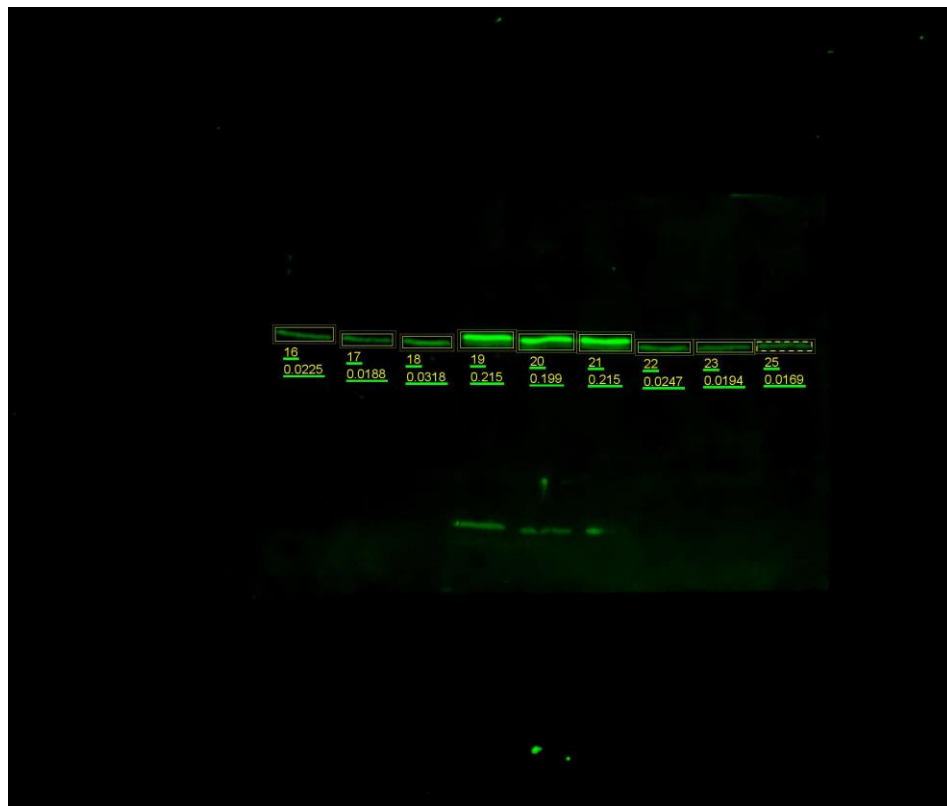


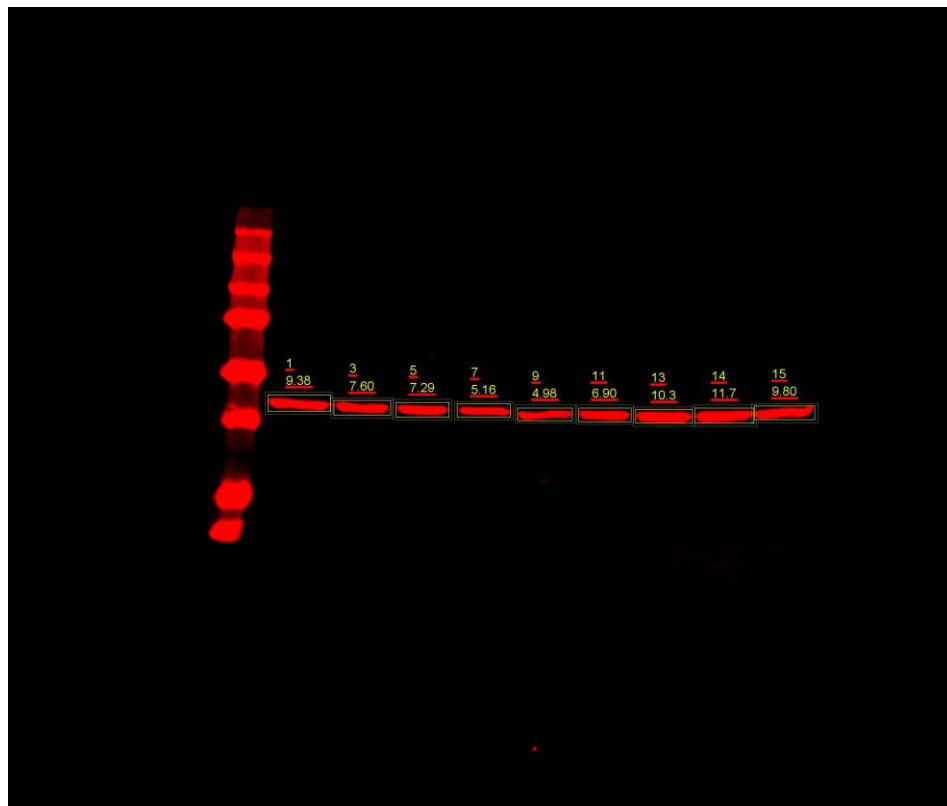
Fig 3-  $\alpha$ -PRMT5 antibody in HepG2 cells

## Acquisition Information

#	Image ID	Acquire Time	Channels	Resolution	Intensities	Image Name	Comment	Image Modifications
1	0001064_01	Aug 11, 2023 12:54:33 PM	700 800	125um		0001064_01		

## Image Display Values

Channel	Color	Minimum	Maximum	K
700	Red	0.00478	0.0102	1

Fig 4-  $\alpha$ -  $\beta$ -actin antibody in HepG2 cells.

## 9 Appendix D- Albumin-Cre documentation

Original documentation for Alb-Cre mice received from the David Johnson lab:



610 Main Street Bar Harbor, ME 04609 US  
Tel: 1-800-422-6423 or 1-207-288-5845  
Fax: 1-207-288-6150  
Email:

To: Ms. Lisa Cooper  
Email: lcooper@mdanderson.org

Page 1 of 1

### NOTIFICATION OF ORDER RECEIPT

Sales order: 3602677	PO: 3000450367	
Standing Sales Order:	Ref. No:	Investigator: Dr. David Johnson
Order date: 01Dec14		Ship via: AUS-AP

**Bill To:**  
UT - MD Anderson Cancer Center  
Accounts Payable - Box 1699  
PO Box 301401  
Houston, TX 77230

**Ship To:**  
UT - MD Anderson Cancer Center  
Dr David Johnson  
Science Park  
1808 Park Rd 1C  
Smithville, TX 78957

**End User:**

Order placed on: 01Dec14 by Dorsey Britt

Ship	Arrive	Qty	Description	Price	Adj.	Ext. Price
		2	CryoRecov, Stock 016833, Sex F,FVB(Cg)-Tg(Alb1-cre)1Dlr/J, Genotype: , JAXEAST:G200 ,Est. Boxes: 1 Notes: 13-16 weeks typical, but could be up to 25 if a second recovery is needed			0.00
		1	RPS0041,Cryo Recovery	2,140.00		2,140.00
		2	CryoRecov, Stock 016833, Sex M,FVB(Cg)-Tg(Alb1-cre)1Dlr/J, Genotype: , JAXEAST:G200 ,Est. Boxes: 1 Notes: 13-16 weeks typical, but could be up to 25 if a second recovery is needed			0.00

<b>Please Note:</b> Number of containers and freight charges are estimates based on average packing allowances. The actual number of boxes required to ship your order will vary depending on original cage density and a number of other factors. For an exact quote, please contact our Customer Service Department on the day of shipping.	TOTAL LINE ITEMS	2,140.00
	TOTAL MISC CHARGES	0.00
	TOTAL TAX	0.00
	<b>TOTAL EXCLUDING SHIPPING</b>	<b>2,140.00</b>
	<i>Est. Box Charges (subject to change)</i>	26.00
	<i>Est. Freight (subject to change)</i>	110.00

#### IMPORTANT NOTES ABOUT YOUR ORDER

1. **Please review this notification carefully!!** Your order will ship as described above unless you notify us of any changes prior to the scheduled ship dates.
2. The Jackson Laboratory's policies on cancellations, changes to orders, and credits apply to this order (see: <http://jaxmice.jax.org/support/orderchanges/index.html>).
3. If your organization has animal health restrictions, please review the animal health report of the shipping room (e.g., RB04, AX5, etc.) for your order on-line at: [www.jax.org/jaxmice/health](http://www.jax.org/jaxmice/health).
4. The Jackson Laboratory's current General Terms and Conditions apply to this order (see: <http://jaxmice.jax.org/cou/index.html>).

JAX is a registered Trademark of The Jackson Laboratory. All rights reserved.

## 10 Appendix E- BioRender license



49 Spadina Ave. Suite 200  
Toronto ON M5V 2J1 Canada  
www.biorender.com

### Confirmation of Publication and Licensing Rights

September 3rd, 2023  
Science Suite Inc.

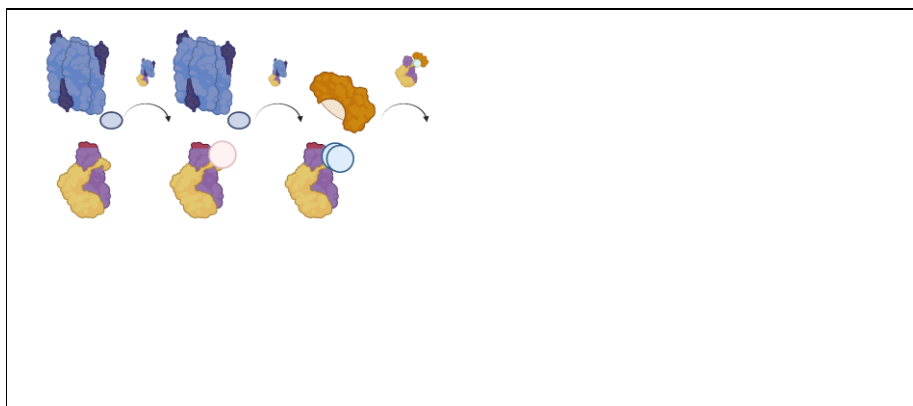
<b>Subscription:</b>	<i>Institution</i>
<b>Agreement number:</b>	<i>NX25T4KDGC</i>
<b>Journal name:</b>	<i>Thesis</i>

To whom this may concern,

This document is to confirm that Tanner Wright has been granted a license to use the BioRender content, including icons, templates and other original artwork, appearing in the attached completed graphic pursuant to BioRender's [Academic License Terms](#). This license permits BioRender content to be sublicensed for use in journal publications.

All rights and ownership of BioRender content are reserved by BioRender. All completed graphics must be accompanied by the following citation: "Created with BioRender.com".

BioRender content included in the completed graphic is not licensed for any commercial uses beyond publication in a journal. For any commercial use of this figure, users may, if allowed, recreate it in BioRender under an Industry BioRender Plan.



For any questions regarding this document, or other questions about publishing with BioRender refer to our [BioRender Publication Guide](#), or contact BioRender Support at [support@biorender.com](mailto:support@biorender.com).

## 11 Bibliography

1. Liu, K., Chen, C., Guo, Y., Lam, R., Bian, C., Xu, C., Zhao, D. Y., Jin, J., MacKenzie, F., Pawson, T., and Min, J. (2010) Structural basis for recognition of arginine methylated Piwi proteins by the extended Tudor domain. *Proceedings of the National Academy of Sciences of the United States of America*. **107**, 18398-18403  
10.1073/PNAS.1013106107
2. Han, X., Li, R., Zhang, W., Yang, X., Wheeler, C. G., Friedman, G. K., Province, P., Ding, Q., You, Z., Fathallah-Shaykh, H. M., Gillespie, G. Y., Zhao, X., King, P. H., and Nabors, L. B. (2014) Expression of PRMT5 correlates with malignant grade in gliomas and plays a pivotal role in tumor growth in vitro. *Journal of Neuro-Oncology*. **118**, 61-72  
10.1007/s11060-014-1419-0
3. Yan, F., Alinari, L., Lustberg, M. E., Martin, L. K., Cordero-Nieves, H. M., Banasavadi-Siddegowda, Y., Virk, S., Barnholtz-Sloan, J., Bell, E. H., Wojton, J., Jacob, N. K., Chakravarti, A., Nowicki, M. O., Wu, X., Lapalombella, R., Datta, J., Yu, B., Gordon, K., Haseley, A., Patton, J. T., Smith, P. L., Ryu, J., Zhang, X., Mo, X., Marcucci, G., Nuovo, G., Kwon, C. H., Byrd, J. C., Chiocca, E. A., Li, C., Sif, S., Jacob, S., Lawler, S., Kaur, B., and Baiocchi, R. A. (2014) Genetic validation of the protein arginine methyltransferase PRMT5 as a candidate therapeutic target in glioblastoma. *Cancer Research*. **74**, 1752-1765  
10.1158/0008-5472.CAN-13-0884
4. Huang, J., Gillian, V., Yu, Z., Almazan, G., and Richard, S. (2011) Type II arginine methyltransferase PRMT5 regulates gene expression of inhibitors of differentiation/DNA binding Id2 and Id4 during glial cell differentiation. *J Biol Chem*. **289**, 44424-44432  
10.1074/jbc.M111.277046
5. Bezzi, M., Teo, S. X., Muller, J., Mok, W. C., Sahu, S. K., Vardy, L. A., Bonday, Z. Q., and Guccione, E. (2013) Regulation of constitutive and alternative splicing by PRMT5 reveals



- a role for Mdm4 pre-mRNA in sensing defects in the spliceosomal machinery. *Genes and Development*. **27**, 1903-1916 10.1101/gad.219899.113
6. Nicholas, C., Yang, J., Peters, S. B., Bill, M. A., Baiocchi, R. A., Yan, F., Sif, S., Tae, S., Gaudio, E., Wu, X., Grever, M. R., Young, G. S., and Lesinski, G. B. (2013) PRMT5 Is Upregulated in Malignant and Metastatic Melanoma and Regulates Expression of MITF and p27Kip1. *PLoS ONE*. **8**, 1-9 10.1371/journal.pone.0074710
  7. AbuHammad, S., Cullinane, C., Martin, C., Bacolas, Z., Ward, T., Chen, H., Slater, A., Ardley, K., Kirby, L., Chan, K. T., Brajanovski, N., Smith, L. K., Rao, A. D., Lelliott, E. J., Kleinschmidt, M., Vergara, I. A., Papenfuss, A. T., Lau, P., Ghosh, P., Haupt, S., Haupt, Y., Sanij, E., Poortinga, G., Pearson, R. B., Falk, H., Curtis, D. J., Stuppel, P., Devlin, M., Street, I., Davies, M. A., McArthur, G. A., and Sheppard, K. E. (2019) Regulation of PRMT5-MDM4 axis is critical in the response to CDK4/6 inhibitors in melanoma. *Proc Natl Acad Sci U S A*. **116**, 17990-18000 10.1073/pnas.1901323116
  8. Liu, F., Cheng, G., Hamard, P. J., Greenblatt, S., Wang, L., Man, N., Perna, F., Xu, H., Tadi, M., Luciani, L., and Nimer, S. D. (2015) Arginine methyltransferase PRMT5 is essential for sustaining normal adult hematopoiesis. *Journal of Clinical Investigation*. **125**, 3532-3544 10.1172/JCI81749
  9. Scaglione, A., Patzig, J., Liang, J., Frawley, R., Bok, J., Mela, A., Yattah, C., Zhang, J., Teo, S. X., Zhou, T., Chen, S., Bernstein, E., Canoll, P., Guccione, E., and Casaccia, P. (2018) PRMT5-mediated regulation of developmental myelination. *Nature Communications*. **9**, 2840 10.1038/s41467-018-04863-9
  10. Chiang, K., Zielinska, A. E., Shaaban, A. M., Sanchez-Bailon, M. P., Jarrold, J., Clarke, T. L., Zhang, J., Francis, A., Jones, L. J., Smith, S., Barbash, O., Guccione, E., Farnie, G., Smalley, M. J., and Davies, C. C. (2017) PRMT5 Is a Critical Regulator of Breast Cancer Stem Cell Function via Histone Methylation and FOXP1 Expression. *Cell Rep*. **21**, 3498-3513 10.1016/j.celrep.2017.11.096

11. Ramachandran, J., Liu, Z., Gray, R. S., and Vokes, S. A. (2019) PRMT5 is necessary to form distinct cartilage identities in the knee and long bone. *Dev Biol.* **456**, 154-163  
10.1016/j.ydbio.2019.08.012
12. Norrie, J. L., Li, Q., Co, S., Huang, B.-L., Ding, D., Uy, J. C., Ji, Z., Mackem, S., Bedford, M. T., Galli, A., Ji, H., and Vokes, S. A. (2016) PRMT5 is essential for the maintenance of chondrogenic progenitor cells in the limb bud. *Development.* **143**, 4608-4619  
10.1242/dev.140715.
13. Tripsianes, K., Madl, T., Machyna, M., Fessas, D., Englbrecht, C., Utz, F., Neugebauer, K. M., and Sattler, M. (2011) Structural basis for dimethylarginine recognition by the Tudor domains of human SMN and SPF30 proteins. *Nature Structural & Molecular Biology.* **18**, 1414-1420 10.1038/nsmb.2185
14. Välineva, T., Jie, Y., Palovuori, R., and Silvennoinen, O. (2005) The transcriptional co-activator protein p100 recruits histone acetyltransferase activity to STAT6 and mediates interaction between the CREB-binding protein and STAT6. *J Biol Chem.* **280**, 14989-14996 10.1074/jbc.M410465200
15. Wang, J., Huang, X., Zheng, D., Li, Q., Mei, M., and Bao, S. (2022) PRMT5 determines the pattern of polyploidization and prevents liver from cirrhosis and carcinogenesis. *Journal of Genetics and Genomics.* 10.1016/J.JGG.2022.04.008
16. Wright, T., Wang, Y., and Bedford, M. T. (2021) The Role of the PRMT5–SND1 Axis in Hepatocellular Carcinoma. *Epigenomes.* **5**, 2-2 10.3390/epigenomes5010002
17. Antonyamy, S., Bonday, Z., Campbell, R. M., Doyle, B., Druzina, Z., Gheyi, T., Han, B., Jungheim, L. N., Qian, Y., Rauch, C., Russell, M., Sauder, J. M., Wasserman, S. R., Weichert, K., Willard, F. S., Zhang, A., and Emtage, S. (2012) Crystal structure of the human PRMT5:MEP50 complex. *Proceedings of the National Academy of Sciences of the United States of America.* **109**, 17960-17965 10.1073/pnas.1209814109
18. Tan, D. Q., Li, Y., Yang, C., Li, J., Tan, S. H., Chin, D. W. L., Nakamura-Ishizu, A., Yang, H., and Suda, T. (2019) PRMT5 Modulates Splicing for Genome Integrity and Preserves

- Proteostasis of Hematopoietic Stem Cells. *Cell Reports*. **26**, 2316-2328.e2316  
10.1016/j.celrep.2019.02.001
19. Powers, M. A., Fay, M. M., Factor, R. E., Welm, A. L., and Ullman, K. S. (2011) Protein arginine methyltransferase 5 accelerates tumor growth by arginine methylation of the tumor suppressor programmed cell death 4. *Cancer Research*. **71**, 5579-5587  
10.1158/0008-5472.CAN-11-0458
  20. Hamard, P. J., Santiago, G. E., Liu, F., Karl, D. L., Martinez, C., Man, N., Mookhtiar, A. K., Duffort, S., Greenblatt, S., Verdun, R. E., and Nimer, S. D. (2018) PRMT5 Regulates DNA Repair by Controlling the Alternative Splicing of Histone-Modifying Enzymes. *Cell Reports*. **24**, 2643-2657 10.1016/j.celrep.2018.08.002
  21. Litzler, L. C., Zahn, A., Meli, A. P., Hébert, S., Patenaude, A.-M., Methot, S. P., Sprumont, A., Bois, T., Kitamura, D., Costantino, S., King, I. L., Kleinman, C. L., Richard, S., and Di Noia, J. M. (2019) PRMT5 is essential for B cell development and germinal center dynamics. *Maulbeerstrasse*. **3775**, 4002-4002 10.1038/s41467-018-07884-6
  22. Tanaka, Y., Nagai, Y., Okumura, M., Greene, M. I., and Kambayashi, T. (2020) PRMT5 Is Required for T Cell Survival and Proliferation by Maintaining Cytokine Signaling. *Frontiers in Immunology*. **11**, 10.3389/fimmu.2020.00621
  23. Jeon, J. Y., Lee, J. S., Park, E. R., Shen, Y. N., Kim, M. Y., Shin, H. J., Joo, H. Y., Cho, E. H., Moon, S. M., Shin, U. S., Park, S. H., Han, C. J., Choi, D. W., Gu, M. B., Kim, S. B., and Lee, K. H. (2018) Protein arginine methyltransferase 5 is implicated in the aggressiveness of human hepatocellular carcinoma and controls the invasive activity of cancer cells. *Oncology Reports*. **40**, 536-544 10.3892/or.2018.6402
  24. Liu, L., Zhao, X., Zhao, L., Li, J., Yang, H., Zhu, Z., Liu, J., and Huang, G. (2016) Arginine methylation of SREBP1a via PRMT5 promotes de novo lipogenesis and tumor growth. *Cancer Research*. **76**, 1260-1272 10.1158/0008-5472.CAN-15-1766
  25. Zheng, B. N., Ding, C. H., Chen, S. J., Zhu, K., Shao, J., Feng, J., Xu, W. P., Cai, L. Y., Zhu, C. P., Duan, W., Ding, J., Zhang, X., Luo, C., and Xie, W. F. (2019) Targeting PRMT5

- activity inhibits the malignancy of hepatocellular carcinoma by promoting the transcription of HNF4 $\alpha$ . *Theranostics*. **9**, 2606-2617 10.7150/thno.32344
26. Jiang, H., Zhu, Y., Zhou, Z., Xu, J., Jin, S., Xu, K., Zhang, H., Sun, Q., Wang, J., and Xu, J. (2018) PRMT5 promotes cell proliferation by inhibiting BTG2 expression via the ERK signaling pathway in hepatocellular carcinoma. *Cancer Medicine*. **7**, 869-882 10.1002/cam4.1360
  27. Wang, Y., Li, Q., Liu, C., Han, F., Chen, M., Zhang, L., Cui, X., Qin, Y., Bao, S., and Gao, F. (2015) Protein arginine methyltransferase 5 (Prmt5) is required for germ cell survival during mouse embryonic development. *Biol Reprod*. **92**, 104 10.1095/biolreprod.114.127308
  28. Wang, Y., Zhu, T., Li, Q., Liu, C., Han, F., Chen, M., Zhang, L., Cui, X., Qin, Y., Bao, S., and Gao, F. (2015) Prmt5 is required for germ cell survival during spermatogenesis in mice OPEN. 10.1038/srep11031
  29. Duan, Z., Zhao, X., Fu, X., Su, C., Xin, L., Saarikettu, J., Yang, X., Yao, Z., Silvennoinen, O., Wei, M., and Yang, J. (2014) Tudor-SN, a novel coactivator of peroxisome proliferator-activated receptor  $\gamma$  protein, is essential for adipogenesis. *Journal of Biological Chemistry*. **289**, 8364-8374 10.1074/jbc.M113.523456
  30. Yang, N., Wang, W., Wang, Y., Wang, M., Zhao, Q., Rao, Z., Zhu, B., and Xu, R. M. (2012) Distinct mode of methylated lysine-4 of histone H3 recognition by tandem tudor-like domains of Spindlin1. *Proceedings of the National Academy of Sciences of the United States of America*. **109**, 17954-17959 10.1073/PNAS.1208517109
  31. Zhao, F., Liu, Y., Su, X., Lee, J. E., Song, Y., Wang, D., Ge, K., Gao, J., Zhang, M. Q., and Li, H. (2020) Molecular basis for histone H3 "K4me3-K9me3/2" methylation pattern readout by Spindlin1. *The Journal of biological chemistry*. **295**, 16877-16887 10.1074/JBC.RA120.013649
  32. Deng, X., Shao, G., Zhang, H. T., Li, C., Zhang, D., Cheng, L., Elzey, B. D., Pili, R., Ratliff, T. L., Huang, J., and Hu, C. D. (2017) Protein arginine methyltransferase 5 functions as

- an epigenetic activator of the androgen receptor to promote prostate cancer cell growth. *Oncogene*. **36**, 1223-1231 10.1038/onc.2016.287
33. Li, Q., Jiao, J., Li, H., Wan, H., Zheng, C., Cai, J., and Bao, S. (2018) Histone arginine methylation by Prmt5 is required for lung branching morphogenesis through repression of BMP signaling. *J Cell Sci*. **131**, 10.1242/jcs.217406
  34. Chang, X., Liu, X., Wang, H., Yang, X., and Gu, Y. (2022) Glycolysis in the progression of pancreatic cancer. *Am J Cancer Res*. **12**, 861-872,
  35. Qin, Y., Hu, Q., Xu, J., Ji, S., Dai, W., Liu, W., Xu, W., Sun, Q., Zhang, Z., Ni, Q., Zhang, B., Yu, X., and Xu, X. (2019) PRMT5 enhances tumorigenicity and glycolysis in pancreatic cancer via the FBW7/cMyc axis. *Cell Commun Signal*. **17**, 30 10.1186/s12964-019-0344-4
  36. Välineva, T., Jie, Y., and Silvennoinen, O. (2006) Characterization of RNA helicase A as component of STAT6-dependent enhanceosome. *Nucleic Acids Res*. **34**, 3938-3946 10.1093/nar/gkl539
  37. Klein, B. J., Wang, X., Cui, G., Yuan, C., Botuyan, M. V., Lin, K., Lu, Y., Wang, X., Zhao, Y., Bruns, C. J., Mer, G., Shi, X., and Kutateladze, T. G. (2016) PHF20 Readers Link Methylation of Histone H3K4 and p53 with H4K16 Acetylation. *Cell Rep*. **17**, 1158-1170 10.1016/j.celrep.2016.09.056
  38. Gu, Z., Zhang, F., Wang, Z. Q., Ma, W., Davis, R. E., and Wang, Z. (2013) The p44/wdr77-dependent cellular proliferation process during lung development is reactivated in lung cancer. *Oncogene*. **32**, 1888-1900 10.1038/onc.2012.207
  39. Zhang, T., Günther, S., Looso, M., Künne, C., Krüger, M., Kim, J., Zhou, Y., and Braun, T. (2015) Prmt5 is a regulator of muscle stem cell expansion in adult mice. *Nat Commun*. **6**, 7140 <https://doi.org/10.1038/ncomms8140>
  40. Hu, G., Wang, X., Han, Y., and Wang, P. (2018) Protein arginine methyltransferase 5 promotes bladder cancer growth through inhibiting NF-kB dependent apoptosis. *Excli J*. **2018**, 1157-1166 10.17179/excli2018-1719

41. Ma, J., He, X., Cao, Y., O'Dwyer, K., Szigety, K. M., Wu, Y., Gurung, B., Feng, Z., Katona, B. W., and Hua, X. (2020) Islet-specific Prmt5 excision leads to reduced insulin expression and glucose intolerance in mice. *J Endocrinol.* **244**, 41-52 10.1530/JOE-19-0268
42. Bao, X., Zhao, S., Liu, T., Liu, Y., Liu, Y., and Yang, X. (2013) Overexpression of PRMT5 promotes tumor cell growth and is associated with poor disease prognosis in epithelial ovarian cancer. *J Histochem Cytochem.* **61**, 206-217 10.1369/0022155413475452
43. Chung, J., Karkhanis, V. A.-O., Baiocchi, R. A., and Sif, S. A.-O. Protein arginine methyltransferase 5 (PRMT5) promotes survival of lymphoma cells via activation of WNT/ $\beta$ -catenin and AKT/GSK3 $\beta$  proliferative signaling.
44. Pal, S., Baiocchi, R. A., Byrd, J. C., Grever, M. R., Jacob, S. T., and Sif, S. (2007) Low levels of miR-92b/96 induce PRMT5 translation and H3R8/H4R3 methylation in mantle cell lymphoma. *EMBO Journal.* **26**, 3558-3569 10.1038/sj.emboj.7601794
45. Li, Y., Chitnis, N., Nakagawa, H., Kita, Y., Natsugoe, S., Yang, Y., Li, Z., Wasik, M., Klein-Szanto, A. J., Rustgi, A. K., and Diehl, J. A. (2015) PRMT5 is required for lymphomagenesis triggered by multiple oncogenic drivers. *Cancer Discovery.* **5**, 288-303 10.1158/2159-8290.CD-14-0625.
46. Aggarwal, P., Vaites, L. P., Kim, J. K., Mellert, H., Gurung, B., Nakagawa, H., Herlyn, M., Hua, X., Rustgi, A. K., McMahon, S. B., and Diehl, J. A. (2010) Nuclear cyclin D1/CDK4 kinase regulates CUL4 expression and triggers neoplastic growth via activation of the PRMT5 methyltransferase. *Cancer Cell.* **18**, 329-340 10.1016/j.ccr.2010.08.012
47. Gao, S., Wu, H., Wang, F., and Wang, Z. (2010) Altered differentiation and proliferation of prostate epithelium in mice lacking the androgen receptor cofactor p44/WDR77. *Endocrinology.* **151**, 3941-3953 10.1210/en.2009-1080
48. Jing, P., Xie, N., Zhu, X., Dang, H., and Gu, Z. (2018) The methylation induced by protein arginine methyltransferase 5 promotes tumorigenesis and progression of lung cancer. *Journal of Thoracic Disease.* **10**, 7014-7019 10.21037/jtd.2018.10.100

49. Wei, T. Y., Juan, C. C., Hisa, J. Y., Su, L. J., Lee, Y. C., Chou, H. Y., Chen, J. M., Wu, Y. C., Chiu, S. C., Hsu, C. P., Liu, K. L., and Yu, C. T. (2012) Protein arginine methyltransferase 5 is a potential oncoprotein that upregulates G1 cyclins/cyclin-dependent kinases and the phosphoinositide 3-kinase/AKT signaling cascade. *Cancer Sci.* **103**, 1640-1650 10.1111/j.1349-7006.2012.02367.x
50. Cho, E. C., Zheng, S., Munro, S., Liu, G., Carr, S. M., Moehlenbrink, J., Lu, Y. C., Stimson, L., Khan, O., Konietzny, R., McGouran, J., Coutts, A. S., Kessler, B., Kerr, D. J., and Thangue, N. B. (2012) Arginine methylation controls growth regulation by E2F-1. *EMBO J.* **31**, 1785-1797 10.1038/emboj.2012.17
51. Hartley, A. V., Wang, B., Jiang, G., Wei, H., Sun, M., Prabhu, L., Martin, M., Safa, A., Sun, S., Liu, Y., and Lu, T. (2020) Regulation of a PRMT5/NF- $\kappa$ B Axis by Phosphorylation of PRMT5 at Serine 15 in Colorectal Cancer. *International journal of molecular sciences.* **21**, 10.3390/IJMS21103684
52. Low, S. H., Shivakumar, V., Larson, C. H., Mukherjee, S., Sharma, N., Kinter, M. T., Kane, M. E., Obara, T., and Weimbs, T. (2006) Polycystin-1, STAT6, and P100 function in a pathway that transduces ciliary mechanosensation and is activated in polycystic kidney disease. *Dev Cell.* **10**, 57-69 10.1016/j.devcel.2005.12.005
53. Sikorsky, T., Fruzsina, H., Krizanova, E., Pasulka, J., Kubicek, K., and Stefl, R. (2012) Recognition of asymmetrically dimethylated arginine by TDRD3. *Nucleic Acids Res.* **40**, 11748-11755 10.1093/nar/gks929
54. Kaushik, S., Liu, F., Veazey, K. J., Gao, G., Das, P., Neves, L. F., Lin, K., Zhong, Y., Lu, Y., Giuliani, V., Bedford, M. T., Nimer, S. D., and Santos, M. A. (2018) Genetic deletion or small-molecule inhibition of the arginine methyltransferase PRMT5 exhibit anti-tumoral activity in mouse models of MLL-rearranged AML. *Leukemia.* **32**, 499-509 10.1038/leu.2017.206

55. Rho, J., S., C., Seong, Y. R., Cho, W. K., Kim, S. H., and Im, D. S. (2001) Prmt5, which forms distinct homo-oligomers, is a member of the protein-arginine methyltransferase family. *J Biol Chem.* **276**, 11393-11401 10.1074/jbc.M008660200
56. Gullà, A., Hideshima, T., Bianchi, G., Fulciniti, M., Kemal Samur, M., Qi, J., Tai, Y. T., Harada, T., Morelli, E., Amodio, N., Carrasco, R., Tagliaferri, P., Munshi, N. C., Tassone, P., and Anderson, K. C. (2018) Protein arginine methyltransferase 5 has prognostic relevance and is a druggable target in multiple myeloma. *Leukemia.* **32**, 996-1002 10.1038/leu.2017.334
57. Pauku, K., Kalkkinen, N., Silvennoinen, O., Kontula, K. K., and Lehtonen, J. Y. A. (2008) p100 increases AT1R expression through interaction with AT1R 3'-UTR. *Nucleic Acids Research.* **36**, 4474-4487 10.1093/nar/gkn411
58. Su, C., Zhang, C., Tecele, A., Fu, X., He, J., Song, J., Zhang, W., Sun, X., Ren, Y., Silvennoinen, O., Yao, Z., Yang, X., Wei, M., and Yang, J. (2015) Tudor Staphylococcal Nuclease (Tudor-SN), a Novel Regulator Facilitating G1/S Phase Transition, Acting as a Co-activator of E2F-1 in Cell Cycle Regulation. *Journal of Biological Chemistry.* **290**, 7208-7220 10.1074/JBC.M114.625046
59. Bian, C., Chao, X., Ruan, J., Lee, K. K., Burke, T. L., Tempel, W., Barsyte, D., Li, J., Wu, M., Zhou, B. O., Fleharty, B. E., Paulson, A., Allali-Hassani, A., Zhou, J.-Q., Mer, G., Grant, P. A., Workman, J. L., Zang, J., and Min, J. (2011) Sgf29 binds histone H3K4me2/3 and is required for SAGA complex recruitment and histone H3 acetylation. *EMBO J.* **30**, 2829-2842 10.1038/emboj.2011.193
60. Tong, X., Drapkin, R., Yalamanchili, R., Mosialos, G., and Kieff, E. (1995) The Epstein-Barr Virus Nuclear Protein 2 Acidic Domain Forms a Complex with a Novel Cellular Coactivator That Can Interact with TFIIE. *Molecular and Cellular Biology.* **15**, 4735-4744 10.1128/MCB.15.9.4735



61. Guo, F., Wan, L., Zheng, A., Stanevich, V., Wei, Y., Satyshur, K. A., Shen, M., Lee, W., Kang, Y., and Xing, Y. (2014) Structural insights into the tumor-promoting function of the MTDH-SND1 complex. *Cell Rep.* **8**, 1704-1713 10.1016/j.celrep.2014.08.033
62. Santhekadur, P. K., Das, S. K., Gredler, R., Chen, D., Srivastava, J., Robertson, C., Baldwin, A. S., Jr., Fisher, P. B., and Sarkar, D. (2012) Multifunction protein staphylococcal nuclease domain containing 1 (SND1) promotes tumor angiogenesis in human hepatocellular carcinoma through novel pathway that involves nuclear factor kappaB and miR-221. *J Biol Chem.* **287**, 13952-13958 10.1074/jbc.M111.321646
63. Rogne, M., B., L. H., Van Eynde, A., Beullens, M., Bollen, M., Collas, P., and Küntziger, T. (2006) The KH-Tudor domain of a-kinase anchoring protein 149 mediates RNA-dependent self-association. *Biochemistry.* **45**, 14980-14989 10.1021/bi061418y
64. Yoo, B. K., Santhekadur, P. K., Gredler, R., Chen, D., Emdad, L., Bhutia, S., Pannell, L., Fisher, P. B., and Sarkar, D. (2011) Increased RNA-induced silencing complex (RISC) activity contributes to hepatocellular carcinoma. *Hepatology.* **53**, 1538-1548 10.1002/hep.24216
65. Gao, X., Shi, X., Fu, X., Ge, L., Zhang, Y., Su, C., Yang, X., Silvennoinen, O., Yao, Z., He, J., Wei, M., and Yang, J. (2014) Human Tudor staphylococcal nuclease (Tudor-SN) protein modulates the kinetics of AGTR1-3'UTR granule formation. *FEBS letters.* **588**, 2154-2161 10.1016/j.febslet.2014.04.045
66. Gao, X., Ge, L., Shao, J., Su, C., Zhao, H., Saarikettu, J., Yao, X., Yao, Z., Silvennoinen, O., and Yang, J. (2010) Tudor-SN interacts with and co-localizes with G3BP in stress granules under stress conditions. *FEBS letters.* **584**, 3525-3532 10.1016/J.FEBSLET.2010.07.022
67. Weissbach, R., and Scadden, A. D. (2012) Tudor-SN and ADAR1 are components of cytoplasmic stress granules. *Rna.* **18**, 462-471 10.1261/rna.027656.111
68. Yang, J., Välineva, T., Hong, J., Bu, T., Yao, Z., Jensen, O. N., Frilander, M. J., and Silvennoinen, O. (2007) Transcriptional co-activator protein p100 interacts with snRNP

- proteins and facilitates the assembly of the spliceosome. *Nucleic Acids Research*. **35**, 4485-4494 10.1093/nar/gkm470
69. Yang, Y., Hadjikyriacou, A., Xia, Z., Gayatri, S., Kim, D., Zurita-Lopez, C., Kelly, R., Guo, A., Li, W., Clarke, S. G., and Bedford, M. T. (2015) PRMT9 is a Type II methyltransferase that methylates the splicing factor SAP145. *Nature Communications*. **6**, 10.1038/ncomms7428
70. Nady, N., Lemak, A., Walker, J. R., Avvakumov, G. V., Kareta, M. S., Achour, M., Xue, S., Duan, S., Allali-Hassani, A., Zuo, X., Wang, Y.-X., Bronner, C., Chédin, F., Arrowsmith, C. H., and Dhe-Paganon, S. (2011) Recognition of multivalent histone states associated with heterochromatin by UHRF1 protein. *J Biol Chem*. **286**, 24300-24311 10.1074/jbc.M111.234104
71. Gao, X., Zhao, X., Zhu, Y., He, J., Shao, J., Su, C., Zhang, Y., Zhang, W., Saarikettu, J., Silvennoinen, O., Yao, Z., and Yang, J. (2012) Tudor staphylococcal nuclease (Tudor-SN) participates in small ribonucleoprotein (snRNP) assembly via interacting with symmetrically dimethylated Sm proteins. *J Biol Chem*. **287**, 18130-18141 10.1074/jbc.M111.311852
72. Law, J. A., Du, J., J., C., Feng, S., Krajewski, K., Palanca, A. M. S., Strahl, B. D., Patel, D. J., and Jacobsen, S. E. (2013) Polymerase IV occupancy at RNA-directed DNA methylation sites requires SHH1. *Nature*. **498**, 385-389 10.1038/nature12178
73. Cappellari, M., Bielli, P., Paronetto, M. P., Ciccocanti, F., Fimia, G. M., Saarikettu, J., Silvennoinen, O., and Sette, C. (2014) The transcriptional co-activator SND1 is a novel regulator of alternative splicing in prostate cancer cells. *Oncogene*. **33**, 3794-3802 10.1038/onc.2013.360
74. Wang, Y., Wang, X., Cui, X., Zhuo, Y., Li, H., Ha, C., Xin, L., Ren, Y., Zhang, W., Sun, X., Ge, L., Liu, X., He, J., Zhang, T., Zhang, K., Yao, Z., Yang, X., and Yang, J. (2020) Oncoprotein SND1 hijacks nascent MHC-I heavy chain to ER-associated degradation, leading to impaired CD8(+) T cell response in tumor. *Sci Adv*. **6**, 10.1126/sciadv.aba5412

75. Levenson, J. D., Koskinen, P. J., Orrico, F. C., Rainio, E. M., Jalkanen, K. J., Dash, A. B., Eisenman, R. N., and Ness, S. A. (1998) Pim-1 kinase and p100 cooperate to enhance c-Myb activity. *Molecular cell*. **2**, 417-425 10.1016/S1097-2765(00)80141-0
76. Musselman, C. A., Nikita, A., Watanabe, R., Abraham, C. G., Lalonde, M.-E., Hong, Z., Allen, C., Roy, S., Nuñez, J. K., Nickoloff, J., Kulesza, C. A., Yasui, A., Côté, J., and Kutateladze, T. G. (2012) Molecular basis for H3K36me3 recognition by the Tudor domain of PHF1. *Nat Struct Mol Bio*. **19**, 1266-1272 10.1038/nsmb.2435
77. Tee, W. W., Pardo, M., Theunissen, T. W., Yu, L., Choudhary, J. S., Hajkova, P., and Surani, M. A. (2010) Prmt5 is essential for early mouse development and acts in the cytoplasm to maintain ES cell pluripotency. *Genes and Development*. **24**, 2772-2777 10.1101/gad.606110
78. Wang, W. L., Anderson, L. C., Nicklay, J. J., Chen, H., Gamble, M. J., Shabanowitz, J., Hunt, D. F., and Shechter, D. (2014) Phosphorylation and arginine methylation mark histone H2A prior to deposition during *Xenopus laevis* development. *Epigenetics & Chromatin*. **7**, 22-22 10.1186/1756-8935-7-22
79. Murn, J., and Shi, Y. (2017) The winding path of protein methylation research: milestones and new frontiers. *Nat Rev Mol Cell Biol*. **18**, 517-527 10.1038/nrm.2017.35
80. Sims, R. J., 3rd, Rojas, L. A., Beck, D. B., Bonasio, R., Schüller, R., Drury, W. J., 3rd, Eick, D., and Reinberg, D. (2011) The C-terminal domain of RNA polymerase II is modified by site-specific methylation. *Science*. **332**, 99-103 10.1126/science.1202663
81. Brahms, H., Raymackers, J., Union, A., de Keyser, F., Meheus, L., and Lührmann, R. (2000) The C-terminal RG dipeptide repeats of the spliceosomal Sm proteins D1 and D3 contain symmetrical dimethylarginines, which form a major B-cell epitope for anti-Sm autoantibodies. *J Biol Chem*. **275**, 17122-17129 10.1074/jbc.M000300200
82. Boisvert, F. M., Rhie, A., Richard, S., and Doherty, A. J. (2005) The GAR motif of 53BP1 is arginine methylated by PRMT1 and is necessary for 53BP1 DNA binding activity. *Cell Cycle*. **4**, 1834-1841 10.4161/cc.4.12.2250

83. Xu, J., and Richard, S. (2021) Cellular pathways influenced by protein arginine methylation: Implications for cancer. *Mol Cell.* **81**, 4357-4368  
10.1016/j.molcel.2021.09.011
84. Bedford, M. T., and Clarke, S. G. (2009) Protein Arginine Methylation in Mammals: Who, What, and Why. *Molecular Cell.* **33**, 1-13 10.1016/j.molcel.2008.12.013
85. Blanc, R. S., and Richard, S. (2017) Arginine Methylation: The Coming of Age. *Molecular Cell.* **65**, 8-24 10.1016/j.molcel.2016.11.003
86. Yang, Y., Hadjikyriacou, A., Xia, Z., Gayatri, S., Kim, D., Zurita-Lopez, C., Kelly, R., Guo, A., Li, W., Clarke, S. G., and Bedford, M. T. (2015) PRMT9 is a type II methyltransferase that methylates the splicing factor SAP145. *Nat Commun.* **6**, 10.1038/ncomms7428
87. Mellacheruvu, D., Wright, Z., Couzens, A. L., Lambert, J. P., St-Denis, N. A., Li, T., Miteva, Y. V., Hauri, S., Sardi, M. E., Low, T. Y., Halim, V. A., Bagshaw, R. D., Hubner, N. C., Al-Hakim, A., Bouchard, A., Faubert, D., Fermin, D., Dunham, W. H., Goudreault, M., Lin, Z. Y., Badillo, B. G., Pawson, T., Durocher, D., Coulombe, B., Aebersold, R., Superti-Furga, G., Colinge, J., Heck, A. J. R., Choi, H., Gstaiger, M., Mohammed, S., Cristea, I. M., Bennett, K. L., Washburn, M. P., Raught, B., Ewing, R. M., Gingras, A. C., and Nesvizhskii, A. I. (2013) The CRAPome: A contaminant repository for affinity purification-mass spectrometry data. *Nature Methods.* **10**, 730-736 10.1038/nmeth.2557
88. Gao, G., Dhar, S., and Bedford, M. T. (2017) PRMT5 regulates IRES-dependent translation via methylation of hnRNP A1. *Nucleic Acids Research.* **45**, 4359-4369  
10.1093/nar/gkw1367
89. Friesen, W. J., Wyce, A., Paushkin, S., Abel, L., Rappsilber, J., Mann, M., and Dreyfuss, G. (2002) A novel WD repeat protein component of the methylosome binds Sm proteins. *Journal of Biological Chemistry.* **277**, 8243-8247 10.1074/jbc.M109984200
90. Yang, Y., and Bedford, M. T. (2013) Protein arginine methyltransferases and cancer. *Nat Rev Cancer.* **13**, 37-50 10.1038/nrc3409

91. Wang, M., Xu, R. M., and Thompson, P. R. (2013) Substrate specificity, processivity, and kinetic mechanism of protein arginine methyltransferase 5. *Biochemistry*. **52**, 5430-5440  
10.1021/bi4005123
92. Mulvaney, K. M., Blomquist, C., Acharya, N., Li, R., Ranaghan, M. J., O'Keefe, M., Rodriguez, D. J., Young, M. J., Kesar, D., Pal, D., Stokes, M., Nelson, A. J., Jain, S. S., Yang, A., Mullin-Bernstein, Z., Columbus, J., Bozal, F. K., Skepner, A., Raymond, D., LaRussa, S., McKinney, D. C., Freyzon, Y., Baidi, Y., Porter, D., Aguirre, A. J., Ianari, A., McMillan, B., and Sellers, W. R. (2021) Molecular basis for substrate recruitment to the PRMT5 methylosome. *Molecular Cell*. **81**, 3481-3495.e3487  
10.1016/J.MOLCEL.2021.07.019
93. Hartley, A. V., and Lu, T. (2020) Modulating the modulators: regulation of protein arginine methyltransferases by post-translational modifications. *Drug discovery today*. **25**, 1735-1735  
10.1016/J.DRUDIS.2020.06.031
94. Botuyan, M. V., and Mer, G. (2016) Tudor Domains as Methyl-Lysine and Methyl-Arginine Readers. *Chromatin Signaling and Diseases*. 149-165  
10.1016/B978-0-12-802389-1.00008-3
95. Lu, R., and Wang, G. G. (2013) Tudor: A versatile family of histone methylation 'readers'. *Trends in Biochemical Sciences*. **38**, 546-555  
10.1016/J.TIBS.2013.08.002
96. Su, X., Zhu, G., Ding, X., Lee, S. Y., Dou, Y., Zhu, B., Wu, W., and Li, H. (2014) Molecular basis underlying histone H3 lysine-arginine methylation pattern readout by Spin/Ssty repeats of Spindlin1. *Genes & development*. **28**, 622-636  
10.1101/GAD.233239.113
97. Wang, W., Chen, Z., Mao, Z., Zhang, H., Ding, X., Chen, S., Zhang, X., Xu, R., and Zhu, B. (2011) Nucleolar protein Spindlin1 recognizes H3K4 methylation and stimulates the expression of rRNA genes. *EMBO reports*. **12**, 1160-1166  
10.1038/EMBOR.2011.184
98. Wright, T., Wang, Y., and Bedford, M. T. (2021) The Role of the PRMT5–SND1 Axis in Hepatocellular Carcinoma. *Epigenomes*. **5**, 2  
10.3390/epigenomes5010002

99. Broadhurst, M. K., and Wheeler, T. T. (2001) The p100 coactivator is present in the nuclei of mammary epithelial cells and its abundance is increased in response to prolactin in culture and in mammary tissue during lactation. *The Journal of endocrinology*. **171**, 329-337 10.1677/JOE.0.1710329
100. Fu, X., Zhang, C., Meng, H., Zhang, K., Shi, L., Cao, C., Wang, Y., Su, C., Xin, L., Ren, Y., Zhang, W., Sun, X., Ge, L., Silvennoinen, O., Yao, Z., Yang, X., and Yang, J. (2018) Oncoprotein Tudor-SN is a key determinant providing survival advantage under DNA damaging stress. *Cell Death & Differentiation*. **25**, 1625-1637 10.1038/s41418-018-0068-9
101. Saarikettu, J., Lehmusvaara, S., Pesu, M., Junttila, I., Partanen, J., Sipilä, P., Poutanen, M., Yang, J., Haikarainen, T., and Silvennoinen, O. (2023) The RNA-binding protein Snd1/Tudor-SN regulates hypoxia-responsive gene expression. *FASEB BioAdvances*. **5**, 183-198 10.1096/FBA.2022-00115
102. Su, C., Gao, X., Yang, W., Zhao, Y., Fu, X., Cui, X., Zhang, C., Xin, L., Ren, Y., Li, L., Shui, W., Yang, X., Wei, M., and Yang, J. (2017) Phosphorylation of Tudor-SN, a novel substrate of JNK, is involved in the efficient recruitment of Tudor-SN into stress granules. *Biochim Biophys Acta Mol Cell Res*. **1864**, 562-571 10.1016/j.bbamcr.2016.12.018
103. Pauku, K., Yang, J., and Silvennoinen, O. (2003) Tudor and nuclease-like domains containing protein p100 function as coactivators for signal transducer and activator of transcription 5. *Molecular Endocrinology*. **17**, 1805-1814 10.1210/me.2002-0256
104. Keenan, T. W., Winter, S., Rackwitz, H. R., and Heid, H. W. (2000) Nuclear coactivator protein p100 is present in endoplasmic reticulum and lipid droplets of milk secreting cells. *Biochimica et Biophysica Acta (BBA) - General Subjects*. **1523**, 84-90 10.1016/S0304-4165(00)00106-9
105. Caudy, A. A., Ketting, R. F., Hammond, S. M., Denli, A. M., Bathoorn, A. M. P., Tops, B. B. J., Silva, J. M., Myers, M. M., Hannon, G. J., and Plasterk, R. H. A. (2003) A

- micrococcal nuclease homologue in RNAi effector complexes. *Nature*. **425**, 411-414  
10.1038/NATURE01956
106. Scadden, A. D. J. (2005) The RISC subunit Tudor-SN binds to hyper-edited double-stranded RNA and promotes its cleavage. *Nature Structural & Molecular Biology* 2005 **12:6**, 489-496 10.1038/nsmb936
107. Yang, W., Chendrimada, T. P., Wang, Q., Higuchi, M., Seeburg, P. H., Shiekhattar, R., and Nishikura, K. (2006) Modulation of microRNA processing and expression through RNA editing by ADAR deaminases. *Nature structural & molecular biology*. **13**, 13-21  
10.1038/NSMB1041
108. Friberg, A., Corsini, L., Mourao, A., and Sattler, M. (2009) Structure and ligand binding of the extended Tudor domain of *D. melanogaster* Tudor-SN. *J Mol Biol*. **387**, 921-934  
10.1016/j.jmb.2009.02.018
109. Zheng, S., Moehlenbrink, J., Lu, Y. C., Zalmas, L. P., Sagum, C. A., Carr, S., McGouran, J. F., Alexander, L., Fedorov, O., Munro, S., Kessler, B., Bedford, M. T., Yu, Q., and La Thangue, N. B. (2013) Arginine methylation-dependent reader-writer interplay governs growth control by E2F-1. *Molecular Cell*. **52**, 37-51 10.1016/j.molcel.2013.08.039
110. Roworth, A. P., Carr, S. M., Liu, G., Barczak, W., Miller, R. L., Munro, S., Kanapin, A., Samsonova, A., and La Thangue, N. B. (2019) Arginine methylation expands the regulatory mechanisms and extends the genomic landscape under E2F control. *Science Advances*. **5**, 1-14 10.1126/sciadv.aaw4640
111. Kim, M., Ki, B. S., Hong, K., Park, S. P., Ko, J. J., and Choi, Y. (2016) Tudor Domain Containing Protein TDRD12 Expresses at the Acrosome of Spermatids in Mouse Testis. *Asian-Australas J Anim Sci*. **29**, 944-951 10.5713/ajas.15.0436
112. Cui, X., Zhang, X., Liu, M., Zhao, C., Zhang, N., Ren, Y., Su, C., Zhang, W., Sun, X., He, J., Gao, X., and Yang, J. (2020) A pan-cancer analysis of the oncogenic role of staphylococcal nuclease domain-containing protein 1 (SND1) in human tumors. *Genomics*. **112**, 3958-3967 10.1016/J.YGENO.2020.06.044

113. Wang, X., Zhang, C., Wang, S., Rashu, R., Thomas, R., Yang, J., and Yang, X. (2021) SND1 promotes Th1/17 immunity against chlamydial lung infection through enhancing dendritic cell function. *PLoS pathogens*. **17**, e1009295-e1009295 10.1371/JOURNAL.PPAT.1009295
114. Dong, F., Li, Q., Yang, C., Huo, D., Wang, X., Ai, C., Kong, Y., Sun, X., Wang, W., Zhou, Y., Liu, X., Li, W., Gao, W., Liu, W., Kang, C., and Wu, X. (2018) PRMT2 links histone H3R8 asymmetric dimethylation to oncogenic activation and tumorigenesis of glioblastoma. *Nat Commun*. **9**, 4552 10.1038/s41467-018-06968-7.
115. Gao, G., Hausmann, S., Flores, N. M., Benitez, A. M., Shen, J., Yang, X., Person, M. B., Gayatri, S., Cheng, D., Lu, Y., Liu, B., Mazur, P. K., and Bedford, M. T. (2023) The NFIB/CARM1 partnership is a driver in preclinical models of small cell lung cancer. *Nat Commun*. **14**, 363 10.1038/s41467-023-35864-y
116. Karakashev, S., Fukumoto, T., Zhao, B., Lin, J., Wu, S., Fatkhutdinov, N., Park, P. H., Semenova, G., Jean, S., Cadungog, M. G., Borowsky, M. E., Kossenkov, A. V., Liu, Q., and Zhang, R. (2020) EZH2 Inhibition Sensitizes CARM1-High, Homologous Recombination Proficient Ovarian Cancers to PARP Inhibition. *Cancer Cell*. **37**, 157-167 10.1016/j.ccell.2019.12.015.
117. Jarrold, J., and Davies, C. C. (2019) PRMTs and Arginine Methylation: Cancer's Best-Kept Secret? *Trends in Molecular Medicine*. **25**, 993-1009 10.1016/j.molmed.2019.05.007
118. Metz, P. J., Ching, K. A., Xie, T., Delgado Cuenca, P., Niessen, S., Tatlock, J. H., Jensen-Pergakes, K., and Murray, B. W. (2020) Symmetric Arginine Dimethylation Is Selectively Required for mRNA Splicing and the Initiation of Type I and Type III Interferon Signaling. *Cell Rep*. **30**, 1935-1950 10.1016/j.celrep.2020.01.054
119. Feustel, K., and Falchook, G. S. (2022) Protein Arginine Methyltransferase 5 (PRMT5) Inhibitors in Oncology Clinical Trials: A review. *J Immunother Precis Oncol*. **5**, 58-67 10.36401/jipo-22-1



120. Shen, Y., Gao, G., Yu, X., Kim, H., Wang, L., Xie, L., Schwarz, M., Chen, X., Guccione, E., Liu, J., Bedford, M. T., and Jin, J. (2020) Discovery of First-in-Class Protein Arginine Methyltransferase 5 (PRMT5) Degraders. *Journal of Medicinal Chemistry*. **63**, 9977-9989 10.1021/acs.jmedchem.0c01111
121. Palte, R. L., Schneider, S. E., Altman, M. D., Hayes, R. P., Kawamura, S., Lacey, B. M., Mansueto, S., Reutershan, M., Siliphaivanh, P., Sondey, C., Xu, H., Xu, Z., Ye, Y., and Machacek, M. R. (2020) Allosteric Modulation of Protein Arginine Methyltransferase 5 (PRMT5). *ACS Med Chem Lett*. **11**, 1688-1693 10.1021/acsmedchemlett.9b00525
122. Smith, C. R., Aranda, R., Bobinski, T. P., Briere, D. M., Burns, A. C., Christensen, J. G., Clarine, J., Engstrom, L. D., Gunn, R. J., Ivetac, A., Jean-Baptiste, R., Ketcham, J. M., Kobayashi, M., Kuehler, J., Kulyk, S., Lawson, J. D., Moya, K., Olson, P., Rahbaek, L., Thomas, N. C., Wang, X., Waters, L. M., and Marx, M. A. (2022) Fragment-Based Discovery of MRTX1719, a Synthetic Lethal Inhibitor of the PRMT5•MTA Complex for the Treatment of MTAP-Deleted Cancers. *Cite This: J Med Chem*. **2022**, 1749-1766 10.1021/acs.jmedchem.1c01900
123. Kalev, P., Hyer, M. L., Gross, S., Konteatis, Z., Chen, C. C., Fletcher, M., Lein, M., Aguado-Fraile, E., Frank, V., Barnett, A., Mandley, E., Goldford, J., Chen, Y., Sellers, K., Hayes, S., Lizotte, K., Quang, P., Tuncay, Y., Clasquin, M., Peters, R., Weier, J., Simone, E., Murtie, J., Liu, W., Nagaraja, R., Dang, L., Sui, Z., Biller, S. A., Travins, J., Marks, K. M., and Marjon, K. (2021) MAT2A Inhibition Blocks the Growth of MTAP-Deleted Cancer Cells by Reducing PRMT5-Dependent mRNA Splicing and Inducing DNA Damage. *Cancer Cell*. **39**, 209-224 10.1016/j.ccell.2020.12.010.
124. Blanco, M. A., Masa, A., Hua, Y., Li, T., Wei, Y., Xu, Z., Cristea, I. M., and Kang, Y. (2011) Identification of staphylococcal nuclease domain-containing 1 (SND1) as a Metadherin-interacting protein with metastasis-promoting functions. *J Biol Chem*. **286**, 19982-19992 10.1074/jbc.M111.240077

125. Yu, L., Liu, X., Cui, K., Di, Y., Xin, L., Sun, X., Zhang, W., Yang, X., Wei, M., Yao, Z., and Yang, J. (2015) SND1 Acts Downstream of TGFbeta1 and Upstream of Smurf1 to Promote Breast Cancer Metastasis. *Cancer Res.* **75**, 1275-1286 10.1158/0008-5472.CAN-14-2387
126. Emdad, L., K., D. S., Dasgupta, S., Hu, B., Sarkar, D., and Fisher, P. B. (2013) AEG-1/MTDH/LYRIC: signaling pathways, downstream genes, interacting proteins, and regulation of tumor angiogenesis. *Adv Cancer Res.* **120**, 75-111 10.1016/B978-0-12-401676-7.00003-6
127. Tsuchiya, N., Masako, O., Nakashima, K., Ubagai, T., Sugimura, T., and Nakagama, H. (2007) SND1, a component of RNA-induced silencing complex, is up-regulated in human colon cancers and implicated in early stage colon carcinogenesis. *Cancer Res.* **67**, 9568-9576 10.1158/0008-5472.CAN-06-2707
128. Bard-Chapeau, E. A., Nguyen, A. T., Rust, A. G., Sayadi, A., Lee, P., Chua, B. Q., New, L. S., De Jong, J., Ward, J. M., Chin, C. K. Y., Chew, V., Toh, H. C., Abastado, J. P., Benoukraf, T., Soong, R., Bard, F. A., Dupuy, A. J., Johnson, R. L., Radda, G. K., Chan, E. C. Y., Wessels, L. F. A., Adams, D. J., Jenkins, N. A., and Copeland, N. G. (2014) Transposon mutagenesis identifies genes driving hepatocellular carcinoma in a chronic hepatitis B mouse model. *Nature Genetics.* **46**, 24-32 10.1038/ng.2847
129. Jariwala, N., Rajasekaran, D., Mendoza, R. G., Shen, X. N., Siddiq, A., Akiel, M. A., Robertson, C. L., Subler, M. A., Windle, J. J., Fisher, P. B., Sanyal, A. J., and Sarkar, D. (2017) Oncogenic role of SND1 in development and progression of hepatocellular carcinoma. *Cancer Research.* **77**, 3306-3316 10.1158/0008-5472.CAN-17-0298
130. Kodama, T., Yi, J., Newberg, J. Y., Tien, J. C., Wu, H., Finegold, M. J., Kodama, M., Wei, Z., Tamura, T., Takehara, T., Johnson, R. L., Jenkins, N. A., and Copeland, N. G. (2018) Molecular profiling of nonalcoholic fatty liver disease-associated hepatocellular carcinoma using SB transposon mutagenesis. *Proceedings of the National Academy of Sciences of the United States of America.* **115**, E10417-E10426 10.1073/pnas.1808968115

131. Gao, X., Xin, L., Yao, Z., Silvennoinen, O., and Yang, J. (2023) Friend or Foe? The fascinating Tudor-SN protein. *Visualized Cancer Medicine*. **4**, 5-5 10.1051/VCM/2023001
132. Rumgay, H., Arnold, M., Ferlay, J., Lesi, O., Cabasag, C. J., Vignat, J., Laversanne, M., McGlynn, K. A., and Soerjomataram, I. (2022) Global burden of primary liver cancer in 2020 and predictions to 2040. *Journal of Hepatology*. **77**, 1598-1606 10.1016/j.jhep.2022.08.021
133. Weledji, E. P., Enow Orock, G., Ngowe, M. N., and Nsagha, D. S. (2014) How grim is hepatocellular carcinoma? *Annals of Medicine and Surgery*. **3**, 71-71 10.1016/J.AMSU.2014.06.006
134. Ashem, H., Erag, L. S., Ndrew, A., and Ason, C. M. (1999) RISING INCIDENCE OF HEPATOCELLULAR CARCINOMA IN THE UNITED STATES A BSTRACT Background and Methods Clinical observations have. **340**, 745-745,
135. Llovet, J. M., Kelley, R. K., Villanueva, A., Singal, A. G., Pikarsky, E., Roayaie, S., Lencioni, R., Koike, K., Zucman-Rossi, J., and Finn, R. S. (2021) Hepatocellular carcinoma. *Nature Reviews Disease Primers 2021 7:1*. **7**, 1-28 10.1038/s41572-020-00240-3
136. Kumari, R., Kumar Sahu, M., Tripathy, A., Uthansingh, K., and Behera, M. (2018) Hepatocellular carcinoma treatment: hurdles, advances and prospects. *Hepat Oncol*. **5**, 8-8 10.2217/hep-2018-0002
137. Zhong, C., Li, Y., Yang, J., Jin, S., Chen, G., Li, D., Fan, X., and Lin, H. (2021) Immunotherapy for Hepatocellular Carcinoma: Current Limits and Prospects. *Frontiers in Oncology*. **11**, 10.3389/fonc.2021.589680
138. Dupuy, A. J., Keiko, A., Largaespada, D. A., Copeland, N. G., and Jenkins, N. A. (2005) Mammalian mutagenesis using a highly mobile somatic Sleeping Beauty transposon system. *Nature*. **436**, 221-226 10.1038/nature03691.
139. Mátés, L., L., C. M. K., Belay, E., Jerchow, B., Manoj, N., Acosta-Sanchez, A., Grzela, D. P., Schmitt, A., Becker, K., Matrai, J., Ma, L., Samara-Kuko, E., Gysemans, C.,

- Pryputniewicz, D., Miskey, C., Fletcher, B., VandenDriessche, T., Ivics, Z., and Izsvák, Z. (2009) Molecular evolution of a novel hyperactive Sleeping Beauty transposase enables robust stable gene transfer in vertebrates. *Nat Genet.* **41**, 753-761 10.1038/ng.343
140. Copeland, N. G., and Jenkins, N. A. (2010) Harnessing transposons for cancer gene discovery. *Nat Rev Cancer.* **10**, 696-706 10.1038/nrc2916
141. Moriarity, B. S., and Largaespada, D. A. (2015) Sleeping Beauty transposon insertional mutagenesis based mouse models for cancer gene discovery. *Curr Opin Genet Dev.* **30**, 66-72 10.1016/j.gde.2015.04.007
142. Shimizu, D., Kanda, M., Sugimoto, H., Shibata, M., Tanaka, H., Takami, H., Iwata, N., Hayashi, M., Tanaka, C., Kobayashi, D., Yamada, S., Nakayama, G., Koike, M., Fujiwara, M., Fujii, T., and Kodera, Y. (2017) The protein arginine methyltransferase 5 promotes malignant phenotype of hepatocellular carcinoma cells and is associated with adverse patient outcomes after curative hepatectomy. *International Journal of Oncology.* **50**, 381-386 10.3892/ijo.2017.3833
143. Zhang, B., Dong, S., Li, Z., Lu, L., Zhang, S., Chen, X., Cen, X., and Wu, Y. (2015) Targeting protein arginine methyltransferase 5 inhibits human hepatocellular carcinoma growth via the downregulation of beta-catenin. *Journal of Translational Medicine.* **13**, 1-10 10.1186/s12967-015-0721-8
144. Lin, Z., Jia, H., Hong, L., Zheng, Y., Shao, W., Ren, X., Zhu, W., Lu, L., Lu, M., Zhang, J., and Chen, J. (2018) Prognostic impact of SET domain-containing protein 8 and protein arginine methyltransferase 5 in patients with hepatocellular carcinoma following curative resection. *Oncology Letters.* **16**, 3665-3673 10.3892/ol.2018.9083
145. Li, Z., Zhang, J., Liu, X., Li, S., Wang, Q., Di, C., Hu, Z., Yu, T., Ding, J., Li, J., Yao, M., Fan, J., Huang, S., Gao, Q., Zhao, Y., and He, X. (2018) The LINC01138 drives malignancies via activating arginine methyltransferase 5 in hepatocellular carcinoma. *Nat Commun.* **9**, 1572 10.1038/s41467-018-04006-0

146. Hou, Z., Peng, H., Ayyanathan, K., Yan, K.-P., Langer, E. M., Longmore, G. D., and Rauscher, F. J. (2008) The LIM Protein AJUBA Recruits Protein Arginine Methyltransferase 5 To Mediate SNAIL-Dependent Transcriptional Repression. *Molecular and Cellular Biology*. **28**, 3198-3207 10.1128/mcb.01435-07
147. Gu, J., Yao, M., Yao, D., Wang, L., Yang, X., and Yao, D. (2016) Nonalcoholic Lipid Accumulation and Hepatocyte Malignant Transformation. *Journal of Clinical and Translational Hepatology*. **4**, 123-130 10.14218/jcth.2016.00010
148. Barczak, W., Jin, L., Carr, S. M., Munro, S., Ward, S., Kanapin, A., Samsonova, A., and La Thangue, N. B. (2020) PRMT5 promotes cancer cell migration and invasion through the E2F pathway. *DCell Death Dis*. **11**, 572 10.1038/s41419-020-02771-9.
149. Pastore, F., Bhagwat, N., Pastore, A., Radziszewska, A., Karzai, A., Krishnan, A., Li, B., Bowman, R. L., Xiao, W., Viny, A. D., Zouak, A., Park, Y. C., Cordner, K. B., Braunstein, S., Maag, J., Grego, A., Mehta, J., Wang, M., Lin, H., Durham, B. H., Koche, R. P., Rampal, R., Helin, K., Scherle, P., Vaddi, K., and Levine, R. L. (2020) PRMT5 Inhibition Modulates E2F1 Methylation and Gene-Regulatory Networks Leading to Therapeutic Efficacy in JAK2(V617F)-Mutant MPN. *Cancer Discovery*. **10**, 1742-1757 10.1158/2159-8290.CD-20-0026
150. Farra, R., Grassi, G., Tonon, F., Abrami, M., Grassi, M., Pozzato, G., Fiotti, N., Forte, G., and Dapas, B. (2017) The Role of the Transcription Factor E2F1 in Hepatocellular Carcinoma. *Curr Drug Deliv*. **14**, 272-281 10.2174/1567201813666160527141742.
151. Zheng, L., Hill, J., Zheng, L., Rumi, M. A. K., and Zheng, X. L. (2022) A Simple, Robust, and Cost-effective Method for Genotyping Small-scale Mutations. *J Clin Transl Pathol*. **2**, 108-115 10.14218/JCTP.2022.00014
152. Wang, Y., Person, M. D., and Bedford, M. T. (2022) Pan-methylarginine antibody generation using PEG linked GAR motifs as antigens. *Methods*. **200**, 80-86 10.1016/j.ymeth.2021.06.005.

153. Schulien, I., and Hasselblatt, P. (2021) Diethylnitrosamine-induced liver tumorigenesis in mice. *Methods in Cell Biology*. **163**, 137-152 10.1016/BS.MCB.2020.08.006
154. Liu, F., Y, S., and Liu, D. (1999) Hydrodynamics-based transfection in animals by systemic administration of plasmid DNA. *Gene Ther.* **6**, 1258-1266 10.1038/sj.gt.3300947
155. Molina-Sánchez, P., Ruiz de Galarreta, M., Yao, M. A., Lindblad, K. E., Bresnahan, E., Bitterman, E., Martin, T. C., Rubenstein, T., Nie, K., Golas, J., Choudhary, S., Bárcena-Varela, M., Elmas, A., Miguela, V., Ding, Y., Kan, Z., Grinspan, L. T., Huang, K. L., Parsons, R. E., Shields, D. J., Rollins, R. A., and Lujambio, A. (2020) Cooperation Between Distinct Cancer Driver Genes Underlies Intertumor Heterogeneity in Hepatocellular Carcinoma. *Gastroenterology*. **159**, 2203-2220 10.1053/j.gastro.2020.08.015.
156. Lecocq, M., Andrianaivo, F., Warnier, M., Wattiaux-De Coninck, S., Wattiaux, R., and Jadot, M. (2003) Uptake by mouse liver and intracellular fate of plasmid DNA after a rapid tail vein injection of a small or a large volume. *J Gene Med.* **5**, 142-156 10.1002/jgm.328.
157. Boswell, R. E., and Mahowald, A. P. (1985) tudor, a gene required for assembly of the germ plasm in *Drosophila melanogaster*. *Cell*. **43**, 97-104 10.1016/0092-8674(85)90015-7
158. Xin, X., Mains, R. E., and Eipper, B. A. (2004) Monooxygenase X, a member of the copper-dependent monooxygenase family localized to the endoplasmic reticulum. *J Biol Chem*. **279**, 48159-48167 10.1074/jbc.M407486200.
159. Chambers, K. J., Tonkin, L. A., Chang, E., Shelton, D. N., Linskens, M. H., and Funk, W. D. (1998) Identification and cloning of a sequence homologue of dopamine beta-hydroxylase. *Gene*. **1-2**, 111-120 10.1016/s0378-1119(98)00344-8.
160. Tolba, R., Kraus, T., Liedtke, C., Schwarz, M., and Weiskirchen, R. (2015) Diethylnitrosamine (DEN)-induced carcinogenic liver injury in mice. *Laboratory animals*. **49**, 59-69 10.1177/0023677215570086

161. Swenberg, J. A., Hoel, D. G., and Magee, P. N. (1991) Mechanistic and statistical insight into the large carcinogenesis bioassays on N-nitrosodiethylamine and N-nitrosodimethylamine. *Cancer Research*. **51**, 6409-6414, <https://pubmed.ncbi.nlm.nih.gov/1933905/>
162. Liu, L. L., Li-Kun, G., Qi, X.-m., Cai, Y., Wang, H., Wu, X.-f., Xiao, Y., and Ren, J. (2005) Altered expression of cytochrome P450 and possible correlation with preneoplastic changes in early stage of rat hepatocarcinogenesis. *Acta Pharmacol Sin*. **26**, 737-744 10.1111/j.1745-7254.2005.00737.x
163. Reed, C. A., Mayhew, C. N., McClendon, A. K., and Knudsen, E. S. (2010) Unique impact of RB loss on hepatic proliferation: tumorigenic stresses uncover distinct pathways of cell cycle control. *J Biol Chem*. **285**, 1089-1096 10.1074/jbc.M109.043380
164. Garcia-Arcos, I., Y, R., González-Kother, P., Palacios, L., Ochoa, B., and Fresnedo, O. (2010) Association of SND1 protein to low density lipid droplets in liver steatosis. *J Physiol Biochem*. **66**, 73-83 10.1007/s13105-010-0011-0
165. Navarro-Imaz, H., Rueda, Y., and Fresnedo, O. (2016) SND1 overexpression deregulates cholesterol homeostasis in hepatocellular carcinoma. *Biochim Biosphys Acta*. **1861**, 988-996 10.1016/j.bbailip.2016.05.011.
166. Gao, X., L., G., Shao, J., Su, C., Zhao, H., Saarikettu, J., Yao, X., Yao, Z., Silvennoinen, O., and Yang, J. (2010) Tudor-SN interacts with and co-localizes with G3BP in stress granules under stress conditions. *FEBS letters*. **584**, 3525-3532 10.1016/j.febslet.2010.07.022
167. Elbarbary, R., Miyoshi, K., Hedaya, O., Myers, J., and Maquat, L. (2017) UPF1 helicase promotes TSN-mediated miRNA decay. *Genes Dev*. **31**, 1483-1493 10.1101/gad.303537.117
168. Elbarbary, R., Miyoshi, K., Myers, J., Du, P., Ashton, J. M., Tian, B., and Maquat, L. E. (2017) Tudor-SN-mediated endonucleolytic decay of human cell microRNAs promotes G(1)/S phase transition. *Science*. **356**, 859-862 10.1126/science.aai9372.

169. Ku, H. Y., Gangaraju, V. K., Qi, H., Liu, N., and Lin, H. (2016) Tudor-SN Interacts with Piwi Antagonistically in Regulating Spermatogenesis but Synergistically in Silencing Transposons in *Drosophila*. *PLoS Genetics*. **12**, 10.1371/journal.pgen.1005813
170. Sun, J. G., A, J., and Casper, R. F. (1997) Detection of deoxyribonucleic acid fragmentation in human sperm: correlation with fertilization in vitro. *Biol Reprod*. **56**, 602-607 10.1095/biolreprod56.3.602
171. Kroeger-Koepke, M. B., Koepke, S. R., McClusky, G. A., Magee, P. N., and Michejda, C. J. (1981) alpha-Hydroxylation pathway in the in vitro metabolism of carcinogenic nitrosamines: N-nitrosodimethylamine and N-nitroso-N-methylaniline. *Proc Natl Acad Sci USA*. **78**, 6489-6493 10.1073/pnas.78.10.6489.
172. Kot, M., and Daujat-Chavanieu, M. (2018) Altered cytokine profile under control of the serotonergic system determines the regulation of CYP2C11 and CYP3A isoforms. *Food Chem Toxicol*. **116**, 369-378 10.1016/j.fct.2018.04.051.
173. Chowdhury, G., W., C. M., and Guengerich, F. P. (2010) Oxidation of N-Nitrosoalkylamines by human cytochrome P450 2A6: sequential oxidation to aldehydes and carboxylic acids and analysis of reaction steps. *J Biol Chem*. **285**, 8031-8044 10.1074/jbc.M109.088039
174. Klyushova, L. S., Perepechaeva, M. L., and Grishanova, A. Y. (2022) The Role of CYP3A in Health and Disease. LID - 10.3390/biomedicines10112686 [doi] LID - 2686. *Biomedicines*. **10**, 2686 10.3390/biomedicines10112686
175. Yang, J., Aittomäki, S., Pesu, M., Carter, K., Saarinen, J., Kalkkinen, N., Kieff, E., and Silvennoinen, O. (2002) Identification of p100 as a coactivator for STAT6 that bridges STAT6 with RNA polymerase II. *The EMBO journal*. **21**, 4950-4958 10.1093/EMBOJ/CDF463
176. Gabay, C., and Kushner, I. (1999) Acute-phase proteins and other systemic responses to inflammation. *N Engl J Med*. **340**, 448-454 10.1056/NEJM199902113400607



177. Dempsey, E., and Rudd, P. M. (2012) Acute phase glycoproteins: bystanders or participants in carcinogenesis? *Ann N Y Acad Sci.* **1253**, 122-132 10.1111/j.1749-6632.2011.06420.x
178. Gao, X., X, F., Song, J., Zhang, Y., Cui, X., Su, C., Ge, L., Shao, J., Xin, L., Saarikettu, J., Mei, M., Yang, X., Wei, M., Silvennoinen, O., Yao, Z., He, J., and Yang, J. (2015) Poly(A)(+) mRNA-binding protein Tudor-SN regulates stress granules aggregation dynamics. *FEBS J.* **282**, 874-890 10.1111/febs.13186
179. Dasovich, M., Beckett, M. Q., Bailey, S., Ong, S. E., Greenberg, M. M., and Leung, A. K. L. (2021) Identifying Poly(ADP-ribose)-Binding Proteins with Photoaffinity-Based Proteomics. *Journal of the American Chemical Society.* **143**, 3037-3042 10.1021/JACS.0C12246/ASSET/IMAGES/LARGE/JA0C12246\_0004.JPEG
180. Pare, J. M., N, T., López-Orozco, J., LaPointe, P., Lasko, P., Hobman, T. C., and Hobman, T. C. (2009) Hsp90 regulates the function of argonaute 2 and its recruitment to stress granules and P-bodies. *Mol Biol Cell.* **20**, 3273-3284 10.1091/mbc.e09-01-0082
181. Brown, Z. J., Heinrich, B., and Greten, T. F. (2018) Mouse models of hepatocellular carcinoma: an overview and highlights for immunotherapy research. *Nat Rev Gastroenterol Hepatol.* **15**, 536-554,
182. Horie, Y., A, S., Kataoka, E., Sasaki, T., Hamada, K., Sasaki, J., Mizuno, K., Hasegawa, G., Kishimoto, H., Iizuka, M., Naito, M., Enomoto, K., Watanabe, S., Mak, T. W., and Nakano, T. (2004) Hepatocyte-specific Pten deficiency results in steatohepatitis and hepatocellular carcinomas. *J Clin Invest.* **113**, 1774-1783 10.1172/JCI20513.
183. Katz, S. F., A, L., Obenauf, A. C., A.C., O., Begus-Nahrmann, Y., Kraus, J. M., Hoffmann, E. M., Duda, J., Eshraghi, P., Hartmann, D., Liss, B., Schirmacher, P., Kestler, H. A., Speicher, M. R., and Rudolph, K. L. (2012) Disruption of Trp53 in livers of mice induces formation of carcinomas with bilineal differentiation. *Gastroenterology.* **142**, 1229-1239 10.1053/j.gastro.2012.02.009

184. Sato, S., H, S., Takeda, K., Ninomiya-Tsuji, J., Yamamoto, M., Kawai, T., Matsumoto, K., Takeuchi, O., and Akira, S. (2005) Essential function for the kinase TAK1 in innate and adaptive immune responses. *Nat Immunol.* **6**, 1087-1095 10.1038/ni1255
185. Wang, Q., Yu, W. N., Chen, X., Peng, X. D., Jeon, S. M., Birnbaum, M. J., Guzman, G., and Hay, N. (2016) Spontaneous Hepatocellular Carcinoma after the Combined Deletion of Akt Isoforms. *Cancer Cell.* **29**, 523-535 10.1016/j.ccell.2016.02.008.
186. Chen, W. T., C., T. C., Pfaffenbach, K., Kanel, G., Luo, B., Stiles, B. L., and Lee, A. S. (2014) Liver-specific knockout of GRP94 in mice disrupts cell adhesion, activates liver progenitor cells, and accelerates liver tumorigenesis. *Hepatology.* **59**, 947-957 10.1002/hep.26711
187. Llovet, J. M., Zucman-Rossi, J., Pikarsky, E., Sangro, B., Schwartz, M., Sherman, M., and Gores, G. (2016) Hepatocellular carcinoma. *Nature reviews Disease primers.* **2**, 10.1038/NRDP.2016.18
188. Wang, J., Kaur, S., Westermeier, F., Porat-Shliom, N., and Cunningham, R. P. (2021) Liver Zonation – Revisiting Old Questions With New Technologies. *Front Physiol.* **12**, 732929-732929 10.3389/fphys.2021.732929
189. Zhang, Q., Lou, Y., Bai, X. L., and Liang, T. B. (2020) Intratumoral heterogeneity of hepatocellular carcinoma: From single-cell to population-based studies. *World Journal of Gastroenterology.* **26**, 3720-3720 10.3748/WJG.V26.I26.3720
190. Zheng, J., Li, B., Wu, Y., Wu, X., and Wang, Y. (2023) Targeting Arginine Methyltransferase PRMT5 for Cancer Therapy: Updated Progress and Novel Strategies. *J Med Chem.* 10.1021/acs.jmedchem.3c00250
191. Caruso, S., Calatayud, A. L., Pilet, J., La Bella, T., Rekik, S., Imbeaud, S., Letouze, E., Meunier, L., Bayard, Q., Rohr-Udilova, N., Peneau, C., Grasl-Kraupp, B., de Koning, L., Ouine, B., Bioulac-Sage, P., Couchy, G., Calderaro, J., Nault, J. C., Zucman-Rossi, J., and Rebouissou, S. (2019) Analysis of Liver Cancer Cell Lines Identifies Agents With

- Likely Efficacy Against Hepatocellular Carcinoma and Markers of Response. *Gastroenterology*. **157**, 760-776 10.1053/j.gastro.2019.05.001
192. Mueller, H. S., Fowler, C. E., Dalin, S., Moiso, E., Udomlumleart, T., Garg, S., Hemann, M. T., and Lees, J. A. (2021) Acquired resistance to PRMT5 inhibition induces concomitant collateral sensitivity to paclitaxel. LID - 10.1073/pnas.2024055118 [doi] LID - e2024055118. *Proc Natl Acad Sci U S A*. **118**, doi: 10.1073/pnas.2024055118
193. Liu, Y., Iqbal, A., Li, W., Ni, Z., Wang, Y., Ramprasad, J., Abraham, K. J., Zhang, M., Zhao, D. Y., Qin, S., Loppnau, P., Jiang, H., Guo, X., Brown, P. J., Zhen, X., Xu, G., Mekhail, K., Ji, X., Bedford, M. T., Greenblatt, J. F., and Min, J. (2022) A small molecule antagonist of SMN disrupts the interaction between SMN and RNAP II. *Nat Commun*. **13**, 5453 10.1038/s41467-022-33229-5
194. Enders, L., Siklos, M., Borggräfe, J., Gaussmann, S., Koren, A., Malik, M., Tomek, T., Schuster, M., Reiniš, J., Hahn, E., Rukavina, A., Reicher, A., Casteels, T., Bock, C., Winter, G. E., Hannich, J. T., Sattler, M., and Kubicek, S. (2023) Pharmacological perturbation of the phase-separating protein SMNDC1. *Nat Commun*. **14**, 1504 10.1038/s41467-023-40124-0.
195. Liu, L., Yan, H., Ruan, M., Yang, H., Wang, L., Lei, B., Sun, X., Chang, C., Huang, G., and Xie, W. (2021) An AKT/PRMT5/SREBP1 axis in lung adenocarcinoma regulates de novo lipogenesis and tumor growth. *Cancer Sci*. **112**, 3083-3098 10.1111/cas.14988
196. Han, X., Wei, L., and Wu, B. (2020) PRMT5 Promotes Aerobic Glycolysis and Invasion of Breast Cancer Cells by Regulating the LXR $\alpha$ /NF- $\kappa$ Bp65 Pathway. *Onco Targets Ther*. **13**, 3347-3357 10.2147/OTT.S239730
197. Ji, S., Ma, S., Wang, W. J., Huang, S. Z., Wang, T. Q., Xiang, R., Hu, Y. G., Chen, Q., Li, L. L., and Yang, S. Y. (2017) Discovery of selective protein arginine methyltransferase 5 inhibitors and biological evaluations. *Chem Biol Drug Des*. **89**, 585-598 10.1111/cbdd.12881

198. Suda, T., and Liu, D. (2007) Hydrodynamic gene delivery: its principles and applications. *Mol Ther.* **15**, 2063-2069 10.1038/sj.mt.6300314
199. Espejo, A. B., Gao, G., Black, K., Gayatri, S., Veland, N., Kim, J., Chen, T., Sudol, M., Walker, C., and Bedford, M. T. (2017) PRMT5 C-terminal Phosphorylation Modulates a 14-3-3/PDZ Interaction Switch. *J Biol Chem.* **292**, 2255-2265 10.1074/jbc.M116.760330
200. Zhou, L., H, W., Lee, P., and Wang, Z. (2006) Roles of the androgen receptor cofactor p44 in the growth of prostate epithelial cells. *J Mol Endocrinol.* **37**, 283-300 10.1677/jme.1.02062
201. Stopa, N., Krebs, J. E., and Shechter, D. (2015) The PRMT5 arginine methyltransferase: Many roles in development, cancer and beyond. *Cellular and Molecular Life Sciences.* **72**, 2041-2059 10.1007/s00018-015-1847-9
202. Guderian, G., C, P., Wiesner, J., Sickmann, A., Schulze-Osthoff, K., Fischer, U., and Grimmmler, M. (2011) RioK1, a new interactor of protein arginine methyltransferase 5 (PRMT5), competes with pICln for binding and modulates PRMT5 complex composition and substrate specificity. *J Biol Chem.* **286**, 1976-1986 10.1074/jbc.M110.148486
203. Lacroix, M., S, E. M., Rodier, G., Le Cam, A., Sardet, C., and Fabrizio, E. (2008) The histone-binding protein COPR5 is required for nuclear functions of the protein arginine methyltransferase PRMT5. *EMBO Reports.* **9**, 452-458 10.1038/embor.2008.45
204. Pesiridis, G. S., E, D., and Van Duyne, G. D. (2009) Role of pICln in methylation of Sm proteins by PRMT5. *J Bio Chem.* **284**, 21347-21359 10.1074/jbc.M109.015578
205. Ancelin, K., Uc, L., Hajkova, P., Schneider, R., Bannister, A. J., Kouzarides, T., and Surani, M. A. (2006) Blimp1 associates with Prmt5 and directs histone arginine methylation in mouse germ cells. *Nat Cell Biol.* **8**, 623-630 10.1038/ncb1413
206. Fu, T., Lv, X., Kong, Q., and Yuan, C. (2017) A novel SHARPIN-PRMT5-H3R2me1 axis is essential for lung cancer cell invasion. *Oncotarget.* **8**, 54809-54820 10.18632/oncotarget.18957

207. Yang, M., Lin, X., Segers, F., Suganthan, R., Hildrestrand, G. A., Rinholm, J. E., Aas, P. A., Sousa, M. M. L., Holm, S., Bolstad, N., Warren, D., Berge, R. K., Johansen, R. F., Yndestad, A., Kristiansen, E., Klungland, A., Luna, L., Eide, L., Halvorsen, B., Aukrust, P., and Bjørås, M. (2020) OXR1A, a Coactivator of PRMT5 Regulating Histone Arginine Methylation. *Cell Reports*. **30**, 4165-4178.e4167 10.1016/j.celrep.2020.02.063
208. Paul, C., C, S., and Fabrizio, E. (2012) The histone- and PRMT5-associated protein COPR5 is required for myogenic differentiation. *Cell Death & Differentiation*. **19**, 900-908 10.1038/cdd.2011.193.
209. Meister, G., C, E., Bühler, D., Brahms, H., Kambach, C., and Fischer, U. (2001) Methylation of Sm proteins by a complex containing PRMT5 and the putative U snRNP assembly factor pICln. *Curr Biol*. **11**, 1990-1994 10.1016/s0960-9822(01)00592-9
210. Zhang, H., Z.H., C., and Savarese, T. M. (1996) Codeletion of the genes for p16INK4, methylthioadenosine phosphorylase, interferon-alpha1, interferon-beta1, and other 9p21 markers in human malignant cell lines. *Cancer Genet Cytogenet*. **86**, 22-28 10.1016/0165-4608(95)00157-3
211. Marjon, K., Cameron, M. J., Quang, P., Clasquin, M. F., Mandley, E., Kunii, K., McVay, M., Choe, S., Kernytsky, A., Gross, S., Konteatis, Z., Murtie, J., Blake, M. L., Travins, J., Dorsch, M., Biller, S. A., and Marks, K. M. (2016) MTAP Deletions in Cancer Create Vulnerability to Targeting of the MAT2A/PRMT5/RIOK1 Axis. *Cell Reports*. **15**, 574-587 10.1016/j.celrep.2016.03.043
212. Li, C. L., Yang, W. Z., Chen, Y. P., and Yuan, H. S. (2008) Structural and functional insights into human Tudor-SN, a key component linking RNA interference and editing. *Nucleic acids research*. **36**, 3579-3589 10.1093/NAR/GKN236
213. Nakagawa, H., Umemura, A., Taniguchi, K., Font-Burgada, J., Dhar, D., Ogata, H., Zhong, Z., Valasek, M. A., Seki, E., Hidalgo, J., Koike, K., Kaufman, R. J., and Karin, M. (2014) ER stress cooperates with hypernutrition to trigger TNF-dependent spontaneous HCC development. *Cancer Cell*. **26**, 331-343 10.1016/j.ccr.2014.07.001

214. Chisari, F. V., K, K., Moriyama, T., Pasquinelli, C., Dunsford, H. A., Sell, S., Pinkert, C. A., Brinster, R. L., and Palmiter, R. D. (1989) Molecular pathogenesis of hepatocellular carcinoma in hepatitis B virus transgenic mice. *Cell*. **59**, 1145-1156 10.1016/0092-8674(89)90770-8
215. Huang, L., Liu, J., Zhang, X. O., Sibley, K., Najjar, S. M., Lee, M. M., and Wu, Q. (2018) Inhibition of protein arginine methyltransferase 5 enhances hepatic mitochondrial biogenesis. *Journal of Biological Chemistry*. **293**, 10884-10894 10.1074/jbc.RA118.002377
216. Zhang, Y., Verwilligen, R. A. F., Van Eck, M., and Hoekstra, M. (2023) PRMT5 inhibition induces pro-inflammatory macrophage polarization and increased hepatic triglyceride levels without affecting atherosclerosis in mice. *J Cell Mol Med*. **27**, 1056-1068 10.1111/jcmm.17676

## 12 Vita

Tanner Janson Wright is the son of VaLee Loertscher Wright and the late Todd Lee Wright. He completed his Bachelor of Science at Utah Valley University with honors and a minor in chemistry in December 2017. While at his *alma mater*, Tanner helped start the lab of Eric T. Domyan, PhD and worked in the laboratory of Joshua Schiffman, MD and Lisa Abegglen, PhD. Following his undergraduate work, he entered The University of Texas MD Anderson Cancer Center UTHealth Houston Graduate School of Biomedical Sciences in 2018.

Permanent address:

3517 W 8180 S

West Jordan, UT 84044